This electronic thesis or dissertation has been downloaded from the King's Research Portal at https://kclpure.kcl.ac.uk/portal/



Functional analysis of the KDM5B demethylase
In vitro and in vivo studies

Catchpole, Steven

Awarding institution:
King's College London

The copyright of this thesis rests with the author and no quotation from it or information derived from it may be published without proper acknowledgement.

END USER LICENCE AGREEMENT



Unless another licence is stated on the immediately following page this work is licensed

under a Creative Commons Attribution-NonCommercial-NoDerivatives 4.0 International

licence. https://creativecommons.org/licenses/by-nc-nd/4.0/

You are free to copy, distribute and transmit the work

Under the following conditions:

- Attribution: You must attribute the work in the manner specified by the author (but not in any way that suggests that they endorse you or your use of the work).
- Non Commercial: You may not use this work for commercial purposes.
- No Derivative Works - You may not alter, transform, or build upon this work.

Any of these conditions can be waived if you receive permission from the author. Your fair dealings and other rights are in no way affected by the above.

Take down policy

If you believe that this document breaches copyright please contact librarypure@kcl.ac.uk providing details, and we will remove access to the work immediately and investigate your claim.

Download date: 08. Oct. 2023

King's College London

Functional analysis of the KDM5B demethylase: *In vitro* and *in vivo* studies

Steven Catchpole

August 2013

A thesis submitted in accordance with the requirements for examination for the degree of Doctor of Philosophy

Division of Cancer Studies
Breast Cancer Biology
Guy's Hospital
London
SE1 9RT

Declaration

All of the experimental work, results and ideas presented in this thesis, except where acknowledged accordingly, are entirely my own.

None of the work contained within this thesis has previously been submitted for examination by the University of London or any other degree awarding body.

The work was carried out under the supervision of Professor Joyce Taylor-Papadimitriou and Professor Joy Burchell at King's College London, Guy's Hospital.

Abstract

Thesis abstract

The KDM5 family consists of four proteins, namely KDM5A, KDM5B, KDM5C and KDM5D. The KDM5 family of demethylase proteins counteract the tri-methylation of H3K4 and can function as transcriptional repressors. They can form a number of different multi-protein complexes that contain other chromatin-modifying factors and co-factors that aid in the recruitment of the protein complex to the genome, whilst also possessing the ability to bind to DNA directly through the ARID domain. Furthermore the KDM5 family has also been implicated in mediating nuclear receptor signalling. The KDM5 family are highly homologous and where co-expressed may act redundantly. A picture is emerging where the KDM5 family may dictate the shift in balance between cellular proliferation and differentiation and are therefore important during development. Although the KDM5 demethylase activity has attracted the greatest attention, it is apparent that this family is an important multi-faceted group of proteins.

To study the function of KDM5B two knockout murine lines were generated. The *Kdm5b* null murine line resulted in early embryonic lethality, whereas a second murine line expressing a KDM5B protein lacking the ARID domain (ΔARID) was viable and fertile but displayed a mammary gland phenotype, where terminal end bud development and side branching were delayed at puberty. Since intact oestrogen receptor (ER alpha) signaling is a prerequisite for nulliparous mammary gland development we examined the expression of the progesterone receptor in the adult nulliparous KDM5B ΔARID murine mammary gland and found levels to be reduced as compared to the wild-type. Furthermore, co-immunoprecipition of tagged human KDM5B and ER alpha proteins demonstrated an *in vivo* interaction. These studies suggest that KDM5B is required during embryonic development and may be involved in the ER alpha signaling pathway during nulliparous mammary gland development. Our analysis of the C57BL/6J-*Kdm5b* ΔARID pregnant mammary gland showed a delay in mammary gland morphogenesis and the female could nurse her pups at parturition. Investigation into the molecular mechanisms that may relate to this showed that KDM5B expression is required to positively regulate the PRLR/JAK2/STAT5 signalling pathway associated with mammary gland development during gestation

Acknowledgements

First, I would like to thank Joyce Taylor-Papadimitriou and Joy Burchell for their help and supervision and above all, for giving me the opportunity to complete this thesis. Thank you.

I would like to thank all those who have contributed to this work. To Dr Samantha Santangelo who designed and constructed the targeting constructs used to generate the B6;129-*Kdm5b Exon 1* knock out and the C57BL/6-*Kdm5b ΔARID* murine lines. To Dr Ian Rosewell and colleagues at Cancer Research UK for their participation in the generation of the B6;129-*Kdm5b Exon 1* knock out and the C57BL/6-*Kdm5b ΔARID* murine lines and Janet Macdonald who carried out the breeding programs and always went beyond the call of duty – thanks Janet. To Debbie Hall for her help with the screening of the mice and for sharing both good times and bad! I would also like to give my special thanks to Dr Bradley Spencer-Dene for being a great guy who helped me with the studies on the murine mammary gland. Finally, I would like to thank Professor Gordon Stamp who provided the pathology reports and Dr. Richard Poulson and colleagues for help with the *in situ* hybridisation data.

Contents page

Contents

Title page i

Declaration ii

Thesis abstract iii

Acknowledgements v

Chapters vii

Index of figures xv

Index of tables xxiii

Abbreviations xxvi

Chapter 1. Introduction: Section 1A: The regulation of chromatin: Methylation of histone lysine residues. 1

1A Prologue 2

1A.1 The regulation of chromatin: Methylation of histone lysine residues 2

1A.1.1 The nucleosome and histone tail 2

1A.1.2 It takes a PHD to be a reader in H3K4 methylation 4

1A.2 Histone marks and murine mammary development 5

1A.3 The KDM5 family and gene regulation 6

1A.3.1 The conserved domains of the KDM5 family of proteins 7

1A.3.2 The KDM5 family as H3K4 demethylase enzymes 9

1A.3.3 The KDM5 family of transcriptional repressors 9

1A.3.4 A function for the KDM5 family of proteins in the activation of transcription 11

1A.3.5 Direct Recruitment of the KDM5 family to the genome 12

1A.3.6 Recruitment of the KDM5 family to the genome as part of a multi-protein complex 13

1A.3.7 Lessons from the past: Studies in *C. Elegans* and *D. Melangaster* 14

1A.4 The expression patterns of the KDM5 family of proteins 16

1A.4.1 The expression profile of KDM5A and KDM5B in human adult tissue 16

1A.4.2 The expression profile of KDM5B in murine adult tissue 16

1A.4.3 KDM5B expression during murine embryonic development 17

1A.4.4 A function for KDM5B during ES cell commitment 19

1A.4.5 The expression profile of KDM5C and KDM5D 19

1A.4.6 A role for the KDM5 family of proteins during neurogenesis 20

1A.5 A role for KDM5A and KDM5B during senescence and differentiation 20

1A.5.1 A function for KDM5B during the G1 to S phase transition of the cell cycle 20

1A.5.2 KDM5A and KDM5B link H3K4 demethylation to retinoblastoma 21

binding protein mediated senescence
1A.5.3 A function for KDM5A during differentiation 22
1A.6 KDM5B and cancer 23
1A.6.1 KDM5B expression and melanoma 24
1A.6.2 KDM5B expression and prostate cancer 24
1A.6.3 KDM5B and breast cancer 25
1A.7 Clinical sub-types of breast cancer 26
1A.8 The relevance of murine models to study mammary gland morphogenesis 26

Chapter 1. Introduction: Section 1B: Development, differentiation and involution of the murine mammary gland 28
1B Overview 29
1B.1 Murine mammary gland stem cells, the epithelial cell hierarchy **31**
1B.1.1 The existence of a murine multi-potent adult mammary gland stem cell 31
1B.1.2 Murine postnatal mammary gland development is defined in the embryonic mammary bud and completed after birth by uni-potent stem cells 34
1B.1.3 Both multi-potent and uni-potent murine mammary gland stem cells contribute to postnatal mammary gland development 35
1B.1.4 Ovarian hormone control of mammary epithelial cell hierarchy organisation during postnatal mammary gland development 35
1B.1.5 Cell fate and histone marks in the mammary gland 37
(A) The chromatin effector protein, Pygo-2 37
(B) The EZH2 histone methyltransferase 38
1B.2 Studies on pubertal mammary gland development 39
1B.2.1 Oestrogen receptor signalling 39
1B.2.2 Progesterone receptor signalling in the adult mammary gland 41
1B.2.3 Growth factor regulation of ductal morphogenesis 42
1B.3 Morphogenesis and Differentiation of the mammary gland at Pregnancy and Lactation 44
1B.3.1 Progesterone and prolactin in alveologenesis and terminal differentiation 45
1B.3.2 The function of the Ets transcription factor ELF5 during cell fate determination in the pregnant mammary gland 46
1B.4 Post weaning and Involution of the mammary gland 47
1B.5 The JAK/STAT pathways during mammary gland development 48

1B.5.1 STAT6 in luminal cell development 50
1B.5.2 The role of STAT5 in alveologenesis and expression of milk proteins 52
1B.5.3 STAT3 function during involution 53

1C Aims 56

Chapter 2. Materials and methods 59
2.1 Solutions and buffer 60
2.2 General statement 61
2.3 Cell culture 61
2.4 Preparation and analysis of DNA 62
2.4.1 Phenol:chloroform extraction and precipitation of tail-snip genomic DNA 62
2.4.2 Determining the concentration of DNA 62
2.4.3 Restriction endonuclease digest of (A) B6;129-*Kdm5b-Exon 1* knock out and (B) B6;129-*Kdm5b ΔARID* genomic DNA for Southern blot analysis 62
2.4.4 Agarose gel electrophoresis of DNA 63
2.4.5 Genotyping by Southern transfer 63
2.4.6 End point PCR on C57BL/6J mammary gland cDNA and sequencing 64
2.4.7 B6;129-*Kdm5b-Exon 1* knock out PCR screen to identify homologous recombination 65
2.4.8 PCR screen used to detect heterozygous B6;129-*Kdm5b ΔARID* offspring during backcross to the C57BL/6J genetic background 65
2.4.9 PCR screen used to detect the polyoma virus middle T antigen transgene (PyV-mT) 65
2.4.10 Generation of chemically competent *Escherichia coli* (*E.coli*) 65
2.4.11 Transformation of competent *E. Coli* 66
2.4.12 Large-scale preparation of plasmid DNA 66
2.4.13 Plasmid constructs 67
2.5 Preparation and analysis of RNA 67
2.5.1 Extraction of total RNA 67
2.5.2 Determining the concentration of RNA 67
2.5.3 cDNA synthesis 67
2.5.4 Quantitative PCR and PCR primers 68
2.6 Preparation and analysis of protein 69
2.6.1 Nuclear and cytoplasmic protein extraction 69
2.6.2 SDS-PAGE electrophoresis and Western blot transfer 69

2.6.3 Primary antibodies used for Western blot 71
2.6.4 Secondary antibodies used for Western blot 72
2.6.5 Transient transfection of plasmid DNA 72
2.6.6 Immunoprecipitation 73
2.6.7 Antibodies used for immunoprecipitation 73
2.7 Murine studies 74
2.7.1 Development of the B6;129-*Kdm5b ΔARID* mouse strain and backcross to the C57BL/6J genetic background 74
2.7.2 Development of the B6;129-*Kdm5b-Exon 1* knock out murine line 74
2.7.3 Breeding program between the C57BL/6-*Kdm5b ΔARID -/-* and the FVB-MMTV-*PyV-mT +/-* murine lines 74
2.7.4 Staging pregnancy and synchronising oestrous cycle 75
2.8 Cell biology techniques 75
2.8.1 Histology 75
2.8.2 Mammary gland whole mount 76
2.8.3 Immunohistochemistry 76
2.8.4 Primary antibody used for immunohistochemistry 77
2.8.5 Secondary antibody used for immunohistochemistry 77
2.8.6 *Microscopy* and data analysis 78

Chapter 3. Studies on the function of KDM5B in vivo 79
3.1 Aim 80
3.2 Introduction: A role for KDM5B during development 80
3.3 Results 81
3.3.1 Ablation of murine KDM5B results in embryonic lethality 81
3.3.2 Development, screening and preliminary characterisation of the chimeric B6;129-*Kdm5b ΔARID* murine line 87
3.3.2.1 The B6;129-*Kdm5b ΔARID* murine line are viable and fertile 87
3.3.2.2 Expression of a less abundant KDM5B protein lacking the entire ARID domain and part of the JmjN domain 89
(A) KDM5B protein expression 89
(B) Processing of the KDM5B transcript 90
3.3.2.3 Development of adult tissues in the B6;129-Kdm5b ΔARID murine line 93
(A) Histological analysis of male and female adult tissue 93
(B) A possible defect in mammary gland ductal morphogenesis 94
3.4 Discussion 98
3.4.1 Assessing the developmental role of KDM5B 98

3.4.2 KDM5B protein expression in the adult testis and mammary gland at pd18.5 100
3.4.3 A demethylase independent function for KDM5B? 101
3.4.4 Recruitment of KDM5B to the genome 102
3.4.5 The B6;129-*Kdm5b ΔARID* male is fertile 102
3.5 Supplemental materials 104

Chapter 4. KDM5B is expressed during mammary gland ductal morphogenesis and is required for normal mammary gland development 107
4.1 Aims 108
4.2 Introduction: Murine mammary gland ductal morphogenesis 108
4.3 Results 110
4.3.1 Documentation of KDM5B expression during C57BL/6J murine mammary gland development 110
4.3.1.1 Cellular localisation of the *Kdm5b* transcript expressed during murine C57BL/6J mammary gland development 112
4.3.1.2 Quantification of the *Kdm5b* transcript during murine C57BL/6J mammary gland development 114
4.3.1.3 KDM5B protein expression during murine C57BL/6J mammary gland development 115
4.3.1.4 Backcross of the chimeric homozygous B6;129-*Kdm5b ΔARID* murine line onto the inbred C57BL/6 genetic strain 116
4.3.1.5 Generation of the homozygous C57BL/6-*Kdm5b ΔARID* murine line 118
4.3.1.6 *Kdm5b* transcript levels in the C57BL/6J-*Kdm5b ΔARID* female mammary gland do not reflect KDM5B protein levels 119
4.3.2 Mammary gland development in the C57BL/6-*Kdm5b ΔARID* nulliparous female 121
4.3.2.1 The C57BL/6-*Kdm5b ΔARID* 4-week old mammary gland presents with fewer terminal end buds and a defect in ductal elongation and side branching 121
4.3.2.2 The C57BL/6-*Kdm5b ΔARID* 12-week old mammary gland presents with fewer bifurcation points, a defect in ductal elongation and side branching 123
4.3.2.3 Defective mammary gland development in the C57BL/6-*Kdm5b ΔARID* pregnant female 126
4.4 Discussion 132
4.4.1 KDM5B is expressed during mammary gland morphogenesis

and may suggest a role in epithelial cell proliferation, differentiation and survival 132
4.4.2 An increase in *Kdm5b* transcript level translates to a less abundant KDM5B protein in the C57BL/6J-*Kdm5b ΔARID* female at pd 18.5 133
4.4.3 A function for KDM5B during nulliparous mammary gland development 133
4.4.4 A function for KDM5B during pregnancy associated mammary gland morphogenesis 135
4.5 Supplemental material 138

Chapter 5. Investigation into the effect of KDM5B ΔARID expression on gene regulation and breast cancer development 139
5.1 Aims 140
5.2 Introduction 140
5.2.1 KDM5B and gene regulation 140
5.3 Results 143
5.3.1 Studies on a possible role for KDM5B in ER alpha signalling 143
5.3.1.1 Analysis of transcription levels in the C57BL/6J-*Kdm5b ΔARID* nulliparous mammary gland 143
5.3.1.2 KDM5B interacts with ER alpha in vivo in an ARID independent manner 144
5.3.2 Studies on KDM5B repressor function in the adult C57BL/6J-*Kdm5b ΔARID* mammary gland 145
5.3.3 Molecular assessment of the role of KDM5B during development of the C57BL/6J-*Kdm5b ΔARID* pregnant mammary gland 146
5.3.3.1 Molecular analysis in the C57BL/6J-Kdm5b ΔARID mammary gland at mid-pregnancy 146
(A) Steroid receptor expression at mid pregnancy 146
(B) Changes in the JAK/STAT and AKT signaling axis at mid pregnancy 148
5.3.3.2 Molecular analysis in the C57BL/6J-Kdm5b ΔARID mammary gland at late pregnancy 152
(A) Steroid receptor expression at late pregnancy 152
(B) Changes in the JAK/STAT and AKT signaling axis at late pregnancy 154
(C) Analysis of Kdm5a transcript expression in the C57BL/6J-Kdm5b WT and ΔARID mammary gland at late pregnancy 160

5.4 Discussion 162

5.4.1 A potential role for KDM5B during oestrogen receptor signaling in the pubertal mammary gland 163

5.4.2 Analysis of KDM5B target genes in the adult C57BL/6J-*Kdm5b ΔARID* mammary gland 164

5.4.3 Importance of epigenetic factors in mammary gland development 165

5.4.4 KDM5B function during pregnancy associated mammary gland development 165

(A) Early to mid-pregnancy 165

(B) Late pregnancy 167

5.4.5 The relative ratio of phosphorylated to un-phosphorylated STAT5 167

5.4.6 The regulation of STAT5 activation 168

Chapter 6. Investigation into the effect of KDM5B ΔARID expression on mammary gland tumour development 169

6.1 Aims 170

6.2 Introduction 170

6.3 Results 171

6.3.1 The expression of a KDM5B ΔARID results in a delay in mammary gland tumour development 171

6.4 Discussion 175

6.4.1 KDM5B ΔARID expression and breast cancer 175

6.5 Supplemental material 138

Chapter 7 Discussion 178

7.1 Summary 179

7.2 The KDM5B null phenotype 179

7.3 Deciphering the role of the KDM5 family of proteins during development 180

7.4 KDM5B function during pubertal mammary gland 181

7.5 KDM5B, stem cells and progenitor cells 183

7.6 KDM5B, pregnancy and involution 184

7.6.1 KDM5B and the STAT signalling pathway 184

7.7 KDM5B, signalling pathways and the development of the mammary gland 186

7.8 Demethylase independent function of the KDM5 family of proteins 188

Chapter 8 References 190

Index of figures

Index of figures

Figure 1. Chromatin, the nucleosome and the histone tail cooperate to control gene regulation 3

Figure 1.1. Schematic representation of the protein domain position for the KDM5 family of H3K4 demethylase enzymes 8

Figure 1.2. Model for KDM5 mediated repression 10

Figure 1.3. Model for C-MYC/KDM5 target gene activation 11

Figure 1.4. Model for PcG/KDM5B binding to the bivalent promoters of developmental genes 14

Figure 1.5. Model for KDM5/NOTCH signalling 15

Figure 1.6. Homology between the human KDM5B and the murine KDM5B proteins 17

Figure 1.7. A model 'switch' in repression during differentiation 23

Figure 1.8. Murine postnatal mammary gland development 30

Figure 1.9. Nulliparous mammary gland development is completed by adulthood through the bifurcation of TEB structures and the generation of ductal side-branches 31

Figure 1.10. Murine mammary gland epithelial cell hierarchy 32

Figure 1.11. The JAK/STAT signalling pathway in the mammary gland 49

Figure 1.12 Schematic representation of mammary gland development In the virgin, at pregnancy, lactation and involution showing the expression of different phosphorylated STAT proteins 49

Figure 3 Schematic representation of B6;129-*Kdm5b-Exon1* knock out strategy detailing an outline for the production of gene targeted mice by manipulation and injection of ES cells 82

Figure 3.1 Schematic representation showing the KDM5B protein domains with genomic sequence detailing the positions of the neomycin targeting construct (neo) used to replace exon1 (which codes for part of the JmjN domain) and homologous regions HR1 and HR2 83

Figure 3.2 Schematic representation of the *Kdm5b-WT* allele and the *Kdm5b-Exon1* targeting construct together with the screening strategy used to detect homologous recombination in transfected embryonic stem cells 83

Figure 3.3 PCR screen on genomic DNA isolated from the off-spring of the heterozygous B6;129-*Kdm5b-Exon1* knock out breeding programs 84

Figure 3.4 Normal mammary gland development in the heterozygous B6;129-*Kdm5b-Exon 1* knock out murine line 86

Figure 3.5 Schematic representation showing the KDM5B protein domains with genomic sequence detailing the positions of the neo targeting construct used to replace part of exon 2 and exons 3 to 4 88

Figure 3.6 Schematic representation of *Kdm5b ΔARID* targeting construct and the screening strategy used to detect homologous recombination in murine tail snip DNA 88

Figure 3.7 Expression of a of a smaller less abundant KDM5B protein in the B6;129-*Kdm5b ΔARID* mammary gland and testis 90 and 101

Figure 3.8 Processing of the *Kdm5b* primary transcript in the (A) B6;129-*Kdm5b WT* and (B) B6;129-*Kdm5b* ΔARID murine line 92

Figure 3.9 DNA trace from the B6;129-*Kdm5b ΔARID* mammary gland transcript at pd 18.5 93

Figure 3.10 Abnormal mammary gland development in the adult

B6;129-Kdm5b ΔARID murine line 95

Figure 3.11 Abnormal mammary gland development in the *B6;129-Kdm5b ΔARID* murine line at pd12.5 97

Figure 3.12 Mammary gland development at pd18.5 in the B6;129-*Kdm5b ΔARID* murine line 97

Figure 3S1. DNA trace from the B6;129-*Kdm5b WT* mammary gland transcript at pd 18.5 105

Figure 3S2. Murine *Kdm5b* coding sequence 106

Figure 4. Schematic representation of mammary gland ductal morphogenesis detailing the techniques employed to examine KDM5B expression levels 111

Figure 4.1. *In situ* hybridization showing the *Kdm5b* transcript is restricted to epithelial cells in the C57BL/6J mammary gland 113

Figure 4.2. The *Kdm5b* transcript is differentially expressed in the C57BL/6J *WT* murine mammary gland. 114

Figure 4.3. KDM5B protein expression in the C57BL/6J murine mammary gland 115

Figure 4.4. Representative neomycin specific PCR reaction on genomic DNA isolationed from the ear-snips of a heterozygous B6;129-*Kdm5b ΔARID* and C57BL/6J-*Kdm5b WT* breeding program 116

Figure 4.5. Representative Southern blot on tail-snip genomic DNA isolated from a heterozygous C57BL/6J-*Kdm5b ΔARID* breeding program 118

Figure 4.6. Representative Southern blot on tail-snip genomic DNA isolated from a homozygous C57BL/6J-*Kdm5b ΔARID* breeding program 118

Figure 4.7. Elevated *Kdm5b* transcript level in the C57BL/6J-*Kdm5b ΔARID* mammary gland at pd18.5 results in the translation of a less abundant KDM5B ΔARID protein 120

Figure 4.8. Fewer TEB structures in the 4-week old C57BL/6J-*Kdm5b ΔARID* nulliparous female 122

Figure 4.9. Abnormal mammary gland ductal development in the 4-week old C57BL/6J-*Kdm5b* ΔARID nulliparous female 123

Figure 4.10. Abnormal mammary gland development in the 12 weeks old (adult) C57BL/6J-*Kdm5b ΔARID* nulliparous female 124

Figure 4.11. The relatively quiescent state of the adult C57BL/6J-*Kdm5b WT* nulliparous mammary gland is not mirrored in the adult C57BL/6J-*Kdm5b ΔARID* female 125

Figure 4.12. Defective mammary gland development in the C57BL/6J-*Kdm5b ΔARID* female at pd12.5 126

Figure 4.13. Representative immunohistochemistry showing Ki67 staining in the C57BL/6J-*kdm5b WT* and C57BL/6J-*Kdm5b ΔARID* thoracic mammary glands at day 12.5 of pregnancy 127

Figure 4.14. Ki67 levels in the (A) alveoli and (B) ductal epithelia of C57BL/6J-*kdm5b WT* and C57BL/6J-*Kdm5b ΔARID* thoracic mammary glands at day 12.5 of pregnancy 128

Figure 4.15. A defect in mammary gland development at mid-pregnancy is over come at late pregnancy. 129

Figure 4.16 The number of alveoli are significant reduced in the C57BL/6J-*Kdm5b ΔARID* mammary gland compared to the wild type counterpart at late pregnancy 129

Figure 4.17 Representative immunohistochemistry showing Ki67 staining in the C57BL/6J-*kdm5b WT* and C57BL/6J-*Kdm5b ΔARID* thoracic mammary glands at day 18.5 of pregnancy 130

Figure 4.18 Ki67 levels in the C57BL/6J-*kdm5b WT* and C57BL/6J-*Kdm5b ΔARID* thoracic mammary glands at day 12.5 of pregnancy 130

Figure 4.19 C57BL/6J-Kdm5b WT and ΔARID alveoli perimeters are comparable and fat globules are secreted into the lumen 131

Figure 4S1 Screening strategy used to backcross the chimeric heterozygous B6;129-*Kdm5b ΔARID* murine line onto the inbred C57BL/6J genetic strain 138

Figure 5. Relative transcript levels of *Esr1* in the C57BL/6J-*Kdm5b WT* and C57BL/6J-*Kdm5b ΔARID* nulliparous mammary gland at 4 weeks of age 144

Figure 5.1. Relative transcript levels of *Esr1, Pgr*, and *Wnt4* in the C57BL/6J-*Kdm5b WT* and C57BL/6J-*Kdm5b ΔARID* nulliparous mammary gland at 12 weeks of age 144

Figure 5.2. KDM5B interacts with ER alpha *in vivo* in an ARID independent manner 145

Figure 5.3. Relative transcript levels of *Bub1, Brca1* and *Mt1F* in the C57BL/6J-*Kdm5b WT* and C57BL/6J-*Kdm5b ΔARID* nulliparous mammary gland at 12 weeks of age 146

Figure 5.4. Expression of ER alpha in the C57BL/6J-Kdm5b WT and ΔARID mammary gland at mid-pregnancy 147

Figure 5.5. Transcript levels of *Pgr* and *Wnt4* in the C57BL/6J-*Kdm5b WT* and C57BL/6J-*Kdm5b ΔARID* mammary gland at pd12.5 148

Figure 5.6. Expression of STAT6 in the C57BL/6J-Kdm5b WT and ΔARID mammary gland at mid-pregnancy 148

Figure 5.7. The relative ratio of pSTAT5 to STAT5 is reduced in the C57BL/6J-*Kdm5b ΔARID* mammary gland at mid pregnancy 150

Figure 5.8. AKT expression is reduced in the C57BL/6J-*Kdm5b ΔARID* mammary gland at mid pregnancy 151

Figure 5.9. A delay in mammary gland differentiation is suggested by the reduced beta casein expression level in the C57BL/6J-*Kdm5b*

ΔARID mammary gland at mid pregnancy 152

Figure 5.10. Expression of ER alpha in the C57BL/6J-*Kdm5b WT* and *ΔARID* mammary gland at late pregnancy 153

Figure 5.11. Progesterone receptor expression level is reduced in the C57BL/6J-*Kdm5b ΔARID* mammary gland at late-pregnancy 154

Figure 5.12. Expression of STAT6 in the C57BL/6J-Kdm5b WT and ΔARID mammary gland at late-pregnancy 155

Figure 5.13. The relative ratio of pSTAT5 to STAT5 is markedly reduced in the C57BL/6J-Kdm5b ΔARID mammary gland at late pregnancy 156

Figure 5.14. Phosphorylated STAT5 expression level is reduced in the C57BL/6J-*Kdm5b ΔARID* mammary gland at late-pregnancy 157

Figure 5.15. AKT expression in the C57BL/6J-Kdm5b ΔARID mammary gland at late pregnancy is comparable with the wild type counterpart 158

Figure 5.16. Beta casein and WAP expression level in the C57BL/6J-*Kdm5b ΔARID* mammary gland at late pregnancy indicative of full differentiation 159

Figure 5.17. Expression of Kdm5a in the in the C57BL/6J-Kdm5b WT and ΔARID mammary gland at late pregnancy 160

Figure 5.18 Summary of molecular analysis in the C57BL/6J-Kdm5b ΔARID mammary gland 162

Figure 6. Schematic representation of the B6;FVB-*Kdm5b ΔARID -/-* : *PyV-mT +/-* breeding program 171

Figure 6.1 PCR generated genotype results of a litter from the C57BL/6J-*Kdm5b ΔARID -/-* female : FVB-*MMTV-PyV-mT +/-* male breeding program (B6FVBF1) 172

Figure 6.2 Genotype results of a litter from the B6;FVB-*Kdm5b ΔARID* +/- : *PyV-mT +/-* male and a C57BL/6J-*Kdm5b ΔARID -/-* female breeding program (B6FVBF2) 172

Figure 6.3 Genotype results of a litter from the B6;FVB-*Kdm5b ΔARID* -/- : *PyV-mT* +/- male and a C57BL/6J-*Kdm5b ΔARID -/-* female breeding program (B6FVBF3) 173

Figure 6.4. Box plot showing the distribution of time (in days) taken to develop mammary gland tumours in the B6;FVB-*Kdm5b WT*:*PyV-mT* +/- and B6;FVB-*Kdm5b ΔARID* -/- : *PyV-mT* +/- females 174

Figure 6.5. Kaplan-Meier plot showing time to tumour development in the B6;FVB-*Kdm5b ΔARID* -/- : *PyV-mT* +/- and B6;FVB- *Kdm5b WT*:*PyV-mT* +/- female mammary gland 174

Index of tables

Index of tables

Table 2 Table listing primer sequences used in quantitative PCR 68

Table 2.1 Table listing primary antibodies used for Western blot 71

Table 2.2 Table listing secondary antibodies used for Western blot 72

Table 2.3 Table listing antibodies used for immunoprecipitation 73

Table 2.4 Table listing primary antibody used for immunohistochemistry 77

Table 2.5 Table listing secondary antibody used for immunohistochemistry 77

Table 3 Genotype of progeny from a heterozygous B6;129-*Kdm5b-Exon1* knock out breeding program 84

Table 3.1 The *Kdm5b* knock out line is embryonic lethal 85

Table 3.2 Genotyping from two B6;129-*Kdm5b ΔARID* heterozygous breeding programs demonstrates that the B6;129-*Kdm5b ΔARID* offspring are born according to Mendelian ratio. 89

Table 3.3 Derived sequence from the DNA trace of B6;129-*Kdm5b ΔARID* cDNA showing exon 1 to 5 boundaries 93

Table 3.4 Histological analysis of organs from the male and female B6;129-*Kdm5b ΔARID* murine line at 9 weeks of age (adult) suggesting normal development 94

Table 3S1 Heterozygous offspring of the B6;129 *Kdm5b-Exon1* knock out murine line are not born according to Mendelian frequencies 104

Table 3S2 Genotyping results from B6;129-*Kdm5b ΔARID* heterozygous breeding program demonstrates that the B6;129-*Kdm5b ΔARID* offspring are born according to Mendelian frequency 104

Table 3S3: Calculations for Chi Squared test (Table 3S2) 105

Table 3S4. Derived sequence from the DNA trace (Fig 3S1) of B6;129-*Kdm5b* WT cDNA showing exon 4 to 5 boundaries 105

Table 4. PCR generated genotyping results from the backcross of the B6;129-*Kdm5b ΔARID* chimeric line onto the C57BL/6J genetic strain 117

Table 6S1: Table showing time to tumour development (in days from birth) in the B6;FVB-*Kdm5b ΔARID* -/- : *PyV-mT* +/- and B6;FVB-*Kdm5b WT* : *PyV-mT* +/- female mammary gland 177

Abbreviations

Abbreviations

A

A	adenosine
aa	amino acid
ADP	adenosine triphosphate
ALPL	alkaline phosphatase
AP2 gamma	transcription factor AP-2 gamma (protein)
AR	androgen receptor
AREG	amphiregulin
ARID	A-T rich interactive domain
ARNTL	aryl hydrocarbon receptor nuclear translocator-like
Asp	aspartic acid

B

BamH1	Bacillus amyloli
BciVI	Bacillus circulans
BGLAP	bone gamma-carboxyglutamate protein
BMAL1	brain and muscle Arnt-like protein-1
bp	base pair
BPTF	bromodomain PHD finger transcription factor
BRCA1	breast cancer 1
BrdU	5-bromo-2-deoxyuridine
BRD2	bromodomain containing 2
BUB	budding uninhibited by benzimidazole
B6;129	A mixed strain derived from C57BL/6J and a 129 ES cell line

C

C	cytosine
CBP	CREB-binding protein
CCL14	chemokine ligand 14
CCNA1	cyclin A
CCND1	cyclin D1
CDKN1B	cyclin-dependent kinase inhibitor 1B
cDNA	complementary DNA
c-ErbB2	receptor tyrosine-protein kinase erbB2
ChIp	chromatin immunoprecipitation
ChIp-Seq	chromatin immunoprecipitation coupled with sequencing
Chi3Li	Chitinase 3-like 1
CITED	cbp/p300-interacting transactivator with Glu/Asp-rich carboxyl-terminal domain 1
CLOCK	circadian locomotor output cycles kaput
CO_2	carbon dioxide
Cre	cis-regulatory element
CSN2	beta casein
C-terminus	carboxyl terminus
c-MYC	myelocytomatosis viral oncogene

D

DAB	3,3'-diaminobenzidine
dCTP	deoxycytidine triphosphate
DMEM	Dulbecco's modified Eagle's medium
DNA	deoxyribonucleic acid
ds	double stranded
DTT	dithiothretiol
DTX1	E3 ubiquitin-protein ligase DTX1

E

e	embryonic day
E-box	enhancer box
EDTA	ethylenediaminetetraacetic acid
EED	embryonic ectoderm development
EGF	epidermal growth factor
EGFR	epidermal growth factor receptor
EGFP	enhanced green fluorescent protein
EHMT2	euchromatic histone-lysine N-methyltransferase 2
ELF5	Ets domain transcription factor
EMSA	electrophorectic mobility shift assay
ER alpha	oestrogen receptor alpha (protein)
ER beta	oestrogen receptor beta
ERE-luc	oestrogen receptor element luciferase reporter
ES	embryonic stem cells
ESR1	oestrogen receptor alpha (gene)
EZH2	enhancer of zeste homologue 2
E2F	E2 promoter binding factor

F

FACS	fluorescence-activated cell sorting
FCS	fetal calf serum
FGF	fibroblast growth factor
FGFR	fibroblast growth factor receptor
FOXA1	forkhead box A1
FVB	friend virus B
F1	filial 1

G

GATA3	trans-acting T-cell specific transcription factor 3
GFP	green fluorescent protein
Gln	glutamine
GR	glucocorticoid receptor
GST	Glutathione S-transferase
G1 phase	gap 1 phase
G418	geneticin

H

HA	hemagglutinin
H and E	hematoxylin and eosin
HCL	hydrochloric acid
HDAC	histone deacetylase
HIS	histidine
HOX	homeobox
HP1-alpha	heterochromatin protein 1 alpha
HR	homologous region
H3K4	histone 3 lysine 4

I

ICM	inner cell mass
IFN	interferon
IL	interleukin
IMS	industrial methylated spirit
ING1	inhibitor of growth 1
iNOS	nitric oxide synthetase
Ip	immunoprecipitation

J

Janus kinase	JAK
Jarid1	jumonji AT-rich interactive domain 1
JMJC	jumonji C
JMJN	jumonji N
JMJD2	jumonji domain 2

K

Kb	kilo base
KDa	kilo dalton
KDM5	lysine demethylase 5
KMT	lysine methyltransferase
KRT18	cytokeratin 18

L

LB	lysogeny broth
lid	little imaginal disc
LIF	Leukemia inhibitory factor
LMP	lysosomal membrane permeabilisation
LN	lymph node
loxP	locus of crossover in P1
LRP5	low density lipoprotein receptor-related protein 5

M

MaSC	mammary gland stem cell
MEF	mouse embryonic fibroblast
MET	mesenchymal to epithelial transition
min	minutes
MLL	mixed-lineage leukemia
M	molar
miRNA	micro-RNA
mM	millimolar
MMTV	mouse mammary tumour virus
MT1F	metallothionein 1F
MW	Molecular weight

N

NaCl	sodium chloride
NaOH	sodium hydroxide
Neo	neomycin gene
NOP60B	nucleolar protein at 60B
N-terminus	amino terminus
NURD	nucleosome remodeling and histone deacetylase
NURF	nucleosome-remodelling factor subunit

O

OCT4	octamer 4
OSM	Oncostatin M

P

PAK1	p21-activated kinase 1
PBS	phoshate buffered saline
PCR	polymerase chain reaction
PcG	polycomb group
PCNA	proliferating cell nuclear antigen
pd	pregnancy day

PGR	progesterone receptor (gene)
PHD	plant homeo domain
PH3	phospho-histone 3 (ser 10)
PIKE-A	PI3-kinase enhancer A
PI3K	phosphoinositide-3-kinase
PKB	Protein kinase B
PolII Ser5	phosphorylation of serine 5 in the C-terminus of polymerase II
POU5F1	POU class 5 homeobox 1
PR	progesterone receptor (protein)
pRb	retinoblastoma-binding protein
PRC2	polycomb repressive complex 2
Prl	prolactin
Prlr	prolactin receptor
Pro	proline
PSA-luc	prostate specific antigen luciferase reporter
PTEN	phosphatase and tensin homologue
PTP1B	protein tyrosine phosphatase 1B
Pygo	Pygopus
PyV-mT	polyoma middle T

Q

qPCR	quantitative PCR

R

RAS	rat sarcoma
RAR	retinoic acid receptor
RBP-J	recombination signal-binding protein 1 for J-kappa
RBP2	retinoblastoma binding protein 2
RBP2-H1	retinoblastoma binding protein 2 homology 1
Rbr-2	retinoblastoma binding protein related
RING1B	ring finger protein 1B
RNA	ribonucleic acid
RNF2	ring finger protein 2
RT	reverse transcription

S

SAHF	senescence-associated heterochromatic foci
Sca1	stem cell antigen 1
SDS	sodium dodecyl sulphate
Serpin2A	Spi2A
SET	su(var)3-9 and enhancer of zeste
siRNA	short interfering RNA
SMA	smooth muscle actin
SMCX	selected mouse cDNA on X
SMCY	selected mouse cDNA on Y
SOCS2	Suppressor of cytokine signaling-2
S-phase	synthesis phase
SSC	sodium chloride and sodium citrate
s-SHIP	SH2-containing inositol 5'-phosphatase (104kd isoform)
STAT	Signal transducer and activator of transcription
Su(h)	suppressor of hairless
SUZ12	suppressor of zeste 12 homolog
SV40	simian virus 40

T

T	thymidine
TAE	tris acetate EDTA

TAF3	transcription initiation factor TFIID subunit 3 (gene)
TEB	terminal end bud
TFAP2C	transcription factor AP-2 gamma (gene)
TFIID	transcription factor II D
Th	T helper cell
TNF	tissue necrosis factor
TPA	tissue plasminogen activator
Try	tryptophan

U

UVB	ultraviolet B

V

VDR	vitamin D receptor

W

Wap	Whey acidic protein
Wnt4	wingless-related MMTV integration site
WRT	with respect to
WT	wild type

X

XLMR	x-linked mental retardation

Y

YFP	yellow fluorescent protein

Z

ZF	zinc finger

Chapter 1: Introduction

Section 1A: The regulation of chromatin: Methylation of histone lysine residues.

Chapter 1. Section 1A: Introduction

1A Prologue

This thesis aims to gain an understanding into the function of a specific histone demethylase, KDM5B (a.k.a PLU-1, JARID1B), by exploring the effect on the murine mammary gland of knocking out the *Kdm5b* gene or introducing a partially defective gene into the *Kdm5b* loci. It is therefore appropriate to introduce the field of histone methylation, and the enzymes which regulate the epigenetic control of transcription (Section 1A) and furthermore, to discuss published work that is relevant to mammary gland biology (Section 1B).

1A.1 The regulation of chromatin: Methylation of histone lysine residues.

1A.1.1 The nucleosome and histone tail

Every cell within the same organism contains the same genes and therefore the same genetic information. Not only during embryonic development but also during the post postnatal development of organs such as the mammary gland, extrinsic cues are incorporated which permit cell fate determination. How cell type-specific chromatin organization at specific genomic loci allows access to and the regulation of genes controlling cellular phenotype is governed in part by the interaction of DNA with histone proteins.

The nucleosome – the basic unit of chromatin – contains 146 bp of DNA, wrapped twice around a histone octamer consisting of two copies of histones H3, H4, H2A and H2B (Kornberg, 1974). The nucleosome is repeated throughout the genome with chromatin being further condensed through its association with linker histone H1. Histone proteins contain a hydrophobic internal region and a flexible amino-terminal tail that protrudes outward from the nucleosome (Luger *et al*., 1997, Figure 1).

A major contributor to the regulation of cellular function governed by chromatin structure is the posttranslational modification of histone tails (Bhaumik *et al*., 2007). These post-translational modifications include acetylation, phosphorylation, methylation, monoubiquitination, sumoylation, and ADP ribosylation (Campos and Reinberg, 2009). For almost every modification identified, there are also machineries involved in their removal (Bhaumik *et al*., 2007). The result of histone post-translational modifications is

to affect protein-DNA, protein-protein, and nucleosome-nucleosome interactions, as well as providing docking sites for chromatin effector proteins (Campos and Reinberg, 2009). Therefore the type and degree of histone modification at any particular genomic site can affect cellular function.

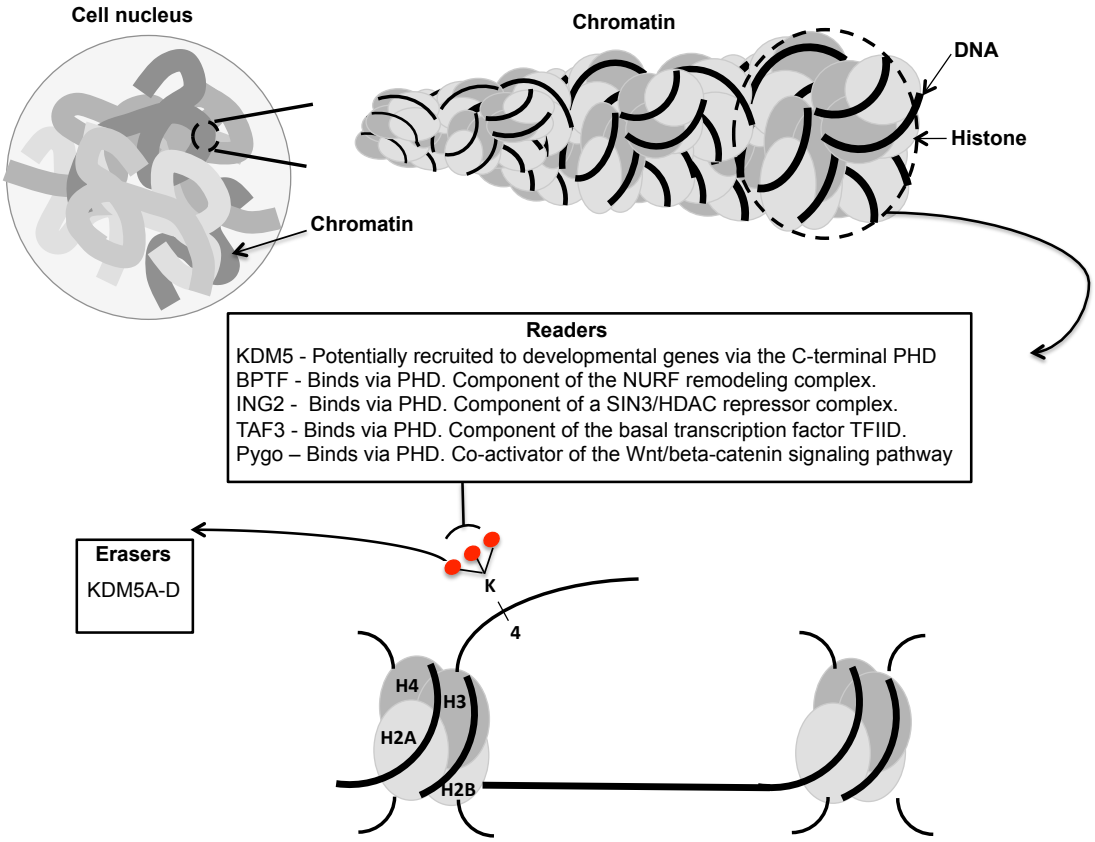


Figure 1. Chromatin, the nucleosome and the histone tail cooperate to control gene regulation. The KDM5 family of demethylase enzymes can erase H3K4me3/2. H3K4 trimethylation can function as a docking site for PHD finger containing proteins (see below).

All histones can be methylated on any of their basic amino acid groups. Specific histone lysine methylation marks are commonly associated with either transcriptional activation or repression (Pokholok *et al*., 2005). In general, methylation of Histone 3 Lysine 9 (H3K9), H3K27 or H3K20 is linked to repression while methylation on H3K4, H3K36 and H3K79 is linked to activation. An additional level of specificity that may serve to influence the recruitment of effecter proteins to chromatin, and therefore functional interpretation of these methyl marks, is whether a particular lysine residue is mono (me1), di (me2) or tri (me3) methylated. Of the lysine residues methylated on the amino acid 'tail' of histone 3, methylation of H3K4, and H3K27 are of particular interest.

Although H3K4me3 is a modification generally associated with transcription (Pokholok *et al*., 2005, Vermeulen *et al*., 2007), and H3K27me3 is widely associated with repression of transcription, H3K4me3 and the H3K27me3 marks have been simultaneously localized to the promoter region of developmental genes (Bernstein *et al*., 2006, Mikkelsen *et al*., 2007) and are uniquely associated with cell fate plasticity and with the regulation of developmental genes (Bernstein *et al*., 2006, Heintzman *et al*., 2009).

Whilst H3K4me3/2 is found at the promoters of actively transcribed genes (Barski *et al*., 2007), H3K4me1 is localized to the enhancer regions of tissue-specific genes (Heintzman *et al*., 2009) suggesting a role during differentiation. Although methylated H3K4 marks areas of the genome that are being transcribed (Pokholok *et al*., 2005) and of developmental importance (Bernstein *et al*., 2006, Heintzman *et al*., 2009), exactly how the methylated H3K4 mark is interpreted or 'read' (Ruthenburg *et al*., 2007) and to what functional end, is determined by the methyl lysine recognition domain of proteins and executed as part of the associated multi-protein complex in response to environmental signals.

1A.1.2 It takes a PHD to be a reader in H3K4 methylation

One such lysine recognition domain found in proteins is the PHD finger (Wysocka *et al*., 2006, Shi *et al*., 2006). The PHD finger is a protein domain that can interact with trimethylated H3K4 to influence transcription positively by promoting the formation of the pre-initiation complex (Vermeulen *et al*., 2007) and by altering chromatin structure (Barak *et al*., 2003, Wysocka *et al*., 2006). Specifically, the PHD finger of TAF(II)140 (a.k.a TAF3) facilitates in the recruitment of the multi-protein complex, TFIID during promoter activation (Vermeulen *et al*., 2007). Moreover, the PHD finger of BPTF is required for the recruitment of the chromatin-remodelling complex NuRF to H3K4 tri-methyl marks and subsequent gene activation (Barak *et al*., 2003, Wysocka *et al*., 2006).

The importance of the PYGO-2 PHD sequence in binding to H3K4me3/2 has been shown to be of particular importance in the mouse mammary gland (Gu *et al*., 2009, 2013. See introduction: Section 1B). The prototype gene, Pygopus (Pygo) was identified in *D. melanogaster* as a specific downstream component of wingless (Wg)/Wnt signalling pathway, and in association with BCL9/Legless, transduces the Wnt signal by promoting Armadillo/beta-catenin mediated transcription (Belenkaya *et*

al., 2002, Kramps *et al*., 2002, Thompson *et al*., 2002). The association of Pygo with BCL9/Legless leads to binding to H3K4me2/3 (Fiedler *et al*., 2008, Kessler *et al*., 2009).

Of the two mammalian orthologs, Pygo2 has been shown to be involved in murine mammary gland development and cell fate determination (Gu *et al*., 2009, 2013. See introduction: Section1B). In mammals, PYGO2 can bind, through the PHD sequence, directly to H3K4me3/2 (Kessler *et al*., 2009, Gu *et al*., 2009), identifying a potential mechanism that directs the recruitment of the beta-catenin/BCL9 complex to the promoters of beta–catenin target genes.

Interestingly, even though H3K4 trimethylation functions to recruit classic factors that are required to promote transcription (Barak *et al*., 2003, Wysocka *et al*., 2006), during situations of cellular stress, H3K4 trimethylation also functions to interpret signalling pathways in response to DNA damage (Shi *et al*., 2006) and cellular senescence (Abad *et al*., 2011,). Specifically, ING2 binding to H3K4 trimethylation via the PHD finger is increased in response to Doxorubicin (Shi *et al*., 2006). Similarly, the ING1 protein is required for oncogene-induced senescence through an interaction of the PHD finger with H3K4 trimethylation (Abad *et al*., 2011).

Peptide-binding studies have shown that KDM5A and KDM5B family can also be recruited to H3K4 trimethylation marks via the C-terminal PHD finger, a feature that is evolutionarily conserved (Wang *et al*., 2009a, Li *et al*., 2010, Figure 1). This is of significant interest given that the C-terminal PHD finger of the single KDM5 orthologue in *Drosophila melanogaster* (*lid*) is essential for viability (Li *et al*., 2010). Furthermore, ChIp-Seq data from embryonic stem cells (ES) has shown that KDM5B is recruited to developmental genes enriched in H3K4 and H3K27 trimethylation ((bivalent domain (Bernstein *et al*., 2006)) which maybe crucial in regulating the temporal expression pattern of developmental genes (Schmitz *et al*., 2011, Albert *et al*., 2013).

1A.2 Histone marks and murine mammary development.

The importance of epigenetics in controlling gene expression during the differentiation of the developing mammary gland is now being investigated, and the methylation status of histone lysine marks is found to play an important role in proliferation, differentiation, and cell fate determination. Binding of signal transducer and activator of transcription 5 (STAT5) to mammary gland specific regulatory sequences can precede the establishment of H3K4me3 marks, suggesting that STAT5 binding is required and responsible for gene expression (Kang *et al*., 2014). Moreover, acquisition of the

H3K4me2 mark together with development of a more open chromatin organisation are also reported to be associated with activation of milk protein genes (Rijnkels *et al*., 2013). A comprehensive analysis of the global maps of H3K4me3 and H3K27me3 marks during the development and differentiation of the murine mammary gland demonstrates that a clear correlation exists between histone modification maps with that of gene expression signatures in the different epithelial cell subpopulations (Pal *et al.,* 2013), thus demonstrating that the epigenome plays a central role in directing cell fate determination.

In considering the enzymes that are responsible for defining the methylation status of histone lysine residues, studies in the murine mammary gland have focused on the methyltransferase protein, enhancer of zeste homologue 2 (EZH2, a.k.a KMT6) and a demethylase that removes methyl groups from H3K9 (JMJD2B/KDM4B). The H3K27 specific histone methyltransferase, EZH2, is a component of the polycomb repressor complex 2 (PRC2), and is responsible for the di and trimethylation of lysine 27 on histone 3 (Cao *et al*., 2002). As genetic ablation of *Ezh2* results in embryonic lethality (O'Carroll *et* al., 2001), studies utilizing an inducible system to knock down *Ezh2* expression (Michalak *et al*., 2013) or through conditional deletion of *Ezh2* (Pal *et al*., 2013) have shown that EZH2 plays an important role in cell fate determination during mammary gland development and differentiation (see introduction: 1B1). Furthermore, MMTV (mouse mammary tumour virus) promoter-driven targeted deletion of the H3K9 specific lysine demethylase KDM4B, from mammary gland epithelia results in a reduction in the number of terminal end bud and ductal side branch structures presented in the nulliparous mammary gland (Kawazu et al 2011). Interpretation of external signals in response to the hormonal environment during mammary gland development is regulated at the level of the gene by the epigenetic landscape. It is therefore not surprising that several demethylase enzymes have also been implicated as co-factors in signalling by the androgen and oestrogen receptors (Kawazu *et al.,* 2011, Svotelis *et al*., 2011, Coffey *et al*., 2013, Chan and Hong, 2001).

1A.3 The KDM5 family and gene regulation

The KDM5 (lysine demethylase 5) family of demethylase proteins counteract the tri-methylation of histone 3 lysine 4 (H3K4) and can function as transcriptional repressors (Christensen *et al*., 2007, Yamane *et al*., 2007, Lopez-Bigas *et al*., 2008, Van Oevelen *et al*., 2008, Beshiri *et al*., 2012, Chicas *et al*., 2012). This family of so-called 'erasers' (Ruthenburg *et al*., 2007) of H3K4 methylation can also 'read' methylated lysine residues (Wang *et al*., 2009a, Li *et al*., 2010). They can form a number of different

multi-protein complexes that contain other chromatin-modifying factors (Barrett *et al*., 2007, Hayakawa *et al*., 2007, Pasini *et al*., 2008, Banck *et al*., 2009, Moshkin *et al*., 2009, Schmitz *et al*., 2011) and co-factors that aid in the recruitment of the protein complex to DNA (Pasini *et al*., 2008, Schmitz *et al*., 2011), whilst also possessing the intrinsic ability to bind to DNA directly (Scibetta *et al*., 2007, Yao *et al*., 2010). The KDM5 family are highly homologous and where co-expressed may act redundantly. A picture is emerging where the KDM5 family may dictate the shift in balance between cellular proliferation (Lopez-Bigas *et al*., 2008, Van Oevelen *et al*., 2008, Beshiri *et al*., 2012) and differentiation (Flowers *et al*., 2010, Flowers *et al*., 2013) and are therefore important during development (Gildea *et al*., 2000, Iwase *et al*., 2007, Klose *et al*., 2007, Albert *et al*., 2013). Although the KDM5 demethylase activity has attracted the greatest attention, it is apparent that the KDM5 family is an important multi-faceted group of proteins with additional functions.

1A.3.1 The conserved domains of the KDM5 family of proteins

As shown in figure 1.1, the mammalian KDM5 family consists of four proteins, namely KDM5A (a.k.a RBP2, JARID1A), KDM5B (a.k.a PLU-1, JARID1B), and 2 homologous proteins encoded by the sex-chromosome-specific genes, KDM5C (a.k.a SMCX, JARID1C) located on the X-chromosome but not inactivated (Agulnik *et al*., 1994a, Wu *et al*., 1994) and KDM5D (a.k.a SMCY, JARID1D) located on the Y-chromosome (Agulnik *et al*., 1994b). The KDM5 family expressed in *D. melanogaster* (*lid*) and *Caenorhabditis elegans* (*rbr-2*) are expressed as single ortholgues with the *D. melanogaster* lid sharing the greatest homology with that of the mammalian KDM5 family.

All the KDM5 family described possess an N-terminal Jumonji N (JMJN), ARID, PHD, catalytic Jumonji C (JMJC) and C5HC2-zinc finger motifs. The greatest divergence in sequence is seen at the C-terminal region of the KDM5 family. Whilst mammalian KDM5A and KDM5B, *D. melanogaster* lid and *C. elegans* rbr-2 possess two PHD fingers, KDM5C and KDM5D possess only one PHD finger in this region.

KDM5A (a.k.a RBP2 Retinoblastoma binding protein 2) was initially identified in a yeast-2-hybrid screen for retinoblastoma binding proteins (pRb) (Defeo-Jones *et al*., 1991). Further studies demonstrated that KDM5A interacts with pRb via a non-T/E1A binding region and p107 via the LXCXE motif (Kim *et al*., 1994), a motif that is unique amongst the KDM5 family of proteins to KDM5A. (Vogt *et al*., 1999).

KDM5B was first reported in the same year by independent labs using different signalling pathways to identify novel transcripts (Lu *et al*., 1999, Vogt *et al*., 1999). *PLU-1* as it was entitled (Lu *et al*., 1999) was identified as a transcript that was positively regulated via the c-ErbB2 signalling pathway in a human mammary epithelial cell line (Lu *et al*., 1999). A splice variant form of KDM5B, named *RBP2-H1* (named due to the homology with the founding family member, RBP2) was identified as a transcript whose expression was down regulated in melanoyctes upon UVB induced DNA damage (Vogt *et al*. 1999). The difference in the two KDM5B splice variants is that the variant RBP2-H1 contains an additional 36 amino acids inserted after amino acid residue 237. Of the two KDM5B splice variants, *PLU-1* expression is the most abundant in a panel of breast cancer and melanoma cell lines examined (Barrett *et al*., 2002). Currently a function for the additional sequence is unknown, and subsequent reports do not always distinguish between the two isoforms.

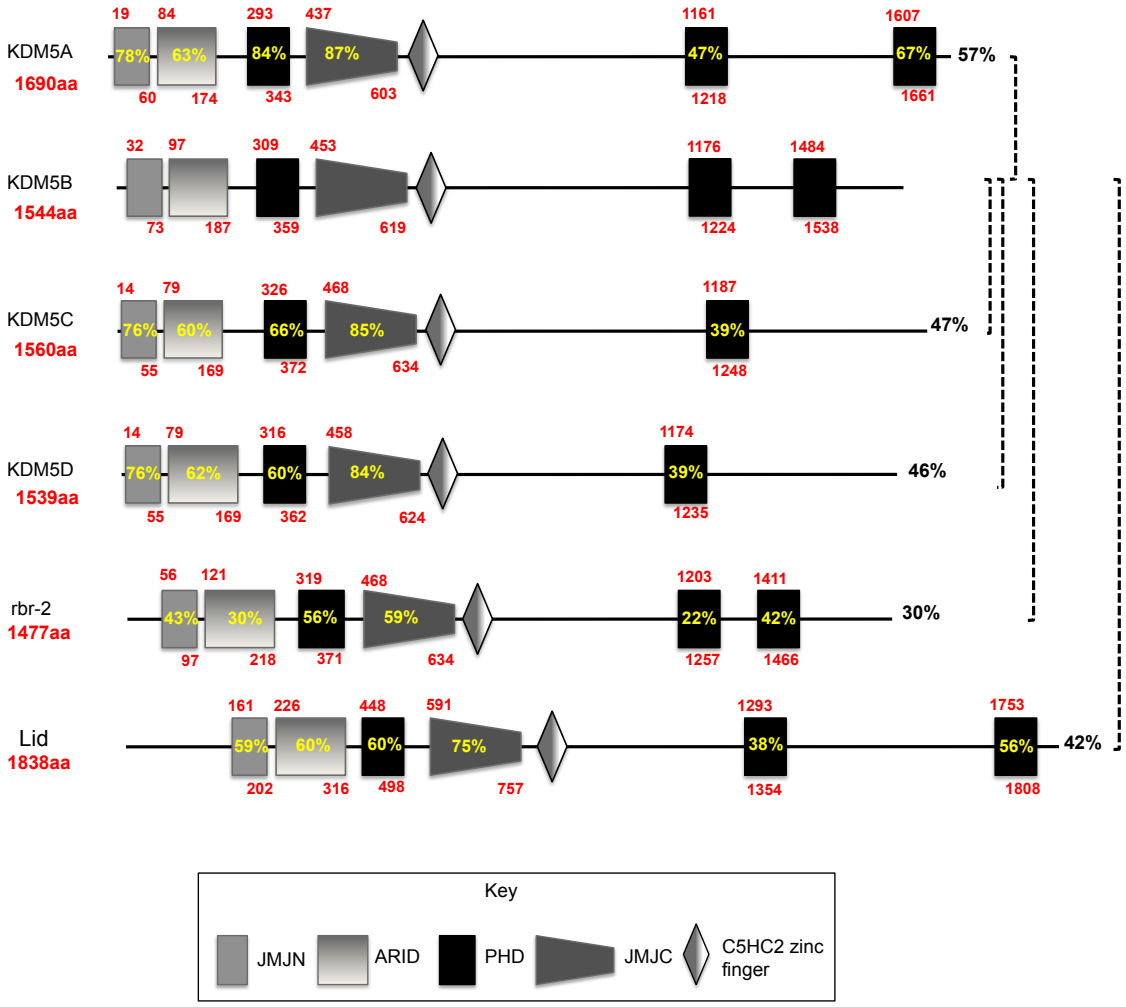


Figure 1.1. Schematic representation of the protein domain position for the KDM5 family of H3K4 demethylase enzymes. KDM5B shares the greatest homology with KDM5A – 57% (See black type with dashed line to the right hand side of the figure. Overall homology for the four KDM5 family members is compared to KDM5B. Red type gives size of proteins in amino acid (aa) and details position of domains in relation to the initiating methionine. Yellow type details homology of domains in relation to KDM5B.

1A.3.2 The KDM5 family as H3K4 demethylase enzymes

The demonstration that methylation is also a reversible histone modification (Shi *et al*., 2004) led to a renewed interest in the KDM5 family of proteins (Trewick *et al*., 2005) Incubation of recombinant KDM5 proteins with synthetic histone peptides or bulk histones followed by analysis by Western blot and by mass spectrometry revealed that the KDM5 family of proteins are demethylase enzymes specific for H3K4.

KDM5A, KDM5C and KDM5D can demethylate H3K4me3 and H3K4me2 but not H3K4me1 *in vitro* (Christensen *et al*., 2007, Eissenberg *et al*., 2007, Iwase *et al*., 2007, Klose *et al*., 2007, Lee *et al*., 2007, Tahiliani *et al*., 2007). However, KDM5B not only demethylates H3K4me3 and H3K4me2 (Christensen *et al*., 2007, Iwase *et al*., 2007, Lee *et al*., 2007) but can also demethylate H3K4me1 to the unmethylated form both *in vitro* (Iwase *et al*., 2007), and *in vivo* (Xiang *et al*., 2007). These data demonstrate that amongst the KDM5 family of proteins, KDM5B may possess unique enzyme specificity.

Immunostaining demonstrated that over-expression of KDM5A, KDM5B or KDM5C *in vivo* resulted in a loss of H3K4me3 or H3K4me2 which was dependent upon a catalytically active JMJC domain (Christensen *et al*., 2007, Iwase *et al*., 2007, Klose *et al*., 2007, Seward *et al*., 2007, Tahiliani *et al*., 2007). For KDM5B, in addition to the catalytic JMJC domain the JMJN, ARID and ZF sequences are also required for demethylase activity *in vivo* (Xiang *et al*., 2007, Yamane *et al*., 2007). Interestingly, structural studies have shown that the JMJN domain of another demethylase, KDM4A (a.k.a JMJD2) (Chen *et al*., 2006) is also required for demethylase activity by contributing to the structural integrity of JMJC catalytic core. (Klose *et al* 2006). Of interest is the observation that point mutations within the KDM5B ARID sequence that ablate binding also negate the demethylase activity of KDM5B when transfected in cell lines (Tu *et al*., 2008). This suggests that recruitment to DNA via the ARID sequence (Scibetta *et al*., 2007) could be required for H3K4me3 demethylase activity.

1A.3.3 The KDM5 family of transcriptional repressors

Consistent with the reported catalytic activity of the KDM5 family (Christensen *et al*., 2007, Eissenberg *et al*., 2007, Iwase *et al*., 2007, Klose *et al*., 2007, Lee *et al*., 2007, Tahiliani *et al*., 2007, Yamane *et al*., 2007) and the localisation of H3K4 trimethylation around transcription start sites (Pokholok *et al*., 2005) the KDM5 family of proteins have been characterised as transcriptional repressors (Christensen *et al*., 2007, Scibetta *et al*., 2007, Yamane *et al*., 2007, Lopez-Bigas *et al*., 2008, Van Oevelen *et al*.,

2008, Beshiri *et al*., 2012, Chicas *et al*., 2012) (Figure 1.2). Functional data also suggest that the demethylase activity of the KDM5 family of proteins is required for the repression of genes involved in development (Schmitz *et al*., 2011, Albert *et al*., 2013), cell cycle (Van Oevelen *et al*., 2008, Beshiri *et al*., 2012), differentiation (Flowers *et al*., 2010, Flowers *et al*., 2013), and senescence (Nijwening *et al*., 2011, Chicas *et al*., 2012).

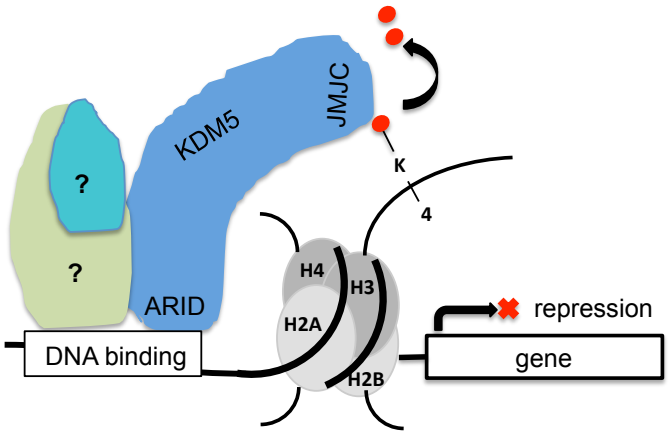


Figure 1.2. Model for KDM5 mediated repression. The KDM5 family may be recruited to the genome via the ARID sequence and/or other co-factors. KDM5 demethylase activity is dependent on the catalytic JMJC domain and the ARID sequence.

Hox (Homeobox) gene expression determines correct patterning during development (Akasaka *et al*., 1996, Del Mar Lorente *et al*., 2000). Both KDM5A and KDM5B have been found bound to the promoter region of *Hox* genes (Pasini *et al*., 2008). While ChIp-seq data on ES cells has localised KDM5B to the promoter region of *Hoxa10, Hoxb4* and *Hoxb8*, in the breast cancer cell line MCF7, KDM5B can bind the promoter of *Hoxa5* and repress transcription in a demethylase-dependent manner (Yamane *et al*., 2007). Likewise, ChIp-PCR has show that KDM5A is bound to the promoter region of *Hoxa1, Hoxa5, Hoxa7* (Christensen *et al*., 2007), *Hoxa4, Hoxa10, Hoxd9, Hoxd11* (Pasini *et al*., 2008) in embryonic stem (ES) cells and is lost upon all-trans retinoic acid induced differentiation from the promoters of *Hoxa1, Hoxa5, Hoxa7*, concomitantly with an increase in H3K4 trimethylation (Christensen *et al*., 2007).

A function for KDM5A in the control of the cell cycle is also suggest by the demonstration that KDM5A can silence the expression of cell cycle dependent genes such as *PCNA* during TPA-induced differentiation of the monocytic U937 cell line (Beshiri *et al* 2012).

KDM5A and KDM5B both play a role during RAS-induced cellular senescence (Chicas *et al*., 2012). Furthermore, using KDM5A as the representative KDM5 family member has shown that during senescence KDM5A can function to repress genes such as *CCNA1* (a.k.a *Cyclin A1*) (Nijwening *et al*., 2012) that is required for cell cycle progression (Resnitzky *et al*., 1995).

1A.3.4 A function for the KDM5 family of proteins in the activation of transcription

The function of the KDM5 family appears context-dependent, determined by protein-protein interactions (Secombe *et al*., 2007, Xiang *et al*., 2007) and genome-recruitment mechanisms (Li *et al*., 2010). With this in mind, data suggests that the KDM5 family may also function as activators of transcription (Xiang *et al*., 2007, Secombe *et al*., 2007).

I*n vitro* binding studies have also shown that *D. melanogaster* proteins lid and dMYC can interact via the JMJC domain, the active domain required for demethylase activity (Secombe *et al*., 2007). This functional interaction is likely to be conserved given that KDM5B and C-MYC can interact *in vivo* via the JMJC domain (SC, JTP unpublished observation). Given that transgenic *D. melanogaster* imaginal wing discs that over-expressed lid and dMYC maintain H3K4 trimethylation levels, suggests that the interaction of lid and dMYC may negate the demethylase activity of lid (Secombe *et al*., 2007). Interestingly, the functional relevance of this interaction is that lid is required for dMYC dependent activation of the MYC target gene *Nop60B* (Secombe *et al*., 2007), a function that could be mediated via the C-terminal PHD domain (Li *et al*., 2010) (Figure1.3).

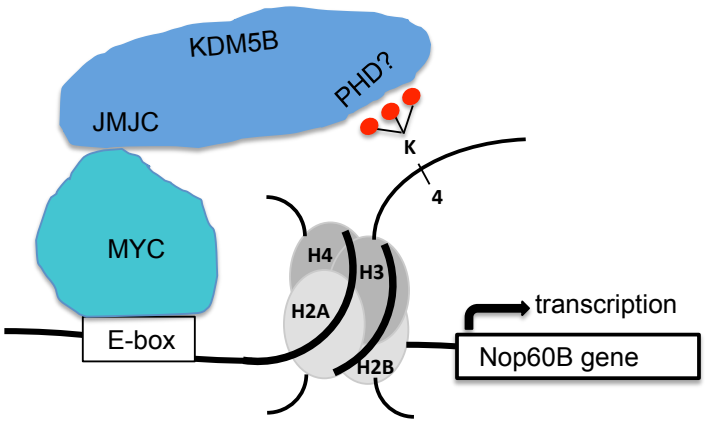


Figure 1.3. Model for C-MYC/KDM5 target gene activation. An interaction of C-MYC with the JMJC domain of KDM5 may negate demethylase activity. The C-terminal PHD finger of the KDM5 family may stabilize a C-MYC complex at E-box target genes.

Although studies implicate KDM5A and KDM5B in functioning as nuclear receptor co-activators (Chan and Hong 2001, Xiang *et al*., 2007), more recent studies demonstrate that KDM5A and KDM5B can function to repress hormone inducible genes prior to activation (Stratmann *et al*., 2011, Vincent *et al*., 2011, Vincent *et al*., 2013).

Initial studies using transiently transfected expression constructs demonstrated that KDM5A can interact with a number of nuclear receptors and using oestrogen receptor alpha (ER alpha) as a co-activator model, that ER alpha and KDM5A can potentiate transcription in a hormone-dependent manner from an *ERE-Luc* reporter construct (Chan and Hong 2001). Similarly, KDM5B can interact with the androgen receptor (AR) and potentiate transcription in a ligand dependent manner from a *PSA-Luc* reporter construction (Xiang *et al*., 2007). However, given that the regulation of chromatin architecture is of central importance to the control of gene expression, the use of transiently transfected DNA templates may not adequately represent the endogenous chromatin structure (Smith *et al*., 1997, Hebbar *et al*., 2008).

With this in mind, studies are beginning to suggest that KDM5B may play a central role in the repression of the progesterone receptor (PR) signalling pathway. Of the four KDM5 family members, *KDM5B* is the most abundant family member expressed in MCF7 cells (Krishnakumar *et al*., 2010. SC, JTP unpublished observation). RNAi-mediated silencing of *KDM5B* suggested a partial role for KDM5B in *PGR* repression but only when MCF7 cells were cultured under hormone-deprived culture conditions (Stratmann *et al*., 2011). In addition to the repression of the *PGR* transcript itself, KDM5B can form a repressive complex with unliganded PR and repress some 20% of hormone regulated genes that are de-repressed upon progestin treatment (Vincent *et al* 2011, 2013).

1A.3.5 Direct Recruitment of the KDM5 family to the genome

A number of observations suggest that two domains, the ARID and the C-terminal PHD finger may work in conjunction to recruit the KDM5 family to the genome of developmental genes (Scibetta *et al*., 2007, Wang *et al*., 2009a, Li *et al*., 2010, Yao *et al*., 2010, Schmitz *et al*., 2011).

In the first instance, genome-wide binding studies in ES cells have shown that the binding of KDM5B correlates with promoter regions that are both GC-rich and enriched for the bivalent histone marks H3K4me3 and H3K27me3 (Schmitz *et al*., 2011). Additionally, using electrophoretic mobility shift assays (EMSA) have demonstrated

that the ARID domain of KDM5B can interact with the derived GC-rich sequence, GCACA. (Scibetta *et al*., 2007, Yao *et al*., 2010) and that mutation of the ARID sequence also ablates the demethylase activity of KDM5B (Yao *et al*., 2010). Finally, the KDM5 family can bind H3K4me3 marks via the C-terminal PHD sequence (Wang *et al*., 2009a, Li *et al*., 2010).

The only study to compare directly KDM5A and KDM5B expression levels suggests that in the main KDM5A and KDM5B display mutually exclusive expression patterns (Islam *et al*., 2011a). However, in the hematopoietic system and ES cells where both KDM5A and KDM5B proteins are expressed, a degree of specificity may be seen at the level of DNA binding via the ARID sequence. Whereas the DNA binding sequence for KDM5B is GCACA (Scibetta *et al*., 2007, Yao *et al*., 2010) the ARID sequence of KDM5A can bind to a CCGCCC sequence motif found in the KDM5A target gene promoter of *BRD2* (Tu *et al*., 2008).

1A.3.6 Recruitment of the KDM5 family to the genome as part of a multi-protein complex

KDM5A and KDM5B are found in protein complexes that also function to modify the chromatin environment or aid in the recruitment to DNA (Barrett *et al*., 2007, Pasini *et al*., 2008, Banck *et al*., 2009, Schmitz *et al*., 2011). For example, KDM5B can interact with the histone deacetylase protein, HDAC1 (Barrett *et al*., 2007), and is also found in a complex with the H3K9 methyltransferase, EHMT2 (a.k.a G9a) (Banck *et al*., 2009). Both KDM5A and KDM5B have been associated with the polycomb group (PcG) protein complex that, as described below, aid in their recruitment to the genome (Pasini *et al*., 2008, Schmitz *et al*., 2011).

The correlation of KDM5B binding with H3K4me3 and H3K27me3 bivalents marks suggests a possible functional relationship between KDM5B and the polycomb group of proteins. In fact, KDM5A and KDM5B can bind to a significant number of PcG target genes in mouse ES cells (Boyer *et al*., 2006, Pasini *et al*., 2008, Schmitz *et al*., 2011), and KDM5A expression has been shown to be necessary for repression (Pasini *et al*., 2008). The potential for KDM5A and KDM5B to regulate PcG target genes in ES cells (Pasini *et al*., 2008, Schmitz *et al*., 2011) does suggest the potential for functional redundancy (Islam *et al*., 2011b). However, the data also suggest that assembly of a KDM5/PcG protein complex and the mechanisms required for recruitment of a KDM5/PcG to the genome may differ between KDM5A and KDM5B-containing complexes (Pasini *et al*., 2008, Schmitz *et al*., 2011). For example, whereas *Kdm5a*

knock down has no affect on SUZ12 DNA binding (Pasini *et al*., 2008), knockdown of *Kdm5b* results in a reduction in the binding of SUZ12 to some PcG-regulated genes (Schmitz *et al*., 2011). This suggests that KDM5B may have more of an influential role in the recruitment to DNA of a PcG complex. Conversely, PcG proteins are required for the recruitment of KDM5A and KDM5B to the genome (Pasini *et al*., 2008, Schmitz *et al*., 2011). KDM5B recruitment is reduced in *Eed* and *Rnf2* (a.k.a *Ring1b*) knockout ES cell lines (Schmitz *et al*., 2011) whereas the recruitment of KDM5A is reduced in *Suz12* knock out ES cell lines (Pasini *et al*., 2008). Although the studies for KDM5A are limited, the recruitment of KDM5A to PcG target genes maybe dependent upon PcG complex-components. Furthermore, these findings demonstrate that although KDM5B and PcG proteins can affect the binding of each other to a subset of target genes, neither KDM5B nor PcG proteins, at least individually, are essential for each other's recruitment to the genome. Furthermore, KDM5A can interact with PcG proteins EZH2 and SUZ12 *in vivo* (Pasini *et al*., 2008), whereas no endogenous interaction with KDM5B and SUZ12 was observed (Schmitz *et al*., 2011). It is therefore plausible that KDM5B may only interact with PcG proteins at PcG-target genes (Figure1.4).

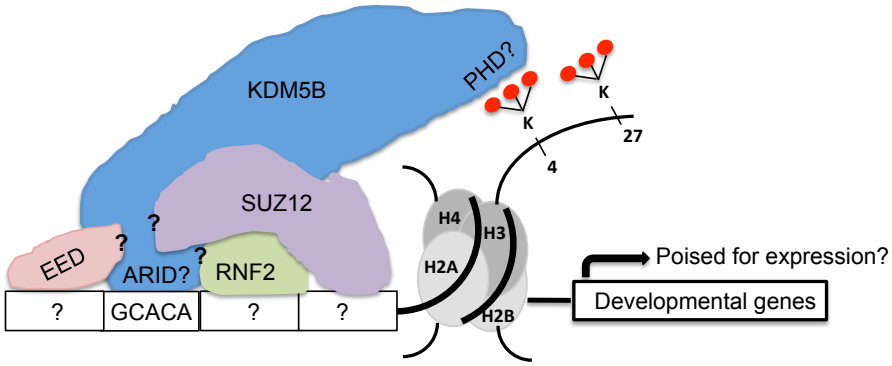


Figure 1.4. Model for PcG/KDM5B binding to the bivalent promoters of developmental genes. The ARID and C-terminal PHD sequence of KDM5B maybe required for complex recruitment to DNA. To date the KDM5B and PcG interacting proteins have not been described.

1A.3.7 Lessons from the past: Studies in C. Elegans and D. Melangaster

Studies on the single ortholgues *lid* and *rbr-2* have confirmed that the function of the KDM5 family as demethylase enzymes is evolutionarily conserved (Christensen *et al*., 2007, Eissenberg *et al*., 2007, Secombe *et al*., 2007). Furthermore, biochemical and functional studies have shown that a role during NOTCH signalling may also be

conserved (Hayakawa *et al*., 2007, Moshkin *et al*., 2009, Liefke *et al*., 2010 Xie *et al*., 2011). KDM5A (Hayakawa *et al*., 2007), KDM5B (Xie *et al*., 2011) and lid (Moshkin *et al*., 2009) have been identified either as a complex (Hayakawa *et al*., 2007, Moshkin *et al*., 2009) or associated by immunoprecipitation (Xie *et al*., 2011) with the core proteins components of a SIN3-complex, SIN3A and HDAC2. In addition to the knock down of either *lid* or *sin3a* resulting in the de-repression of NOTCH target genes (Moshkin *et al*., 2009), an interaction between Su(H) and lid as well as the mammalian homologues RBP-J and KDM5A has been described (Liefke *et al*., 2010). Furthermore KDM5A and RBP-J have been localised to the RBP-J binding site of the NOTCH target gene *DTX1* (a.k.a *Deltex-1*), and are required for repression (Liefke *et al*., 2010) (Figure1.5).

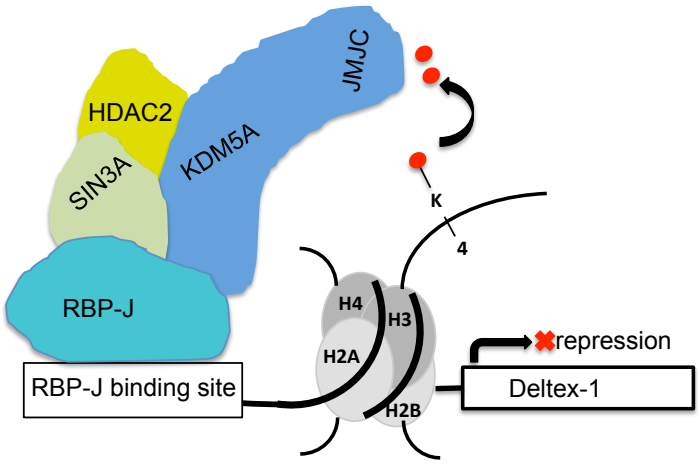


Figure 1.5. Model for KDM5/NOTCH signalling. The KDM5 family are a component of the SIN3/HDAC2 repressor complex. KDM5A can interact with RBP-J and repress the transcription of the NOTCH target gene *DTX1*

Although a great deal of interest in the H3K4 demethylase activity of the KDM5 group has thrust this family into the limelight, the demethylase-independent activity is undoubtedly important (Christensen *et al*., 2007, Catchpole *et al*., 2011, Li *et al*., 2010). Whereas disruption of *lid* expression results in early pupae lethality, presumably due to a defect in optical brain lobe and imaginal disc development (Gildea *et al*., 2000), viability is not dependent upon the demethylase activity of lid (Li *et al*., 2010). Similarly, both a KDM5B murine line (Catchpole *et al*., 2011 and this thesis) and a *C.elegans* rbr-2 (Christensen *et al*., 2007) strain ((*rbr-2(tm1231)*) that express KDM5 proteins that are presumed to lack demethylase activity are both viable. However the *rbr-2 (tm1231)* strain present with a defect in vulvalmorphogenesis, suggestive of a function for rbr-2 in vulva-precursor cell fate specification.

1A.4 The expression patterns of the KDM5 family of proteins

It is apparent from the studies detailed above that some functional aspects of the KDM5 family of proteins are evolutionarily conserved (Hayakawa *et al*., 2007, Moshkin *et al*., 2009, Liefke *et al*., 2010, Xie *et al*., 2011). KDM5B can also be recruited directly or indirectly to KDM5A binding sites post *KDM5A*-targetted RNAi-mediated silencing, suggesting functional compensation (Islam *et al*., 2011b). Knowledge of the expression profile of the KDM5 family during development and in adult tissue would therefore help our understanding of the function of this group of proteins during development, organogenesis and cancer.

1A.4.1 The expression profile of KDM5A and KDM5B in human adult tissue

Studies on the expression and *in vivo* function of the KDM5 family during development as well as in the adult have been limited with the exception of KDM5B (Lu *et al*., 1999, Barrett *et al*., 2002, Madsen *et al*., 2002, McGraw *et al*., 2007, Frankenberg *et al*., 2007, Islam *et al*., 2011a, Albert *et al*., 2013). However, as described below there are data that suggest the potential for functional compensation (Islam *et al*., 2011b) as well as unique functions during developmental (Klose *et al*., 2007, Albert *et al*., 2013).

Only one publication has addressed the pattern of *KDM5A* expression in normal adult human tissue. Strikingly, expression array analysis revealed that *KDM5A* expression is restricted to those cells derived from the bone marrow and peripheral blood as well as the pineal gland (Islam *et al*., 2011a).

The expression of KDM5B in human tissue is also restricted. Northern blot analysis of RNA from a panel of 24 normal adult tissues demonstrated that high levels of KDM5B expression are restricted to the testis (Lu *et al*., 1999). However, Islam and colleagues (2011a) using microarray analysis on an expanded array of whole human tissue, detected robust levels of the *KDM5B* transcript in the kidney and the hematopoietic system.

1A.4.2 The expression profile of KDM5B in murine adult tissue

The murine KDM5B protein shares 94% homology with that of human KDM5B protein with almost 100% identity within the conserved domains, suggesting functional conservation (Figure1.6).

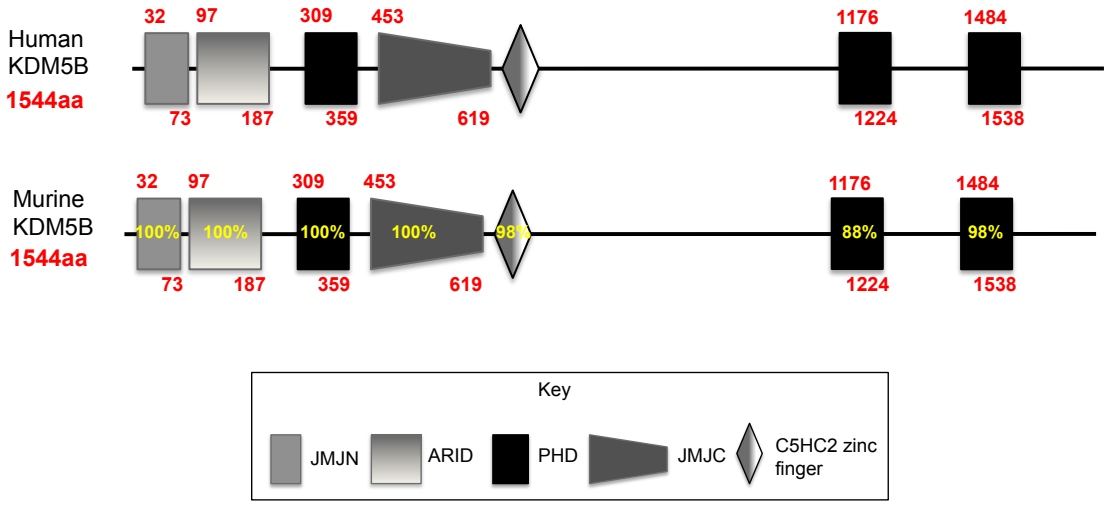


Figure 1.6. Homology between the human KDM5B and the murine KDM5B proteins. Red type gives size of proteins in amino acid (aa) and details position of domains in relation to the initiating methionine. Yellow type details homology of domains in relation to human KDM5B.

As seen with human tissue, the murine *Kdm5b* transcript is also detected at high levels in the testis (Madsen *et al*., 2002). However in addition, the murine KDM5B protein is also detected at moderate levels (compared to the testis), in the colon, prostate, thymus, spleen, and low but detectable levels of KDM5B expression are detected in the mesenteric lymph node, brain, lung, heart and skin (Schmitz *et al*., 2011).

KDM5B is also expressed in the mammary gland (Madsen *et al*., 2002, Barrett *et al*., 2007) as well as the testis (Madsen *et al* 2002, Madsen *et al* 2003), organs that under go cyclic regeneration and are responsive to hormonal stimuli. *Kdm5b* is expressed in the luminal epithelial cells of the nulliparous mammary gland with expression levels increasing through pregnancy associated mammary gland development (Madsen *et al*., 2002, Barrett *et al*., 2007 and this thesis). In the testis, the expression of the *Kdm5b* transcript is restricted to the mitotic spermatogonia and the pachytene/diplotene stage of prophase I during meiosis. This data suggests a potential proliferative function for *Kdm5b* during mitosis and synapsis/homologous recombination during prophase I of meiosis (Madsen *et al*., 2002, Madsen *et al*., 2003).

1A.4.3 KDM5B expression during murine embryonic development

In contrast to KDM5A (McGraw *et al*., 2007), a number of studies have examined the expression profile of *Kdm5b* during embryonic development (Madsen *et al*., 2002, McGraw *et al*., 2007, Frankenberg *et al*., 2007, Schmitz *et al*., 2011). As described

below, the expression pattern of KDM5B highlights the potential functional importance of KDM5B during organogenesis.

Use of an *in vitro* bovine embryo development system to examine the expression profile of a number of histone modification factors demonstrated that KDM5A and KDM5B display two different patterns of expression throughout pre-implantation of the developing embryo. Whereas only trace levels of the *Kdm5b* transcript are detected prior to the maternal to embryonic transition (one to two cell stage in the mouse; e0.5-e1.5), the *Kdm5a* transcript is expressed at more robust levels that are maintained thereafter through to development of the blastocyst (McGraw *et al*., 2007). The expression of the *Kdm5b* transcript is markedly up-regulated at the maternal to embryonic transition (MET) suggestive of a function for KDM5B in the activation of the embryonic genome (McGraw *et al*., 2007).

The pluripotent inner cell mass (ICM) of the implanting blastocysts (mouse: e4-e4.25) gives rise to all future cell lineages. The epiblast is derived from the pluripotent ICM, and is the site for the future lineage restricted endoderm (the epithelium), mesoderm (e.g. the vasculature and lymphatic system including the blood and the urogenital organs) and ectoderm (e.g. the epidermis of the skin and its derivatives including the mammary gland). The expression of *Kdm5b* is restricted to the epiblast at e5.5 suggesting a function for KDM5B during cell fate determination. Furthermore, by gastrulation (e6.5) the expression of *Kdm5b* is ubiquitous and weaker than the levels detected in the epiblast at e5.5 (Frankenberg *et al*., 2007). Significantly, gastrulation is defined by the formation of the primitive streak and subsequent germ cell layer specification further implicating the function of KDM5B during cell fate decision.

The expression of *Kdm5b* is also detected at robust levels in whole embryonic tissue extracts at e7.5 (Madsen *et al*., 2002, Frankenberg *et al*., 2007) before the levels increase dramatically at e11.5 and subsequently fall by e15.5 and e17.5 (prior to parturition) to levels similar to that detected at e11.5 (Madsen *et al*., 2002). Whole mount *in situ* hybridisation on e12.5 to e15.5 embryos localised the *Kdm5b* transcript to a number of developing organs including the whisker follicle, thymus, limbs, teeth, eye (neural retina, optic nerve, olfactory epithelium) and stomach. The *Kdm5b* transcript is also expressed in the invaginating epithelium of the mammary bud at e14.5 (Madsen *et al*., 2002). Furthermore extensive expression of the *Kdm5b* transcript was observed in the developing brain, for example in the telencephalon, the precursor cells to the formation in the adult brain of the cerebral hemispheres.

1A.4.4 A function for KDM5B during ES cell commitment

In keeping with a function for KDM5B during development, the Wynder lab, in 2008 were the first group to describe a role for KDM5B during ES cell commitment (Dey *et al*., 2008). Inducing ES cells over-expressing KDM5B to undergo neuronal differentiation demonstrated that whilst no effect on neurosphere formation was noted, delineation using POU5F1 (a.k.a OCT4) and phospho-histone H3 (PH3) as markers suggested that the ES cell/ progenitor population failed to commit at the same rate as the control population. However, the majority of neurospheres over-expressing KDM5B failed to adhere to poly-D-lysine plates and differentiate toward a neuronal cell fate, further suggesting a function for KDM5B in the maintaining the balance between pluripotency and a differentiated phenotype. The defect in ES cell/progenitor cell commitment may be due to a KDM5B-dependent increase in proliferation (Dey *et al*., 2008), which upon *Kdm5b* knock down results in an accumulation of ES cells in the G1 phase of the cell cycle and ultimately morphological differentiation (Xie *et al*., 2011).

In contrast to these authors, upon *Kdm5b* knock down Schmitz and colleagues (2011) did not describe a function for KDM5B during ES cell proliferation, within the ES cell cell-cycle profile, on ES cell morphology nor on the expression levels of the pluripotency markers, *Pou5f1* and *Nanog*. However, as described by Dey and colleagues (2008), knock down of *Kdm5b* was permissive for neurospheres formation but not terminal neuronal differentiation. Schmitz and colleagues (2011) attributed this defect upon neural differentiation on the inability of KDM5B deficient neural progenitor cells to incompletely silence stem and germ cell specific genes.

1A.4.5 Expression profile of KDM5C and KDM5D

Based on the limited number of tissues examined the transcripts of *KDM5C* and *KDM5D* (in males) are ubiquitously expressed in both human and murine adult tissue. Northern blot hybridisation with *KDM5C* and *KDM5D* specific probes detected transcripts from RNA isolated from human heart, pancreas, skeletal muscle and lung tissue (Jensen *et al*., 2005). Including those human adult tissues detailed above, murine *Kdm5c*, and *Kdm5d* are also expressed in the adult murine kidney, liver and spleen. Similarly, the *Kdm5c* and *Kdm5d* transcripts are also detected in the developing embryonic brain (Sheardown *et al*., 1996, Xu *et al*., 2002). Taking *Kdm5c* expression analysis further demonstrated that the transcript was also detected in haematopoietic stem cells (Sheardown *et al*., 1996), embryonic stem cells and neuronal progenitor cells (Outchkourov *et al*., 2013).

The *Kdm5d* gene is mapped to the azoospermia factor region (AZF) (Agulnik *et al*., 2004b), a hot spot for genes involved in spermatogenesis (Ma *et al*., 1992, Reijo *et al*., 1995). Examination of the *Kdm5d* expression pattern during post natal development of murine spermatogenesis, from germ cell renewal (mitosis) through differentiation to mature sperm cells (spermatid) demonstrated that *Kdm5d* is not expressed during mitosis but is expressed throughout meiosis being maximally expressed at the pachytene stage of prophase I with high levels of expression being maintained during the diplotene stage of meiosis as well as in the differentiating spermatid (Akimoto *et al*., 2008).

1A.4.6 A role for the KDM5 family of proteins during neurogenesis

There is significant evidence for a function for the KDM5 family during neurogenesis. Disruption of *D. melanogaster lid* expression results in a lethal defect in optical brain lobe development (Gildea *et al*., 2000). KDM5C expression is required for dentritic development of rat neuronal cells (Iwase *et al*., 2007) and mutations of the KDM5C gene have been linked with the neurological disorder X-linked mental retardation (XLMR) (Tzschach *et al*., 2006, Santos-Reboucas *et al*., 2011). KDM5A knockout mice displayed abnormal behaviour when held up-side down (Klose *et al*., 2007) suggesting mental dysfunction. At the time of writing this thesis a report was published describing a neurological function for KDM5B during murine development (Albert *et al*., 2013) and will be discussed later.

1A.5 A role for KDM5A and KDM5B during senescence and differentiation

1A.5.1 A function for KDM5B during the G1 to S phase transition of the cell cycle

A function for the KDM5 family in the control of the cell cycle is beginning to emerge. In ES cells the expression of CDKN1B (a.k.a p27) promotes cells cycle arrest in the G1-phase of the cell cycle (Menchon *et al*., 2011). KDM5B can repress the transcription of *CDKN1B* and KDM5B expression is required for the G1 to S phase transition of the cell cycle (Dey *et al*., 2008, Xie *et al*., 2011).

The role of KDM5B in the progression from the G1 to the S-phase of the cell cycle is not limited to ES cells (Yamane *et al*., 2007, Mitra *et al*., 2011, Wong *et al*., 2012). For example, co-transfection of KDM5B together with *TFAP2C* (a.k.a. AP-2γ) and *c-MYC*, into HepG2 cells lead to a significant shift from the G1 to S phase of the cell cycle

(Wong *et al*., 2012). In keeping with this, Yamane and colleagues (2007) have reported that *KDM5B* knock down in the breast cancer cell line, MCF7 cells results in reduced cell proliferation, an accumulation of cells in the G_1 phase of the cell cycle and a delay in cell cycle exit. In addition to repressing *CDKN1B* transcription, as described above (Dey *et al*., 2008), a function for KDM5B downstream of the cyclin-dependent kinase inhibitor protein family has been described. In MCF7 cells, KDM5B represses the expression of Let-7e, a negative regulator of *CCND1* (a.k.a *Cyclin D1*) thereby promoting G1 to S phase transition (Mitra *et al*., 2011).

As described below the repression of E2F-target genes by KDM5A and KDM5B is required during senescence and differentiation.

1A.5.2 KDM5A and KDM5B link H3K4 demethylation to retinoblastoma binding protein mediated cellular senescence

RAS-induced senescence of the human foetal lung cell line IMR90 is associated with a global reduction in H3K4me3/2 levels, of which many of the gene categories affected are enriched for cell cycle progression and DNA replication (Chicas *et al*., 2012). The pRb-pathway mediates cellular senescence through the ability to repress E2F target genes, the promoter regions of which become concomitantly depleted of H3K4me3 (Narita *et al*., 2003, Chicas *et al*., 2012). Both KDM5A and KDM5B contribute to the global reduction in H3K4me3/2 levels seen during RAS-induced senescence (Chicas *et al*., 2012). Over-expression of KDM5A in IMR90 cells induced cell cycle arrest and the formation of senescence associated heterochromatin foci (SAHF), which was dependent upon the demethylase activity of KDM5A and the expression of pRb (Chicas *et al*., 2012).

Whereas both KDM5A and KDM5B can contribute to RAS-induced cellular senescence, using a system in which murine neuronal cells undergo temperature induced senescence, identified KDM5B as the sole member of the KDM5 family that upon knock down was capable of by-passing senescence. Furthermore, KDM5A is not required for replication-induced senescence of mouse embryonic fibroblasts (MEF) (Lin *et al*., 2011). Genome binding studies on late passage MEF cells that bore the hallmarks of replication-induced senescence, demonstrated that KDM5B was recruited to senescence-associated E2F-target genes concomitantly with a decrease in transcriptional expression and H3K4me3 levels (Nijwening *et al*., 2011).

1A.5.3 A function for KDM5A during differentiation

Cellular differentiation requires that the cell exits its cycle and enters quiescence when cell cycle genes are repressed and the expression of tissue-specific differentiation markers are initiated. In quiescent cells E2F4, p130, SIN3B, and HDAC1 are the predominant complex bound to the E2F-regulated promoter of cell cycle genes (Catchpole *et al*., 2002, Rayman *et al*., 2002).

During the monocytic differentiation of U937 cells, concomitantly with cell cycle arrest, KDM5A functions as a transcriptional repressor of cell cycle genes (Lopez-Bigas *et al*., 2008). Using the same monocytic differentiation system, ChIp-PCR demonstrated that those genes bound by KDM5A could potentially do so as a complex with E2F4/p130, and further that KDM5A and E2F4 co-operate during transcriptional repression (Beshiri *et al*., 2012). Similarly, promoter array studies on C2C12 myoblast cells induced to undergo differentiation revealed that SIN3, E2F4, and KDM5A significantly enrich, and repress the expression of cell cycle genes (Van Oevelen *et al*., 2008). These finding taken together, link a potential E2F4, p130, SIN3, HDAC1, and KDM5A complex to the repression of cell-cycle dependent genes during the differentiation of monocytes and myocytes.

In addition to a role for KDM5A during the differentiation-associated repression of cell-cycle dependent genes, data to date suggests that KDM5A functions to repress the expression of tissue-specific lineage markers prior to the on-set of differentiation. During osteoblast proliferation p130 together with E2F4/5 occupy the promoters, and repress the inappropriate expression of two markers of differentiation namely, alkaline phosphatase (*Alpl*) and osteocalcin (*Bglap*), (Flowers *et al*., 2010). However, upon a signal to differentiation there is a shift in binding of the repressor p130, E2F4, KDM5A complex to an activating pRb, E2F1 complex that promotes polymerase II binding to the promoters of *Alpl* and *Bglap* and subsequent transcription (Flowers *et al*., 2013). It is certainly intriguing to imagine that the 'switch' from proliferation toward differentiation that is intimately linked with KDM5A, is conserved amongst the family members during organogenesis (Figure1.7).

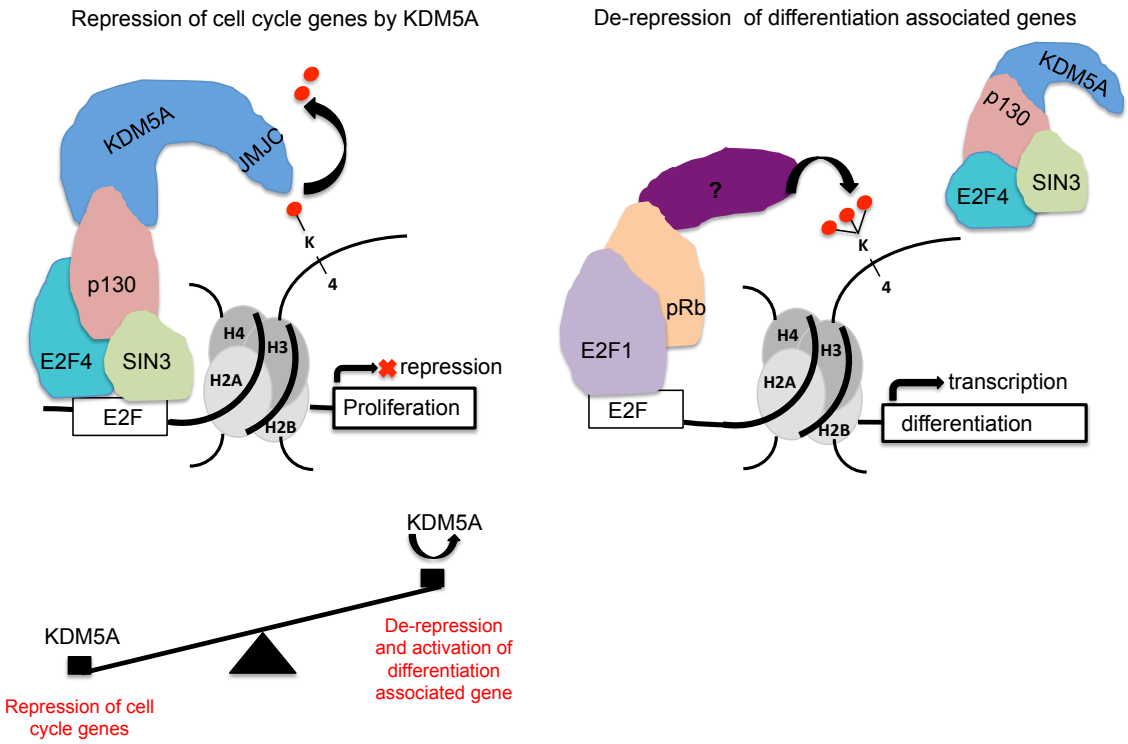


Figure 1.7. A model 'switch' in repression during differentiation. A KDM5A-repressor complex silences E2F-target gene expression during differentiation. A KDM5A repressor complex is displaced from the promoter of differentiation associated genes leading to gene activation.

1A.6 KDM5B and cancer

A function during ES cell commitment and cell cycle control suggests that aberrant expression of KDM5B may contribute to disease development. Indeed KDM5B is over expressed in a number of solid tumours (Lu *et al*., 1999, Yamane *et al*., 2007, Xiang *et al*., 2007, Hayami *et al*., 2010, Catchpole *et al*., 2011, Coleman *et al*., 2011, Islam *et al*., 2011a, Kuzbicki *et al*., 2012, Radberger *et al*., 2013).

In a comprehensive study using a cDNA array containing 337 samples from 17 primary cancers of different tissue types revealed that *KDM5B* is expressed at high levels in cancers of the breast tissue, adrenal glands and the cervix. *KDM5B* expression also correlated with lung tumour stages, increasing in stages IIB, IIIA and IV (Islam *et al*., 2011a). In addition, immunohistochemistry has confirmed that the KDM5B protein is expressed in lung cancer but also bladder cancer (Hayami *et al*., 2010) as well as melanoma (Roesch *et al*., 2005, Kuzbicki *et al*., 2012, Radberger *et al*., 2013), tissues not included in the array data published by Islam and colleagues (2011a).

1A.6.1 KDM5B expression and melanoma

Immunohistochemical studies used to examine the expression of KDM5B during the transformation of melanocytes have yielded contrary findings. Roesch and colleagues (2005) reported that whilst 70% of nevi express KDM5B, a lack of KDM5B expression was detected in 90% of primary melanoma and 70% of melanoma metastases. This lack in KDM5B expression was represented as KDM5B being expressed in single melanoma cells that represented approximately 5 to 10% of the tumour bulk (Roesch *et al*., 2005). However more recent immunohistochemistry studies, report that 90% of nevi, and all melanomas as well as melanoma metastases expressed KDM5B (Kuzbicki *et al*., 2012), as well as 55% of uveal melanomas (Radberger *et al*., 2013). This discrepancy in KDM5B protein levels expressed between nevi and advanced melanoma maybe due to antibody specificity. The antibody used by Roesch and colleagues (2005) was specific to the splice variant of KDM5B in contrast to the studies conducted by Kuzbicki and colleagues (2012) as well as by Radberger and colleagues (2013) which would detect both isoforms of KDM5B.

In order to examine the function of KDM5B during the pathogenesis of melanoma, *KDM5B*-promoter driven EGFP (enhanced green fluorescent protein) positive melanoma cells were FACS sorted and xenotransplanted into NOD/LtS*scid*IL2Rγ *null* mice. Subsequent oral administration of BrdU, suggested that those tumour cells that express KDM5B represented a slow cycling population. Interestingly, regardless of whether KDM5B positive or KDM5B negative melanoma cells were used for xenotransplantation, the resulting tumour was heterogeneous for KDM5B expression. Further studies suggested that KDM5B is not required for the initiation of tumours but for the maintenance of continuous tumour growth (Roesch *et al*., 2010).

1A.6.2 KDM5B expression and prostate cancer

The androgen receptor plays an important role in prostate cancer development and progression (Chen *et al*., 2004). Analysis of a set of data in the Oncomine cancer-profiling database revealed that *KDM5B* expression is limited in benign prostate but is up regulated in prostate cancer, with highest levels of *KDM5B* expressed in metastatic prostate tissue suggesting a potential link with KDM5B and patient survival (Xiang *et al*., 2007). Consistent with Xiang and colleagues (2007), analysis of a data set from the GeneSapiens database identified *KDM5B* as over expressed in prostate adenocarcinoma compared to normal prostate tissue (Bjorkman *et al*., 2011). Significantly KDM5B and the AR can interact *in vivo* (Xiang *et al*., 2007) further

supporting a causal link between KDM5B expression and the pathogenesis of prostate cancer.

1A.6.3 KDM5B and breast cancer

KDM5B is expressed in breast tumours (Lu *et al*., 1999, Islam *et al*., 2011a) and correlates positively with breast cancer grade (Coleman *et al*., 2011). Furthermore, KDM5B maybe required for breast cancer cell proliferation (Yamane *et al*., 2007) and as demonstrated using both a syngenic (Yamane *et al*., 2007) and an ER alpha positive xenograft tumour murine model (Catchpole *et al*., 2011) that KDM5B is required for mammary tumour growth.

Other KDM5B expression data also suggests a role for KDM5B in the progression of breast cancer (Lu *et al*., 1999, Coleman *et al*., 2011, Yoshida *et al*., 2011). A positive effect of KDM5B on breast cancer progression is consistent with transwell migration assays using two breast cancer cell lines MDA-MB-231, BT549 and a prostate cancer cell line DU145 (Yoshida *et al*., 2011). However, a tumour suppressive function has also been suggested during the progression of advanced breast cancer, through the ability of the KDM5B/KDM1/NURD complex to repress the *CCL14* promoter resulting in the suppression of MDA-MB-231 transwell invasion. Furthermore KDM5B expression suppressed angiogenesis both *in vitro* and *in vivo* (Li *et al*., 2011). To clarify the function of KDM5B during breast cancer metastasis, *in vivo* models are required.

Human KDM5B was initially identified as a gene whose expression is positively regulated through the c-ErbB2-signalling pathway in luminal epithelial cells (Lu *et al*., 1999). Subsequently, KDM5B was identified as being expressed in breast tumour biopsies (Lu *et al*., 1999, Coleman *et al*., 2011, Islam *et al*., 2011a) the expression of which positively correlates with breast cancer grade (Coleman *et al*., 2011). From a clinical perspective breast cancer can be broadly classified into 3 therapeutic groups; ER alpha positive, c-ErbB2 positive (ER alpha positive or ER alpha negative), and triple-negative.

1A.7 Clinical sub-types of breast cancer

Over half of breast cancer patients are categorized as oestrogen receptor positive and are therefore the most numerous of the clinical sub-groups (Perou *et al*., 2000, Sorlie *et al*., 2001). Sustained exposure to the ovarian hormones progesterone and oestrogen are established risk factors with early menarche and late menopause increasing the risk of developing breast cancer (Trichopoulos *et al*., 1972, Apter *et al*., 1989, Bernstein *et al*., 2002). Clinically these patients respond well to endocrine therapy. In fact the use of tamoxifen and aromatase inhibitors on hormone receptor positive breast cancer patients has almost halved the rate of disease recurrence (EBCTCG. 2005, Cuzick *et al*., 2010).

Amplification of the *ERBB2* gene occurs for some 25% of breast cancer patients (Slamon *et al*., 1987). Amplification and over-expression of c-ErbB2 is associated with a poorer prognosis (Slamon *et al*., 1987, Perou *et al*., 2000, Sorlie *et al*., 2001). However the use of treatments, such as trastuzumab have significantly improved the survival rates of this category of breast cancer patient (Cobleigh *et al*., 1998).

Patients that present with a triple-negative breast tumour; so called because the tumours lack the expression of ER alpha, PR and c-ErbB2 (Reis-Filho *et al*., 2008), represent some 10-20% of breast cancers (Perou *et al*., 2000, Sorlie *et al*., 2001). Patients with triple-negative tumours have a worse prognosis than patients with ER alpha positive tumours (Sorlie *et al*., 2001), with a higher relapse rate within the first three years (Dent *et al*., 2007).

Significantly, immunohistochemistry on a cohort of over 300 breast cancers demonstrated that KDM5B is widely expressed in all breast cancer sub-types.

1A.8 The relevance of murine models to study mammary gland morphogenesis

One question that remains relevant to scientific research on normal mammary gland development and breast cancer is: What are the most suitable experimental models to use that can best represent the signalling pathways that drive human mammary gland morphogenesis and disease development? In the first instance and from an *in vivo* stand point, the murine gestation period is approximately 20 days and postnatal adult development is completed by approximately 8 weeks. This timeframe provides a suitable window in which to study the signalling pathways involved in mammary gland morphogenesis. It is well documented that exposure to ovarian hormones can increase

a woman's chance of developing breast cancer (Trichopoulos *et al*., 1972, Apter *et al*., 1989, Bernstein *et al*., 2002). Murine models of mammary gland development provide a suitable model due to the similarities between the mouse oestrous cycle and the human menstrual cycle. The human follicular phase has a surge of circulating oestrogen that is reflected in the murine pro-oestrus/oestrus, whereas there is a surge of circulating progesterone during the human luteal phase that is reflected in the murine dioestrus. Further supporting the use of murine models to study normal mammary gland morphogenesis and breast cancer are the similarities between the human and murine mammary hierarchical organisation (Shehata *et al*., 2012) and the signalling pathways involved (Lim *et al*., 2010, Shehata *et al*., 2012).

Using murine models to understand the factors that are important to normal mammary gland epithelial cell hierarchy determination will hopefully provide essential information with respect to the development of breast cancer. The next section of the introduction therefore highlights some of those factors that are crucial for the development of the murine mammary gland.

Chapter 1: Introduction

Section 1B: Development, differentiation, and involution of the murine mammary gland

Chapter 1. Introduction

Section 1B: Development, differentiation, and involution of the murine mammary gland.

1B Overview Although the mammary gland is established during embryonic development, the majority of development occurs after birth. In response to the endocrine signal emanating from the hypothalamus-pituitary-axis at puberty the epithelial cells at the distal ends of the mammary duct proliferate to form bulbous structures known as terminal end buds. Ramification of the fat pad through ductal elongation and bifurcation at TEB structures is completed by adulthood. This is followed by cycles of cell proliferation, differentiation and apoptosis during the oestrous cycle and at each recurring pregnancy. From the onset of puberty and throughout the reproductive period of the female, the mammary gland will undergo extensive cyclic regeneration and remodelling suggesting the presence of mammary gland stem cells and an epithelial cell hierarchy. The balance between mammary progenitor cell proliferation and mammary cell fate specification is therefore critical for normal mammary morphogenesis.

The adult mammary gland structure is comprised of two main lineages that are derived from multi-potent (Shackleton *et al*., 2006, Stingl *et al*., 2006) and/or uni-potent stem cells (Van Keymeulen *et al* 2011). The luminal cell lineage line the ducts and differentiate into alveolar units and the basal/myoepithelial cells are localised between the luminal cells and the basement membrane. In response to the hormonal influx, at approximately 4 weeks of age bulbous TEB structures form at the distal tip of the rudimentary ductal structure (Nandi, 1958). TEB structures - the unit of elongation, are a putative niche for mammary stem cells, with evidence from murine studies suggesting that although the majority of actively proliferating stem cells reside in the cap cell layer, actively proliferating stem cells have also been detected in the inner body cells during puberty (Bai *et al*., 2010). The TEB structure, is comprised of many layers of highly proliferative yet relatively unpolarized luminal body cells surrounded by cap cells, that via collective cell migration result in the ramification of the fat pad (Ewald *et al*., 2008). Figure 1.8

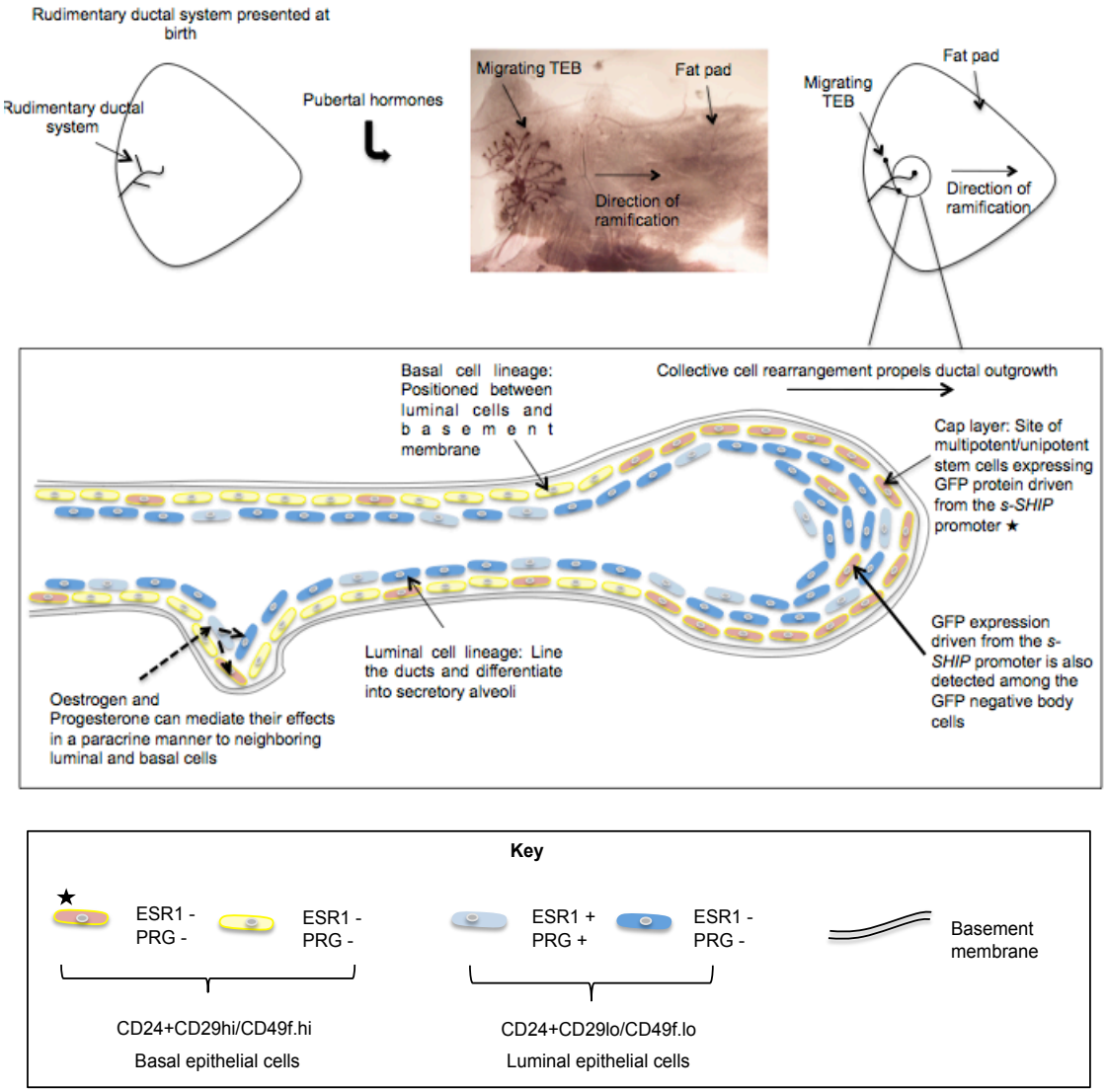


Figure 1.8 Murine postnatal mammary gland development. The adult mammary gland is comprised of two main lineages. The luminal cell lineage line the ducts and the basal/myoepithelial cells are localised between the luminal cells and the basement membrane. At the on-set of pubertal mammary gland development, TEB structures are formed resulting in and the ramification of the fat pad. Ovarian hormones dictate nulliparous mammary epithelial cell hierarchy determination. (Amalgamated from: Shackleton *et al*., 2007, Stingl *et al*., 2007, Ewald *et al*., 2008, Bai *et al*., 2010, Asselin-Labat *et al.,* 2010, Joshi *et al*., 2010, Van Keymeulen *et al*., 2011, Shehata *et al*., 2012). *s-SHIP* is the acronym for SH2-containing inositol 5'-phosphatase (104kd isoform), and GFP is green fluorescent protein.

Mammary gland ductal patterning through the bifurcation of TEB structures and subsequent side branching at stem/progenitor rich sites, occurs at regions of little myoepithelial coverage. The completion of ductal morphogenesis occurs once the luminal epithelial cells attain full apicobasal polarity and simple epithelial organisation by approximately 8 weeks of age (Ewald *et al*., 2008). Coincidentally, as the ductal tree

approaches the outer limits of the fat pad so the mouse reaches sexual maturity (Figure 1.9).



Figure 1.9 Nulliparous mammary gland development is completed by adulthood through the bifurcation of TEB structures and the generation of ductal side-branches.

During pubertal mammary gland development mammary epithelia are exposed to cyclic rounds of oestrogen and progesterone exposure. The mouse estrous cycle is divided into proestrus, estrus, metestrus and diestrus and lasts for 4-5 days. Although estradiol and progesterone serum levels are detected throughout the estrous cycle, levels do fluctuate. Estradiol levels peak at estrus, and progesterone serum levels peak at diestrus (Fata *et al*., 2001, Joshi *et al*., 2010). Mammary gland stem cells are responsive to steroid hormones (Asselin-Labat *et al*., 2010, Joshi *et al*., 2010) despite lacking oestrogen and progesterone receptors (Asselin-Labat *et al*., 2006, Sleeman *et al*., 2007). Whereas oestrogen primes mammary gland stem cells (Asselin-Labat *et al*., 2010) and is required for ductal elongation (Daniel *et al*., 1987), a rise in serum progesterone levels at diestrous is concurrent with an increase in mammary gland cell number and mammary ductal side-branching (Cole *et al*., 1933, Fata *et al*., 2001)

1B.1 Murine mammary gland stem cells, the epithelial cell hierarchy

1B.1.1 The existence of a murine multi-potent adult mammary gland stem cell

In order to generate an adult mammary gland from a rudimentary ductal structure, mammary gland stem cells need to undergo self-renewal and progenitor cell expansion toward a luminal or myoepithelial cell fate. Defining the signalling pathways responsible for progenitor cell expansion and mammary cell fate specification requires the identification and isolation of specific mammary gland cell types.

Using a FACS-based approach has enabled the isolation and characterisation of the mammary gland stem cell (Shackleton *et al*., 2006, Stingl *et al*., 2006). The isolation of the putative mammary gland stem cell was based upon the cell surface expression of CD29 (β1-integrin), which is a skin stem cell marker (Jones *et al*., 1995), CD24 (heat-stable antigen) a neural stem cell marker (Rietze *et al*., 2001), and CD49f (α6-integrin) an epidermal stem cell marker (Li *et al*., 1998). Confirmation of the existence of a multi-potent adult mammary gland stem cell came with the demonstration that a single cell from either the CD24+CD29^{hi} (Shackleton *et al*., 2006) or CD24+CD49f^{hi} (Stingl *et al*., 2006) epithelial population isolated from an adult nulliparous mammary gland could self renew and generate a functional mammary gland when serially transplanted into the cleared fat pad of recipient mice (Figure 1.10).

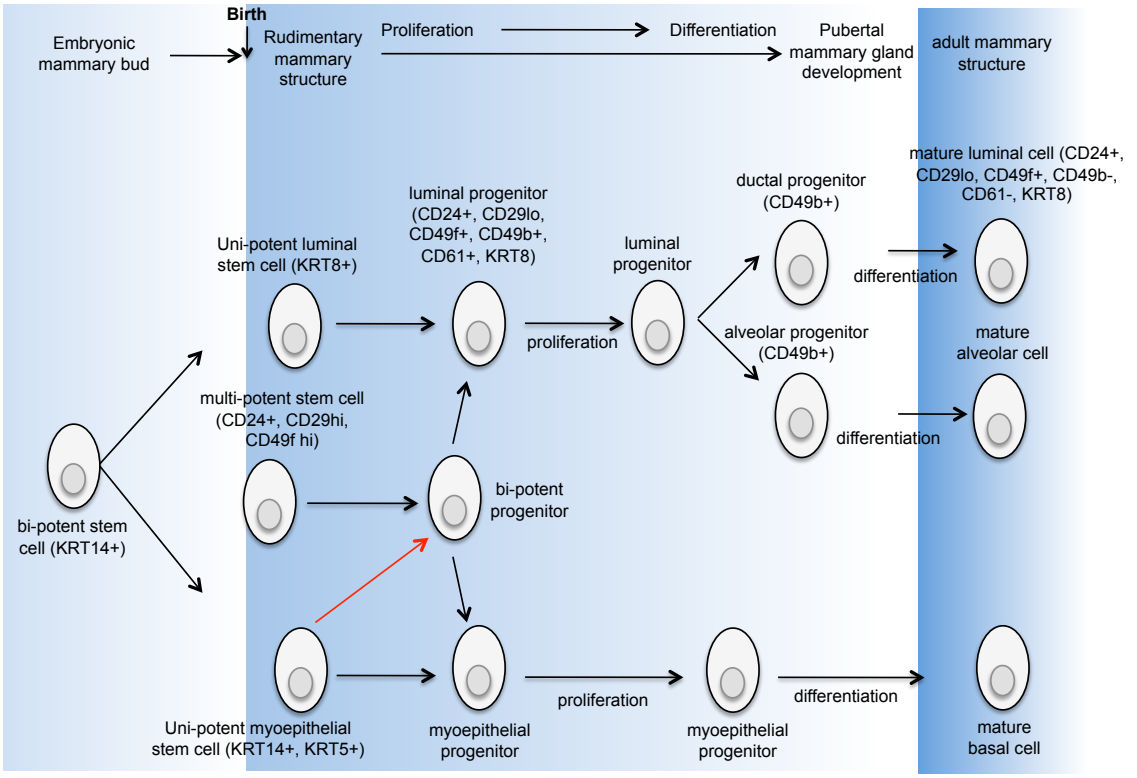


Figure 1.10 Murine mammary gland epithelial cell hierarchy. Lineage trace experiments have identified the existence of a multi-potent embryonic mammary epithelial stem cell. Adult mammary gland maybe generated from multi-potent and/or uni-potent mammary stem cells. Red arrow indicates bi-potent potential of the uni-potent myoepithelial stem cell upon transplantation. (Amalgamated from: Asselin-Labat *et al.,* 2007, Shackleton *et al*., 2007, Stingl *et al*., 2007, Van Keymeulen *et al*., 2011, Shehata *et al*., 2012). KRT is the acronym for cytokeratin.

In order to further delineate a mammary gland epithelial cell hierarchy, Shackleton and colleagues (2006) compared the growth of the CD24+CD29^{hi} stem cell-enriched population with that of the CD24+CD29^{lo} population in Matrigel under lactogenic conditions. Under these conditions, the CD24+CD29^{lo} population formed mainly alveolar like structures (85%) demonstrating a population that is enriched for cells that have a restricted luminal cell fate. In contrast the CD24+CD29^{hi} stem cell-enriched population presented with a more expanded repertoire of distinguishable structures including ducts, multicellular spheroid bodies, as well as the occasional alveolar structure (3%).

Leading on from this, the CD24+CD29^{lo} luminal enriched population of mammary cells can be further subdivided based upon the expression of the cell surface marker CD61 (β3-integrin). The CD61+ sub-population when grown in Matrigel could generate colonies that exclusively expressed KRT18 (cytokeratin 18), indicative of luminal progenitors. In keeping with this the greatest proportion of mammary epithelial cells at the onset of puberty are of the luminal enriched progenitor subtype, CD61+ cells (~60%). As the female reaches adulthood, the mammary gland becomes more differentiated and is composed of fewer luminal progenitor cells (~38% CD61+ epithelial cells). By day 18.5 of pregnancy (pd18.5), the mammary gland is fully differentiated in preparation for parturition. Consistent with this, the mammary gland is comprised of few luminal progenitor cells (~3% CD61+ epithelial cells) (Asselin-Labat *et al*., 2007).

The cell surface markers, stem cell antigen (Sca1) and CD49b (α2-integrin) can also be used to isolate luminal progenitor cells (Li *et al*., 2009). Using these cell surface markers has demonstrated that the adult mammary gland consists of two luminal progenitor cell types based on their genotypic and phenotypic characteristics, with the Sca1+CD49b+ population representing the luminal progenitors restricted to a ductal luminal cell fate and the Sca1-CD49b+ population representing the luminal progenitors restricted to a alveolar cell fate (Shehata *et al*., 2012). Although both luminal progenitor populations are clonogenic, the Sca1+CD49b+ enriched population express higher levels of *Esr1*, *Foxa1* and *Gata3* (Shehata *et al*., 2012). Given that ER alpha (Feng *et al*., 2007), FOXA1 (Bernado *et al*., 2010) and GATA3 (Asselin-Labat *et al*., 2007) are required for ductal development may suggest that the Sca1+CD49b+ enriched population represent a ductal progenitor cell type. In contrast the Sca1-CD49b+ enriched population may represent the alveolar progenitor population. The Sca1-CD49b+ enriched population express no to low detectable levels of *Esr1* but do

express milk protein transcripts and markers of alveolar differentiation (Shehata *et al*., 2012)

As researchers attempt to delineate the mammary gland epithelial cell hierarchy and the controlling factors involved, a number of issues require redress. Firstly, what is the contribution of the embryonic mammary bud to adult mammary gland morphogenesis? Secondly, what effect, if any, do mammary epithelial cell transplantation assays have on cell behaviour and thirdly, what influence do steroid hormones have on stem cell and progenitor cell numbers and differentiation potential?

1B.1.2 Murine postnatal mammary gland development is defined in the embryonic mammary bud and completed after birth by uni-potent stem cells

In order to address these first two issues, Blanpain and colleagues (2011) used a lineage trace approach to decipher the cellular hierarchy of mammary epithelia under the physiological setting of embryonic, pubertal and pregnancy-associated mammary gland development (Van Keymeulen *et al*., 2011). Monitoring yellow fluorescent protein (YFP) expression, driven indirectly from lineage specific cytokeratin promoters has demonstrated that a multi-potent stem cell population resides in the embryonic mammary bud and that pubertal and pregnancy-associated mammary gland development is supported by a uni-potent stem cell population as detailed below.

Using an inducible approach to trace KRT14-specific YFP protein expression in the embryonic mammary bud through to birth demonstrated that mammary epithelial cells of the rudimentary ductal system presented at birth were all positive for YFP protein expression. Furthermore, the YFP positive mammary epithelial cells from the rudimentary ductal structure could be divided into 2 populations; a CD24+CD29^{hi} population enriched for myoepithelial cells and a CD24+CD29^{lo} population enriched for luminal epithelial cells.

Transcription profiling identified *Krt14* and *Krt5* as transcripts enriched in the CD24+CD29^{hi} stem cell enriched population (Shackleton *et al*., 2006, Stingl *et al*., 2006). To determine under physiological conditions the contribution of a multi-potent stem cell (Shackleton *et al*., 2006, Stingl *et al*., 2006) to mammary gland morphogenesis Van Keymeulen and colleagues (2011) again used an inducible approach to trace KRT14-specific and KRT5-specific YFP protein expression in the pubertal and adult mammary gland. Significantly, these data demonstrated that KRT14

or KRT5 specific YFP protein expression marked only myoepithelial cells. Similarly, KRT8-luminal specific YFP protein expression traced only luminal cells, demonstrating that post-natal mammary epithelial cell fate is determination by uni-potent stem cells specific to the myoepithelial or luminal lineage (Figure 1.10)

1B.1.3 Both multi-potent and uni-potent murine mammary gland stem cells contribute to postnatal mammary gland development

In order to establish whether mammary gland transplantation assays can unlock a differentiation potential not seen under physiological conditions, chimeric mammary glands were generated. Whether the mixing experiments used YFP-protein marked luminal or YFP-protein marked myoepithelial cells, the resulting mammary glands were generated from uni-potent stem cells. Significantly, when YFP positive myoepithelial cells are co-transplanted with a 10x fold reduction in the number of luminal cells normally present during physiological conditions, the KRT14-specific YFP-traced myoepithelial cells can adopt a bi-potent phenotype and can differentiate along both the myoepithelial and the luminal cell lineage. These data suggest that a stem cell hierarchy exist in the adult mammary gland that includes stem cells with uni-potent and bi-potent activity that may perform unique functions during the morphogenesis and maintenance of the murine mammary gland (Van Keymeulen *et al*., 2011, Figure 1.10).

Given that postnatal murine mammary gland development is absolutely dependent on ovarian hormones (Nandi, 1958) would indicate a role for ovarian hormones in dictating murine stem cell function and mammary epithelial cell hierarchy determination. It is therefore essential to understand the role of ovarian hormones on mammary epithelial cell hierarchy determination during postnatal mammary gland development.

1B.1.4 Ovarian hormone control of mammary epithelial cell hierarchy organisation during postnatal mammary gland development

Studies of the effects of the ovarian hormones oestrogen and progesterone on postnatal mammary gland stem cell stasis have certainly added to the current understanding of mammary gland development. In the first instance, although ovarian hormone deprivation as a result of ovariectomy, had no effect on the total number of the mammary gland stem cell-enriched population (CD24+CD29^{hi}), transplantation of an ovarian hormone deprived CD24+CD29^{hi} stem cell enriched population into the clear fat pad of recipient adult females presented as a delay in ductal morphogenesis. This mammary gland phenotype maybe due to an effect on the cell cycle given that the

hormone deprived CD24+CD29^{hi} stem cell enriched population accumulated in the G0/G1-phase of the cell cycle (Asselin-Labat at al., 2010). Therefore, these results demonstrate that the exposure of mammary epithelial cells to a normal hormonal milieu is essential for proper mammary gland stem cell function and that mammary epithelial cells appear to retain a memory of their hormone environment (Asselin-Labat at al., 2010).

Of the ovarian hormones, oestrogen is a potent mitogen in the pubertal mammary gland where it promotes ductal elongation (Daniel *et al*., 1987), but acts merely permissively in the adult mammary gland where it induces progesterone receptor expression (Haslam *et al*., 1979, Beleut *et al*., 2010). Furthermore, data thus far implicates oestrogen in mediating stem cell function and epithelial cell hierarchy determination (Asselin-Labat *et al*., 2010). Treatment of young adult mice with the aromatase inhibitor Letrozole, which inhibits the production of oestrogen, not only reduced the repopulating frequency of the CD24+CD29^{hi} stem cell enriched population, but also the ductal outgrowth potential of transplants. Furthermore, fewer of the CD24+CD29^{lo} luminal cell enriched population were detected in Letrozole treated mice. Oestrogen may therefore be required for the survival of the luminal-enriched population (Asselin-Labat *et al*., 2006, Asselin-Labat *et al*., 2010, Shehata *et al*., 2012).

During post-natal mammary gland development, mammary epithelial cells are exposed to cyclic rounds of ovarian hormones. Whilst estradiol serum levels peak at oestrus, progesterone serum levels peak at dioestrus, the stage of the oestrus cycle that is associated with tertiary side branching and lobuloalveolar development (Fata *et al*., 2001, Joshi *et al*., 2010). These observed changes in the gross morphology of the mammary gland would therefore suggest that the hormonal changes imposed on the mammary gland during the oestrus cycle could therefore influence mammary epithelial cell hierarchy determination. In contrast to the number of mammary epithelial cells at oestrus; during dioestrus the CD24+CD49f^{hi} stem cell enriched population had expanded some six-fold whilst the CD24+CD49f^{lo} luminal cell enriched population had expanded some three-fold. A rise in progesterone therefore drives not only the proliferation of the CD24+CD49f^{hi} stem cell enriched population but also the proliferation and differentiation of the CD24+CD49f^{lo} luminal cell enriched population as the expanded luminal population were CD61-.

1B.1.5 Cell fate and histone marks in the mammary gland

(A) The chromatin effector protein, PYGO-2

Genetic studies in mice have shown an effect of the H3K4me3/2 reader, PYGO-2 (see Section 1A) on stem and progenitor cells during embryonic and postnatal murine mammary gland development (Gu *et al.,* 2009). In an epithelial specific *Pygo2* null murine line, reduced formation of the rudimentary ductal tree was observed, due to a reduction in embryonic progenitor cell proliferation, whilst in the adult mammary gland, fewer terminal end bud structures are present, ductal elongation is delayed and the female presents with fewer ductal side branches (Gu *et al.,* 2009).

Examination of the differentiation potential of the *Pygo2* deficient stem cell enriched population *ex-vivo* using a 3D Matrigel assay demonstrated a propensity for acinar-like structures and an increase in the transcript levels of *Csn2* (beta-casein) and *Stat5a*, indicating that the expression of PYGO2 is required to suppress the luminal/alveolar differentiation potential of the mammary gland stem cell enriched population. At a molecular level, *Pygo2* deficient mammary gland stem cells exhibited a transcriptional expression profile consistent with that of a mature luminal gene set including elevated members of the NOTCH signalling pathway such as *Notch3*.

The NOTCH signalling pathway promotes the commitment/differentiation of mammary gland stem cells to the luminal cell fate (Buono *et al*., 2006, Bouras *et al*., 2008). In contrast, the WNT/beta-catenin signalling pathway promotes the self-renewal of mammary gland stem cells (Zeng and Nusse 2010). Interestingly, the activation of the WNT/beta-catenin signalling pathway suppressed luminal/alveolar differentiation, and *Notch3* expression in a PYGO2 dependent manner (Gu *et al*., 2013). To elucidate the mechanism of action responsible for the suggested PYGO2 dependent cross-talk between the NOTCH-signalling and WNT/beta-catenin signalling pathways these authors demonstrated that beta-catenin binding to the promoter region of the *Notch3* gene was reduced in *Pygo2* deficient mammary gland stem cells (Gu *et al*., 2013). Importantly, the nucleosomes surrounding the PYGO2/beta-catenin enriched binding site at the *Notch3* locus was enriched with the 'bivalent' H3K27me3 and H3K4me3 mark. This chromatin configuration is reminiscent of the 'bivalent domain' found at the promoter region of developmental genes whose silence is required in embryonic stem cells yet are poised for activation upon lineage differentiation (Bernstein *et al*., 2006, Mikkelsen *et al*., 2007). In *Pygo2* deficient mammary gland stem cells an increase in the H3K4me3 mark was observed at the *Notch3* locus with a concomitant decrease in the H3K27me3 mark (Gu *et al*., 2013). These data indicate that in the absence of

Pygo2 the 'bivalent domain' at the *Notch3* locus was resolved to an active chromatin configuration.

(B) The EZH2 histone methyltransferase

Development of the mammary gland requires interpretation of upstream hormonal signalling at the level of the genome resulting in the alteration of chromatin structure that permits gene regulation, progenitor cell expansion and lineage determination. This results in milk protein synthesis and therefore the ultimate aim of the developing mammary gland - the nourishment of the offspring. Although studies have identified a number of signalling pathways and downstream transcription factors that control mammary gland epithelial cell differentiation, knowledge on the epigenetic factors that regulate chromatin structure during mammary gland development is now only coming to the fore.

Changes in histone methylation are associated with gene expression changes during lineage restriction and is therefore a likely mediator of the mammary epithelial cell hierarchy (Pal *et al*., 2013). Genes differentially expressed in the mammary gland stem cell enriched population or the luminal progenitor enriched population display an increase in the H3K4me3 mark and a decrease in the H3K27me3 mark upon increased expression, whilst those gene that are silenced display the opposite epigenetic change (Pal *et al*., 2013).

The hormone environment influences the dynamics of the mammary gland epithelial cell hierarchy (Asselin-Labat *et al*., 2010, Joshi *et al*., 2010). Cell cycle genes expressed in the mammary gland stem cell and luminal enriched populations of epithelia of ovariectomized mice are enriched in the H3K27me3 mark (Pal *et* al., 2013) accounting for the delay in ductal morphogenesis (Asselin-Labat *et al*., 2010) and linking the hormonal environment with chromatin modifications, gene expression and cell fate determination (Asselin-Labat *et al*., 2010, Josh *et al*., 2010, Pal *et al*., 2013). As could be predicted therefore, during pregnancy, key luminal-specific genes such as whey acidic protein (Wap), the Ets domain transcription factor (Elf5) and beta casein, whose expression increases during pregnancy and are required for differentiation and milk protein synthesis, display reduced levels of the H3K27me3 mark (Pal *et al*., 2013).

The histone methyltransferase EZH2, is a component of the polycomb repressor complex 2 (PRC2), and is responsible for the di and trimethylation of lysine 27 on histone 3 (Cao *et al*., 2002). Of the major pregnancy hormones, progesterone but not

prolactin regulates the increase in the phosphorylation of EZH2 on threonine 487 detected from early to mid pregnancy (Pal *et al*., 2013) linking further the relationship between the hormonal environment and the function of epigenetic factors during the development of the mammary gland.

Ablation of *Ezh2* expression from mammary gland epithelia not only delays ductal elongation during puberty, but also alveoli development during pregnancy due to defective cell cycle control (Pal *et al*., 2013). Furthermore, using fat pad reconstitution assays, and limited dilutions of FAC-sorted stem cell enriched (CD24+CD29^{hi}) epithelia the frequency of repopulating cells was reduced by 14 fold in the absence of *Ezh2* expression. Moreover, the stem cell enriched and the luminal cell enriched population of epithelia isolated from the *Ezh2*-deficent mammary gland had poor colony forming ability *in vitro* (Pal *et al*., 2013). These observations suggest a critical role for EZH2 in regulating the activity of multiple progenitor subtypes during mammary gland development.

Of interest, one of the top de-repressed gene sets in the stem cell enriched population of *Ezh2* deficient mammary epithelia other than those related to cell cycle regulation, was keratinocyte differentiation (Pal *et al*., 2013), suggesting that a function of EZH2 during mammary gland morphogenesis is to silence inappropriate gene expression. This finding is consistent with observations in other biological systems in which mis-expression of non-myogenic lineage specific genes has been observed in *Ezh2* null skeletal muscle (Juan *et al*., 2011).

1B.2 Studies on pubertal mammary gland development

1B.2.1 Oestrogen receptor signalling

Oestrogen elicits some of its effects on pubertal mammary gland development through the oestrogen receptor. Of the two oestrogen receptors (ER alpha and ER beta) only epithelial ER alpha expression is required for TEB formation and development of the mammary gland beyond the rudimentary ductal system presented at birth (Krege *et al*., 1998, Forster *et al*. 2002, Mallepell *et al*., 2006, Feng *et al*., 2007). Factors central to the oestrogen receptor signalling-cascade are therefore also important for maintaining pubertal mammary gland development (Asselin-Labat *et al*., 2007, Bernado *et al*., 2010, Kawazu *et al*., 2011). For example, the expression of factors such as FOXA1 (Bernado *et al*., 2010) and GATA3 (Asselin-Labat *et al*., 2007) - whose expression is

required for ER alpha expression in the normal mammary gland - are also required for development beyond the rudimentary ductal structure (Asselin-Labat *et al*., 2007, Bernado *et al*., 2010). Furthermore, ER alpha can elicit transcriptional control as part of a dynamic multi-protein complex (Metivier *et al*., 2003). Members of an ER alpha complex can include histone-remodelling proteins such as the histone acetyl-transferase protein p300/CBP (Metivier *et al*., 2003) and the H3K9me3 demethylase KDM4B (a.k.a JMJD2B) (Kawazu *et al*., 2011, Gaughan *et al*., 2013). Depending on how significant these co-factors are to ER alpha function determines the degree to which deletion studies phenocopy the mammary gland defect presented in a *Esr1* epithelial knock out murine line (Feng *et al*., 2007).

GATA3 is a critical regulator of lineage determination and differentiation in a number of cellular systems (Ting *et al*., 1996, Grote *et al*., 2006), including the murine mammary gland (Asselin-Labat *et al*., 2007). Although not exclusively, the expression of ER alpha and GATA3 are also intimately linked during normal murine mammary gland development. GATA3 positively regulates the expression of *Esr1* with co-expression being more prevalent in the more mature luminal CD61- epithelial population (Asselin-Labat *et al*., 2007). Therefore as does the ablation of epithelial ESR1 expression halt pubertal mammary gland development at the rudimentary ductal stage (Feng *et al*., 2007), similarly, employment of either *Krt-14-cre* or *MMTV-cre* to mediate *Gata3* deletion during pubertal mammary gland development also results in a severely stunted ductal tree (Asselin-Labat *et al*., 2007). Interestingly, expression of *Gata3* from one allele resulted in an expansion of the luminal-enriched progenitor (CD61+) population in the adult mammary gland, highlighting the importance of GATA3 expression, and potentially ER alpha in the drive toward a mature luminal mammary phenotype.

As described ER alpha expression is a prerequisite for pubertal mammary gland development (Feng *et al*., 2007). However, deletion of the transcriptional co-activator CITED1 which stabilises the oestrogen dependent interaction between p300/CBP and ER alpha (Yahata *et al*., 2001) only affected the expression of a sub-set of oestrogen responsive genes in the developing pubertal mammary gland (McBryan *et al*., 2007). The resulting *Cited1* knock out mammary gland presented with fewer terminal end bud structures, a delay in ductal tree development, together with a disorganised lateral branching structure (Howlin *et al*., 2006).

A number of observations place the expression of the H3K9 demethylase, KDM4B centrally within the oestrogen receptor signalling pathway (Kawazu *et al*., 2011, Shi *et*

al., 2011, Gaughan *et al*., 2013). Using human breast cancer cell lines, oestrogen can induce KDM4B expression (Kawazu *et al*., 2011) and KDM4B can also cooperate with GATA3 to regulate *ESR1* expression itself (Gaughan *et al*., 2013). KDM4B expression is also required for breast cancer cell proliferation both *in vitro* and *in vivo* (Kawazu *et al*., 2011, Shi *et al*., 2011). In addition KDM4B expression is required for the proper recruitment of ER alpha to the genome (Kawazu *et al*., 2011). Furthermore, *MMTV-Cre* driven deletion of KDM4B from pubertal mammary epithelial cells results is a delay in ductal morphogenesis (Kawazu *et al*., 2011).

By acting through the epidermal growth factor receptor (EGFR), Amphiregulin (AREG) is a major paracrine mediator of ER alpha function during pubertal mammary gland development (Kenney *et al*., 1995, Luetteke *et al*., 1999, Ciarloni *et al*., 2007). The expression of AREG, the most abundant EGF-family member expressed during pubertal mammary gland development (Kenney *et al*., 1995) is regulated by ER alpha (Ciarloni *et al*., 2007). The expression of AREG is essential for pubertal mammary gland development (Luetteke *et al*., 1999, Ciarloni *et al*., 2007) and recombinant AREG expression can promote TEB formation and ductal development in ovariectomised mice (Kenney *et al*., 1996).

1B.2.2 Progesterone receptor signalling in the adult mammary gland

As described above, serum progesterone influences stem cell expansion and luminal progenitor cell differentiation in the adult mammary gland (Joshi *et al*., 2010). As is the case with the oestrogen receptor (Feng *et al*., 2007), only the epithelial expression of the progesterone receptor (PR) is required for mammary gland development (Brisken *et al*., 1998). Furthermore, engraftment of progesterone receptor null epithelial cells into the clear fat pad of the recipient host has shown that the epithelial expression of the progesterone receptor is required for lateral side branching but not the initial ramification of the pubertal mammary fat pad (Brisken *et al*., 1998). Mammary gland stem cells are oestrogen and progesterone receptor negative (Asselin-labat *et al*., 2006, Sleeman *et al*., 2007) and are instructed via paracrine mechanisms (Joshi *et al*., 2010). The canonical WNT-signalling pathway is one pathway that can mediate the effects of progesterone and is therefore of central importance to mammary gland development (Brisken *et al*., 2000, Joshi *et al*., 2010, Van Amerongen *et al* 2012). Use of an oestrogen and progesterone replacement regime on ovariectomised mice demonstrated that the *Wnt4* transcript is induced in the FACS-sorted luminal enriched epithelial cell population ($CD24+CD49f^{lo}$), whilst a canonical WNT-signalling co-

receptor *Lrp5* is induced in the CD24+CD49f^{hi} stem cell enriched population (Joshi *et al*., 2010).

Hormonal cues together with locally produced growth factors stimulate the formation of TEB structures, which as a consequence of mammary epithelial proliferation results in the ramification of the fat pad through the bifurcation of TEB structures and the production of side-branches. This results in an ordered and amply spaced pubertal tree-like structure in anticipation for infilling by alveolar structures. Described below are some of those factors that function downstream or in parallel to ER alpha to mediate the development of the pubertal mammary gland.

1B.2.3 Growth factor regulation of ductal morphogenesis

Of the epidermal growth factor receptor family members, EGFR (c-ErbB1), c-ErbB2 and c-ErbB3 are required for pubertal mammary ductal development (Sebastian *et al* 1998, Jackson-Fisher *et al*., 2004, Jackson-Fisher *et al*., 2008).

AREG is regulated by ER alpha (Ciarloni *et al*., 2007) and is the major ligand for EGFR (Sternlicht *et al*., 2005). EGFR therefore mediates ER alpha signaling during pubertal mammary gland development (Sebastian *et al*., 1998). *Egfr* null neonatal mammary glands fail to undergo ductal morphogenesis when grafted under the renal capsule of recipient female mice (Sebastian *et al*., 1998) and therefore phenocopy mammary gland development in an *Esr1* null murine line (Feng *et al*., 2007).

In contrast to the mammary gland phenotype presented in the *Egfr* knockout line, studies have shown that c-ErbB2 signalling is not absolutely required for pubertal development and is dispensable during pregnancy-associated differentiation (Jackson-Fisher *et al*., 2004, Andrechek *et al*., 2005). Whether the approach to examining the role of c-ErbB2 during mammary gland ductal morphogenesis utilized transplanted *Erbb2* null epithelial (Jackson-Fisher *et al*., 2004) or a murine line harbouring a mammary epithelia specific *Erbb2* deletion, these females presented with a delay in pubertal ductal morphogenesis yet eventually recovered to ramify the fat pad fully. Moreover, the *Erbb2* null female could support her pups at parturition with no difference in the size of the offspring noted (Andrechek *et al*., 2005).

Similar to the *Erbb2* null pubertal mammary gland phenotype (Jackson-Fisher *et al*., 2004, Andrechek *et al*., 2005), the *Erbb3* null pubertal mammary gland also present with a delay in ductal morphogenesis (Jackson-Fisher *et al*., 2008). Gene expression

analysis on murine mammary epithelial sub-populations revealed that high levels of *Erbb3* are expressed in committed luminal progenitors and mature luminal epithelial cells (Balko *et al*., 2012). Immunohistochemical staining of TEB structures demonstrates that ablation of *Erbb3* results in an increase in the cap cell number (SMA+) and a decrease in body cell number (increased cleaved caspase 3) (Jackson-Fisher *et al*., 2008). In keeping with this, using an organoid system to replicate mammary gland development demonstrated that in the absence of c-ErbB3 expression the gene expression signature switched from that of a luminal signature to one of basal epithelial in origin (Balko *et al*., 2012)

In addition to ER alpha and EGFR acting synergistically to promote pubertal mammary gland development (Kenney *et al*., 1995, Luetteke *et al*., 1999, Sternlicht *et al*., 2005, Ciarloni *et al*., 2007), FGF signalling may also act in parallel to, or in concert with EGFR signalling. Specifically, the FGF2 ligand can induce branching in *Egfr* null mammary organoids grown in 3-D matrigel (Sternlicht *et al*., 2005). With respect to mammary gland development both FGFR1 and FGFR2 are expressed in the developing mammary bud, and are the primary FGF receptors expressed in the mouse mammary epithelium during ductal morphogenesis suggestive of a function during pre- and postnatal mammary gland development (Chodosh *et al*., 2000, Lu *et al*., 2008). Both FGFR1 and FGFR2 are expressed in the basal and luminal mammary epithelial suggesting that together they may function during the determination of the mammary epithelial hierarchy. In order to study the function of FGFR2 during adult mammary gland development, Lu and colleagues (2008) utilized the inefficiency of the MMTV-Cre transgene to generate a murine line whose mammary glands are chimeric, that is a combination of mammary gland epithelial cells that are *Fgfr2* null and *Fgfr2* heterozygous. These chimeric females presented with a delay in pubertal mammary gland development and had completely ramified the fad pad some 3 weeks later than the control counterpart. In addition to a delay in ductal elongation these chimeric females also presented with fewer bifurcation points, a phenomenon which was more pronounced during the earlier stages of pubertal development. The mammary gland epithelial cells of these chimeric females were able to undergo pregnancy-associated differentiation with milk secretion during lactation, despite having fewer alveolar units. These authors demonstrated that the pre-pubertal mammary gland had a substantial number of *Fgfr2* null cells distributed evenly throughout the rudimentary ductal structure. However, during puberty as the mammary gland undergoes proliferation at TEB structures and consequently ductal elongation and bifurcation, the *Fgfr2* null epithelial cells, being at a proliferative disadvantage compared to the *Fgfr2* heterozygous epithelial cells are diluted out of the TEB structure. These authors

conclude that the delay in ductal elongation could be due to the substantial number of *Fgfr2* null epithelial cells at the onset of puberty, that due to their defective proliferative capability manifest in a delay in ductal elongation. As ductal development proceeds the proliferative-defective *Fgfr2* null epithelial cells are out competed by the proliferative-able *Fgfr2* heterozygous epithelial cells allowing completion of pubertal ductal development (Lu *et al*., 2008).

A delay in pubertal development was also displayed using a conditional deletion of *Fgfr1* through *Krt14* mediated Cre expression. The *Fgfr1* null mammary gland presented with fewer terminal end buds as well as ductal branch points and a defect in ductal elongation. The *Fgfr1* null phenotype presented from the on-set of puberty at 3 weeks of age until 5 weeks, after which the mammary gland resembled that of the wild type female. Immunohistochemical analysis post BrdU incorporation demonstrated that during the delay in mammary gland development (between weeks 3 and 5), fewer TEB epithelia were positive for BrdU suggesting that FGFR1 may function to drive the initial stages of pubertal mammary gland development. Additionally, adenoviral-cre mediated deletion of both *Fgfr1* and *Fgfr2* from mammary epithelial cells ablated mammary gland development upon transplantation into cleared fat pads. Furthermore, subsequent FACS-sorted isolation of the CD24+CD29^{hi} stem cell enriched population, revealed that the *Fgfr1/2* null transplanted mammary gland contained significantly fewer CD24+CD29^{hi} stem cell enriched epithelia (Pond *et al*., 2013).

1B.3 Morphogenesis and differentiation of the mammary gland at pregnancy and lactation

The morphological changes which the mammary gland has to undergo during pregnancy to proceed to lactation involves a large increase in secondary and tertiary branching leading to the development of alveoli, a process known as alveologenesis. Alveoli buds that develop from the proliferating alveolar progenitor cells cleave and differentiate into the alveoli that will form the milk secreting lobules at lactation. Two factors known to play major roles in the development of alveoli structures, and in the production of milk, are progesterone from the ovaries and prolactin secreted by the pituitary gland and - as has been recently demonstrated – prolactin is produced by the mammary gland epithelial cells themselves (Chen *et al.,* 2012. See below). However, in addition to ovarian hormones and prolactin, a role for immune cell cytokines operating through the STAT6 signalling pathway have also been shown to be involved in regulating luminal cell fate (see below and reviews by Watson and Khaled 2008, Macias and Hinck 2012, Oliver and Watson 2013).

1B.3.1 *Progesterone and prolactin in alveologenesis and terminal differentiation*.

With a rise in circulating progesterone serum levels during pregnancy the mammary gland undergoes morphogenesis. Combined hormone replacement regimes have demonstrated that progesterone and 17-beta estradiol can drive the expansion of the mammary gland stem cell enriched (CD24+ CD61+ CD49f^{hi}) and the differentiated luminal (CD24+ CD61- CD49f^{lo}) populations of epithelial cells (Joshi *et al*., 2010). From a physiological perspective the isolation of FAC-sorted epithelial cells has demonstrated that there is an increase in the number of the mammary gland stem cell enriched population (CD24+CD29^{hi}) during pregnancy associated mammary gland development with a marked increase in the frequency of repopulating units at mid pregnancy (day 12.5) compared to late pregnancy (day 18.5) (Asselin-Labat *et al*., 2010) consistent with the physiological drive toward the development of the pregnant mammary gland.

The mitogenic effects of progesterone are elicited via the progesterone receptor, the deletion of which results in a failure of the mammary gland to instigate side branching and alveolar development during pregnancy (Lydon *et* al., 1995, Brisken *et al*., 1998). Progesterone, acting through the progesterone receptor functions in a paracrine manner (Brisken *et al*., 1998, Beleut *et al*., 2010). Of the two isoforms of the progesterone receptor expressed, progesterone receptor alpha (PR-A) and progesterone receptor beta (PR-B), only PR-B is required for side branching and alveologenesis (Mulac-Jericevic *et al*., 2003).

Both WNT4 and TNFSF11 (a.k.a RANKL) have been implicated in mediating the mitogenic effects of progesterone (Brisken *et* al., 2002, Asselin-Labat *et al*., 2010, Beleut *et al*., 2010, Joshi *et* al., 2010). Progesterone induces WNT4 expression (Brisken *et* al., 2002, Joshi *et* al., 2010) and gene ablation studies have shown that WNT4 expression is required for ductal side branching at mid-pregnancy (pd12.5) but not at late pregnancy (Brisken *et al*., 2000). The expression of TNFSF11 is induced by progesterone in PR positive cells and mediates its function in a paracrine fashion to neighboring cells expressing tumor necrosis factor receptor superfamily, member 11a (TNFRSF11A, a.k.a RANK) (Fernandez-Valdivia *et* al., 2008). Deletion of *Tnfsf11* or *Tnfrsf11a* results in a failure in alveologenesis during pregnancy (Fata *et* al., 2000) reminiscent of the phenotype presented in the mammary gland of the *Pr-b* knock out model (Mulac-Jericevic *et al*., 2003).

Until recently the pituitary gland was consider the primary source of prolactin required for alveologenesis (Vomachka et al 2000). However, a recent study (Chen *et al.,* 2012) has demonstrated that the phosphoinositide-3-kinase - protein kinase B/AKT (PI3K-PKB/AKT) signalling pathway mediates autocrine prolactin production by the mammary epithelia, downstream STAT5 activation and mammary gland secretory differentiation. The importance of this pathway was demonstrated by conditional activation of the PI3K-AKT signalling pathway by doxycyclin-inducible expression of activated *Akt1* in mammary epithelia and by conditional ablation of the inhibitor of this pathway, phosphatase and tensin homologue (Pten). These authors demonstrated that epithelial cells in the adult virgin mammary gland could be induced to differentiate, producing milk proteins, when the AKT signalling pathway was activated, in spite the absence of alveoli development that is normally seen during pregnancy. AKT1 induced mammary gland differentiation was abrogated in mice that harbour prolactin (Prl) null, prolactin receptor (Prlr) null or *Stat5* null genetic backgrounds (Chen *et al*., 2012), demonstrating the requirement for the PRLR/JAK2/STAT5 signalling pathway (JAK, Janus kinase 2).

The PI3K-AKT signalling pathway is essential for the synthesis of milk components such as lipids and lactose (Anderson *et al*., 2007). Significantly, following *Akt1* induction the *Stat5* or *Prlr* null epithelia failed to accumulate cytoplasmic lipid droplets or induce lactose synthesis, demonstrating that the major components of milk require a functional PRLR/JAK2/STAT5 signalling pathway (Chen *et al*., 2012).

1B.3.2 The function of the Ets transcription factor ELF5 during cell fate determination in the pregnant mammary gland.

Genetic ablation studies have demonstrated that mediators of progesterone and prolactin signalling are required for alveologenesis (Lydon *et* al., 1995, Lui *et al.,* 1997, Ormandy *et al*., 1997, Brisken *et al*., 1998, Teglund *et al*., 1998, Mulac-Jericevic *et al*., 2003, Cui *et al*., 2004, Wagner *et al*., 2004, Lee *et al*., 2013). Expression of the transcription factor ELF5 is dispensable for pubertal mammary gland development but required for alveoli development, implicating ELF5 as a mediator of pregnancy hormone function (Oakes *et al*., 2008, Choi *et al*., 2009). Progesterone induces ELF5 expression *in vivo* and these two factors act synergistically to promote alveoli development (Lee *et al*., 2013). Not only does ELF5 transcriptionally activate *Stat5* expression but also indirectly regulates the phosphorylation of STAT5 (Choi *et al*., 2009). Furthermore, STAT5 activates *Elf5* transcription (Yamaji *et al*., 2013) suggesting a positive regulatory feedback loop. Although autocrine prolactin is induced by the PI3K-AKT signalling pathway and mediates alveoli development and secretory

activation via the PRLR/JAK2/STAT5 signalling pathway (Chen *et al*., 2012), AKT1 can induce *Elf5* expression in the mammary gland of nulliparous *Stat5* null and *Prlr* null mice (Chen *et al*., 2013). This indicates that AKT1 is an upstream transcriptional regulator of *Elf5* in a manner that is independent of PRLR/JAK2/STAT5 signalling and that ELF5 expression alone is insufficient to substitute for the differentiation effects of prolactin receptor signalling. However, ELF5 is necessary for mammary gland development since conditional deletion of *Elf5* during pregnancy results in a block in alveologenesis and lactational failure (Choi *et al*., 2009) and over expression of *Elf5* in the nulliparous mammary gland results in precocious alveolar development and secretory differentiation (Oakes *et al*., 2008). This data suggests a function for ELF5 in mammary gland epithelial cell hierarchy determination. Consistent with this, an increase in the FAC-sorted CD61+ subpopulation of luminal progenitor cells has been reported to be present in the pregnant mammary gland of *Elf5* null mice, suggestive of a block in differentiation (Oakes *et al*., 2008, Chakrabarti *et al*., 2012).

1B.4 Post weaning and Involution of the mammary gland

Following the lack of demand for milk, which can be induced by the removal of the pups, the process of involution is initiated in order to remodel the mammary gland back to its pre-pregnant architecture. This process takes place in two phases, the first is reversible, and no obvious morphological change occurs, but alveolar cells detach and are shed into the lumen. The cell death that occurs during the first phase of involution has been attributed to both intrinsic mitochondrial and extrinsic - death receptor - apoptotic pathways (Marti *et al*., 2001, Baxter *et al*., 2006). However, more recent data show that lysosomal membrane permeabilisation (LMP) is responsible for the earliest cell death (Kreuzaler *et al*., 2011). After 48 hours this phase is followed by a second phase, which is irreversible, when the alveoli begin to collapse, and activation of proteases induce a second wave of cell death that is accompanied by an influx of neutrophils and macrophages leading to the remodelled mammary gland.

The first phase of involution is orchestrated by local cues. This was shown using models where milk release was disrupted in the presence of systemic lactogenic hormones by sealing of the teats, transplanting mammary glands unable to release milk due to no teat connection, or by inactivation of the oxytocin gene (Li *et al*., 1997). Two groups have performed a detailed transcript analysis during the two phases of involution, and have documented the genes that are expressed (Clarkson *et al*., 2003, Stein *et al*., 2003). Along with the signal transducer and activator of transcription 3 (Stat3), which was know to be a crucial factor during involution (Chapman *et al*., 1999,

Humphreys *et al*., 2002), genes encoding for death receptors, immune mediators and factors involved in the acute phase response were found to be elevated. The specific immune response resembles a wound healing process involving macrophage infiltration of the mammary gland concurrent with an increase in the expression of several acute phase response genes. The importance of STAT3 in the regulation of several acute phase response genes has recently been reported by specifically documenting the effects of deletion of STAT3 expression in the mammary gland epithelia during involution (Hughes *et al*., 2012).

1B.5 The JAK/STAT signalling pathways during mammary gland development

The JAK/STAT signalling pathways, which transduce external stimuli to regulate gene transcription, involve two JAK proteins (Janus kinase, JAK1 and JAK2), and seven signal transducers and activators of transcription (STAT - STAT1, STAT2, STAT3, STAT4, STAT5A, STAT5B and STAT6). The basic signalling mechanism is illustrated diagrammatically in Figure1.11. A signal is generated by interaction of a ligand with its surface receptor triggering the activation of an associated JAK protein which phosphorylates tyrosine residues on the intracellular domain of the receptor to which the specific STAT then binds and is itself phosphorylated. The phosphorylated STAT protein dimerises and moves to the nucleus where it can associate with specific promoters to activate transcription. The JAK/STAT signalling pathway has proved to be crucial to the determination of cell fate and in directing the changes in gene expression and morphology occurring in the development of the mammary gland. Evaluating the role of the different STAT proteins has largely been achieved by gene deletion or overexpression studies using transgenic murine lines, in many cases using mammary gland specific promoters to achieve genetic change at specific stages of mammary gland development. Different STAT proteins are expressed in association with JAK1/2, and are activated at different stages of mammary gland development, as is illustrated in Figure1.12 for the expression of activated STAT proteins 1,3,5 and 6 (For review see Hughes and Watson 2012).

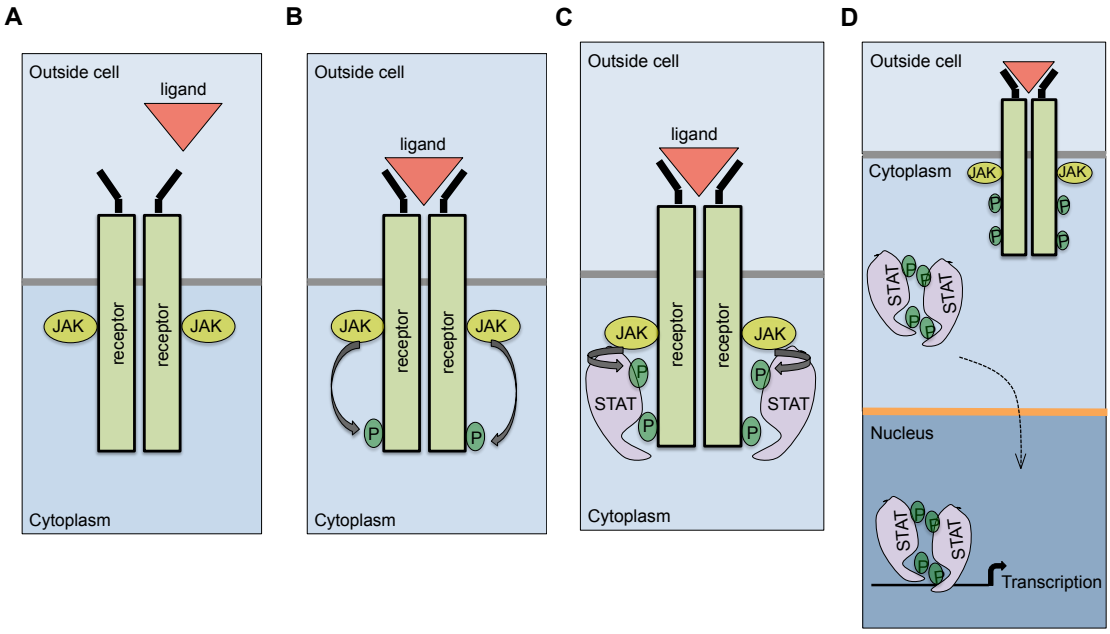


Figure 1.11 The JAK/STAT signalling pathway in the mammary gland. (A and B) Binding of cytokines (red triangle) to their receptor (green rectangle) results in receptor dimerization and activation of JAK (yellow circle). (C and D) The downstream consequence of JAK activation is the phosphorylation and activation of the STAT protein, STAT translocation to the nucleus, DNA binding and gene regulation.

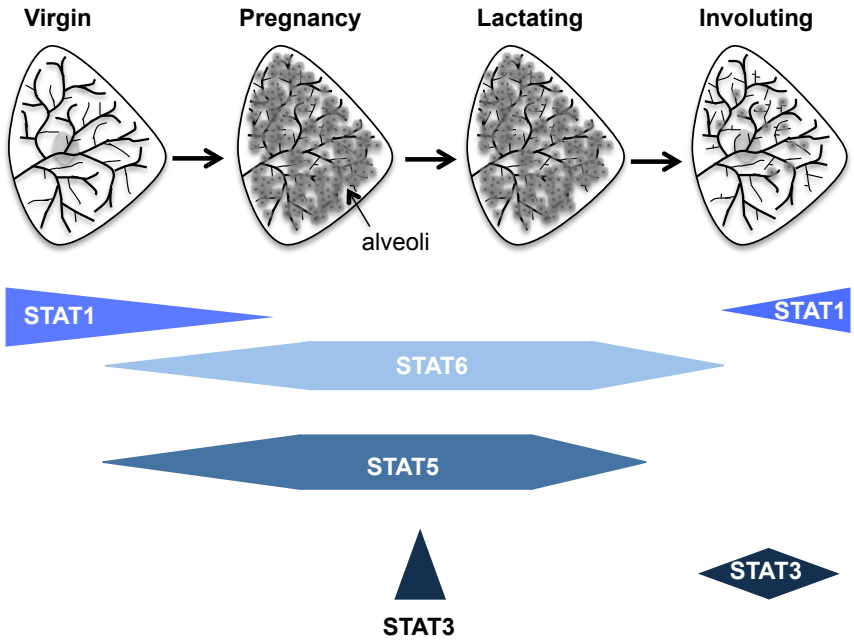


Figure 1.12 Schematic representation of mammary gland development in the virgin, at pregnancy, lactation and involution, showing the expression of the different phosphorylated STAT proteins (Amended from Hughes and Watson 2012).

With the exception of STAT2, all other STAT family members are expressed during mammary gland development (Philp *et al*., 1996, Khaled *et al*., 2007). Furthermore, whilst the *Stat4* transcript could be detected in the nulliparous mammary gland, *Stat4* expression was not detected in a mammary gland cell line suggesting that *Stat4* expression could be limited to non-epithelial cells (Philp *et al*., 1996). Phosphorylation of STAT proteins is the readout for functionality and activated STAT1 is detected in the nulliparous mammary gland and during late involution (Philp *et al*., 1996). However, studies using *MMTV-Cre* and *Wap-Cre* transgenic murine lines to delete *Stat1* expression from mammary gland epithelia demonstrated that STAT1 expression is dispensable for development of the nulliparous mammary gland and at lactation (Klover *et al*., 2010). Whilst activated STAT5 and activated STAT6 proteins are detected in the nulliparous mammary gland (Liu *et* al., 1996, Khaled *et* al., 2007) no apparent defect in development was observed in the absence of STAT6 (Khaled *et al*., 2007). However STAT5 expression is required for the generation of the alveolar progenitor pool required during pregnancy (Yamaji *et al*., 2009), and is required to mediate secondary side branching during oestrus (Santos *et al*., 2010). The function for STAT5 and STAT6 during pregnancy associated mammary gland development and the function for STAT3 during involution of the mammary gland will be discussed in more detail below.

1B.5.1 *STAT6 in luminal cell development*

In the immune system, it has been demonstrated that the differentiation of CD4+ T helper (Th) cells to the T helper 1 (Th1) lineage is induced by interleukin 12 (IL12) signalling through STAT4 (Jacobson *et al*., 1995, Thierfelder *et al*., 1996), whereas differentiation toward the T helper 2 (Th2) lineage is mediated through IL4/IL13 activation of STAT6 (Kaplan *et al*., 1996). Phosphorylated STAT6 is also expressed in the mammary gland being limited to a minority of virgin epithelia, induced at day 5 of gestation where expression is then seen in the majority of ductal/luminal epithelia and remains up regulated at day 15 of pregnancy (Khaled *et al.,* 2007). The importance of the IL4/IL13/STAT6 signalling pathway during pregnancy associated mammary gland development was demonstrated by the observation that in a *Stat6* null murine line, or in mice with the genes for both *IL4* and *IL13* deleted, mammary gland morphogenesis was delayed (Khaled *et al*., 2007). Examination of the *Stat6* null female mammary gland revealed a striking reduction in the number of side-branches and alveolar structures (70%) at pregnancy day 5. This is a potential consequence of reduced proliferation as seen in the reduced number of Ki67 positive alveolar cells and the reduction in cyclin B1/B2 and AKT1 expression levels. As suggested by the ability of

the *Stat6* null female to nurse her pups at parturition, pregnancy associated mammary gland development is not arrested at pregnancy day 5. In fact, by day 15 of pregnancy, although the *Stat6* null mammary gland presents with fewer alveolar structures, alveolar progenitor cells are proliferating at a significantly greater rate, than the alveolar cells in the wild type counterpart (Khaled et al., 2007).

The delay in *Stat6* null mammary gland development during pregnancy, and the ability of the *Stat6* null female to nurse her offspring is reflected in the delayed induction of beta-casein expression (Kahled *et al*., 2007). Interestingly Khaled and colleagues (2007) demonstrated that whilst *IL4* and *IL13* transcript levels were reduced at day 5 of pregnancy, expression levels recovered by day 15 of pregnancy and in fact the expression of *IL4* was increased above that expressed in the wild type counterpart commensurate with the recovery of the *Stat6* null mammary gland. Significantly, in the *Stat6* null murine background, *IL12 alpha* transcript levels were detected at increased levels at day 5 of pregnancy and were still elevated by day 15 of pregnancy. Using opposing systems, these authors (Khaled *et* al., 2007) proceeded to demonstrate a potential role for IL4/IL13 signalling through STAT6 activation by examining pregnancy associated mammary gland morphology in a double *IL4*/*IL13* null genetic background as well as in *Socs5* null genetic background that results in activated *IL4*/*IL13* signalling (Seki *et al*., 2002).

The *IL4/IL13* null double mutant strain also presented with a delay in alveologenesis similar to the mammary gland phenotype presented in the *Stat6* null genetic background, whilst the deletion of *Socs5* resulted in precocious alveolar development (Kahled *et al*., 2007). The KIM-2 cell line can be induced to undergo differentiation upon stimulation with lactogenic hormones (prolactin, dexamethasone and insulin) a process that mimics the differentiation of alveolar cells during pregnancy (Gordon *et al*., 2000). Elegantly, the cytokine expression profile of KIM-2 cells switches from a type-1 to a type-2 cytokine expression profile upon induction of differentiation (Khaled *et al*., 2007). The type-1 cytokines IL12 alpha, interferon (IFN) gamma and tissue necrosis factor (TNF) alpha are expressed by undifferentiated KIM-2 cells at day 2 of differentiation. When the milk protein beta-casein is first expressed, the expression of the type-1 cytokines is markedly down-regulated and the expression of the type-2 cytokines IL4, IL5 and IL13 is induced (Khaled *et al*., 2007). By analogy with the T-helper lymphocyte differentiation system in which Th2 cells secrete IL4 and IL13 that promotes the differentiation of naïve T-helper cells toward the Th2 lineage, Khaled and colleagues (2007) proposed that in the mammary gland, the differentiated luminal population secrete IL4 and IL13 that acts upon the luminal progenitor population to

promote proliferation and differentiation. These data suggest that the elevated expression of *IL12 alpha* expressed in the *Stat6* null genetic background could indicate an imbalance in epithelial lineage determination. The involvement of STAT6 in the regulation of luminal progenitor cell proliferation and commitment to an alveolar lineage demonstrates how cell fate determination during early pregnancy is linked to IL4/IL13 mediated activation of STAT6 (Khaled *et al*., 2007).

1B.5.2 The role of STAT5 in alveologenesis and expression of milk proteins.

STAT5 has a well defined role in the regulation of stem and progenitor cells in the hematopoietic system (Yao *et al*., 2006, Wang *et al*., 2009b). In the mammary gland, binding of prolactin to the prolactin receptor results in receptor dimerization and activation of JAK2 (Darnell *et* al., 1994, Schindler and Darnell 1995). The downstream consequence of JAK2 activation is the phosphorylation and activation of STAT5 (Ihle and Kerr 1995, Schindler and Darnell 1995). Two STAT5 isoforms exist (STAT5A and STAT5B, collectively known as STAT5), sharing 96% homology (Liu *et al*., 1995). Activated STAT5A is expressed in the nulliparous mammary gland at 5 weeks of age (Santos *et* al., 2008) and whilst STAT5A expression is not required for ductal elongation (Yamaji *et al*., 2009), side branching is impaired in the *Stat5a* null genetic background (Santos *et al*., 2010).

Early studies demonstrated the importance of STAT5 in the regulation of the milk protein genes such as beta-lactoglobulin (BLG) (Watson *et al*., 1991, Burdon *et al*., 1994), whey acidic protein (Li and Rosen, 1995) and beta casein (Happ and Groner 1993) an observation later confirmed by genome wide interrogation of STAT5 binding and gene expression analysis in the murine mammary gland of the pregnant female (Yamaji *et al*., 2013).

During the oestrus cycle the murine mammary gland can develop alveoli structures (Fata *et al*., 2001), which consist of epithelial cells that bare the gene signature of an alveolar progenitor population (Shehata *et al*., 2012). Significantly, STAT5A expression in the nulliparous mammary gland is required for the generation and proliferation of alveolar progenitor cells the precursor cells required during pregnancy (Yamaji *et al*., 2009). Expression levels of phosphorylated activated STAT5 increase in the mammary gland during pregnancy (Liu *et* al., 1996) suggesting that the level of STAT5 can control distinct biological programs at different stages of mammary gland development (Cui *et al*., 2004, Yamaji *et al*., 2013). In fact studies have shown that STAT5 expression is required for luminal progenitor cell proliferation and differentiation

toward alveolar buds and the survival of mammary gland epithelia (Liu *et* al., 1997, Liu *et* al., 1998, Cui *et al*., 2004, Yamaji *et* al., 2009 and 2013).

The contribution of the two isoforms of STAT5 (STAT5A and STAT5B) to the development of the pregnant mammary gland most likely reflects expression levels as STAT5A is more abundant than STAT5B and constitutes approximately 70% of STAT5 expression levels (Liu *et al*., 1995). Thus whilst STAT5A expression is required for lobuloalveolar development and terminal differentiation (Liu *et al*., 1997), a phenotype that can be rescued upon STAT5A re-expression (Yamaji *et al*., 2009), an increase in the expression of STAT5B in the *Stat5a* null genetic background can partially compensate for the absence of STAT5A after several rounds of pregnancy (Liu *et al*., 1998).

Interestingly, Yamaji and colleagues (2013) have proposed a two-stage model of STAT5 dose-dependent mammary gland development whereby expression from either a single *Stat5a* or *Stat5b* allele is sufficient for the generation of histologically undifferentiated alveolar units, expression from two alleles is required for the initiation of mammary gland differentiation and the expression of the lactation gene signature, similar to that found with all four alleles (Yamaji *et al*., 2013).

1B.5.3 STAT3 function during involution

During the later stages of pregnancy pSTAT5 expression is required for the survival of the mammary gland epithelia (Cui *et al*., 2004) by positively regulating the expression of pro-survival genes such as AKT (Creamer *et al*., 2010). After the young are weaned, the differentiated mammary gland epithelial cells are redundant and activated STAT5 levels are reduced as STAT3 is activated (Liu *et al*., 1996, Philp *et al*., 1996). This switch between survival and the involution of the mammary is exemplified by the demonstration that inducing the over expression of STAT5 (Creamer *et* al., 2010) or the expression of a constitutive active form of AKT1 (Schwertfeger *et al*., 2001) delays involution of the mammary gland. In keeping with this, mammary gland specific conditional deletion of *Stat3* results in a delay of the first phase of involution and is therefore essential for the initiation of cell death and remodeling of the mammary gland (Chapman *et al*., 1999, Humphreys *et al*., 2002).

Accumulation of milk in the mammary gland lumen post weaning results in the production of leukemia inhibitory factor (LIF) and activation of STAT3 via the glycoprotein 130/JAK complex (glycoprotein 130, gp130) (Kritikou *et* al., 2003, Schere-Levy *et al*., 2003, Zhao *et al*., 2004). Thus, activated STAT3 is absent in *LIF* null

(Kritikou *et* al., 2003) and *gp130* null (Zhao *et al*., 2004) genetic backgrounds and involution of the mammary gland is delayed (Kritikou *et* al., 2003, Zhao *et al*., 2004). Implantation of LIF containing pellets in lactating mammary glands induced STAT3 phosphorylation resulting in an increase in apoptosis (Schere-Levy *et al*., 2003). Significantly, the use of *Stat3* null and *LIF* null murine lines suggested that the regulatory subunits of phosphoinositide-3-OH kinase (PI3K), p55-alpha and p50-alpha are positively regulated downstream of the LIF/JAK/STAT3 signaling pathway, an observation further substantiated by the demonstration that STAT3 can bind the promoter of p55-alpha and p50-alpha *in vivo*. Significantly, in the *Stat3* null background up-regulation of p55-alpha and p50-alpha is abrogated, activated levels of AKT are sustained and apoptosis is prevented (Abell *et al*., 2005). Whilst molecular profiling (Clarkson *et* al., 2004) and studies in *Stat3* null genetic background (Chapman *et al*., 1999) suggested that cell death during the initial, reversible phase of involution was mediated by the classical apoptotic pathway, involution occurs in the absence of executioner caspase 3 and 6 (Kreuzaler et al., 2011). In fact classic signatures of apoptosis such as membrane blebbing and chromatin fragmentation are not observed during the first phase of involution (Kreuzaler et al., 2011). These studies demonstrated that during the first stage of mammary gland involution, epithelia undergo lysosomal membrane permeabilization (LMP) concomitant with an increase in lysosomal protease cathepsin B and L expression. In the absence of STAT3, cathepsin B and L expression is diminished and the expression of the endogenous inhibitor Serpin2A (Spi2A) is up-regulated. Importantly, chemical inhibition (CA-074Me) of cathepsin B delayed involution in wild type mice, and resulted in a reduction in cell death when applied to the murine epithelial cell line EpH4. Furthermore, using the same mammary epithelial cell line EpH4, Kreuzaler and colleagues (2011) further substantiated STAT3 in mediating LMP by demonstrating that chemical inhibition (S3I-201) of STAT3 activation decreased cathepsins B and L protein expression levels and significantly reduced cell death.

During involution there is a marked up-regulation of genes involved in the acute phase response and inflammation (Clarkson *et al*., 2004, Stein *et al*., 2004, Hughes *et al.,* 2012). STAT3 expression mediates cell death (Kreuzaler *et al*., 2011) and regression, post-weaning (Chapman *et al*., 1999). Hughes and colleagues (2012) therefore proposed a potential role for STAT3 in influencing the innate immune environment and the influx of inflammatory cells into the mammary gland. Using the *BLG-Cre* system to produce a mammary gland specific *Stat3* null murine line, the acute phase response genes were analysed 24 and 48 hours after forced weaning. The ablation of *Stat3* resulted in the down-regulation of several acute phase response genes, as compared

to the wild type counterpart. Expression of CD14 on the apical surface of the mammary luminal epithelia was also reduced at 24 hours but not later, suggesting that the proposed acquisition of a phagocytic phenotype by mammary gland epithelia (Stein *et al*., 2003) is part of the involution program dependent upon STAT3 expression. In the second phase of involution – after 48 hours, the expression of chitinase 3-like 1 (Chi3Li) a factor associated with inflammatory conditions and wound healing (Lee *et al*., 2011), was decreased in the *Stat3* null murine line. In this second phase of involution STAT3 transcriptional activation of *Chi3Li* expression is induced by oncostatin M (OSM) operating through the OSM receptor, indicating a causal link between STAT3 expression, the regulation of *Chi3Li* and therefore wound healing response. The increase in the number of macrophages and mast cells normally seen in the second phase of involution is also reduced in the *Stat3* null mammary gland, a phenomenon that may be indirectly related to STAT3 and thus reflect a delay in involution and therefore a reduction in the number of dead epithelia. Interestingly during involution macrophages are polarized towards an alternatively activated (M2) phenotype (O'Brien *et al*., 2010), yet in the absence of STAT3 the macrophage phenotype is also altered, favouring the M1 phenotype, evidenced by an increase expression of inducible nitric oxide synthetase (iNOS) (Hughes *et al*., 2012). This is a significant observation given that macrophage M1 activity results in tissue damage whereas macrophage M2 activity promotes tissue repair (*Mills,* 2012).

Thesis aims

1C Aims:

Chapter 3

In order to study the function of KDM5B *in vivo*, the *Kdm5b* locus was targeted. The aims were to:

(1) Assess the effect of ablating KDM5B *in vivo* (*B6;129-Kdm5b-Exon 1* knockout)
(2) To develop and characterise the *B6;129-Kdm5b ΔARID* murine line

Chapter 4

In Chapter 3 preliminary studies on the chimeric B6;129-*Kdm5b ΔARID* murine line have indicated that KDM5B is required for normal mammary gland ductal morphogenesis. However the influence of genetic background on mammary gland morphogenesis has complicated the interpretation of the presenting phenotype in the chimeric B6;129-*Kdm5b ΔARID* female. In addition, studies on WT KDM5B expression in the mammary gland are limited. Therefore, understanding the role of KDM5B during mammary gland development could be advanced by the following aims:

(1) To examine the pattern and level of KDM5B expression during mammary gland morphogenesis in the C57BL/6J female.
(2) To backcross the chimeric B6;129-*Kdm5b ΔARID* murine line onto the inbred C57BL/6J genetic background.
(3) To characterise the mammary gland phenotype presented in the C57BL/6J-*Kdm5b ΔARID* female

Chapter 5

Using the C57BL/6J-*Kdm5b ΔARID* murine line we have investigated the effect of KDMB ΔARID expression on gene expression by:

(1) Examining the effect of KDM5B ΔARID expression on ER alpha target gene regulation during mammary gland development.
(2) Investigating the ability of KDM5B and KDM5B ΔARID to interact with ER alpha.
(3) Examining in the mammary gland, the effect of KDM5B ΔARID expression on the repression of demethylase-dependent KDM5B target genes.
(4) Examining in the mammary gland, the effect of KDM5B ΔARID expression on the AKT and STAT5 signaling pathways.

Chapter 6

Using the C57BL/6J-*Kdm5b ΔARID* murine line we have investigated the effect of KDMB ΔARID expression on mammary gland tumour development.

Chapter 2: Materials and methods

Chapter 2 Materials and methods

All chemicals and solvents were supplied by Merck Ltd (unless otherwise stated)

2.1 Solutions and buffers

Carmine solution	0.5% carmine dye w/v, 0.2% aluminum potassium sulfate
Carnoy's fixative	75% ethanol, 25% glacial acetic acid
lysis buffer	50mM Tris.HCl (pH 8.0), 150mM NaCl, 10% glycerol, 0.5% Triton X-100
TE	10mM Tris.HCL (pH8.0), 1mM EDTA
Tissue lysis buffer	50mM Tris.HCl (pH 8.0), 100mM EDTA, 100mM NaCl, 1% SDS
1% acid alcohol	1% HCL, 70% IMS
6x DNA loading buffer	30% (v/v) glycerol, 0.25% (w/v) bromophenol blue, 0.25% (w/v) xylene cyanol FF
1x TAE	40mM Tris, 20mM acetic acid, 1mM EDTA
20x SSC	3M sodium chloride, 0.3M sodium citrate
2x Laemmli sample buffer	120mM Tris-HCL (pH6.8), 4% SDS, 20% (w/v) glycerol, 0.02% (w/v) bromophenol blue

1x SDS-PAGE running buffer	25mM Tris (pH8.3), 192mM glycine, 0.1% SDS
1x Towbin buffer (PAGE transfer buffer)	25mM Tris (pH8.3), 192mM glycine, 20% methanol

2.2 General statement

Targeting construct used to generate the B6;129-*Kdm5b-Exon 1* knock out and the C57BL/6J-*Kdm5b ΔARID* murine lines was designed and constructed by Dr Samantha Santangelo, KCL.

Transfection of targeting vector into ES cells and subsequent injection of positive clones into the blastocysts or 8-cell embryos and pseudopregnant female was carried out by the Cancer Research UK Transgenic Mouse Service Laboratory, headed by Dr Ian Rosewell.

Southern blot of transfected embryonic stem (ES) cells and screening of the B6;129-*Kdm5b-Exon 1* knock out line was done with the help of Debbie Hall, KCL

I would like to thank Dr. Bradley Spencer-Dene at the London Research Institute, Cancer Research UK, for his patience in teaching me how to dissect inguinal mammary glands (4th from the neck) and the thoracic mammary glands (3rd from the neck) from the B6;129-*Kdm5b WT* and B6;129-*Kdm5b* ΔARID females (as well as on the C57BL/6J genetic background).

Staged pregnancies were arranged with Janet Macdonald at the Biological Service Unit, Cancer Research UK.

Pathology on the B6;129-*Kdm5b* ΔARID murine line was performed by Professor Gordon Stamp, Cancer Research UK. *In situ* hybridization on the C57BL/6J-*Kdm5b WT* mammary gland series was performed by Dr Richard Poulson at Cancer Research Services.

2.3 Cell culture

COS-7 (CV-1 in origin, carrying SV40), an African green monkey kidney fibroblast-like cell line was maintained in Dulbecco's modified Eagle's medium (DMEM, Life

technologies), supplemented with 10% FCS (Fisher scientific), 2mM L-glutamine and 100U/ml Penicillin-Streptomycin (Life technologies). COS-7 cells were maintained in a humidified atmosphere of 5% CO_2 and 37^{o}C. A sub-cultivation ratio of 1:5 was used to maintain the cell line.

2.4 Preparation and analysis of DNA

2.4.1 Phenol:chloroform extraction and precipitation of tail-snip genomic DNA

5mm of tail-snip tissue was incubated overnight at 55°C in 180 μl of tissue lysis buffer (Qiagen) supplemented with 2mg/ml of proteinase K (Qiagen). The DNA was extracted from the aqueous phase following addition of an equal volume of 25:24:1 phenol:chloroform:isoamylalcohol (Sigma-Aldrich), emulsification and centrifugation at 16,000g for 5 minutes at room temperature. Extraction and centrifugation were repeated with 25:24:1 phenol:chloroform:isoamylalcohol and water saturated chloroform. The DNA was precipitated from the aqueous phase at room temperature for 1 minute with an equal volume of isopropyl alcohol and 1/10th volume of 3M sodium acetate (pH4.8, Sigma-Aldrich). The DNA was pelleted by centifugation at 16,000g for 1 minute at room temperature. The DNA pellet was washed twice with 70% ethanol, air-dried for 5 minutes at room temperature and re-suspended in 40μl TE (pH8.0)

2.4.2 Determining the concentration of DNA

The concentration of dsDNA was determined using a spectrophotmeter where the absorbance reading of 1 unit at 260nm is equivalent to 50μg/ml of dsDNA

2.4.3 Restriction endonuclease digest of (A) B6;129-Kdm5b-Exon 1 knock out and (B) *B6;129-Kdm5b ΔARID genomic DNA for Southern blot analysis*

(A) *B6;129-Kdm5b-Exon 1* knock out

Stock Solution	Final concentration
10x buffer 4 (NEB)	1x
10,000U/ml BciVI (NEB)	200U
Genomic DNA	10μg
Water	upto100μl

(B) *B6;129-Kdm5b ΔARID*

Stock Solution	Final concentration
10x BamH1 buffer (NEB)	1x
20,000U/ml BamH1(NEB)	200U
Genomic DNA	10μg
10mg/ml BSA (100x)	10μg (1x)
Water	upto 100μl

Genomic DNA was incubated over night at 37°C and the DNA precipitated at -20 °C in 2.5 volumes of ethanol (v/v) and 1/10th volume of 3M sodium acetate (pH4.8) for 60 minutes. The DNA was pelleted by centifugation at 14,000g for 5 minutes, washed twice in 70% ethanol, air dried at room temperature and re-suspended in 20μl of TE (pH8.0)

2.4.4 Agarose gel electrophoresis of DNA

Agarose gel electrophoresis was performed using a 2% (w/v) agarose gel for quantitative PCR, a 1.0% (w/v) or a 1.5% (w/v) agarose gel for end-point PCR and 1% (w/v) agarose for Southern transfer containing 0.5 μg/ml ethidium bromide in 1x TAE buffer.

2.4.5 Genotype screening by Southern transfer

Digested genomic DNA separated by agarose gel electrophoresis (1% w/v) over night at 1V/cm was partially depurinated in 10 volumes of 0.25M HCL for 10 minutes followed by incubation in 10 volumes of 0.4M NaOH for 20 minutes at room temperature. DNA was covalently linked to positively charged nylon membrane (GE Healthcare Life Sciences) by downward alkaline capillary transfer for 60 minutes. After transfer the nylon membrane was neutralised by a briefly wash in 2x SSC.

To screen the B6;129-Kdm5b-Exon 1 knock out murine line for integration of the targeting construct a 999bp fragment was amplified with *Kdm5b* specific primers (sense: 5'-GTATGCCCCTCACTAAAGGG-'3 and anti-sense: 5'-GCGCGTTAGACACTATCACG-3') using 100ηg of the targeting construct plasmid DNA, and the following PCR cycling conditions: 94°C for 5 minutes, then 30 cycles at, 94°C for 1 minutes, 60°C for 1 minutes, 72°C for 1 minutes.

To screen the B6;129-Kdm5b ΔARID murine line for integration of the targeting construct a 1.2Kb fragment was amplified with *Kdm5b* specific primers (sense: 5'-TCCAGCGTAAGTCTGTTCTCC-'3 and anti-sense 5'-CTTTACTAGCAACGGCAACACG-'3) using 100ηg of the targeting construct plasmid DNA, and the following PCR cycling conditions: 94°C for 5 minutes, then 30 cycles at, 94°C for 1 minute, 56°C for 1 minute, 72°C for 1 minute.

PCR products were resolved on a 1% agarose gel, excised and purified using Wizard SV gel and PCR clean up systems (Promega) according to manufacture's instructions. Incorporation of [α-^{32}P]-dCTP (PerkinElmer) was achieved by internal random primer extension using 50ηg of template DNA and unincorporated [α-^{32}P]-dCTP removed using Sephadex S-300 spin columns according to manufacture's instructions (GE Healthcare Life Sciences).

Prior to the addition of the probe, the nylon membrane was blocked for 3hrs at 42^{O}C in Ultrahyb (Ambion). Hybridisation was overnight in Ultrahyb at 42^{O}C followed by increasingly stringent washes as follows. The membranes were washed twice using an excess volume of 2xSSC/0.1%SDS at 42^{O}C for 10 minutes. Non-specific binding of the probe to the nylon membrane was checked using a Geiger counter with a beta probe. The nylon membrane was then washed twice using an excess volume of 0.1xSSC/0.1%SDS at 65^{O}C for 10 minutes or until the non-specific signal was reduced to background levels. The nylon membrane was then exposed to autoradiography film (GE Healthcare) and the cassette stored overnight at -80^{O}C. The cassette was warmed on the bench to room temperature and signal developed using a X-ray film developer.

2.4.6 End point PCR on C57BL/6J mammary gland cDNA and sequencing

PCR primers specific to *Kdm5b exon 1 and exon 5* (sense: 5'-CGCTTTCATCCACAAGATCC–3' and anti-sense 5'– CAGACTGCCTCTGGGGAATA-3' respectively), were used to amplify cDNA generated from RNA isolated from mammary gland tissue or testis, using the following PCR cycling conditions: 94°C for 5 minutes, then 30 cycles at, 94°C for 1 minute, 60°C for 1 minute, 72°C for 1 minute. PCR products were resolved on a 1.5% (w/v) agarose gel, excised and purified using Wizard SV gel and PCR clean up systems (Promega) according to manufacture's instructions. DNA sequencing reactions were performed using BigDye terminator v3.1

Cycle Sequencing kit and the 3730 DNA Analyzer (Life Technologies) at Cancer Research UK.

2.4.7 B6;129-Kdm5b-Exon 1 knock out *PCR screen to identify homologous recombination*

PCR amplification reactions were performed using the following PCR cycling conditions: 94°C for 5 minutes, then 30 cycles at, 94°C for 1 minute, 60°C for 1 minute, 72°C for 1 minute.
To amplify the *WT allele* the following primer pairs were used:
Sense 5'-TGGATTGTAACTCTGTTCTCCCTAC-3'
Anti-sense 5'-TTCTACTAGCAACGGCAACACCTAG-3'
To amplify the integrated targeting vector the following primer pairs were used:
Sense 5'-CATCTGTCAGACCCTTAGTACGCTA-3'
Anti-sense 5'- GCTACCGGTGGATGTGGAATGTGTG-3'

2.4.8 PCR screen used to detect heterozygous B6;129-Kdm5b ΔARID offspring during backcross to the C57BL/6J genetic background

PCR amplification reactions were performed using neomycin specific PCR primers:
Sense 5'-TGCTCCTGCCGAGAAAGTATC-'3
Antisense 5'- CCACCCCCCAGAATAGAATGAC-'3 and the following PCR cycling conditions: 94°C for 5 minutes, then 30 cycles at, 94°C for 1 minute, 60°C for 1 minute, 72°C for 1 minute.

2.4.9 PCR screen used to detect the polyoma virus middle T antigen transgene (PyV-mT)

PCR amplification reactions were performed using PyV-mT specific PCR primers:
Sense 5'-CCAGAACTCCTGTATCCAGAAGC-3'
Anti-sense 5'-GGATGAGCTGGGGTACTTGTTCCC-3' and the following PCR cycling conditions: 94°C for 5 minutes, then 30 cycles at, 94°C for 1 minute, 60°C for 1 minute, 72°C for 1 minute.

2.4.10 Generation of chemically competent Escherichia coli (E.Coli)

The *E.Coli* stain DH5 alpha were inoculated in 5ml of LB broth and grown overnight at 37^{O}C with shaking. 100ml of LB broth was inoculated with 1ml of overnight culture,

incubated at 37^{O}C and grow until mid-log phase (OD@550nm = 0.2-0.5). *E.Coli* where chilled on ice, pelleted by centrifugation at 4000g for 5 minutes at 4^{O}C and re-suspended in ice-cold sterile 60mM calcium chloride. *E.Coli* were Incubated on ice for 30 minutes, pelleted by centrifugation at 4000g for 5 minutes at 4^{O}C, re-suspended in 5ml of ice-cold sterile 60mM calcium chloride and stored in 100μl aliquots at -80^{O}C.

2.4.11 Transformation of competent E. Coli

A 100μl aliquot of competent DH5 alpha bacterial cells were thawed on ice spiked with 100ηg of plasmid DNA, mixed gently and then incubated on ice for 30 minutes followed by heat-shock at 42^{O}C for 30 seconds. The transformed DH5 alpha bacterial cells were incubated in 1ml of LB broth at 37^{O}C for 60 minutes, centrifuged at 500g for 5 minutes and re-suspended in 20μl of LB broth. Re-suspended DH5 alpha bacterial cells were spread on LB-agar plates under selection with 100μg/ml ampicillin (Life technologies). Following incubation of LB-agar plates overnight at 37^{O}C, an ampicillin resistant colony was picked and used to inoculate 5mls of LB broth containing 100μg/ml ampicillin. Inoculated LB broth was incubated overnight at 37^{O}C with agitation in a shaking incubator (300rpm).

2.4.12 Large-scale preparation of plasmid DNA

Large-scale preparation and purification of plasmid DNA was achieved using Qiagen maxi-prep kit as detailed in manufacture's instructions. Briefly, 1ml of the overnight culture (detailed in 2.4.11) was used to inoculate 500ml of LB broth containing 100μg/ml ampicillin and incubated overnight at 37^{O}C with agitation in a shaking incubator (300rpm). The bacterial culture was centrifuged at 6000g for 15 minutes at 4^{O}C and the bacterial pellet lysed under alkaline conditions. The solution was neutralized and cleared by centrifugation at 20,000g for 30 minutes at 4^{O}C. The plasmid DNA was bound to the column resin under low-salt and low-pH conditions. RNA and proteins were removed by a medium salt wash, followed by elution of plasmid DNA in a high-salt buffer and subsequent isopropanol precipitation. Contaminating salts were removed by a 70% ethanol wash, the pellet air-dried for 10 minutes at room temperature and the DNA re-suspended in 500μl TE (pH8.0).

2.3.13 Plasmid constructs

The human expression constructs, pcDNA3.1 Myc-HisA KDM5B were generated in house (Lu, et al., 1999). pcDNA3.1 Myc-HisA KDM5B ΔARID was a kind gift from Dr C.D.Chen (Xiang, et al., 2007) and pXJ41neo-Ha-ER alpha was a kind gift from Dr W. Hong (Chan et al., 2001).

2.5 Preparation and analysis of RNA

2.5.1 Extraction of total RNA

Inguinal mammary glands including the lymph node (4th from the neck) and the adult testis were collected, snap frozen in liquid nitrogen and total RNA isolated using the RNeasy Lipid tissue kit (Qiagen) according to manufacture's instructions. The extraction procedure couples the guanidine thiocyanate with phenol-chloroform total RNA extraction method (Chomczynski and Sacchi, 1987) with silica gel membrane purification. In brief, tissue was homogenised in QIAzol lysis reagent (guanidine thiocyanate, phenol mix) and mixed vigorously after the addition of chloroform. The RNA containing aqueous phase was separated from the organic phase by centrifugation at 12,000g for 15 minutes at 4^{o}C. The RNA containing upper aqueous phase was removed and the silica-gel binding conditions optimized by the addition of an equal volume of 70% ethanol. The RNA was bound to the silica-gel containing columns by centrifugation at 12,000g for 15 seconds at room temperature and contaminants removed by wash steps and subsequent centrifugation. The RNA was eluted from the silica-gel containing columns in 30μl of RNase-free water by centrifugation at 12,000g for 1 minute at room temperature. The RNA was stored at -80^{o}C.

2.5.2 Determining the concentration of RNA

The concentration of RNA was determined using a spectrophotometer where the absorbance reading of 1 unit at 260nm is equivalent to 40μg/ml of RNA

2.5.3 cDNA synthesis

cDNA was generated from total RNA isolated from the mammary gland or testis using the SuperScript III First-Strand Synthesis System for RT-PCR kit (Life Technologies)

according to manufacturer's instructions. In brief, 0.5μg of total RNA was incubated with random hexamers and a dNTP mix at 65^{O}C for 5 minutes to denature the RNA and then placed on ice for 1 minute. To generate cDNA, a cDNA synthesis cocktail consisting of the M-MLV reverse transcriptase was added to the RNA/random hexamer mix and the sample incubated at room temperature for 10 minutes, followed by incubation at 50^{O}C for 50 minutes. The reaction was terminated at 85^{O}C for 5 minutes and the RNA digested in the presence of RNase H at 37^{O}C for 20 minutes. Samples were stored at -80^{0}C.

2.5.4 Quantitative PCR and PCR primers

Relative quantification of target gene levels was achieved using SYBR Green JumpStart ReadyMix (Sigma-Aldrich) according to manufacture's instructions and the Opticom 2 continuous fluorescence detector. Normalisation was against 18s ribosomal RNA in separate tube reactions. To prevent amplification of genomic DNA PCR primers were designed to span intronic regions. The reactions were visualised by agarose gel electrophoresis to confirm target amplicon size. The $2^{-\Delta\Delta CT}$ method (Applied Biosystems; User Bulletin No. 2) was used to calculate the target gene expression level relative to the mammary gland identified as expressing the highest level of the target gene. Target gene and control gene amplification rates were comparable. Each group is represented as an average. For all the primers listed in table 2 the PCR cycle parameters used are: 94°C for 5 minutes, then 40 cycles at 94°C for 15 seconds, 60°C for 30 seconds, 72°C for 40 seconds.

Gene	Sense primer (5'- 3')	Anti-sense primer (5'- 3')
Kdm5b	CGATAAACTTCATTTCACCCCG	ACCCACCTTCTTCTGCGACTAAC
18s	CTTCTTAGAGGGACAAGTGGCGTTCAG	AACTGATCCTCCAAACCTCTTCTC
Wnt4	GAGTGCCAATACCAGTTCCG	CCAGCCTCGTTGTTG
Pgr	PRCCCACAGGAGTTTGTCAAACT	TCCGGGATTGGATGAATG
Esr1	CTAGCAGATAGGGAGCTGGTTCA	GGAGATTCAAGTCCCCAAAGC
Bub1	CATATGCAAAGCTACACGGGTAA	TGTAGTAGTTCTTTAGGTTCAGCCTC
Mt1f	TGCAAGAACTGCAAGTGCACCTC	CGGCGCCTTTGCAGACACAG
Brca1	TCTTGTGAGCGTTTGAATGAGGAGG	AGGTTGGGTCTGCCTGTTTTTCTTC
Kdm5a	GATTGACTCTGGCGTAGGCTTGGCACC	GGACAACACATTGGGTAGAAAGGCTGG

Table 2 Table listing primer sequences used in quantitative PCR.

2.6 Preparation and analysis of protein

2.6.1 Nuclear and cytoplasmic protein extraction

Inguinal mammary glands (4th from the neck) and testis were collected, snap frozen in liquid nitrogen and nuclear protein extracts isolated using NE-PER nuclear and cytoplasmic extraction reagents (Thermo scientific) as detailed in manufacturer's instruction. All steps were carried out at 4^{O}C. In brief, tissue was cut into small pieces, homogenised in phosphate buffer solution (PBS) and cells pelleted by centrifugation at 500g for 3 minutes at 4^{O}C. The supernatant was removed and a 10-fold packed cell volume of reagent 1 added to the cell pellet. The sample was vortexed at the highest setting for 15 seconds and the sample incubated on ice for 10 minutes. Reagent 2 was then added, the sample vortexed at the highest setting for 5 seconds and the sample incubated on ice for 1 minute. The sample was centrifuged at 16,000g for 5 minutes at 4^{O}C and the cytoplasmic fraction (supernatant) removed. The pelleted nuclear fraction was re-suspended in reagent 3 and vortexed on the highest setting for 15 seconds. The nuclear fraction was returned to ice and vortexed for 15 seconds every 10 minutes for a total of 40 minutes. The nuclear fraction was centrifuged at 16,000g for 10 minutes and the supernatant (nuclear extract) removed and stored at -80^{O}C.

For the detection of KDM5B, ER alpha, STAT6, STAT5 and phosphorylated STAT5 expression, nuclear extracts were subject to SDS-PAGE electrophoresis and Western blot transfer. For the detection of WAP, beta-casein, AKT and phosphorylated AKT expression, cytoplasmic extracts were subject to SDS-PAGE electrophoresis and Western blot transfer.

2.6.2 SDS-PAGE electrophoresis and Western blot transfer

For nuclear or whole cell extracts protein concentration was determined based on the Bradford method (Bradford, 1976, Bio-Rad) according to manufacture's instructions. Either 20 μg of nuclear protein extract or 30 μg of whole cell extract were used. Laemmli sample buffer was added to give a final concentration of 1x Laemmli sample buffer, 0.1M DTT. Samples were heated at 100^{O}C for 5 minutes. Protein samples were separated on a 6% polyacrylamide gel (30% acrylamide:bis-acrylamide, Bio-Rad) using SDS-PAGE running buffer. Samples were run on a Mini-PROTEAN (Bio-Rad) electrophoresis system at 20V/cm for 120 minutes. Proteins were transferred in 1x Towbin buffer to Hybond C extra nitrocellulose membrane (Life technologies) using the

Mini Trans-Blot system (Bio-Rad) at 30V/90mA overnight at 4^{O}C. Non-specific protein binding sites were blocked by incubating the membranes in an excess volume of blocking buffer ((5% non-fat milk powder (w/v), 0.2% Tween-20 in PBS)) at room temperature for 60 minutes. The membranes were incubated with the appropriate primary antibody (see table 2.1) diluted in binding buffer (2% non-fat milk powder, 0.1% Tween-20 in PBS) for 60 minutes at room temperature. The membranes were washed three times in an excess volume of PBS plus 0.2% Tween-20 for 10 minutes at room temperature and incubated with the appropriate secondary antibody at room temperature in binding buffer for 60 minutes (table 2.2). The membranes were washed three times in an excess volume of PBS plus 0.2% Tween-20 for 10 minutes and once in PBS only. Membrane bound immuno-complexes were detected by enhanced chemiluminescence on autoradiography film (GE Healthcare). The signal was developed using a X-ray film developer. To remove membrane bound immuno-complexes, membranes were submerged in stripping buffer (62.5mM Tris-HCL, pH6.7, 2% SDS, 100mM 2-Mercaptoethanol) for 30 minutes at 50^{O}C with occasional agitation,. The membranes were washed in copious amounts of PBS, and the removal of membrane bound immuno-complexes confirmed by enhanced chemiluminescence on autoradiography film (GE Healthcare). The signal was developed using a X-ray film developer.

2.6.3 Primary antibodies used for Western blot

Antibody	Immunogen	Dilution/ concentration[a]	Reference/ supplier
AKT (rabbit polyclonal)	Raised against a peptide mapping at the C-terminus of AKT of mouse origin	1:500[a]	Cell signaling
Beta-casein (goat polyclonal M-14)	Raised against a peptide mapping at the C-terminus of beta-casein of mouse origin	0.4μg/ml	Santa Cruz
ER alpha (rabbit polyclonal MC-20)	Raised against a peptide mapping at the C-terminus of ER alpha of mouse origin	0.4μg/ml	Santa Cruz
Hemagglutinin (mouse monoclonal – clone 16B12)	Raised against the peptide CYPYDVPDYASL	1μg/ml	Covance
KDM5B (rabbit polyclonal)	Raised against the C-terminus domain of KDM5B corresponding to aa 1283-1473 of human origin	1:1500	Barrett et al; 2002
Lamin B (goat polyclonal)	Raised against a peptide mapped to the C-terminus domain of Lamin B1 of human origin	1.3μg/ml	Santa Cruz
Phospho-AKT (rabbit monoclonal 193H12)	Raised against a synthetic phospho-peptide corresponding to residues surrounding Ser473 of mouse AKT	1:500	Cell Signaling
Phospho-STAT5 (rabbit monoclonal C11C5)	Raised against a synthetic phospho-peptide of Stat5a corresponding to residues surrounding Tyr694	1:500	Cell signaling
STAT5 (rabbit polyclonal C-17)	Raised against a peptide mapping at the C-terminus of STAT5 of mouse origin	0.4μg/ml	Santa Cruz
STAT6 (rabbit polyclonal M-20)	Raised against a peptide mapping at the C-terminus of STAT6 of mouse origin	0.4μg/ml	Santa Cruz

2.6.3 Primary antibodies used for Western blot continued

Antibody	Immunogen	Dilution/ concentration[a]	Reference/ supplier
WAP (goat polyclonal M-16)	Raised against a peptide mapping at the C-terminus of whey acidic protein of mouse origin	0.4μg/ml	Santa Cruz

Table 2.1 Table listing primary antibodies used for Western blot ([a]Dilution factor is given where concentration is not know).

2.6.4 Secondary antibodies used for Western blot

Antibody	Concentration	Supplier
Rabbit anti mouse HRP conjugate	1.3μg/ml	Dako
Goat anti rabbit HRP conjugate	1.3μg/ml	Dako
Rabbit anti goat HRP conjugate	1.3μg/ml	Dako

Table 2.2 Table listing secondary antibodies used for Western blot

2.6.5 Transient transfection of plasmid DNA

COS-7 cells were transfected with plasmid DNA using Lipofectamine LTX according to manufacturers instruction (Life technologies). Briefly, COS-7 were seeded at $1x10^6$ per 10cm plate (Gibco) in 10% FCS DMEM media (with supplements as described in 2.3) and allowed to establish overnight (as described in 2.3). To 2ml of serum free, antibiotic free DMEM media, a total of 16μg of plasmid DNA was incubated at room temperature with an equal volume of PLUS Reagent (equal volume of PLUS Reagent to [DNA]) for 15 minutes. 35μl of Lipofectamine LTX was added to the above DNA:PLUS solution, mixed and incubated at room temperature for 25 minutes. The 10% FCS DMEM media was removed from the COS-7 cells and replaced with 8ml of 10% FCS DMEM (with supplements) plus the DNA:liposome complex and incubated at 37°C in a 5% CO_2 incubator overnight. The transfection media was then replaced with 10% FCS DMEM media (with supplements) and the COS-7 cells incubated at 37°C in a 5% CO_2 incubator for 48 hours.

2.6.6 Immunoprecipitation

Forty-eight hours post-transfection, COS-7 cells were washed twice with PBS, then lysed for 15 minutes on ice in lysis buffer, plus EDTA-free complete protease inhibitor cocktail (Roche). Cells were passed ten times on ice through a fine gauge needle, and centrifuged at 16,000g for 5 minutes at 4°C to pellet cell debris. The supernatant was pre-cleared with protein A/G agarose beads (Pierce) with rotation for 60 minutes at 4°C. Samples were centrifuged at 16,000g for 1 minute at 4°C and supernatant removed to a pre-chilled tube. To 300μg of supernatant, antibody conjugated agarose was incubated over-night with rotation at 4°C (Table 2.3). The samples were centrifuged at 16,000g for 1 minute at 4°C to pellet the agarose, the supernatant discarded and the agarose washed three times in ice cold PBS plus 0.1% Nonidet-P40 with rotation at 4°C for 10 minutes. The samples were centrifuged at 16,000g for 1 minute at 4°C and the agarose re-suspended in an equal volume of 2x Laemmli sample buffer (final [DTT] 0.1M). The samples were heated at 100°C for 5 minutes, centrifuged at 16,000g for 1 minute at room temperature and the supernatant removed and stored at -80°C.

2.6.7 Antibodies used for immunoprecipitation

Antibody	Immunogen	Concentration	Supplier
HA.11 (Clone 16B12-mouse monoclonal)	Raised against the peptide epitope YPYDVPDYA	40μg[b]	Covance
Histidine (mouse monoclonal)	Raised against poly-Histidine tagged fusion protein	40μg[b]	Sigma

Table 2.3 Table listing antibodies used for immunoprecipitation

[b] Purified antibody is coupled to cyanogen bromide activated agarose at 2-2.4 mg antibody per ml bed volume.

2.7 Murine studies

2.7.1 Development of the B6;129-Kdm5b ΔARID mouse strain and backcross to the C57BL/6J *genetic background*

A *Kdm5b* targeting vector was designed to replace exon 2 to 4. The targeting vector was generated by flanking the loxP-neomycin-LoxP expression cassette with genomic sequence amplified from the sv129/ola murine strain. The 5' 7.3Kb homologous region comprised of intron 2 and 48bp of exon 2 and the 3' homologous region comprised of 1.2Kb of intron 5. After injection of the construct into male 129/ola ES cells, screening of G418-selected (200μg/ml) ES clones was performed by Southern hybridization using a PCR generated probe (1.2kb) within the 3' homologous region. A positive clone (2F9) carrying the integrated targeting vector was injected into C57BL/6J blastocyst to generate a single mouse lineage homozygous for the transgene. The *B6;129* chimeric strain was backcrossed over six generations onto the C57BL/6J genetic background to give the C57BL/6J-*Kdm5b ΔARID* murine strain.

2.7.2 Development of the B6;129-Kdm5b-Exon 1 knock out murine line

A *Kdm5b* targeting vector designed to replace exon 1 was generated by flanking the loxP-neomycin-LoxP expression cassette with genomic sequence amplified from the 129/ola murine strain. The 5' 2.4 kb homologous region (HR1) and the 3' 5.7 kb homologous region (HR2) comprised of intronic 1 and 2 sequences respectively. After injection of the construct into male B6;129 ES cells, screening of G418-selected (200 μg/ml) ES clones was performed by Southern hybridization using a PCR generated probe within the 3' homologous region. Two positive clones (1A4, strain 1 and 1A8, strain 2) carrying the integrated targeting vector were injected into either C57BL/6J blastocysts (1A8) or C57BL/6J embryos at the 8 cell stage (1A4) of development.

2.7.3 Breeding program between the C57BL/6-Kdm5b ΔARID -/- and the FVB-MMTV-PyV-mT +/- murine lines

Homozygous *Kdm5b* ΔARID female mice on a C57BL/6J background (C57BL/6J-*Kdm5b ΔARID -/-*) were mated with FVB male mice heterozygous for the Polyomavirus middle T driven by the mouse mammary tumour virus promoter (FVB-*MMTV-PyV-mT*+/-). Males from the progeny were screened for the polyoma middle T integration by PCR on DNA prepared from tail snips and neomycin integration (ΔARID) by Southern

blot. Male off-spring (B6FVBF1) heterozygous for *PyV-mT* (+/-) and *Kdm5b* ΔARID (+/-) integration were crossed with homozygous C57BL/6J-*Kdm5b ΔARID (-/-)* female mice to obtain male progeny homozygous for *Kdm5b ΔARID (-/-)* integration and heterozygous for *PyV-mT* integration *(+/-)* (B6FVBF2). The *Kdm5b ΔARID (-/-)* : *PyV-mT* (-/+) male mice were bred with C57BL/6J-*Kdm5b ΔARID* (-/-) female mice and the *Kdm5b ΔARID (-/-)* : *PyV-mT* (-/+) female progeny monitored for tumour development (B6FVBF3). Control mice (Control/PyV-mT mice) were derived by breeding FVB-*MMTV-PyMT*+/- male mice with C57BL/6J female mice for 3 generations, the equivalent number of crosses required to obtain the *Kdm5b ΔARID (-/-)* : *PyV-mT* (-/+) test murine line. Test and control mice were examined three times per week for the development of tumours, and the time of first appearance noted (see figure 5.6).

2.7.4 Staging pregnancy and synchronising oestrous cycle

For staged pregnancies, observation of vaginal plug was designated as day zero. To ensure accuracy of staged pregnancies, embryos were assessed for stage of embryonic development at the point of mammary gland harvest. To study the development of the nulliparous mammary gland the female mice were caged together from birth in order to synchronize the estrous cycle, although cytological smear examinations were not performed to unequivocally stage the cycle. For the collection of mammary gland tissue females were culled by carbon dioxide inhalation.

2.8 Cell biology techniques

2.8.1 Histology

The left-sided thoracic mammary glands (3rd from the neck) were formalin-fixed over night at room temperature in an excess volume of 10% neutral buffered formalin (Sigma-Aldrich) and paraffin embedded. Paraffin-embedded sections (4μm) were mounted on slides and incubated for 2 minutes in two changes of xylene to de-wax the sections. To serially hydrate the sections the slides were incubated for 2 minutes with two changes of 100% ethanol and incubated for 2 minutes with one change of 70% ethanol. Slides were placed in a tray of running tap water for 2 minutes and stained in Mayer's haematoxylin (Sigma-Aldrich) for 5 minutes. The slides were placed in a tray of running tap water for 1 minute and incubated in 1% acid alcohol for 5 second. Slides were placed in a tray of running tap water for 3 minutes and incubated in 1% Eosin for 4 minutes. The slides were placed in a tray of running tap water for a few seconds and

serially dehydrated in 70% ethanol for 5 seconds and incubated for 1 minute with two changes of 100% ethanol. Slides were incubated for 2 minutes in xylene to remove the alcohol and mounted under cover slip. Sections were viewed using an Olympus BX50 microscope.

2.8.2 Mammary gland whole mount

The right-sided thoracic and inguinal mammary glands (3rd and 4th from the neck respectively) were dissected onto glass slides and fixed flat overnight at room temperature in Carnoy's fixative. The slides were rinsed in copious amounts of distilled water and stained overnight at room temperature in Carmine solution. The mammary gland whole mounts were dehydrated by incubation for 15 minutes in increasing concentrations of ethanol (70%, 95% and 100%). Whole mounts were viewed using a Nikon stereomicroscope SMZ1500

2.8.3 Immunohistochemistry

The left-sided thoracic mammary glands (3rd from the neck) were formalin-fixed over night at room temperature in an excess volume of 10% neutral buffered formalin (Sigma-Aldrich) and paraffin embedded. Paraffin-embedded sections (4μm) were mounted on slides and incubated for 2 minutes in two changes of xylene to de-wax the sections. To serially hydrate the sections the slides were incubated for 2 minutes with two changes of 100% IMS and incubated for 2 minutes with one change of 70% ethanol. The sections were washed in PBS and the tissue subject to antigen retrieval by boiling the sections for 10 minutes in 10mM sodium citrate buffer (pH6.0). The slides were placed in PBS and allowed to cool for 20 minutes. Endogenous peroxidase activity was blocked by incubation in 1.6% hydrogen peroxide for 10 minutes. The sections were washed for 5 minutes with distilled water, rinsed in PBS and the sections incubated in blocking buffer ((10% normal rabbit serum (Sigma-Aldrich), 1%BSA in PBS) for 30 minutes. The blocking buffer was blotted from the section and the section incubated with the appropriate primary antibody (see table 2.4) diluted in binding buffer (1%BSA in PBS) for 60 minutes at room temperature. The slides were washed in three changes of PBS for 3 minutes each and incubated with the appropriate biotinylated secondary antibody (see table 2.5) diluted in binding buffer (1%BSA in PBS) for 60 minutes at room temperature. The slides were washed in three changes of PBS for 3 minutes each and incubated with a Avidin-Biotin Complex (ABC, Thermo scientific) for 30 minutes. The slides were washed in three changes of PBS for 3 minutes each and incubated in DAB solution (Sigma-Aldrich) for 3 minutes. The sections were

counterstained with Mayer's haematoxylin (Sigma-Aldrich), dehydrated and mounted under cover slips as detailed above (2.8.1). Sections were viewed using an Olympus BX50 microscope.

2.8.4 Primary antibody used for immunohistochemistry

Antibody	Immunogen	Dilution/ concentration[a]	Supplier
Ki67 (rat monoclonal Clone: TEC-3)	Not detailed	1:125[a]	Dako
KDM5B (rabbit polyclonal)	Raised against the C-terminus domain of KDM5B corresponding to aa 1283-1473 of human origin	1:700	In house
PR (rabbit polyclonal)	Raised against the N-terminus region of PR corresponding to aa 533-547 of human origin.	1:30	Dako
Phospho-STAT5 (rabbit monoclonal C11C5)	synthetic peptide of Stat5a. corresponding to residues surrounding Tyr694	1:25	Cell signalling

Table 2.4 Table listing primary antibody used for immunohistochemistry ([a]Dilution factor is given where concentration is not known).

2.8.5 Secondary antibody used for immunohistochemistry

Antibody	Dilution/ concentration	supplier
Biotinylated rabbit anti-rat	2μgml	Vector labs
Swine anti rabbit HRP conjugate For use with the following primary antibodies:		
KDM5B	1.3μg/ml	Dako
pSTAT5	6.5μg/ml	Dako
PR	1.3μg/ml	Dako

Table 2.5 Table listing secondary antibody used for immunohistochemistry

2.8.6 Microscopy and data analysis

For each of the C57BL/6J-*Kdm5b WT* and *Kdm5b ΔARID* mammary gland whole mounts, the total number of TEB structures (at 4 weeks of age, n=6) or Y-branch points (at 12 weeks of age. WT, n=3. ΔARID, n=4) from the whole mammary gland were counted and expressed as an average.

From each of the C57BL/6J-*Kdm5b WT* and *Kdm5b ΔARID* embedded sections at days 12.5 and 18.5 of pregnancy (n=3) approximately 3000 ductal and alveolar epithelial cells were counted. Those cells within the field of vision positive for the cell proliferation marker Ki67 were expressed as a percentage of total epithelial content. Data is represented as an average.

Murine mammary gland whole mounts were visualized using a Nikon stereomicroscope SMZ1500. Slides stained with heamatoxylin and eosin (H and E) or used for immunohistochemistry were scanned with the Hamamatsu digital slide scanner, NanoZoomer-XR C12000. The slides were visualized with the NanoZoomer Digital Pathology Software viewing platform. Six randomly chosen $1mm^2$ areas were selected and the number of alveoli at day 18.5 of pregnancy in the C57BL/6J-*Kdm5b WT* and *Kdm5b ΔARID* mammary glands were scored. Three randomly chosen $1mm^2$ areas were selected and the perimeter of the alveoli at day 18.5 of pregnancy in the C57BL/6J-*Kdm5b WT* and *Kdm5b ΔARID* mammary glands were determined using NanoZoomer Digital Pathology Software. Quantification of immuno-blots was performed using ImageJ software. Student T-tests were performed using GraphPad software

Chapter 3: Results

Studies on the function of KDM5B *in vivo*

Chapter 3. Studies on the function of KDM5B *in vivo*

3.1 Aim:

In order to study the function of KDM5B *in vivo*, the *Kdm5b* locus was targeted. The specific aims in this chapter were to:

(1) Assess the effect of ablating KDM5B *in vivo* (*B6;129-Kdm5b-Exon 1* knock out)

(2) To develop and characterise the *B6;129-Kdm5b ΔARID* murine line

3.2 Introduction: A role for KDM5B during development

KDM5B is expressed in embryonic stem cells (Dey *et al*., 2008, Schmitz *et al*., 2011, Xie *et al*., 2011) and throughout development of the embryo (Madsen *et al*., 2002, Frankenberg *et al*., 2007, McGraw et al., 2007). In adult tissue, the *Kdm5b* transcript is expressed in the testis during spermatogenesis (Madsen *et al*., 2003) and differentially during mammary gland morphogenesis (Barrett *et al*., 2007, Catchpole *et al*., 2011 and this thesis), two organs containing cells that undergo rounds of proliferation and differentiation. The amino acid sequence of murine KDM5B is 94% homologous with that of human KDM5B, with a high degree of homology within the conserved domains[Δ] (Madsen *et al*., 2002 and Figure 1.6), suggesting functional conservation and the relevance of murine systems for the study of KDM5B function. The embryonic expression profile of *Kdm5b* raises the important issue as to the function and requirement of KDM5B during development. In an attempt to address these issues two candidate approaches to study the function of KDM5B *in vivo* were used.

[Δ] % homology within the conserved domains of human and murine KDM5B: JmjN 100%; ARID 100%; JmjC 100%; PHD1 98%; PHD2 88%; PHD3 98% (Murine NCBI reference sequence NP_690855.2 and human Swiss-Prot sequence Q9UGL1

3.3 Results

3.3.1 Ablation of murine KDM5B results in embryonic lethality

As outlined in the schematic for the production of gene targeted mice (Fig.3), in one approach (referred to hereafter as *Kdm5b-Exon 1* knock out), exon 1 was replaced with a floxed neomycin targeting construct (Fig 3.1), which was expected to result in no KDM5B translation.• Successful integration of the targeting vector into male ES cells derived from the ICM of the B6;129 chimeric murine line was determined by Southern blotting (Fig 3.2)* and the resulting positive ES cells were injected into C57BL/6J blastocysts or 8-cell embryos◆. The resulting chimeric offspring where ES cells have contributed to germ line transmission (black/brown coat colour) were screened by Southern blot for homologous recombination.* Several chimeric heterozygous B6;129-*Kdm5b-Exon1* knock out males were identified by Southern hybridisation, and two murine strains (1A4; derived from 8-cell embryo and 1A8; derived from blastocyst) were propagated with wild type C57BL/6J females. In order to streamline the screening for heterozygous B6;129-*Kdm5b-Exon1* knock out offspring PCR primers were designed, tested and optimal amplification conditions chosen to distinguish the wild type *Kdm5b* allele from the engineered allele.

The expression of the *Kdm5b* transcript at the MET (McGraw *et al*., 2007), within the epiblast (Frankenberg *et al*., 2007) and later during embryonic development (Madsen *et al*., 2002) suggests a role for KDM5B throughout the life of the embryo. In order to explore a function for KDM5B during embryonic development and further whether homozygous B6;129-*Kdm5b-Exon 1* knock out offspring were viable, two heterozygous B6;129-*Kdm5b-Exon1* knock out breeding programs (derived from strains 1A4 and 1A8) were initiated. The genotype of the offspring, as detailed above and shown in figure 3.3, was determined by PCR. From a total of 139 and 106 offspring derived from strains 1A4 and 1A8 respectively, no homozygous B6;129-*Kdm5b-Exon 1* knock out offspring were detected.

• Targeting construct was designed and generated by Dr Samantha Santangelo, KCL.

∗ Southern blot of transfected ES cells and screening of the breeding program was done with the help of Miss Debbie Hall, KCL.

◆ Transfection of targeting vector into ES cells and subsequent injection of positive clones into the blastocysts or 8-cell embryos and pseudopregnant female was carried out by Cancer Research UK Transgenic Mouse Service Laboratory, headed by Dr Ian Rosewell

Furthermore, significantly fewer (approx. 50%. Table 3 and 3S1. 1A4: p=0.0002. 1A8: p=0.0001) heterozygous B6;129-*Kdm5b-Exon 1* knock out offspring from both murine strains were detected at birth suggesting that the expression level of KDM5B is important for viability, at some stage of embryonic development, with only a proportion of embryos developing to full term.

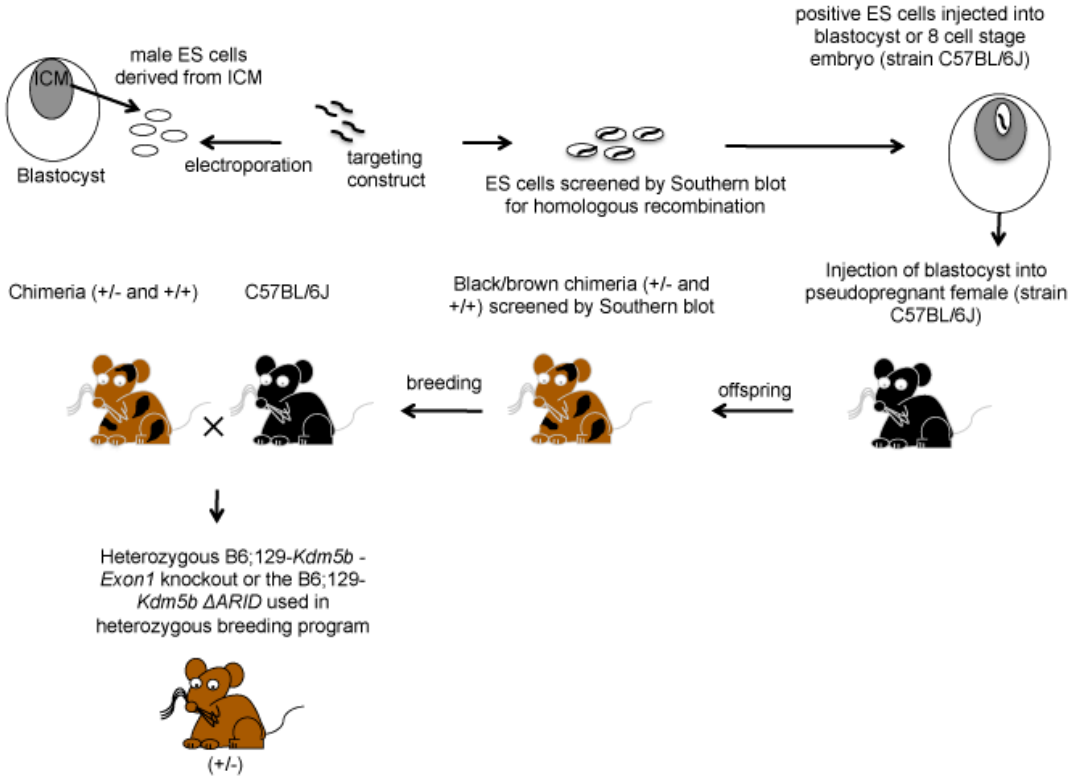


Figure 3 Schematic representation of B6;129-*Kdm5b-Exon1* knock out strategy detailing an outline for the production of gene targeted mice by manipulation and injection of ES cells. (A similar approach was used for the generation of the B6;129-*Kdm5b* ΔARID murine line with the exception that only blastocysts were used).

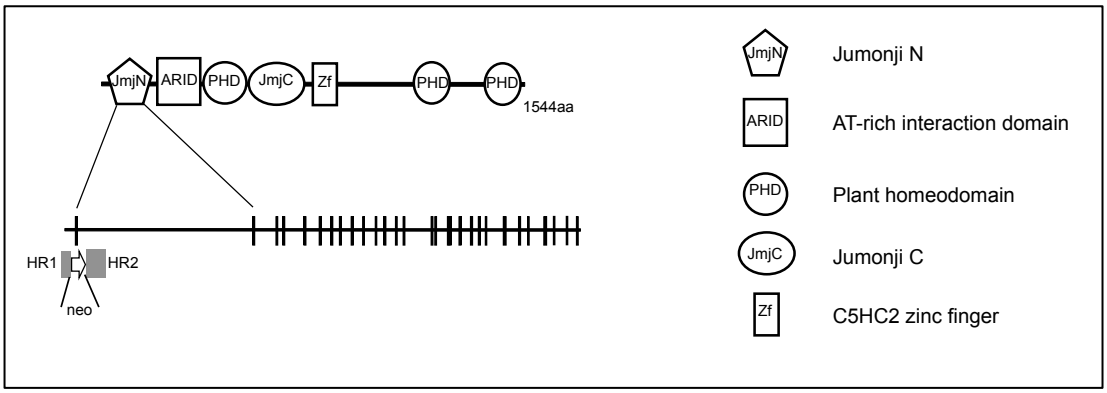


Figure 3.1 Schematic representation showing the KDM5B protein domains with genomic sequence detailing the positions of the neomycin targeting construct (neo) used to replace exon1 (which codes for part of the JmjN domain) and homologous regions HR1 and HR2

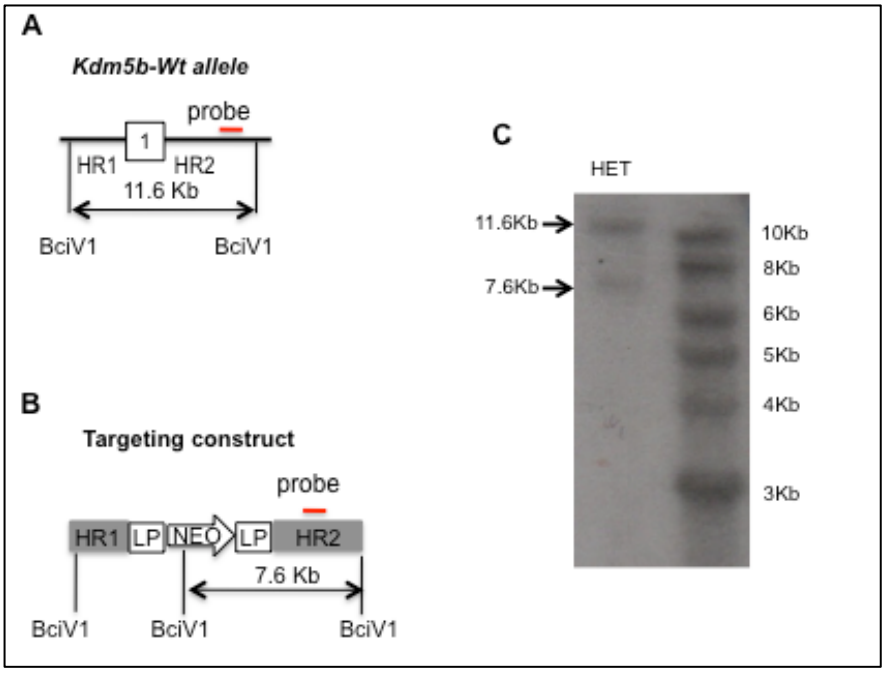


Figure 3.2 Schematic representation of the *Kdm5b-WT* allele and the *Kdm5b-Exon1* targeting construct together with the screening strategy used to detect homologous recombination in transfected embryonic stem cells.
(A) Schematic representation depicting the *Kdm5b-WT* allele with exon 1 (white box 1) and homologous regions (HR1 and HR2) used for the design of the targeting construct.
(B) The targeting construct depicting homologous regions (HR1 and HR2), loxP sites (LP) and the neomycin sequence (arrow) with the screening strategy used to distinguish the WT allele from the engineered allele (BciV1 restriction sites).
(C) Southern blot on genomic DNA isolated from transfected ES cells showing homologous recombination after BcVI digest.

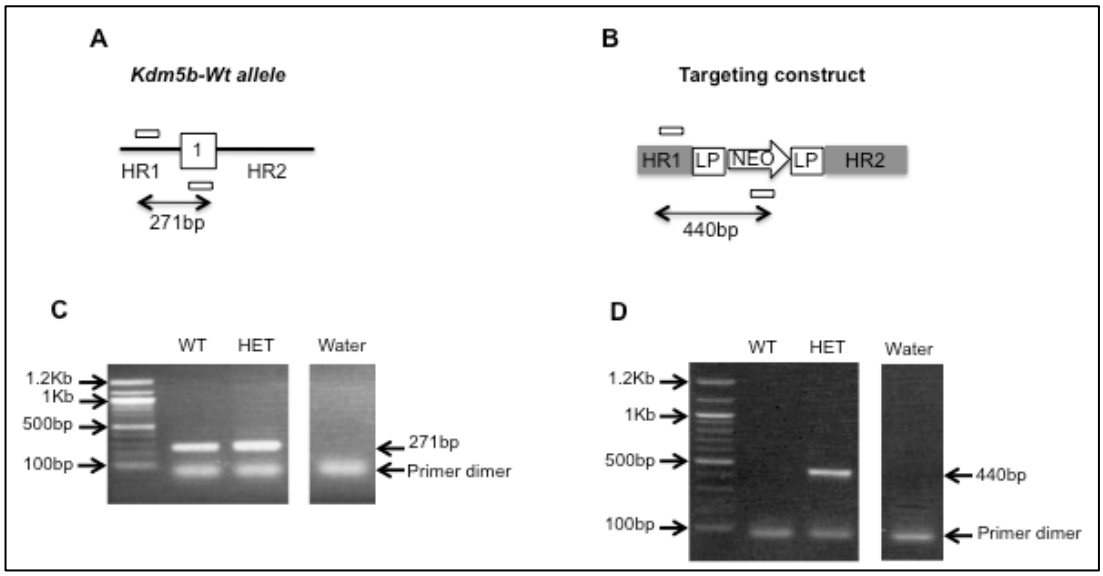


Figure 3.3 PCR screen on genomic DNA isolated from the offspring of the heterozygous B6;129-*Kdm5b-Exon1* knock out breeding programs (A) Schematic representation depicting *Kdm5b-WT* allele with exon 1 (white box 1) and homologous regions (HR1 and HR2) used for the design of the targeting construct. Small white rectangles depict PCR primer location. (B) Schematic representation of the targeting construct depicting homologous regions (HR1 and HR2), loxP sites (LP) and the neomycin sequence (arrow). Small white rectangles depict PCR primer location. (C) PCR product (271bp) generated using PCR primers specific to the *Kdm5b* WT allele. (D) PCR product (440bp) generated using PCR primers designed to amplify the engineered allele.

Strain	total	Wild Type	Heterozygous	Homozygous
Strain 1A4 (14 litters)	139	67	72★	0
Strain 1A8 (18 litters)	106	57	49★★	0

Table 3 Genotype of progeny from a heterozygous B6;129-*Kdm5b-Exon1* knock out breeding program (★, 1A4: p=0.0002. ★★,1A8: p=0.0001).

In order to determine the stage of development at which KDM5B expression is essential for embryonic development and the development of heterozygous embryos, embryos from a heterozygous B6;129-*Kdm5b-Exon 1* knock out breeding program (1A4 and 1A8) were harvested at e7.5, e8-8.5 and e9.5-10.5 and genotyped (Table 3.1). For genotyping of earlier embryos, a collaboration with the Curie Institute was instigated. The data obtained from the mice transferred to the Curie Institute showed that homozygous embryos were detected up to e4.5, which

is suggestive of a function for KDM5B at or around the time of implantation. Surprisingly, although the offspring born consisted of fewer *Kdm5b* heterozygotes than would be expected according to Mendelian genetics (strain 1A4: p=0.0002. strain 1A8: p=0.0001), the embryonic analysis suggested that embryos, heterozygous for *Kdm5*, had a survival advantage at e7.5 (Table 3.1; strain 1A8: $p<0.05$). As the number of embryos analysed at each stage for each strain were small we combined the genotype data. As can be seen from Table 3.1C, the *Kdm5b* heterozygote embryos appear to have a survival advantage from e7.5 to 8-8.5, (e7.5, $p<0.01$), which is lost by e9.5-10.5. Even though the combined number of embryos is still small the data suggest a change in the number of heterozygotes with time. Taken together with the data shown in Table 3 suggests that post e10.5 the heterozygous embryos are disadvantaged leading to the non-Mendelian ratios of the live offspring. Thus, the data suggest that the lower expression of KDM5B in the early embryos may be advantageous to development, while higher levels of KDM5B expression are required for viability in the later embryos.

A

Strain 1A4	Wild Type	Heterozygous	Homozygous
e9.5-10.5	4	4	0
e8-8.5	2	9	0
e7.5	0	7	0

B

Strain 1A8	Wild Type	Heterozygous	Homozygous
e9.5-10.5	0	5	0
e8-8.5	2	5	0
e7.5	1	13★	0

C

Strain 1A4 and 1A8	Wild Type	Heterozygous	Homozygous
e9.5-10.5	4	9	0
e8-8.5	4	14	0
e7.5	1	20★★	0

Table 3.1 The *Kdm5b* knock out line is embryonic lethal. Table showing genotyping results from embryos isolated from 2 heterozygous B6;129 *Kdm5b-Exon1* knock out breeding programs (★, $p<0.05$. ★★, $p<0.01$).

Comparison of the offspring born to the B6;129-*Kdm5b WT* murine line with that of the offspring born to the heterozygous B6;129-*Kdm5b-Exon 1* knock out murine line, indicated that the surviving offspring developed normally, with no difference in the size of the pups noted.

To examine whether the expression levels of KDM5B are important for post-natal development we examine the gross morphology of the mammary gland, an organ known to express KDM5B (Madsen *et al*., 2002, Barrett *et al*., 2007, Catchpole *et al*., 2011 and this thesis). To achieve this, thoracic mammary glands taken from B6;129-*Kdm5b WT* and heterozygous B6;129-*Kdm5b-Exon 1* knock out litter-mates were whole mounted and stained with carmine. As shown in Figure 3.4 development of the B6;129-*Kdm5b WT* and heterozygous B6;129-*Kdm5b-Exon 1* knock out mammary glands appear comparable. This suggests that expression of KDM5B from one allele in the surviving heterozygous B6;129-*Kdm5b-Exon 1* knock out females is sufficient for normal post-natal development of the mammary gland.

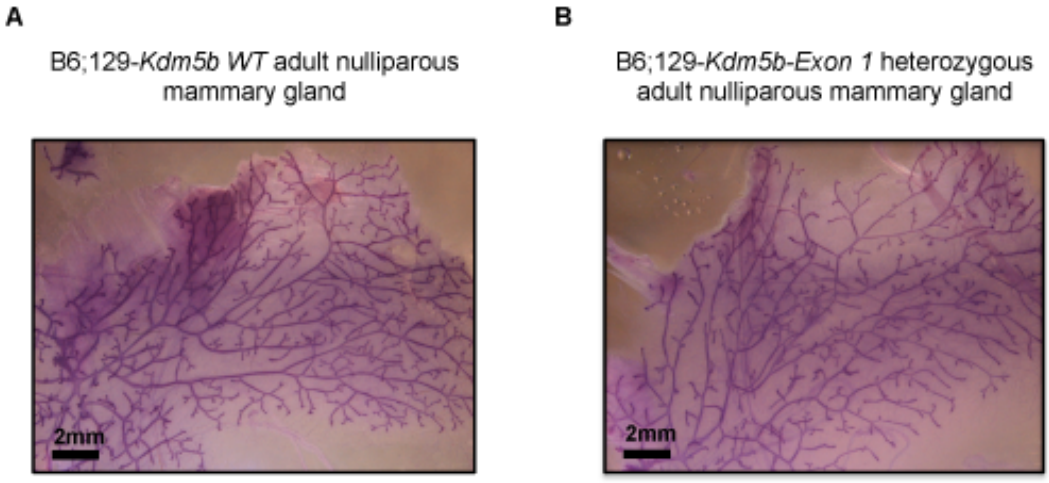


Figure 3.4 Normal mammary gland development in the heterozygous B6;129-*Kdm5b-Exon 1* knock out murine line. Representative carmine on (A) B6;129-*Kdm5b WT* and (B) heterozygous B6;129-*Kdm5b-Exon 1* knockout adult (12 weeks of age) nulliparous mammary gland (n=2 per group).

3.3.2 Development, screening and preliminary characterisation of the chimeric B6;129-*Kdm5b ΔARID* murine line

3.3.2.1 The B6;129-Kdm5b ΔARID murine line are viable and fertile

Data from the B6;129-*Kdm5b-Exon 1* knock out murine line suggested that KDM5B expression is essential for early murine embryonic development. As an alternative strategy, part of exon 2 (48bp from a total of 78bp) and the entirety of exons 3 and 4 (13.8KDa in total) of the *Kdm5b* gene was replaced with a floxed neomycin-targeting construct (Fig 3.5). The region of the *Kdm5b* gene targeted codes for the ARID sequence that is required for demethylase activity (Yamane *et al*., 2007) and has been shown to bind GC rich sequences (Scibetta *et al*., 2007, Yao *et al*., 2010). Successful integration of the targeting vector into male ES cells derived from the ICM of the 129/Ola mouse strain was determined by Southern blotting and the resulting positive ES cells from the only clone identified was injected into C57BL/6J blastocysts followed by injection into a C57BL/6J pseudo-pregnant female. The resulting chimera offspring where ES cells have contributed to germ line transmission (black/brown coat colour) were screened by Southern blot for homologous recombination. The resulting chimeric mouse line generated from injecting 129/Ola derived ES cells into C57BL/6J blastocysts was termed the B6;129-*Kdm5b ΔARID* murine line (See Fig. 3 for an outline for the production of gene targeted mice).

In order to establish whether:

(1) The heterozygous B6;129-*Kdm5b ΔARID* murine line was fertile.

(2) The heterozygous B6;129-*Kdm5b ΔARID* offspring were born according to Mendelian frequencies.

(3) The homozygous B6;129-*Kdm5b ΔARID* offspring were viable, a heterozygous B6;129-*Kdm5b ΔARID* breeding program was initiated and the genotype of the offspring examined by Southern blot. As shown in Figure 3.6, BamH1 restriction digest on genomic DNA isolated from the mice in the heterozygous breeding program was used to distinguish the wild type *Kdm5b* allele from the engineered allele for the identification of wild type, heterozygous and homozygous offspring. Furthermore the genotyping of the offspring from 2 heterozygous B6;129-*Kdm5b ΔARID* breeding pairs demonstrated that the offspring were born according to Mendelian frequencies (Table 3.2 and Table 3S2 and 3S3 in the supplemental material) and subsequently that offspring from the homozygous

B6;129-*Kdm5b ΔARID* breeding program were fertile and viable. Moreover the females could support their pups at parturition with no obvious difference in the size of the pups noted.

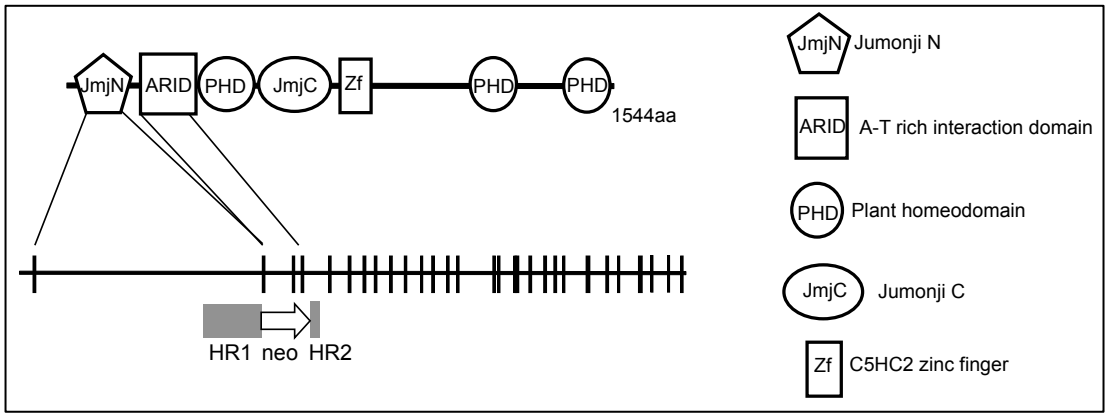


Figure 3.5 Schematic representation showing the KDM5B protein domains with genomic sequence detailing the positions of the neo targeting construct used to replace part of exon 2 and exons 3 to 4 (codes for part of the JmjN domain and the entire ARID domain) and homologous regions HR1 and HR2

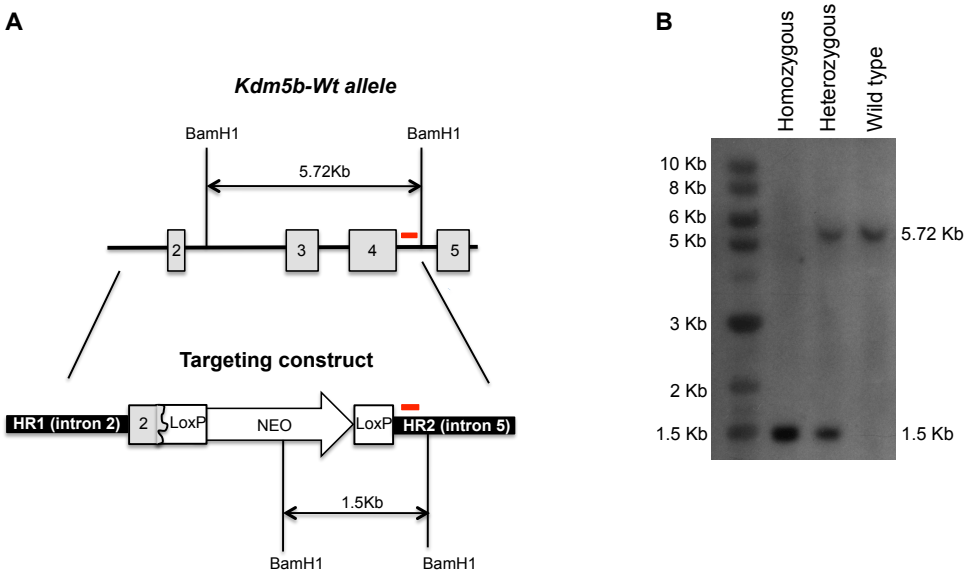


Figure 3.6 Schematic representation of *Kdm5b ΔARID* targeting construct and the screening strategy used to distinguish the wild type allele from the engineered allele in murine tail snip DNA. (A) Schematic representation depicting the WT *Kdm5b* allele showing exons 2 to 5 (grey box), and the targeting construct depicting homologous regions (HR1 and HR2), truncated exon 2 (grey box with serrated edge), loxP sites (LP) and the neomycin targeting construct (arrow) with the screening strategy used to distinguish the WT allele from the engineered allele (BamH1 restriction sites). (B) A Southern blot on genomic DNA isolated from B6;129 murine tail-snips showing the WT allele and homologous recombination after BamH1 digest.

Pair 1 and 2												
	Total from 18 litters			genotype								
				+/+			+/-			-/-		
	total	male	female	total	male	female	total	male	female	total	male	female
total	177	91	86	**48**	24	24	**96**	51	45	**32**	15	17
mendelian ratio				27.12			54.24			18.1		

Table 3.2 Genotyping from two B6;129-*Kdm5b ΔARID* heterozygous breeding programs demonstrates that the B6;129-*Kdm5b ΔARID* offspring are born according to Mendelian ratio. The Chi squared value for 2 degrees of freedom and p=0.05 (5%) is 5.99. As the observed value is lower than 5.99 we accept our hypothesis, that there is no deviation from mendelian ratio.0.1<p<0.5 (See supplemental materials Table 3S3)

3.3.2.2 Expression of a less abundant KDM5B protein lacking the entire ARID domain and part of the JmjN domain

(A) KDM5B protein expression

Given the viability and fertility of the B6;129-*Kdm5b ΔARID* murine line in contrast to the embryonic lethality of the homozygous B6;129-*Kdm5b Exon1* knock out line, we sought to examine whether KDM5B was being expressed by examining tissue known to express high levels of KDM5B, *i.e.* the testis and the mammary gland (Madsen *et al*., 2002, Barrett *et al*., 2007). To achieve this, Western blot transfer of nuclear protein extracts isolated from the B6;129-*Kdm5b WT* and *ΔARID* murine adult testis and the pregnant mammary gland (pd18.5) were probed with a KDM5B specific antibody. A similar profile of bands was observed in the mammary gland and testis (Fig. 3.7). In nuclear protein extracts isolated from wild type tissue, two high molecular weight bands were seen, one at 170KDa - which is the predicted molecular weight (MW) of KDM5B (bands - a and i), the other at around 150KDa (bands - b and j). These bands are likely to be a KDM5B splice variant as Western blot transfer using protein extracts isolated from breast cancer cell lines expressing KDM5B can show this pattern or a single 170KDa band depending on growth conditions. Western blot transfer on KDM5B ΔARID nuclear protein extracts also resolved two bands, but these were smaller and less abundant than seen in the wild type tissue (f and g; l and m). As will be shown below, these bands (f and g; l and m) may correspond to a splicing event that has occurred in the B6;129-*Kdm5b*

ΔARID murine line. Furthermore, Western transfer of nuclear proteins from the B6;129-*Kdm5b ΔARID* mammary gland and testis resolved bands h and n respectively that do not appear to be expressed in the wild type counterpart tissue.

The lower molecular weight band (approx. 130KDa), detected in extracts isolated from the B6;129-*Kdm5b WT* mammary gland and testis (e and k respectively) are not detected in the extracts isolated from the B6;129-*Kdm5b ΔARID* tissue. If this is another splice variant it is clearly not formed in the B6;129-*Kdm5b ΔARID* murine tissue examined. The two faint bands (c and d) observed from wild type murine mammary gland nuclear extracts appear not to be present in the wild type testis and could therefore be tissue specific.

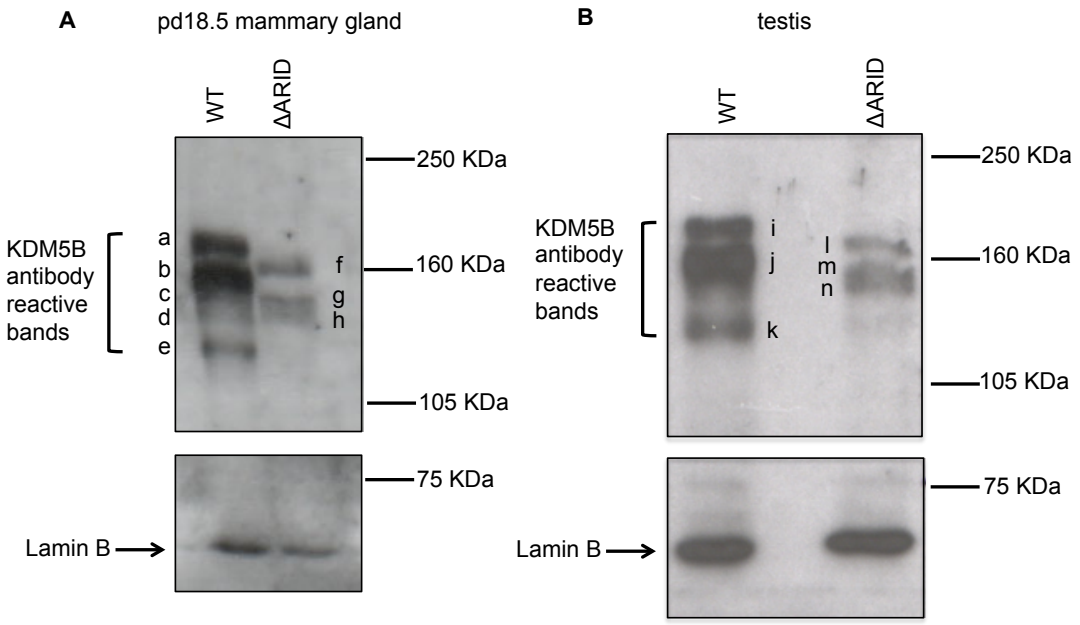


Figure 3.7 Expression of a smaller less abundant KDM5B protein in the B6;129-*Kdm5b ΔARID* mammary gland and testis. Western transfer showing translation of a smaller, less abundant KDM5B ΔARID protein product in (A) the mammary gland at pd18.5 and (B) the adult testis.

(B) Processing of the KDM5B primary transcript

The neomycin selection cassette used to select for recombinant ES cells during gene targeting experiments contains a number of predicted splice sites (Jin *et al*.,

2005). During processing of the primary transcript, utilisation of donor and acceptor sites within the targeted gene can result in the translation of fusion proteins that can consist of elements of both the neomycin cassette and the targeted gene (Kos *et al*., 2002, Shearman *et al*., 2000). Of note is the possibility that integration of the neomycin selection cassette within exon sequences together with the maintenance of naturally occurring splice donor and acceptor splice could lead to splicing out of the neomycin selection cassette (Gawenis *et al*., 2005). The design of the targeting construct detailed here maintained the exon 1 splice donor and exon 5 splice acceptor sites. It was therefore possible that the resulting smaller KDM5B protein seen in the mammary gland and testis is as a consequence of the splicing together of exon 1 and exon 5 resulting in the removal of the neomycin gene. To examine whether the expression of a smaller KDM5B protein in the B6;129-*Kdm5b ΔARID* murine line was as a consequence of:

(1) Aberrant splicing of the primary transcript due to the identification of splice sites within the neomycin construct; or due to the

(2) Splicing together of exon 1 to exon 5 using naturally occurring splice sites within the *Kdm5b* gene. To test this possibility, PCR primers were designed to flank the neomycin construct within exons 1 and 5.

Figure 3.8A shows a schematic representation of the processing of the *WT Kdm5b* primary transcript with the depiction of exon 1 through to exon 5 highlighting the JmJN (grey box) and ARID (red box) domains with the size of the expected PCR product shown (primers: green arrow). In contrast, Figure 3.8B is a schematic representation of one of the predicted splicing events (detailed as 2 above) that would lead to the splicing together of exon 1 to exon 5 with the expected PCR product size shown.

As figure 3.8C shows, the subsequent PCR on the cDNA, that was generated from the RNA, isolated from the B6;129-*Kdm5b WT* and B6;129-*Kdm5b* ΔARID murine testis and mammary gland at pd18.5 results in the amplification of a smaller product in the B6;129-*Kdm5b ΔARID* murine line. (data shown was generated from RNA isolated from the pd18.5 mammary gland). In order to determine the splicing event that lead to the generation of a smaller KDM5B protein product and further to establish whether the neomycin targeting construct had been spliced out during processing of the primary transcript those PCR primers directed to exon 1 and 5 of *Kdm5b* (as detailed above) were used to generate a DNA sequencing trace using the cDNA transcribed from RNA isolated from the B6;129-*Kdm5b WT* and *ΔARID*

testis and pd18.5 mammary gland. Examination of the WT *Kdm5b* DNA sequencing trace confirmed the presence of the exon 4 to exon 5 boundary (See Fig. 3S1 and Table 3S4 in the supplemental material). In contrast, examination of the DNA trace from the B6;129-*Kdm5b ΔARID* at pd18.5 revealed in frame splicing of the primary transcript from exons 1 to 5 resulting in the truncation of the JmjN domain (deletion of amino acids, Asp69, Trp70, Gln71, Pro72, 73) and deletion of the entire ARID domain (Fig 3.9 and Table 3.3) (Exon 1 through to 5 of the WT *Kdm5b* transcript is shown in figure 3S2 of the supplemental material).

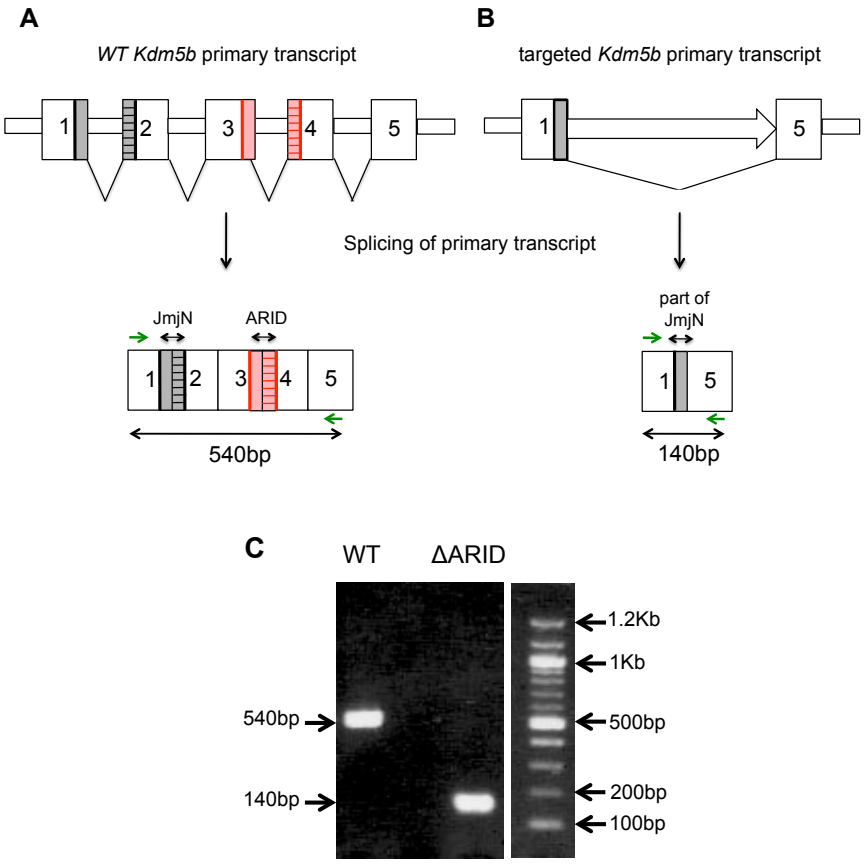


Figure 3.8 Processing of the *Kdm5b* primary transcript in the B6;129-*Kdm5b WT* and B6;129-*Kdm5b* ΔARID murine line. (A) Schematic representation depicting the splicing events of the *WT Kdm5b* primary transcript (boxes labelled 1 to 5 represent exon sequence). Narrow rectangles represent intronic sequence. Grey area in exon 1 and grey area with horizontal line in exon 2 represent the Jumonji N domain (JmjN). Red area in exon 3 and red area with horizontal line in exon 4 represent the ARID sequence. Green arrows represent the 5' and 3' PCR primers specific to exon 1 and exon 5 showing the expected product size. (B) Schematic representation depicting a predicted RNA splicing event of the engineered *Kdm5b* primary transcript resulting in the splicing together of exon 1 to exon 5 and the removal of the neomycin construct (large white arrow). (C) PCR on cDNA generated from RNA isolated from the B6;129-*Kdm5b WT* (540bp) and B6;129-*Kdm5b* ΔARID (140bp) murine mammary glands at pd18.5.

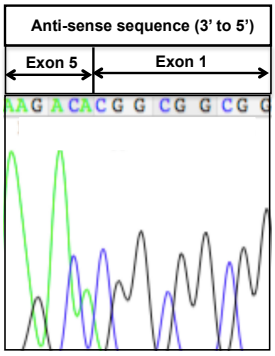


Figure 3.9 DNA trace from the B6;129-*Kdm5b ΔARID* mammary gland transcript at pd 18.5. DNA trace showing anti-sense sequencing data obtained from cDNA reverse transcribed from RNA isolated from B6;129-*Kdm5b ΔARID* mammary gland (schematic representation of PCR primer location within exon 1 and 5 see Fig. 3S2 in the supplemental material)

Exon	Exon1			Exon 2 - 4	Exon 5	
cDNA sequence (Sense)	CCG	CCG	CCG	Exons 1 and 5 are spliced together removing exons 2 to 4	TGT	CTT
cDNA sequence (Anti-sense)	GGC	GGC	GGC		ACA	GAA
Translated sequence	P	P	P		C	L

Table 3.3 Derived sequence from DNA trace (Figure 3.9) of B6;129-*Kdm5b ΔARID* cDNA showing exon 1 to 5 boundaries. Table showing sequencing data obtained from cDNA reverse transcribed from RNA isolated from B6;129 *Kdm5b ΔARID* mammary gland tissue at pd18.5.

3.3.2.3 Development of adult tissues in the B6;129-Kdm5b ΔARID murine line

(A) Histological analysis of male and female adult tissues

In order to examine the gross effect of KDM5B ΔARID expression on adult development, necropsy was performed on litter-matched B6;129-*Kdm5b WT* and B6;129-*Kdm5b ΔARID* male and female mice at 9 weeks of age. However even though *Kdm5b* is expressed during embryonic development and in the adult tissue (Madsen *et al*., 2002, Barrett *et al*., 2007, Frankenberg *et al*., 2007, Schmitz *et al*., 2011), no gross histological differences were noted between the adult B6;129-*Kdm5b WT* and B6;129-*Kdm5b* ΔARID line in any of the tissues examined (Table 3.4)

genotype	organ	Histology
B6;129-*Kdm5b ΔARID* line	**skin**	normal
	mammary gland	normal
	ovaries and oviduct	normal
	penis and urethra	normal
	testis and spermatogenesis	normal
	epididimis and **prostate**	normal
	spleen	normal
	colon	normal
	pancreas	normal
	mesenteric lymph nodes	normal
	small intestine and colon	normal
	kidney and adrenal gland	normal
	stomach, oesophagus and duodenum	normal
	liver and gall bladder	normal
	salivary gland	normal
	thymus	normal
	heart	normal
	lung	normal
	thyroid	normal
	eye	normal
	brain (cerebellum, brain stem, pituitary)	normal
	tongue, nasal passages, tooth development	normal
	spinal cord, vertebral bodies	normal

Table 3.4 Histological examination of organs from the male and female B6;129-*Kdm5b ΔARID* murine line at 9 weeks of age (adult) suggesting normal development. Those organs highlighted in red represent the organs where KDM5B expression has been reported in the adult (n=4 per group) (Madsen *et al*., 2002, Barrett *et al*., 2007, Frankenberg *et al*., 2007, Schmitz *et al*., 2011).

(B) A possible defect in mammary gland ductal morphogenesis

Kdm5b is expressed during mammary gland development (Madsen *et al*., 2002, Barrett *et al*., 2007, Catchpole *et al*., 2011 and this thesis), and a function for KDM5B in breast cancer development *in vivo* has been described (Yamane *et al*., 2007, Catchpole *et al*., 2011). Histological examination is not sufficient to identify

any potential defect in the gross morphology of the B6;129-*Kdm5b ΔARID* female mammary gland. We therefore sought to clarify if an effect on development of the post-natal mammary gland could be seen in the B6;129-*Kdm5b ΔARID* line murine strain. To achieve this thoracic mammary glands from adult B6;129-*Kdm5b WT* and B6;129-*Kdm5b ΔARID* females (> 9 weeks of age) were whole mounted and stained with carmine. Figure 3.10A shows that by adulthood the B6;129-*Kdm5b WT* nulliparous mammary gland had fully ramified the fat pat by ductal elongation, bifurcation at TEB structures and through ductal side branching. In contrast some adult B6;129-*Kdm5b ΔARID* females presented with a lack of secondary ductal side branches, although the mammary gland tree had ramified the fat pad (Fig 3.10B). However, this defect in mammary gland ductal morphogenesis is variable between individual mice, as seen in Figures 3.10B and C.

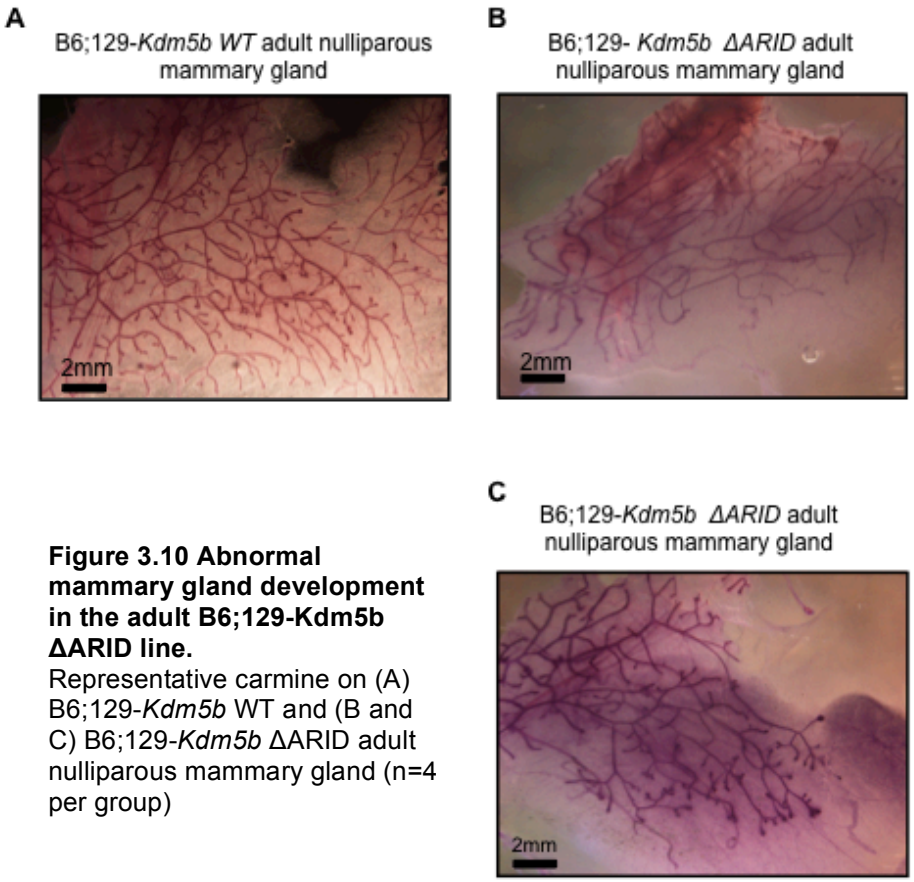


Figure 3.10 Abnormal mammary gland development in the adult B6;129-Kdm5b ΔARID line.
Representative carmine on (A) B6;129-*Kdm5b* WT and (B and C) B6;129-*Kdm5b* ΔARID adult nulliparous mammary gland (n=4 per group)

KDM5B is expressed during pregnancy associated mammary gland development (Madsen *et al*., 2002, Barrett *et al*., 2007, Catchpole *et al*., 2011 and this thesis). To examine whether the expression of the KDM5B ΔARID protein affects development of the mammary gland through pregnancy, the thoracic mammary glands of the

B6;129-*Kdm5b WT* and B6;129-*Kdm5b ΔARID* females at mid and late pregnancy (pd12.5 and pd18.5 respectively) were whole mounted and stained with carmine. In order to ensure the accuracy of staged pregnancies, embryos were assessed for stage of embryonic development at the point of mammary gland harvest. Figure 3.11A shows that the B6;129-*Kdm5b WT* mammary gland at pd12.5 had undergone further side branching and alveolar development. On the other hand, although the mammary gland of some B6;129-*Kdm5b ΔARID* female mice at pd12.5 had ramified the fat pad further, a defect in ductal side branching and alveolar development appeared to be manifest. (Figure 3.11B). As noted for the B6;129-*Kdm5b ΔARID* nulliparous mammary gland, the degree of severity in mammary gland development present in the B6;129-*Kdm5b ΔARID* female at pd12.5 was also variable (compare Fig. 3.11B and Fig. 3.11C). As shown in Figure 3.11C, the B6;129-*Kdm5b ΔARID* mammary gland at pd12.5 had developed only a rudimentary ductal system, had failed to ramify the fat pad and further, presented with few ductal side branches, and an absence of alveolar development.

The B6;129-*Kdm5b ΔARID* females can support their pups at parturition with no obvious difference in the size of the pups noted. This observation suggests that mammary gland ductal morphogenesis recovers sufficiently to support alveolar proliferation and full differentiation. Consistent with this, mammary gland gross morphology, from both the B6;129-*Kdm5b WT* (Fig 3.12A) and B6;129-*Kdm5b ΔARID* (Fig 3.12B) females at pd18.5 were comparable.

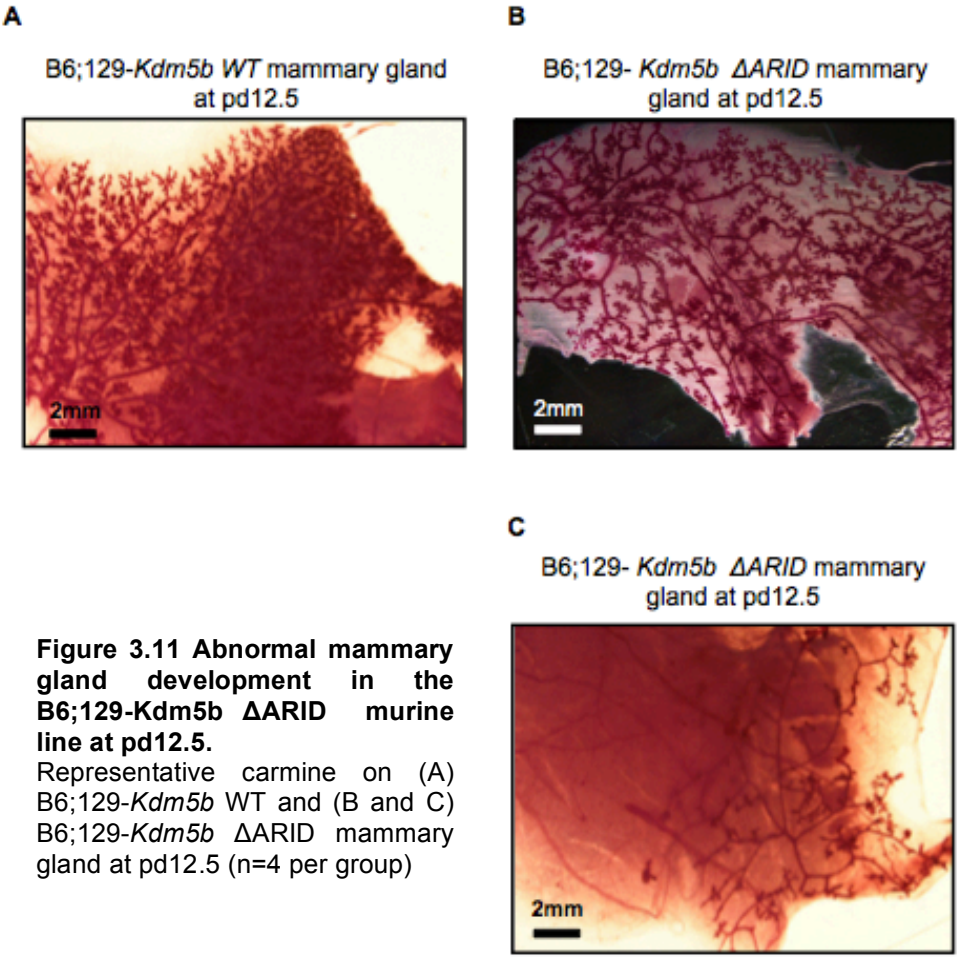


Figure 3.11 Abnormal mammary gland development in the B6;129-Kdm5b ΔARID murine line at pd12.5.
Representative carmine on (A) B6;129-*Kdm5b* WT and (B and C) B6;129-*Kdm5b* ΔARID mammary gland at pd12.5 (n=4 per group)

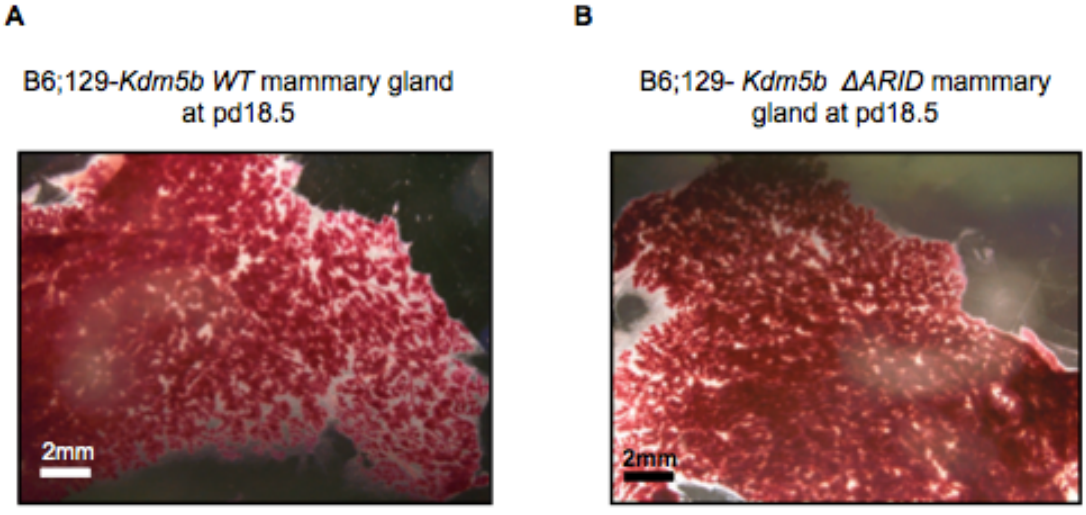


Figure 3.12 Mammary gland development at pd 18.5 in the B6;129-*Kdm5b WT* and *ΔARID* murine line. Representative carmine on (A) B6;129-*Kdm5b WT* and (B) B6;129-*Kdm5b ΔARID* mammary gland at pd18.5 suggests that development of the B6;129-*Kdm5b ΔARID* mammary gland recovered by late pregnancy (n=4 per group)

3.4 Discussion

At the time of writing this thesis a number of outstanding issues remained regarding the function of KDM5B. These include: What function does KDM5B perform during development? Does KDM5B posses a demethylase independent function? How is KDM5B recruited to the genome? Here we attempt to address some of these issues by drawing on the results from our own studies targeting the *Kdm5b* locus.

3.4.1 Assessing the developmental role of KDM5B

The data from the *Kdm5b-Exon 1* knock out line suggests an essential role for KDM5B during embryonic development between e4.5 and e7.5; a role at the time of writing this which is unique amongst the other mammalian KDM5 family members (Klose *et al*., 2007, Catchpole *et al*., 2011 and this thesis). The *Kdm5b-Exon 1* knock out line is viable up to e4.5 (Catchpole *et al*., 2011), even though KDM5B expression is required, through the regulation of H3K4 methylation, to silence pluripotent gene expression as ES cells differentiate (Kidder *et al*., 2013, 2014). An important role for KDM5B expression during post implantation is highlighted by the restricted expression of KDM5B to the epiblast at e5.5 (Frankenberg *et al*., 2007) and the requirement of KDM5B for embryoid body (EB) formation (Kidder *et al*., 2013). In fact, gene categories associated with ectoderm, mesoderm and endoderm formation are under-expressed during EB formation in the absence of KDM5B (Kidder *et al*., 2013) suggesting a requirement for KDM5B during the determination of all future lineages during the early stages of post-implantation. We have also noted that heterozygosity at e7.5 exceeds the numbers expected according to Mendelian frequencies although contamination from the maternal decidua at this early time point cannot be excluded.

However, as described in more detail below, Albert and colleagues (2013) recently reported on the phenotype of a *Kdm5b* null line in which integrated flippase recognition target sites were used to remove the neomycin gene. The *Kdm5b null* line resulted in major neonatal lethality due to respiratory failure. Whilst 95 percent of wild type mice were viable, 50 percent of the *Kdm5b null* offspring died within the first two hours of delivery and another 20 percent died 12 to 24 hours after birth. Our data suggest that the expression level of KDM5B could be important for embryonic viability post e10.5 given that the number of heterozygous *Kdm5b-Exon*

1 knock out offspring born is significantly reduced. These findings are contrary to those of Albert and colleagues (2013) who report that although the viability of the heterozygote offspring born is reduced, this reduction is not significant. In addition, these authors examined whether KDM5B expression is important for embryonic development and observed no significant difference in the expected genotype ratios at mid (e9.5-14.5) and late (e16.5-e18.5) stages of embryonic development. Furthermore, in keeping with *Kdm5b* expression in the developing embryonic brain, eye, and ganglionic nerve centres (Madsen *et al*., 2002), Albert and colleagues (2013) also showed that caesarean recovered embryos presented with neurological defects, such as defects in cranial and spinal nerve development, eye development and exencephaly. The *Kdm5b null* embryos presented with micropthalmic eyes, a disorganised neural retina structure and a significantly smaller lens (Albert *et al*., 2013). Interestingly, KDM5B has also been linked to the signalling pathway that determines rod versus cone photoreceptor cell fate determination (Hao *et al*., 2012). Deregulated *Hox* gene expression in murine polycomb mutant lines results in defective skeletal development (Akasaka *et al*., 1996, Del Mar Lorente *et al*., 2000) and KDM5B has been shown to bind and regulate developmental genes (Schmitz *et al*., 2011, Xie *et al*., 2011) including *Hox* genes (Yamane *et al*., 2007, Pasini *et al*., 2008). With this in mind, null embryos also present with a transformation of the last lumber vertebra (L6), into the first sacral vertebrae (Albert *et al*., 2013).

The *Kdm5b-Exon 1* knock out targeting construct was designed to replace exon 1 with a floxed neomycin gene. It has been reported that the presence of the integrated neomycin targeting construct may have unintended consequences on the targeted gene, and or adjacent genes, if not excised from the genome (Olson *et al*., 1996, Meyers *et al*., 1998, Nagy *et al.,* 1998, Scacheri *et al*., 2001). It is therefore a possibility that the embryonic lethality of the *Kdm5b* knockout and the reduced viability of the *Kdm5b* heterozygote noted at birth, maybe due to the presence of the neomycin targeting construct. The presence of the endogenous *Kdm5b* promoter, and the described cryptic splice sites contained within the neomycin gene (Jin *et al*., 2005) could potentially lead to the expression of hybrid transcripts (Shearman *et al*., 2000, Kos *et al*., 2002) consisting of both the neomycin and *Kdm5b* gene sequences. Furthermore, the presence of the neomycin promoter contained within the neomycin targeting vector could drive transcription that could potentially result in the expression of a truncated *Kdm5b* transcript lacking exon 1 of *Kdm5b.* In order to examine this possibility Northern blot transfer of RNA isolated from surviving *Kdm5b* null embryos at e4.5 and probed with an oligonucleotide sequence directed against

the neomycin gene and the *Kdm5b* gene sequences should be performed. The translation of any potential truncated KDM5B or hybrid neomycin/KDM5B protein should be explored by Western blot, as expression may result in a dominant negative affect thereby altering protein interactions with endogenous KDM5B. The presence of an integrated neomycin targeting vector into the *Kdm5b* locus may therefore explain the different phenotype presented in the *Kdm5b* null murine line reported in this thesis (Catchpole *et al*., 2011) and that reported by the Helin laboratory (Albert *et al*., 2013).

However, the results described in this thesis (Catchpole *et al*., 2011) together with published data (Albert *et al*., 2013) both demonstrate that mice null for the *Kdm5b* gene have severe developmental defects although there is disagreement as to the stage at which the defects manifest. Deciphering the role of KDMB during development has been further complicated by a recent report (Zou *et al*., 2014) and will be discussed at a later point (see Chapter 7 final discussion).

3.4.2 KDM5B protein expression in the adult testis and mammary gland at pd18.5.

The detection of several KDM5B antibody specific bands in the B6;129-*Kdm5b WT* mammary gland at pd18.5 as well as in the adult testis suggests the existence of isoform variants of KDM5B and could be confirmed by peptide sequencing using mass spectrometry. Although the potential splice variants could not be predicted, KDM5B contains numerous domains required for enzyme activity, including the catalytic JmjC domain, the JmjN domain, ARID sequence and the C5HC2 zinc finger sequence (Xiang *et al*., 2007, Yamane *et al*., 2007). The KDM5B protein also contains domains that aid in the recruitment of KDM5B to the genome including the ARID sequence (Scibetta *et al*., 2007, Yao *et al*., 2010) and the N- and C-terminus PHD sequences (Li *et al*., 2011, Klein *et al*., 2014). Therefore, the different KDM5B isoforms suggested from the Western blot analysis (see Figure 3.7 duplicated below for reference) could result in differences in function, and expression of different isoforms by different tissues could reflect these functional differences. In this context, a specific isoform of KDM5B that is expressed in nevi and melanomas and contains an additional 36 amino acids (Roesch *et al., 2005*) is only expressed at low levels in primary breast cancers (Barrett *et al*., 2002).

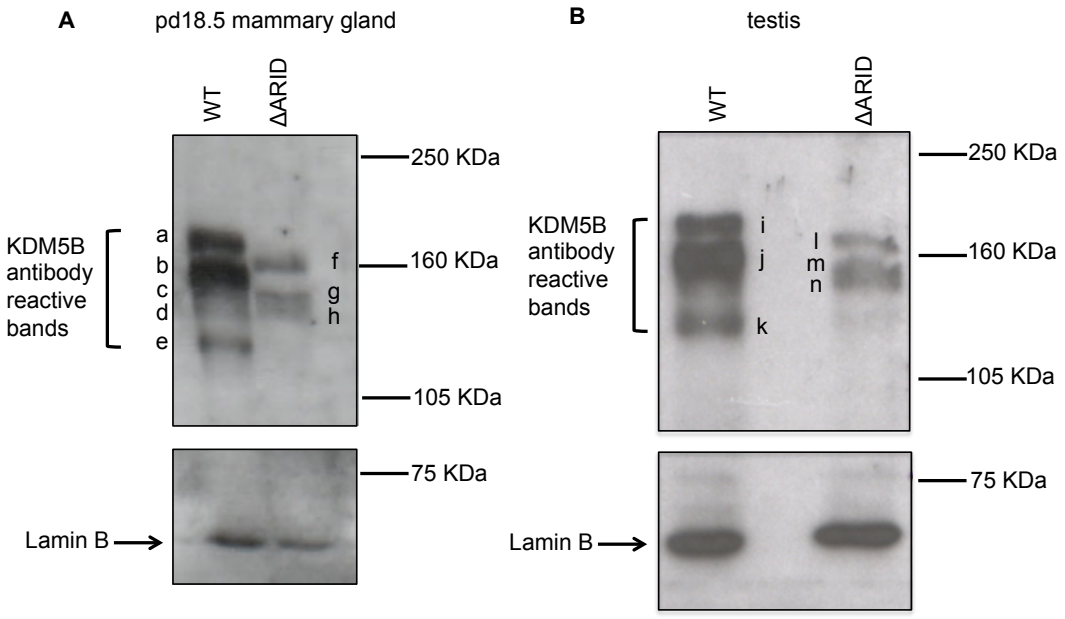


Figure 3.7 Expression of a smaller less abundant KDM5B protein in the B6;129-*Kdm5b ΔARID* mammary gland and testis. Western transfer showing translation of a smaller, less abundant KDM5B ΔARID protein product. in (A) the mammary gland at pd18.5 and (B) the adult testis.

3.4.3 A demethylase independent function for KDM5B?

The ARID sequence of KDM5B is required for demethylase activity (Yamane *et al*., 2007, Xiang *et al*., 2007) and has been deleted from the *Kdm5b ΔARID* murine line. The viability of the *Kdm5b ΔARID* murine line may therefore suggest a crucial demethylase independent function for KDM5B and puts into question which other domains are also important. In fact a demethylase independent function also extends to other members of the KDM5 family of proteins (DiTacchio *et al* 2011) and may be conserved across species (Li *et al*., 2010, DiTacchio *et al* 2011). In a demethylase-independent manner KDM5A functions to regulate circadian rhythms by enhancing transcription by CLOCK-BMAL1 (DiTacchio *et al* 2011). Also, lid is the only KDM5 homolog expressed in *D. Melanogaster* and is essential for development, a function that is independent of its demethylase activity (Li *et al*., 2010). Indeed an enzyme independent function maybe a common mechanism amongst the protein families that regulate the methylation of histone 3 on lysine 4 (Terranova *et al*., 2006, Yu *et al*., 1995, Yagi *et al*., 1998, DiTacchio *et al* 2011). A

case in point can be made regarding the embryonic lethality of the H3K4 methyltransferase *Kmt2a*-null (a.k.a MLL1) mutant (Yu *et al*., 1995, Yagi *et al*., 1998) in contrast to the viability of the catalytically inactive *Kmt2a SET* domain mutant (Terranova *et al*., 2006). These published data, taken together with our studies certainly highlight the functional importance of the remaining protein domains, which may prove to be as significant as the intrinsic catalytic activity.

3.4.4 Recruitment of KDM5B to the genome

In addition to the ARID domain of KDM5B being required for demethylase activity (Xiang *et al*., 2007, Yamane *et al*., 2007), the ARID domain of KDM5B has been shown to bind to DNA (Scibetta *et al*., 2007, Yao *et al*., 2010). Interestingly, deletion of the *ARID* domain of *Kdm5b* results in a mammary gland phenotype that can differentiate during pregnancy. Certainly ChIp-qPCR studies have demonstrated that in *Kdm5a* null cells, some KDM5A gene targets can be bound by KDM5B (Islam *et al*., 2011b) suggesting the propensity for compensation and therefore demethylase activity. Furthermore KDM5B has been identified in different complexes and can potentially be recruited to the genome via different proteins. For example, in the case of a KDM5B/PcG complex neither KDM5B nor PcG proteins, at least individually, are essential for each other's recruitment to the genome (Schmitz *et al*., 2011). In addition the N terminus PHD sequence of KDM5B can bind to unmodified histone H3 and H3K9me1/2/3 (Klein *et al*., 2014) whilst the C-terminus PHD sequences of KDM5B can bind H3K4me1/2/3 (Li *et al*., 2011, Klein *et al*., 2014), providing yet another mechanism for the KDM5B ΔARID protein to be recruited to the genome, where KDM5B could function in a demethylase independent manner. Therefore any effects on transcription maybe subtle, potentially accounting for the delay in mammary gland development presented in the KDM5B ΔARID female.

3.4.5 The B6;129-Kdm5b ΔARID male is fertile

Although germ cell number and the degree of differentiation were not studied, the reduced protein expression levels of the full length KDM5B protein (heterozygous B6;129-*Kdm5b-Exon 1* knock out) or the KDM5B ΔARID protein (*B6;129-Kdm5b*

ΔARID) appear not to grossly affect oogenesis or spermatogenesis. KDM5B and KDM5D expression pattern during spermatogenesis suggests that KDM5D may compensate for KDM5B function during pachytene/diplotene stages of meiosis (Madsen *et al*., 2003, Akimoto *et al*., 2008). However, KDM5D was not detected during the mitotic stage of spermatogenesis (Akimoto *et al*., 2008) suggesting that the reduced expression levels of KDM5B are sufficient and further that alternative H3K4 demethylase activity could be compensated for in the *Kdm5b ΔARID* murine line.

We have presented here an effect of KDM5B ΔARID expression on mammary gland development. However, variations in mammary gland ductal side branching are known to occur between different strains of mice; the mammary gland architecture in the 129ola murine line being highly branched in contrast to the mammary gland architecture presented in the C57BL/6J murine line. Therefore, the variable genetic contribution of mixed genetic backgrounds can complicate interpretation of the resulting phenotype. This issue of a variable mammary gland architecture is highlighted in a study comparing the mammary gland architecture presented in the F2 generation of 45, B6;129 offspring. Of the 45 mice studied, 12 mice demonstrated the highly side branched structure of the 129 murine strain; 8 mice presented with poor ductal branch structure of the C57BL/6J murine line and the remaining 25 mice presented with an intermediary ductal branch structure between the two extremes (Naylor *et al*., 2002). This problem in quantitatively and accurately defining a potential mammary phenotype can be over come by backcrossing the genetically modified mice onto a pure genetic background as detailed in Chapter 4.

3.5 Supplemental materials

A

Strain 1A4		
	genotype	
	+/+	+/-
e	46	92
o	67	72
o-e	21	-20
(o-e)sq	441	400
(o-e)sq/e	9.58695652	4.34782609
sum	13.93478261	

B

Strain 1A8		
	genotype	
	+/+	+/-
e	35	70
o	57	49
o-e	22	-21
(o-e)sq	484	441
(o-e)sq/e	13.8285714	6.3
sum	20.12857143	

Table 3S1 Heterozygous offspring of the B6;129 *Kdm5b-Exon1* knock out murine line are not born according to Mendelian frequences. Calculations for Chi Squared test. The Chi squared value for 1 degrees of freedom and p=0.001 is 10.83. As the observed value is greater than 10.83 we reject our hypothesis, and state that the heterozygous B6;129 *Kdm5b-Exon1* knock out line are not born according to Mendelian frequency (1A4: p=0.0002. 1A8: p=0.0001)

A

Pair 1												
	Total from 9 litters			genotype								
				+/+			+/-			-/-		
	total	male	female	total	male	female	total	male	female	total	male	female
total	88	45	43	**26**	13	13	**48**	25	23	**14**	7	7
mendelian ratio				29.55			54.55			15.9		

B

Pair 2												
	Total from 9 litters			genotype								
				+/+			+/-			-/-		
	total	male	female	total	male	female	total	male	female	total	male	female
total	89	46	43*	**22**	11	11	**48**	26	22	**18**	8	10
mendelian ratio				24.72			53.93			20.22		

Table 3S2 Genotyping results from B6;129-*Kdm5b ΔARID* heterozygous breeding program demonstrates that the B6;129-*Kdm5b ΔARID* offspring are born according to Mendelian frequency. (Pair 1: 0.1<p<0.5 and Pair 2: 0.5<p<0.9)

A

pair 1	genotype		
	+/+	+/-	-/-
e	22	44	22
o	26	48	14
o-e	4	4	-8
(o-e)sq	16	16	64
(o-e)sq/e	0.72727273	0.36363636	2.90909091
sum	4		

B

pair 2	genotype		
	+/+	+/-	-/-
e	22	44	22
o	22	48	18
o-e	0	4	-4
(o-e)sq	0	16	16
(o-e)sq/e	0	0.36363636	0.72727273
sum	1.090909091		

C

pair 1 and 2	genotype		
	+/+	+/-	-/-
e	44	88	44
o	48	96	32
o-e	4	8	-12
(o-e)sq	16	64	144
(o-e)sq/e	0.36363636	0.72727273	3.27272727
sum	4.363636364		

Table 3S3 Calculations for Chi Squared test (data shown in table 3.2 and 3S2). The Chi squared value for 2 degrees of freedom and P=0.05 (5%) is 5.99. As the observed value is lower than 5.99 we accept our hypothesis, that there is no deviation from the expected Mendelian frequency.

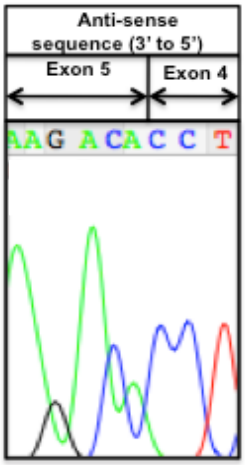


Figure 3S1 DNA trace from the B6;129-*Kdm5b WT* mammary gland transcript at pd 18.5. DNA trace showing anti-sense sequencing data obtained from cDNA reverse transcribed from RNA isolated from B6;129-*Kdm5b WT* mammary gland tissue at pd18.5 using primers specific to *Kdm5b* exon 5 (for schematic representation of PCR primer location within exon 1 and 5 see figure 3S2

Exon	Exon 4	Exon 5	
cDNA sequence (sense)	AGG	TGT	CTT
cDNA sequence (anti-sense)	TCC	ACA	GAA
Translated sequence	R	C	L

Table 3S4 Derived sequence from the DNA trace (Fig 3S1) of B6;129-*Kdm5b* WT cDNA showing exon 4 to 5 boundaries. Table showing sequencing data obtained from cDNA reverse transcribed from RNA isolated from B6;129-*Kdm5b WT* mammary gland tissue at pd18.5

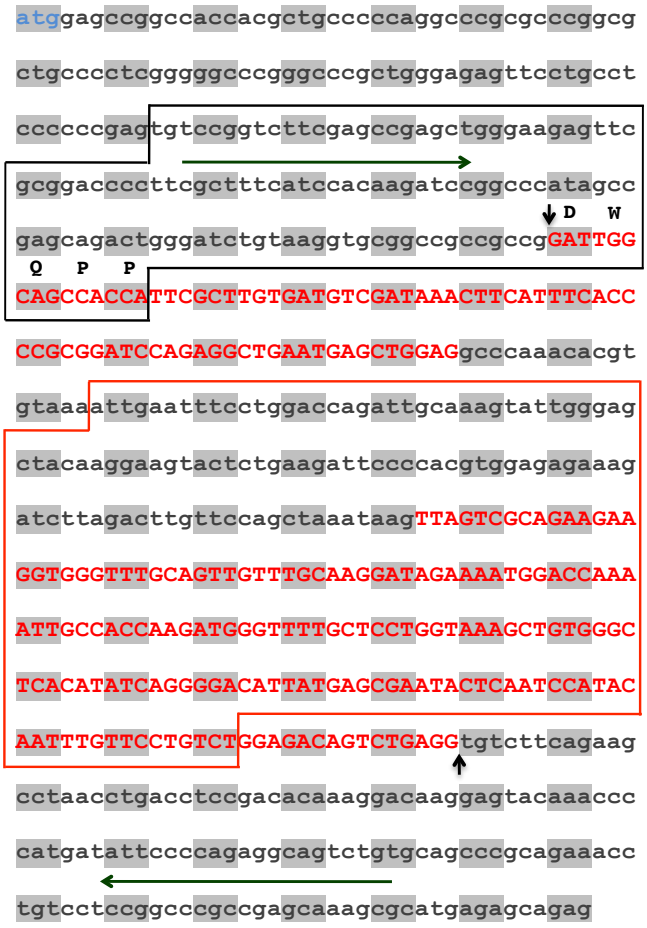


Figure 3S2 Murine *Kdm5b* coding sequence showing translation start site (atg), codon sequence (alternate grey and white highlight), exons 1 to 5 (alternate black (lower case) and red text (upper case)) the JmjN domain (black box), ARID sequence (red box), splice sites (black arrow), exon 1 and exon 5 PCR primer location (horizontal arrow) and amino acid residues removed due to splicing together of exon1 to exon 5 in the ΔARID sequence.
Domain sequence derived from Swiss-Prot:Q80Y84.
NCBI Reference Sequence: NM_152895.2

Chapter 4: Results

KDM5B is expressed during mammary gland ductal morphogenesis and is required for normal mammary gland development

Chapter 4. KDM5B is expressed during mammary gland ductal morphogenesis and is required for normal mammary gland development

4.1 Aims:

In Chapter 3 preliminary studies on the chimeric B6;129-*Kdm5b ΔARID* murine line have indicated that KDM5B is required for normal mammary gland ductal morphogenesis. However the influence of genetic background on mammary gland morphogenesis has complicated the interpretation of the presenting phenotype in the chimeric B6;129-*Kdm5b ΔARID* female. In addition, studies on WT KDM5B expression in the mammary gland are limited. Therefore, understanding the role of KDM5B during mammary gland development could be advanced by the following aims:

(1) To examine the pattern and level of KDM5B expression during mammary gland morphogenesis in the C57BL/6J female.
(2) To backcross the chimeric B6;129-*Kdm5b ΔARID* murine line onto the inbred C57BL/6J genetic background.
(3) To characterise the mammary gland phenotype presented in the C57BL/6J-*Kdm5b ΔARID* female.

4.2 Introduction: Murine mammary gland ductal morphogenesis

The primary function of the mammary gland is to produce and deliver adequate amounts of milk in order for the female to support her offspring at parturition. Mammary gland ductal morphogenesis occurs in distinct stages with the mammary bud providing all future mammary epithelial cell lineages (Van Keymeulen *et al*., 2011). Any further mammary gland development is then not fully realized until after birth where further morphogenesis is in synchrony with sexual maturity (puberty) and reproduction. The expansion of mammary epithelium during puberty and pregnancy together with the regenerative capacity of the epithelium during subsequent pregnancies implicates the existence of mammary stem cells. In line with this, the identification of murine and human stem and progenitor populations has provided evidence of a differential hierarchy within mammary epithelium (Shackleton *et al*., 2006, Stingl *et al*., 2006, Van Keymeulen *et al*., 2011, Shehata *et al*., 2012).

The formation of this extensive tree like network of branched ducts at adulthood provides the foundation for further pregnancy associated alveolar restricted progenitor expansion with differentiation toward milk secreting alveoli lobules in preparation for parturition. At weaning, the milk secreting epithelial cells become redundant and undergo programmed cell death (Kreuzaler *et al*., 2011), with a morphologically distinct biphasic re-modeling of the mammary gland that ultimately resembles the pre-pregnant mammary gland state (6 days post-weaning) - a process termed involution.

In order to study the molecular mechanisms involved during involution, forced weaning at approximately 7 days promotes synchronous involution, a process that is initiated over 2-3 days and involves a reversible event mediated via local factors rather than systemic hormones (Lund *et al*., 1996, Li *et al*., 1997, Marti *et al*., 1997). This is followed by a second stage that initiates programmed cell death as a consequence of mammary gland remodeling mediated via systemic hormones (Feng *et al*., 1995 and Lund *et al*., 1996). Although involution of the mammary gland is marked by two distinct morphological events, these events are under the control of four discrete transcriptional profiles (Clarkson *et al*., 2004 and Stein *et al*., 2004).

This process of mammary gland development therefore requires the timely integration of signaling pathways involved in mammary gland epithelial cell proliferation, migration, branching, invasion, differentiation and programmed cell death that are orchestrated at a local level by co-factor interaction and further mediated by reciprocal paracrine interactions between the ductal epithelial cells and the surrounding stroma. Our understanding of KDM5B function during mammary gland morphogenesis would therefore be improved by examining when and in which cells KDM5B is expressed.

4.3 Results

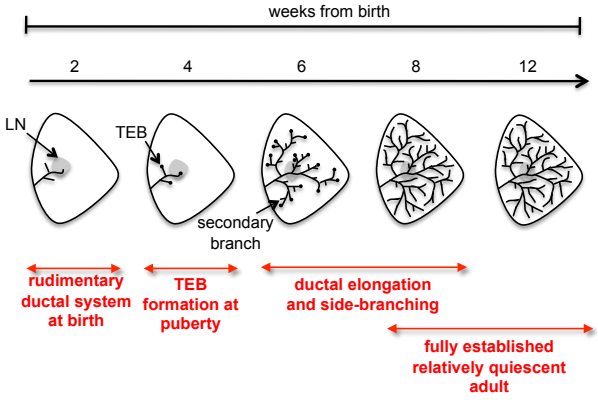
4.3.1 Documentation of KDM5B expression during C57BL/6J murine mammary gland development

To date, studies on KDM5B expression in normal adult mammary gland tissue have been limited (Madsen *et al*., 2002, Stein *et al*., 2003) Thus far, Madsen and colleagues (2002), have shown that using *in situ* hybridisation on sections taken from the adult nulliparous mammary gland, that *Kdm5b* expression is restricted to ductal epithelial cells (Madsen *et al*., 2002). Furthermore, these authors also examined *Kdm5b* expression using Northern hybridization on RNA isolated from mammary gland tissue taken from mid to late pregnancy (day 11, 15 and 18), during lactation (week 1 and 2) and through a period of five days during mammary gland involution (days 1, 2, 3 and 5). This study demonstrated that the expression of the *Kdm5b* transcript is detected at late pregnancy (day 15 and day 17) with maximal expression seen at pregnancy day 17 and no detectable levels of the *Kdm5b* transcript being observed during lactation and involution. Using RNA isolated form the mammary gland of Balb/C females, Stein and colleagues (2003), performed microarray analysis to detect the transcript levels expressed during mammary gland morphogenesis. However, the *Kdm5b* transcript was only detected at low levels throughout mammary gland morphogenesis.

To better understand whether KDM5B may have any potential role during defined stages of murine mammary gland development we embarked on a more detailed examination of the KDM5B cellular localisation and expression profile from puberty through to adulthood (weeks 4 and 12), pregnancy (days 10.5, 12.5, 14.5, 17.5, 18.5) lactation (days 3 and 7) and days 3, 7 and 10 post forced weaning in the C57BL/6J murine line. To achieve this, the thoracic mammary gland was whole mounted and used for *in situ* hybridisation whilst the inguinal mammary gland was snap frozen for the isolation of protein and RNA and subject to western blot and quantitative RT-PCR (qPCR) (See Fig. 4A, B and C for details of mammary gland developmental stage and technique employed).

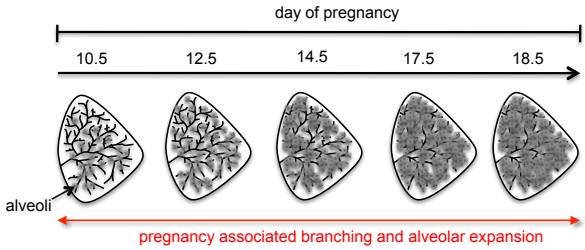
A Nulliparous mammary gland

In situ hybridisation	ND	YES	ND	ND	YES
Western blot	ND	ND	ND	ND	YES
Q-PCR	ND	ND	ND	ND	YES



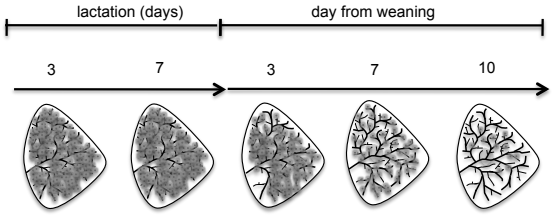
B Pregnant mammary gland

In situ hybridisation	ND	YES	ND	ND	YES
Western blot	ND	ND	YES	ND	YES
Q-PCR	YES	ND	YES	YES	ND



C Lactation and post weaning

In situ hybridisation	ND	ND	ND	ND	ND
Western blot	YES	YES	YES	YES	YES
Q-PCR	YES	YES	YES	YES	YES



ND: Not Determined

Figure 4 Schematic representation of mammary gland ductal morphogenesis detailing the techniques employed to examine KDM5B expression in the C57BL/6J mammary gland (A) nulliparous (B) pregnancy (C) lactation and post weaning.

4.3.1.1 Cellular localisation of the Kdm5b transcript expressed during murine C57BL/6J mammary gland development

Development of the post-natal murine mammary gland is initiated at the onset of puberty (4 weeks of age) with the formation of, and proliferation at TEB structures and then fully realised by adulthood (8 weeks of age) at which point the relatively quiescent mammary gland ductal tree is poised for pregnancy associated development. We therefore sought to explore whether KDM5B may have a potential role at these two important stages in the development of the nulliparous murine mammary gland. In order to examine the cellular localisation of the *Kdm5b* transcript by *in situ* hybridisation, 4 and 12 week old C57BL/6J females were culled and the thoracic mammary gland whole mounted. *In situ* hybridisation using an anti-sense riboprobe homologous to the 3' region of the *Kdm5b* transcript (3.9kb to 4.7kb. (Madsen *et al*., 2002)) has demonstrated that the *Kdm5b* transcript is expressed in a diffuse pattern within epithelial cells of the primary and secondary ductal systems and proliferating TEB structures at 4 weeks of age (Fig 4.1.A). Furthermore, a cross-section through the relatively quiescent adult (12 weeks) mammary gland duct (Fig 4.1.B), demonstrates that the expression of *Kdm5b* is restricted in the main, to the majority of ductal epithelial cells; the expression level being increased compared to that seen in the mammary gland at 4 weeks of age. These data suggest a possible function for KDM5B in the proliferation of mammary gland epithelial cells (at 4 weeks of age) and later the survival and or differentiation of mammary gland epithelial cells in the adult nulliparous mammary gland. We have also demonstrated that at mid-pregnancy (pd12.5) the *Kdm5b* transcript is localised mainly to ductal epithelial cells as well as the epithelium of the alveoli (Fig 4.1.C). Similarly, the *Kdm5b* transcript is detected in the mammary gland at late pregnancy (pd18.5) where the *Kdm5b* transcript is localised to the epithelium of both the duct and alveoli when the murine mammary gland is fully differentiated in preparation for parturition (Fig 4.1.D).

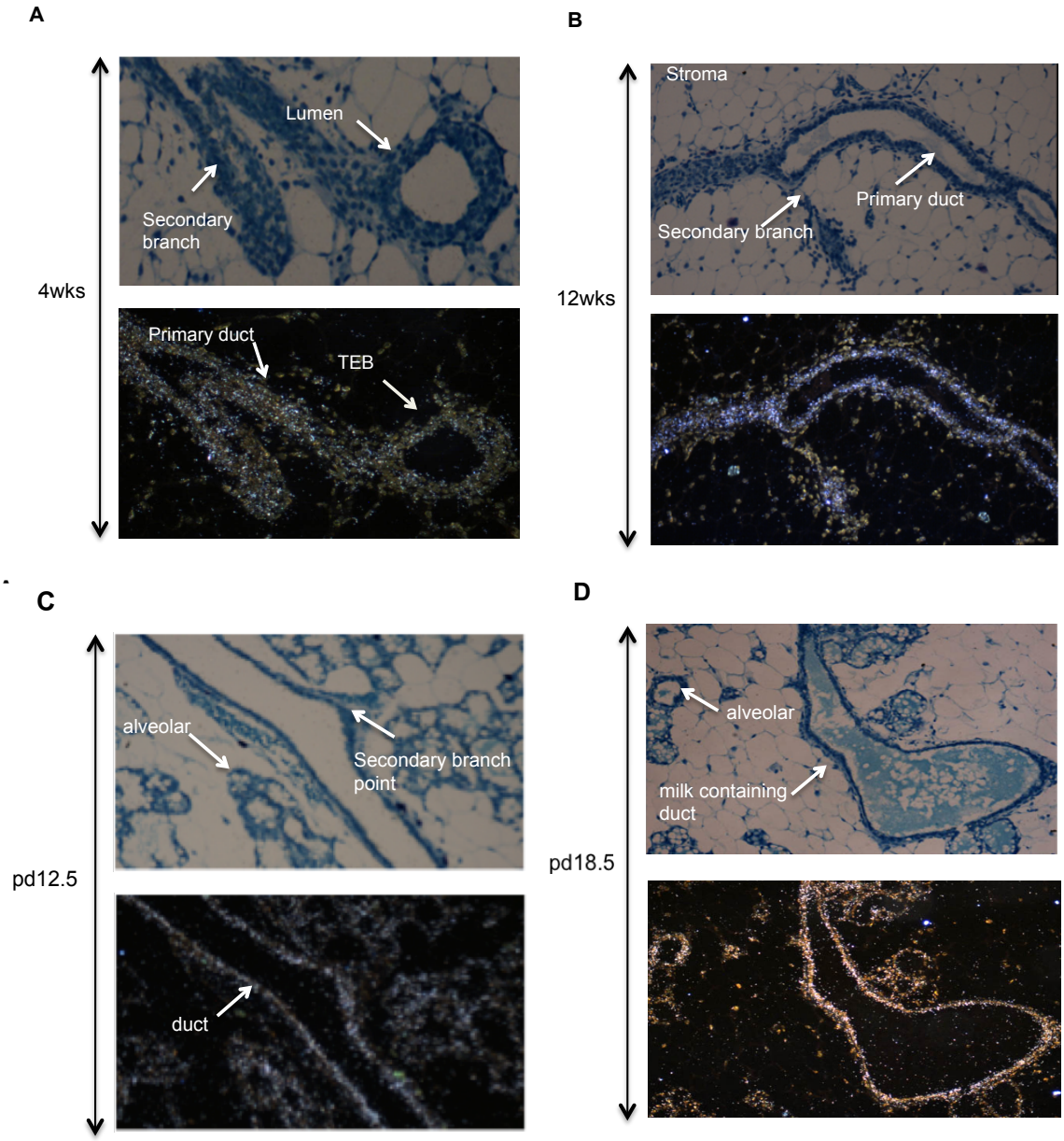


Figure 4.1 *In situ* hybridization showing the *Kdm5b* transcript is restricted in the main to epithelial cells in the C57BL/6J mammary gland. Representative H and E staining on the nulliparous mammary gland at 4 and 12 weeks of age (A and B; top image respectively) and pregnancy at pd12.5 and pd18.5 (C and D; top image respectively). *In situ* hybridization showing the localisation of the *Kdm5b* transcript to mammary gland epithelial cells during C57BL/6J WT mammary gland development (A and B; bottom image at 4 and 12 weeks respectively; C and D; bottom image at pd12.5 and 18.5 respectively). Magnification x20.

4.3.1.2 Quantification of the Kdm5b transcript during murine C57BL/6J mammary gland development

Given the availability of a more sensitive technique – quantitative PCR - for the detection of low-level transcripts, we examined in more detail the level of the *Kdm5b* transcript during mammary gland morphogenesis. In order to achieve this, cDNA was generated from RNA isolated from inguinal mammary glands taken from the adult virgin (12 weeks), during pregnancy (day 10.5, 12,5 and 17.5) during lactation (day 3 and 7) and through days 3, 7 and 10 post forced weaning. Comparing the *Kdm5b* transcript level throughout mammary gland development with that expressed in the adult virgin mammary gland, our findings are consistent with our observations using *in situ* hybridisation, and in part consistent with those findings reported by Madsen and colleagues (2002). We have shown that the *Kdm5b* transcript is differentially expressed in the developing mammary gland, being detected in the adult nulliparous mammary gland and throughout pregnancy (being maximum at 18.5 days) when epithelial cell proliferation leads to further branching and alveolar expansion followed by differentiation in preparation for parturition. Consistent with Madsen and colleagues (2002), *Kdm5b* expression is reduced during lactation, however we have shown that the *Kdm5b* transcript is re-expressed during involution (day 3 post forced weaning) and in the parous mammary gland (Fig 4.2).

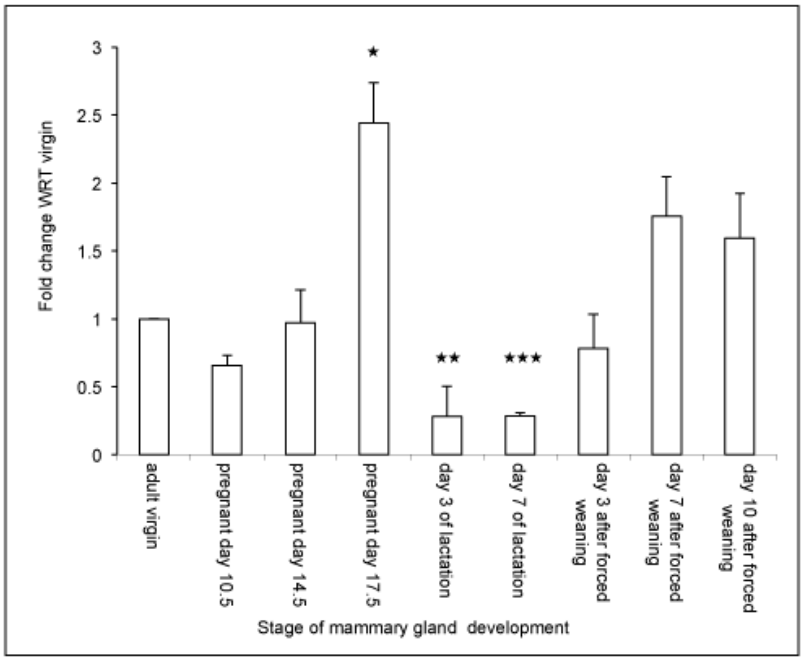


Figure 4.2 The *Kdm5b* transcript is differentially expressed in the C57BL/6J WT murine mammary gland. WRT is an acronym for 'with respect to'. The *Kdm5b* amplicon PCR cycle number was normalized against the 18S ribosomal RNA amplicon PCR cycle number. The average expression of 8 adult virgin mice was used to compare the expression of *Kdm5b* during mammary gland development. RNA was isolated from one mammary gland throughout pregnancy, lactation and post forced weaning. Standard deviation is determined from three RT-PCR experiments. ★, $p<0.02$. ★★, $p<0.05$. ★★★, $p< 0.001$.

4.3.1.3 KDM5B protein expression during murine C57BL/6J mammary gland development

To determine whether the differential *Kdm5b* transcript expression pattern noted during murine mammary gland development correlates with KDM5B protein expression levels, nuclear proteins were extracted from the mammary gland at different stages of development and subject to Western blot analysis (Fig. 4.3). The predicted molecular weight for KDM5B is 170KDa and is expressed in the mammary gland at day 17 of pregnancy (Madsen *et al*., 2002). Using the same KDM5B specific antibody as used by Madsen and colleagues (2002), we have shown by Western blot transfer that two KDM5B antibody specific bands of approximately equal intensities are expressed in the murine mammary gland at pd18.5; one band at the predicted molecular weight of 170KDa and another band with an approximate molecular weight of 150KDa. Interestingly, Western blot transfer of the nuclear extracts prepared from the mammary gland of the adult virgin through pregnancy, lactation and post forced weaning demonstrates that a 170 KDa KDM5B specific band is expressed throughout mammary gland development, with a noticeable increase at pd18.5. However expression of a KDM5B antibody reactive protein is also detected at approx. 150KDa which is most obvious in the mammary gland at pd18.5, and at days 7 and 10 post forced weaning corresponding to the increased level of the *Kdm5b* transcript detected by quantitative PCR. A faster migrating antibody reactive band is also detected throughout mammary gland morphogenesis, and may represent a KDM5B splice variant.

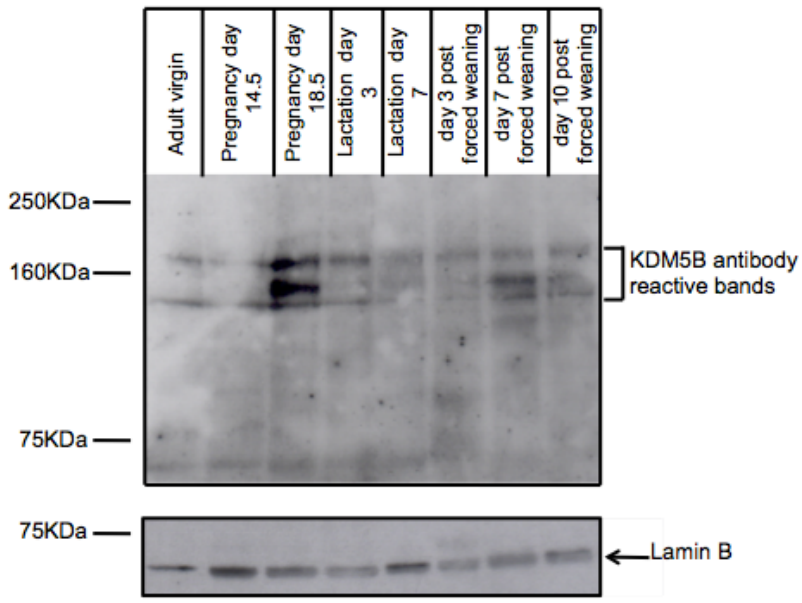


Figure 4.3 KDM5B protein expression in the C57BL/6J murine mammary gland. KDM5B is differentially expressed during murine mammary gland development.

4.3.1.4 Backcross of the chimeric homozygous B6;129-Kdm5b ΔARID murine line onto the inbred C57BL/6J *genetic strain.*

As explained in Chapter 3, the mammary gland morphology presented by chimeric *B6;129* off-spring can resemble that of either the parental strain or a intermediate morphology making interpretation of a phenotype difficult (Naylor *et al.*, 2002). Therefore, to establish genetic and phenotypic uniformity in order to better standardize the characterisation of the mammary gland phenotype, the chimeric homozygous B6;129-*Kdm5b ΔARID* murine line was backcrossed onto the inbred C57BL/6J murine line. A breeding program was instigated between chimeric heterozygous B6;129-*Kdm5b ΔARID* females and inbred C57BL/6J-*Kdm5b WT* males to generate F1 progeny. The F1 progeny were genotyped with neomycin specific PCR (Figure 4.4 and Fig. 4S1 in the supplemental material) using tail-snip genomic DNA, and the resulting heterozygous B6;129-*Kdm5b ΔARID* offspring were paired with the inbred C57BL/6J-*Kdm5b WT* murine line, repeated over a total of 6 generations (Table 4).

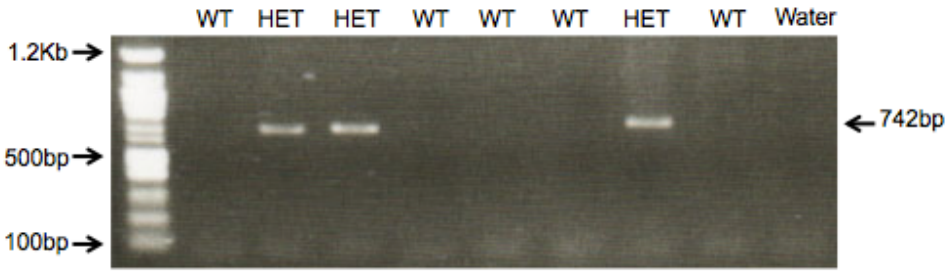


Figure 4.4 Representative neomycin specific PCR reaction on genomic DNA isolation from the ear-snips of a heterozygous B6;129-*Kdm5b ΔARID* and C57BL/6J-*Kdm5b WT* breeding program (Data shown from the forth generation offspring of Pair 7 – see Table 4).

Pair	generation	male	female	genotype								
				Litter size			+/-			+/+		
				total	male	female	total	male	female	total	male	female
Pair 1	1st	C57BL/6-*Kdm5b WT*	B6;129-*Kdm5b ΔARID*	8	3	5	4	3	1	4	0	4
Pair 2	1st	C57BL/6-*Kdm5b WT*	B6;129-*Kdm5b ΔARID*	9	3	6	5	2	3	4	1	3
pair 2 litter 2	1st	C57BL/6-*Kdm5b WT*	B6;129-*Kdm5b ΔARID*	13	11	2	6	5	1	7	6	1
Pair 1 litter 2	1st	C57BL/6-*Kdm5b WT*	B6;129-*Kdm5b ΔARID*	15	7	8	8	2	6	7	5	2
Pair 3	2nd	B6;129-*Kdm5b ΔARID*	C57BL/6-*Kdm5b WT*	7	3	4	1	0	1	6	3	3
Pair 4	2nd	C57BL/6-*Kdm5b WT*	B6;129-*Kdm5b ΔARID*	8	3	5	5	1	4	3	2	1
Pair 5	3rd	B6;129-*Kdm5b ΔARID*	C57BL/6-*Kdm5b WT*	6	5	1	2	2	0	4	3	1
Pair 6	3rd	C57BL/6-*Kdm5b WT*	B6;129-*Kdm5b ΔARID*	5	3	2	4	2	2	1	1	0
Pair 7	4th	B6;129-*Kdm5b ΔARID*	C57BL/6-*Kdm5b WT*	8	5	3	3	1	2	5	4	1
Pair 8	4th	B6;129-*Kdm5b ΔARID*	C57BL/6-*Kdm5b WT*	7	4	3	2	2	0	5	2	3
Pair 9	5th	B6;129-*Kdm5b ΔARID*	C57BL/6-*Kdm5b WT*	10	4	6	1	0	1	9	4	5
Pair 10	5th	B6;129-*Kdm5b ΔARID*	C57BL/6-*Kdm5b WT*	4	2	2	1	1	0	3	1	2
Pair 11	6th	B6;129-*Kdm5b ΔARID*	C57BL/6-*Kdm5b WT*	10	2	8	1	0	1	9	2	7
Pair 12	6th	B6;129-*Kdm5b ΔARID*	C57BL/6-*Kdm5b WT*	5	2	3	2	1	1	3	1	2
Pair 11 litter 2	6th	B6;129-*Kdm5b ΔARID*	C57BL/6-*Kdm5b WT*	11	2	9	4	1	3	7	1	6
Pair 11 litter 3	6th	B6;129-*Kdm5b ΔARID*	C57BL/6-*Kdm5b WT*	6	3	3	2	1	1	4	2	2
			total	132	62	70	51	24	27	81	38	43
			mendelian ratio				38.63636364			61.36363636		

Table 4 PCR generated genotyping results from the backcross of the B6;129-*Kdm5b ΔARID* chimeric line onto the C57BL/6J genetic strain.
Table showing the cumulative genotype results over 6 generations of backcrossing.

4.3.1.5 Generation of the homozygous C57BL/6J-*Kdm5b ΔARID murine line*

In order to generate homozygous C57BL/6J-*Kdm5b ΔARID* offspring, a heterozygous C57BL/6J-*Kdm5b ΔARID* breeding program was established, and the resulting offspring genotyped by Southern blot analysis (Fig. 4.5) using tail-snip genomic DNA (For schematic representation of screening strategy with probe location used in Southern blot analysis see Chapter 3, Fig. 3.6). Those offspring identified as being homozygous for the *Kdm5b ΔARID* allele were bred to generate homozygous C57BL/6J-*Kdm5b ΔARID* females for characterisation of the mammary gland phenotype (For representative Southern blot see Fig. 4.6)

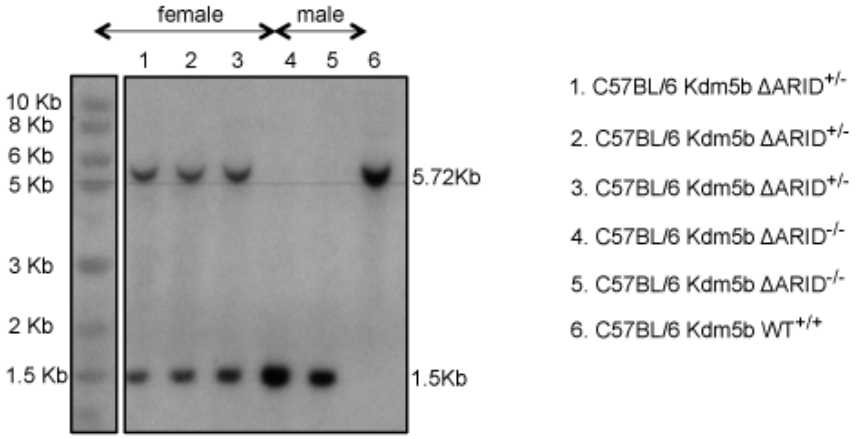


Figure 4.5 Representative Southern blot on tail-snip genomic DNA isolated from a heterozygous C57BL/6J-*Kdm5b ΔARID* breeding program showing the *Kdm5b WT* allele and the engineered allele after BamH1 digest.

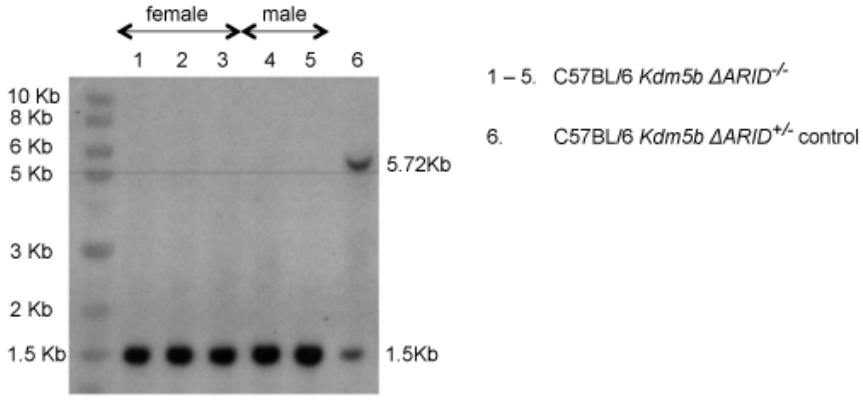


Figure 4.6 Representative Southern blot on tail-snip genomic DNA isolated from a homozygous C57BL/6J-*Kdm5b ΔARID* breeding program showing the engineered allele after BamH1 digest.

4.3.1.6 Kdm5b transcript levels in the C57BL/6J-*Kdm5b ΔARID female mammary gland do not reflect KDM5B protein levels*

The level of KDM5B protein expression in the chimeric B6;129-*Kdm5b ΔARID* female mammary gland at pd18.5 is reduced compared to its chimeric B6;129-*Kdm5b WT* counterpart (Chapter 3, Fig. 3.7). To examine whether this reduced protein expression level is reflected in the C57BL/6J-*Kdm5b ΔARID* female and correlates with *Kdm5b* transcript levels, nuclei were extracted for Western blot analysis and the *Kdm5b* transcript quantified using PCR.

As shown in Fig. 4.7A, the level of the *Kdm5b* transcript is elevated in the C57BL/6J-*Kdm5b ΔARID* mammary gland at pd18.5 compared to the C57BL/6J-*Kdm5b WT* counterpart ($p<0.02$). Interestingly the elevated level of the *Kdm5b* transcript expressed in the C57BL/6J-*Kdm5b ΔARID* mammary gland at pd18.5 does not translate to elevated KDM5B protein levels detected by Western blot analysis (Fig. 4.7B). Furthermore, immunohistochemistry using a KDM5B specific antibody has demonstrated that in comparison with the wild type counterpart, KDM5B specific signal intensity is reduced and slightly fewer KDM5B positive epithelia are detected in the C57BL/6J-*Kdm5b ΔARID* mammary gland at pd18.5 (Fig4.7C and Fig4.7D), and could reflect the reduced KDM5B protein expression level detected by Western blot. In comparison with the C57BL/6J-*Kdm5b WT* counterpart, the reduced expression level of KDM5B expressed in the mammary gland of the C57BL/6J-*Kdm5b ΔARID* female at pd18.5 is in keeping with the reduced level of the KDM5B protein documented at the same stage of pregnancy in the mammary gland of the chimeric B6;129-*Kdm5b ΔARID* female by Western blot analysis.

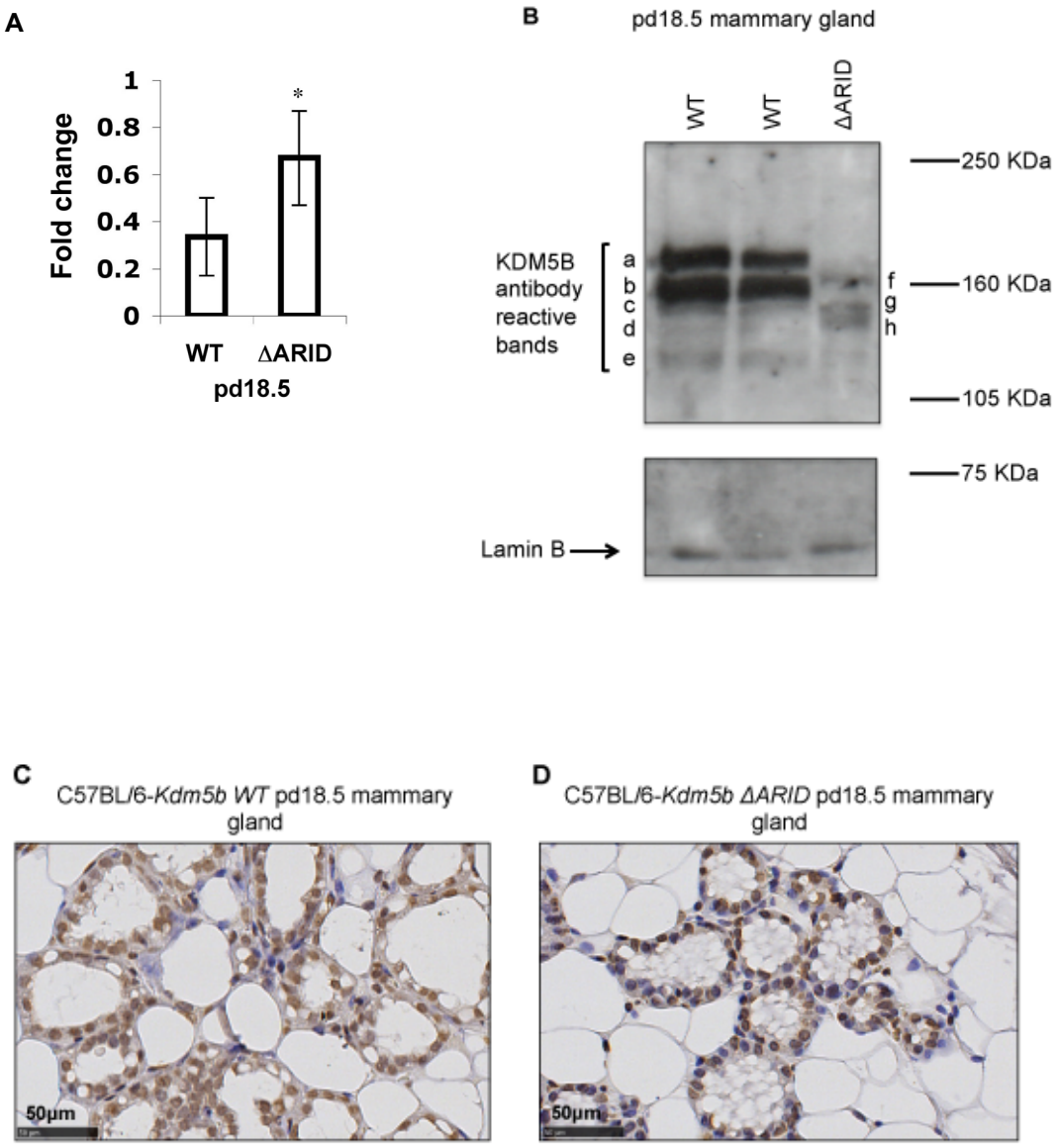


Figure 4.7 Elevated *Kdm5b* transcript level in the C57BL/6J-*Kdm5b ΔARID* mammary gland at pd18.5 results in the translation of a less abundant KDM5B ΔARID protein (A) Quantitative RT-PCR using primers downstream of the ARID domain showing an increase in the *Kdm5b ΔARID* transcript compared to the *Kdm5b WT* transcript at pd18.5. (∗, P<0.02. WT, n=4. ΔARID, n=5). The *Kdm5b* amplicon PCR cycle number was normalized against the 18S ribosomal RNA amplicon PCR cycle number (B) Western blot showing translation of a smaller, less abundant KDM5B ΔARID protein product in the mammary gland at pd18.5. Immunohistochemistry for KDM5B expression on (C) C57BL/6J-*Kdm5b WT* and (D) C57BL/6J-*Kdm5b ΔARID* mammary gland sections at pd18.5.

4.3.2 Mammary gland development in the C57BL/6J-*Kdm5b ΔARID* nulliparous female.

4.3.2.1 The C57BL/6J-*Kdm5b ΔARID 4-week old mammary gland presents with fewer terminal end buds and a defect in ductal elongation and side branching.*

We have shown that the *Kdm5b* transcript is localised to the luminal epithelial cells at the on-set of puberty (at 4 weeks of age) in C57BL/6J mammary gland (Fig. 4.1) and preliminary data suggest that the chimeric B6;129-*Kdm5b ΔARID* nulliparous female mammary gland presents with a defect in ductal morphogenesis (Chapter 3). Development at approximately 4 weeks of age of the pubertal nulliparous murine mammary gland ductal tree requires the formation of, and proliferation at TEB structures. We therefore sought to examine whether the expression of a truncated KDM5B protein affects the initial developmental stages of post-natal mammary gland development (TEB formation) by examining the gross morphology of the nulliparous mammary gland at 4 weeks of age. Therefore, at 4 weeks of age the thoracic and inguinal mammary glands were whole mounted and stained with carmine. Figure 4.8A, shows an organised ductal system with TEB formation in the C57BL/6J-*Kdm5b WT* nulliparous female. However, the C57BL/6J-*Kdm5b ΔARID* nulliparous gland presents with a less organised ductal system with on average a 2.5 fold reduction in TEB number (Fig. 4.8B and C. $*$, $p<0.0005$).

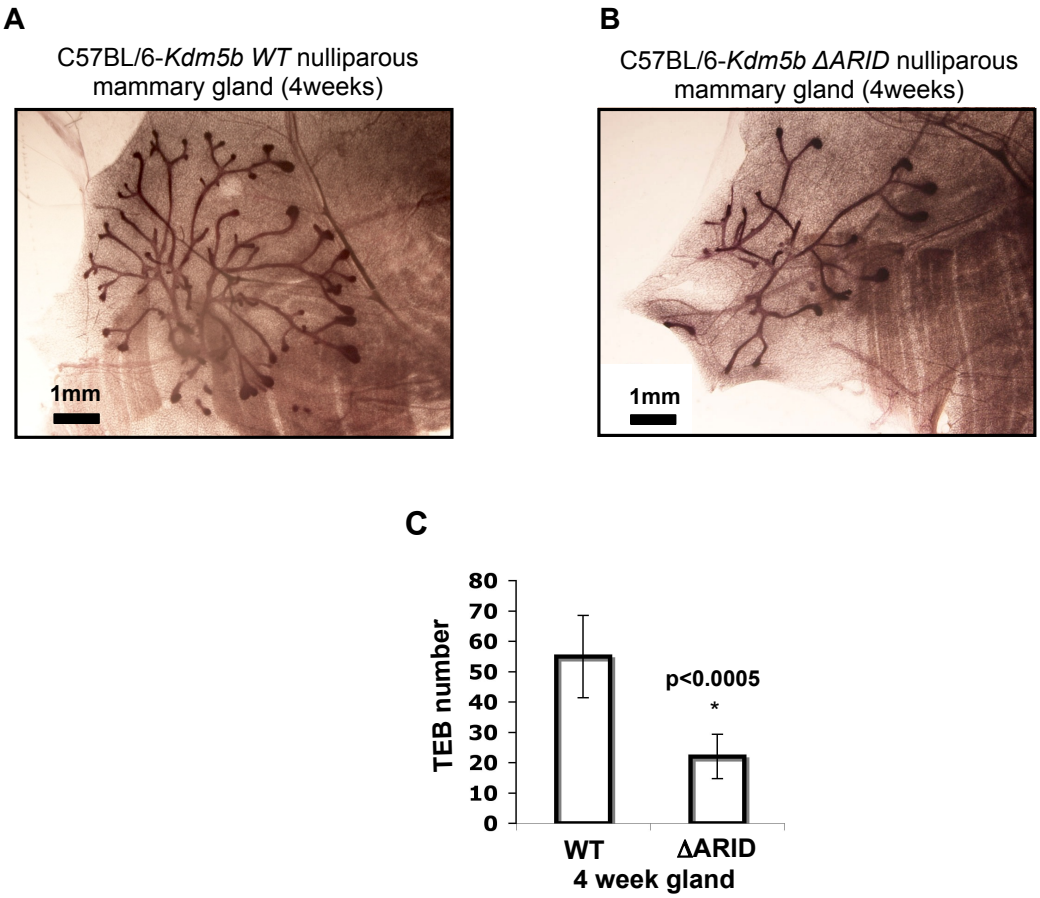


Figure 4.8 Fewer TEB structures in the 4-week old C57BL/6J-*Kdm5b ΔARID* nulliparous female. Representative carmine on (A) C57BL/6J-*Kdm5b WT* and (B) C57BL/6J-*Kdm5b ΔARID* thoracic mammary gland at 4 weeks of age. The C57BL/6J-*Kdm5b ΔARID* presents with a disorganized ductal structure and a reduction in TEB number. (C) Graph showing a 2.5 fold reduction in TEB number in the C57BL/6J *Kdm5b ΔARID* mammary gland at 4 weeks of age. (* p<0.0005 n=6 per group).

Whole mount examination of the C57BL/6J-*Kdm5b ΔARID* inguinal gland demonstrated that abnormal mammary gland development was not specific to the thoracic gland. The use of the lymph node (LN) as a mark for the distance the mammary ductal structures had ramified the fat pad through ductal elongation at TEB structures demonstrated that the C57BL/6J-*Kdm5b ΔARID* female presented with a defect in ductal elongation as compared to the age matched WT counterpart (Fig 4.9 A, B and C).

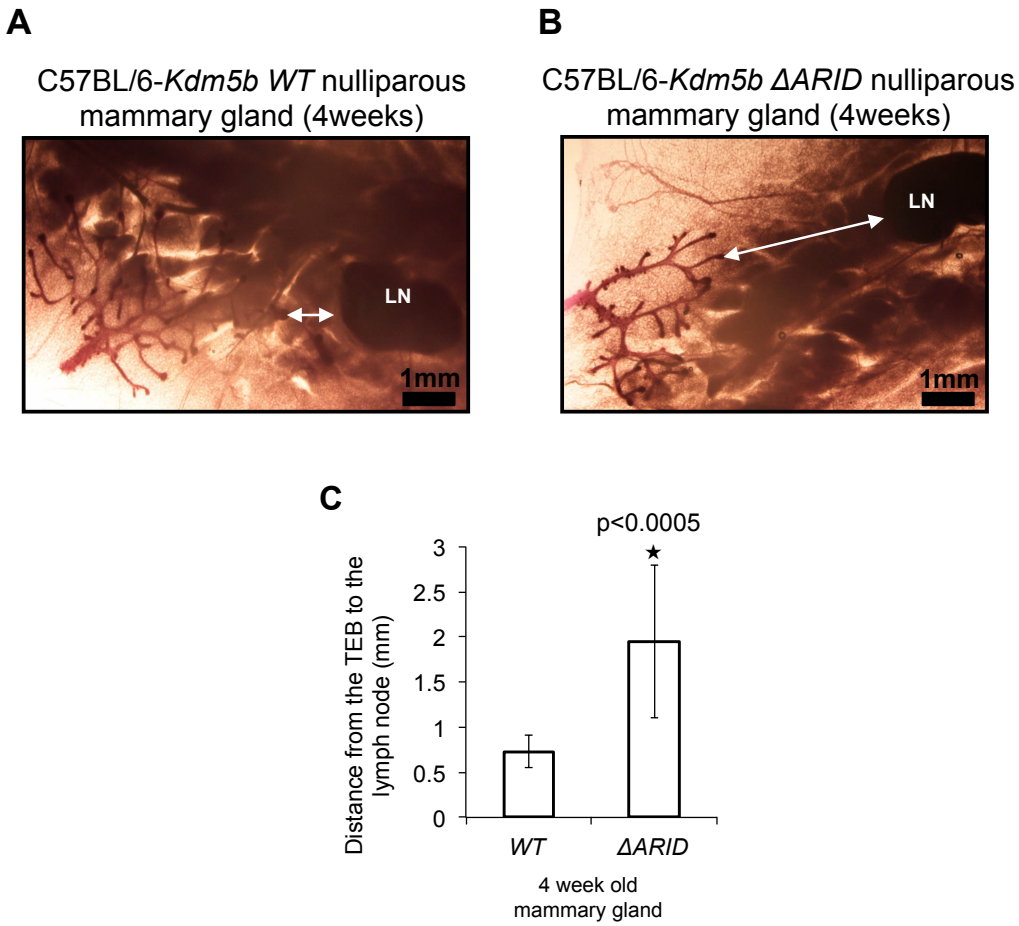


Figure 4.9 Abnormal mammary gland ductal development in the 4-week old C57BL/6J-*Kdm5b* ΔARID nulliparous female. Representative carmine on (A) C57BL/6J-*Kdm5b WT* and (B) C57BL/6J-*Kdm5b ΔARID* inguinal mammary gland at 4 weeks of age. The C57BL/6J-*Kdm5b ΔARID* female presents with a defect in ductal elongation. (C) Graph showing a 3 fold reduction in C57BL/6J-*Kdm5b ΔARID* mammary gland ductal length at 4 weeks of age. (∗, p<0.0005 n=6 per group).

4.3.2.2 The C57BL/6J-*Kdm5b ΔARID 12-week old mammary gland presents with fewer bifurcation points, a defect in ductal elongation and side branching.*

To determine whether the defect presented in the C57BL/6J-*Kdm5b ΔARID* at 4 weeks of age is manifest in the C57BL/6J-*Kdm5b ΔARID* by adulthood (12 weeks) the C57BL/6J-*Kdm5b WT* and C57BL/6J-*Kdm5b ΔARID* adult thoracic mammary glands were whole mounted and stained with carmine.

By adulthood the C57BL/6J-*Kdm5b WT* nulliparous mammary gland had fully ramified the fat pat by ductal elongation, bifurcation at TEB structures and through ductal side branching (Fig. 4.10A). In comparison the mammary gland of the C57BL/6J-*Kdm5b ΔARID* adult female presented with an extremely disorganised ductal pattern, had failed to ramify the fat pad fully and presented as expected, due to the reduced TEB number, with fewer ductal bifurcation points (Figure 4.10B and C; $p<0.005$). Additionally, the C57BL/6J-*Kdm5b ΔARID* adult nulliparous mammary gland presented with a distinct lack of secondary side branches trailing the from the primary ducts (Figure 4.10 B and C).

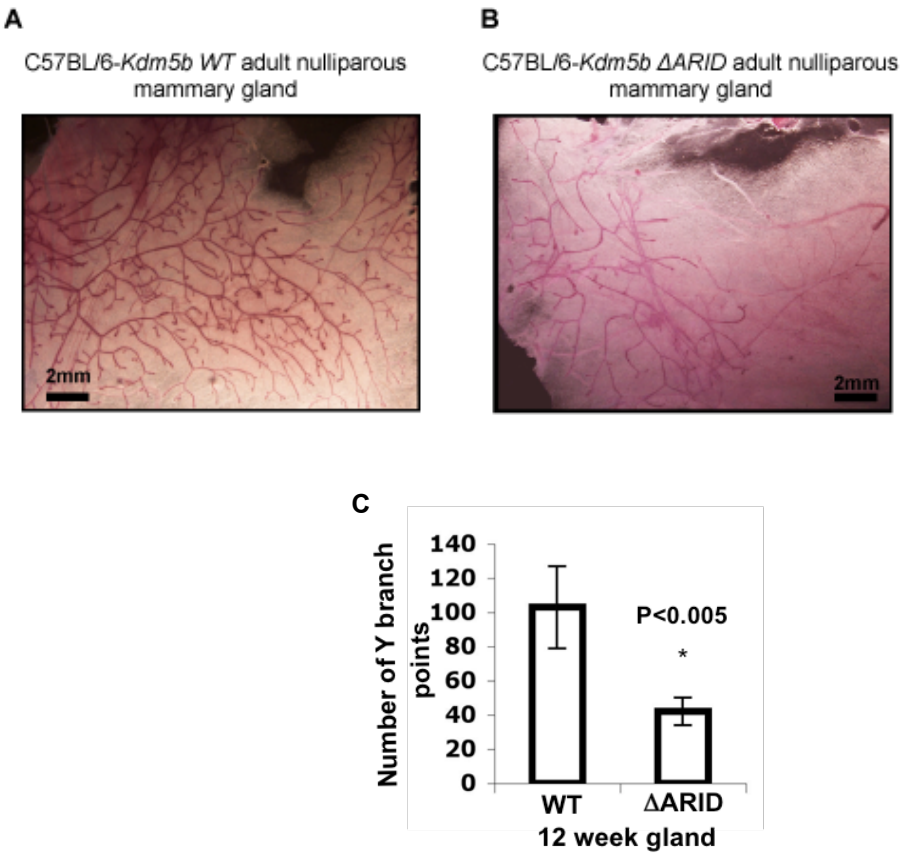


Figure 4.10 Abnormal mammary gland development in the 12 weeks old (adult) C57BL/6J *Kdm5b ΔARID* nulliparous female. Representative carmine on (A) C57BL/6J-*Kdm5b WT* and (B) C57BL/6J-*Kdm5b ΔARID* thoracic mammary glands at 12 weeks of age. The C57BL/6J-*Kdm5b ΔARID* presents with a disorganized ductal pattern and a defect in both ductal elongation and ductal side branching.
(C) Graph showing reduction in 'Y' branch points (bifurcation) in the 12 week old adult (∗, $p<0.005$. WT, n=3. ΔARID, n=4)

The phenotype in the C57BL/6J-*Kdm5b ΔARID* female mammary at 4 and 12 weeks of age suggests a defect in cell proliferation. However, as detailed in Chapter 3, (Figure 3.12) the mammary gland morphology of the chimeric B6;129-*Kdm5b ΔARID* female is comparable to that of the chimeric B6;129-*Kdm5b WT* at pd18.5 and the female can support her pups at parturition. This could suggest that the defect in mammary gland ductal development identified in the nulliparous C57BL/6J-*Kdm5b ΔARID* female mammary gland at 4 and 12 weeks of age is due to a delay in cell proliferation rather than as a consequence of cell cycle arrest. To examine the proliferative status of the C57BL/6J-*Kdm5b WT* and C57BL/6J-*Kdm5b ΔARID* adult mammary gland (12 weeks), sections were stained with the proliferation marker Ki67. By 12 weeks of age the ductal tree of the C57BL/6J-*Kdm5b WT* adult mammary gland is fully established and therefore relatively quiescent. As expected very few Ki67 positive cells were observed (Figure 4.11A). In contrast, the age matched adult C57BL/6J-*Kdm5b ΔARID* nulliparous mammary gland presented with areas of Ki67 positive ductal epithelia cells (Figure 4.11B) indicative of proliferation. This suggests that development in the C57BL/6J-*Kdm5b ΔARID* nulliparous mammary gland is delayed and not arrested, with proliferation signals occurring in the mammary gland ductal epithelia cells of the C57BL/6J-*Kdm5b ΔARID* female at 12 weeks of age in order to ramify the fat pad.

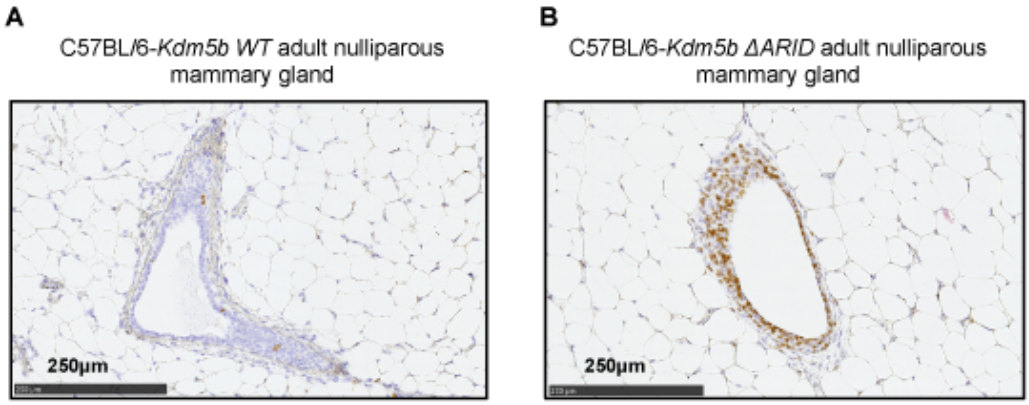


Figure 4.11 The relatively quiescent state of the adult C57BL/6J-*Kdm5b WT* nulliparous gland is not mirrored in the adult C57BL/6J-*Kdm5b ΔARID* female. Representative Ki67 on (A) C57BL/6J-*Kdm5b WT* and (B) C57BL/6J-*Kdm5b ΔARID* mammary gland sections at 12 weeks of age. (WT, n=3. ΔARID, n=4).

4.3.2.3 Defective mammary gland development in the C57BL/6J-*Kdm5b ΔARID pregnant female.*

KDM5B is expressed throughout pregnancy associated epithelial cell proliferation and differentiation (Fig. 4.1, Fig. 4.2 and Fig. 4.3). Therefore, to further examine the affect of KDM5B ΔARID expression on C57BL/6J mammary gland development, we examined the gross morphology of the mammary gland at pd12.5 and pd18.5, mid and late pregnancy respectively. Figures 4.12A and B show the C57BL/6J-*Kdm5 WT* mammary gland at pd12.5 of pregnancy had undergone further ductal elongation, branching and alveoli development. Interestingly the mammary gland of the C57BL/6J-*Kdm5b ΔARID* female at the same stage of pregnancy had over come the defect in ductal elongation presented in the adult nulliparous gland and ramified the fat pad further. However, the C57BL/6J-*Kdm5b ΔARID* female mammary gland at pd12.5 still displayed a defect in ductal side branching and possibly, as a consequence of this, fewer alveoli. (Fig. 4.12 C and D).

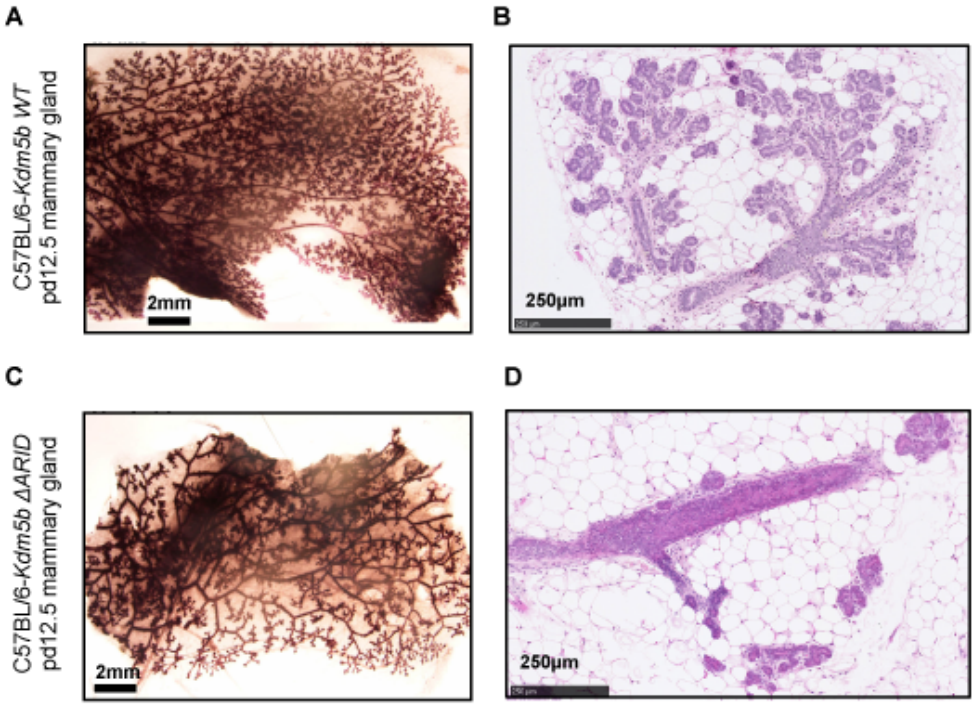


Figure 4.12 Defective mammary gland development in the C57BL/6J-*Kdm5b ΔARID* female at pd12.5. (A, C) Representative carmine and (B, D) Hematoxylin and Eosin staining on (A, B) C57BL/6J-*Kdm5b WT* and (C, D) C57BL/6J-*Kdm5b ΔARID* thoracic mammary glands (n=5).

To determine whether the defect presented in the C57BL/6J-*Kdm5b ΔARID* mammary gland at pd12.5 was due to a possible function of KDM5B in the control of cell proliferation, sections from C57BL/6J-*Kdm5b WT* and C57BL/6J-*Kdm5b ΔARID* mammary gland were stained with Ki67, a marker for cell proliferation (Fig.4.13). However, no significant difference in the proliferation of the ductal or alveolar luminal cell population was observed at pd12.5 using the Ki67 antigen as a marker (Fig 4.14). These data suggest that both the C57BL/6J-*Kdm5b WT* and C57BL/6J-*Kdm5b ΔARID* ductal/alveolar luminal progenitor cells are expanding at the same rate at this stage of pregnancy.

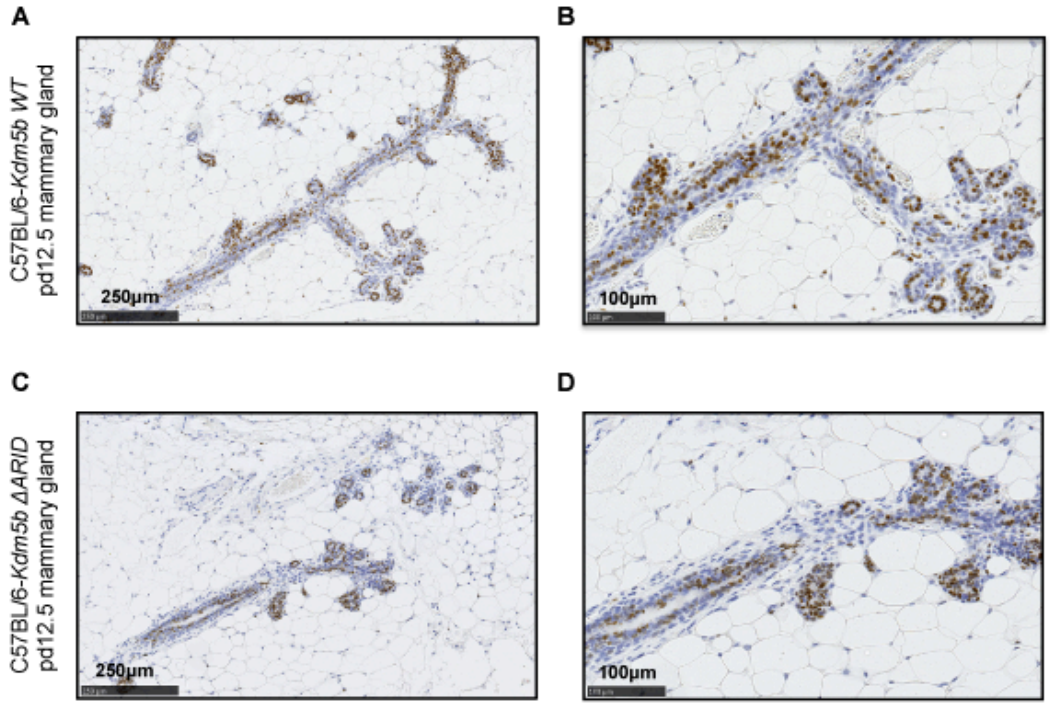


Figure 4.13 Representative immunohistochemistry showing Ki67 staining in the (A and B) C57BL/6J-*kdm5b WT* and (C and D) C57BL/6J-*Kdm5b ΔARID* thoracic mammary glands at day 12.5 of pregnancy (n=4 per group).

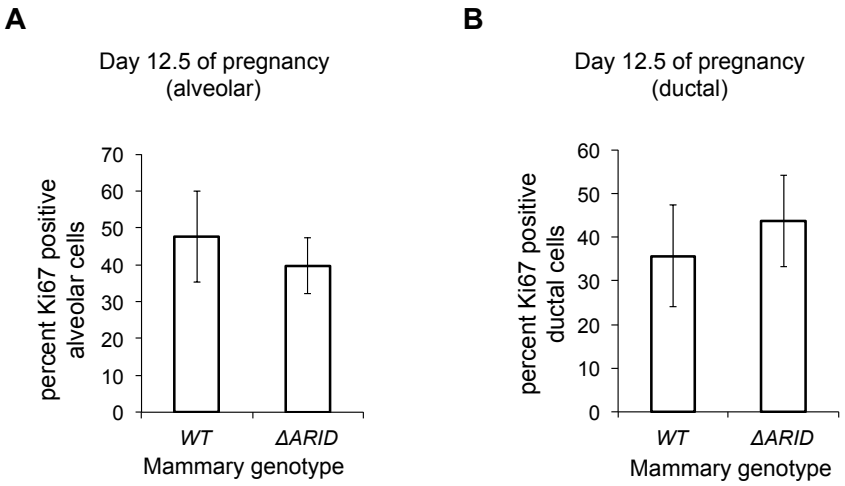


Figure 4.14 Percentage of Ki67 positive luminal epithelial cells in the (A) alveolar and (B) ductal populations of C57BL/6J-*kdm5b WT* and C57BL/6J-*Kdm5b ΔARID* thoracic mammary glands at day 12.5 of pregnancy (n=4 per group).

Consistent with the phenotype presented on the chimeric B6;129 genetic background, the C57BL/6J-*Kdm5b ΔARID* females can support their pups at parturition with no obvious difference in the size of the pups noted. This suggested that side branching recovers sufficiently to support alveolar proliferation and full differentiation. Although the gross morphology of the C57BL/6J-*Kdm5b ΔARID* mammary gland is comparable with the wild type counterpart at late pregnancy (Fig. 4.15A and C), examination of hematoxylin and eosin (H+E) sections demonstrated a significant reduction in the number of alveoli present in the C57BL/6J-*Kdm5b ΔARID* mammary gland (Fig. 4.15B and D; Fig. 4.16). Even though the numbers of alveoli in the C57BL/6J-*Kdm5b ΔARID* mammary gland were significantly reduced, the rate of alveolar proliferation as measured by Ki67 was comparable with the wild type counterpart (Fig. 4.17 and Fig. 4.18). Furthermore, whilst the perimeter of the alveoli were comparable between the C57BL/6J-*Kdm5b WT* and *ΔARID* females, and fat globules were detected in the lumen of both the C57BL/6J-*Kdm5b WT* and *ΔARID* mammary glands, there was a suggestion that secretory activation was more apparent in the C57BL/6J-*Kdm5b ΔARID* mammary gland (Fig. 4.19), indicative of premature differentiation.

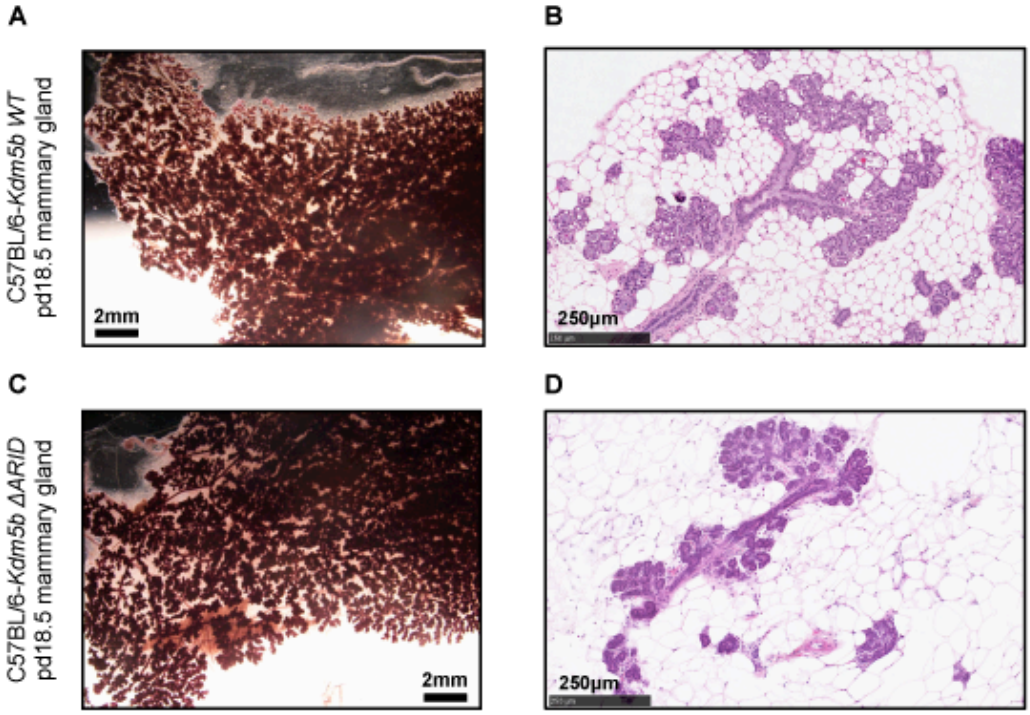


Figure 4.15 ***Mammary gland development in the*** **C57BL/6J-*Kdm5b WT*** **and** ***ΔARID female at late pregnancy.*** (A and C) Representative carmine and (B and D) hematoxylin and eosin staining on (A and B) C57BL/6J-*Kdm5b WT* and (C and D) C57BL/6J-*Kdm5b ΔARID* thoracic mammary glands at pd 18.5 (n=5 per group). Although the C57BL/6J-*Kdm5b ΔARID* female can support her offspring at parturition fewer alveoli are observed at late pregnancy (pd18.5)

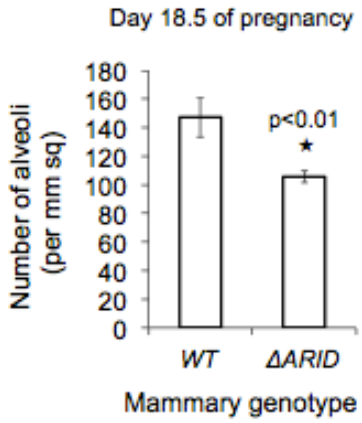


Figure 4.16 The number of alveoli are significantly reduced in the C57BL/6J-*Kdm5b ΔARID* mammary gland compared to the wild type counterpart at late pregnancy. Six randomly chosen 1mm^2 areas were selected and the number of alveoli at day 18.5 of pregnancy (pd18.5) in the C57BL/6J-*Kdm5b WT* and *Kdm5b ΔARID* mammary gland scored.

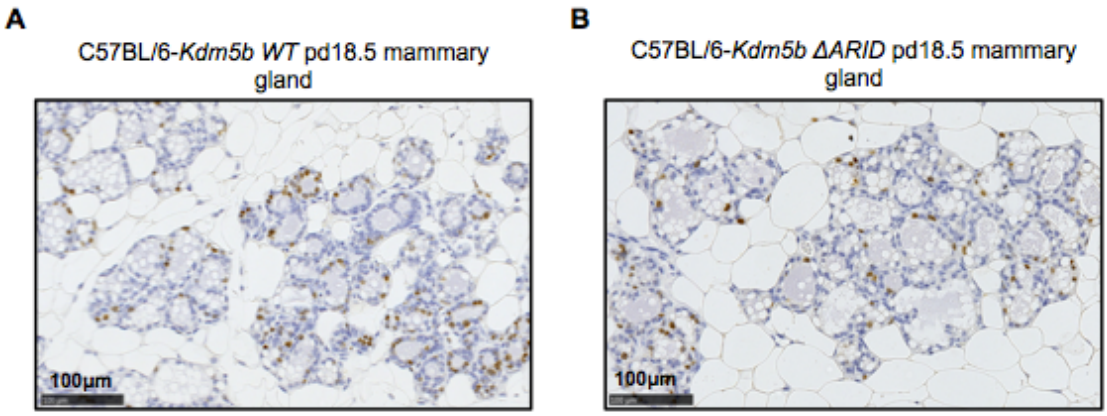


Figure 4.17 Representative immunohistochemistry showing Ki67 staining in (A) C57BL/6J-*Kdm5b WT* and (B) C57BL/6J-*Kdm5b ΔARID* thoracic mammary glands at day 18.5 of pregnancy (n=4 per group).

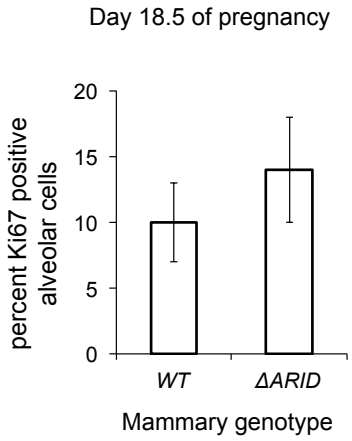


Figure 4.18 Percentage of Ki67 positive alveolar cells in the C57BL/6J-*Kdm5b WT* and C57BL/6J-*Kdm5b ΔARID* thoracic mammary glands at day 12.5 of pregnancy (n=4 per group).

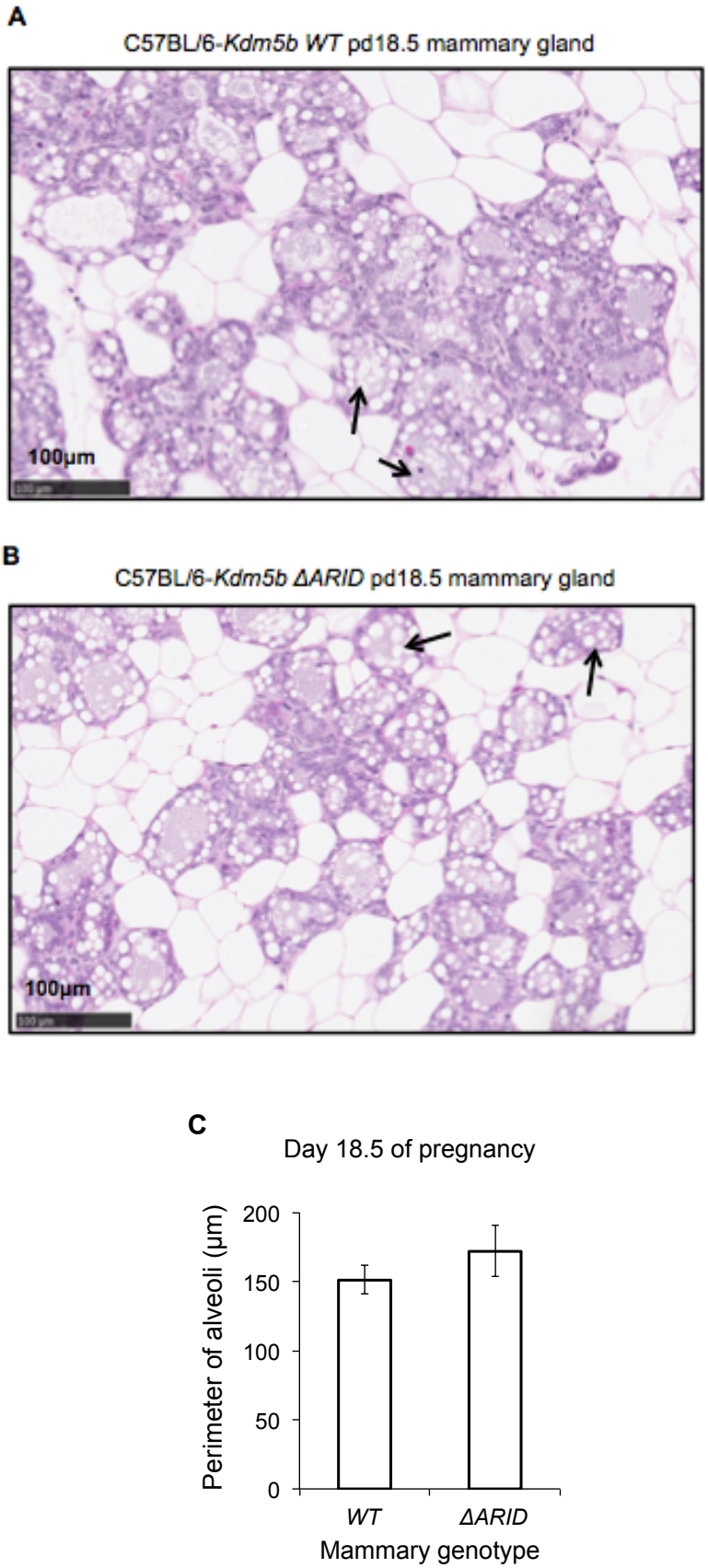


Figure 4.19 C57BL/6J-*Kdm5b WT and ΔARID* alveoli perimeters are comparable and fat globules are secreted into the lumen. (A and B) Representative hematoxylin and eosin staining on (A) C57BL/6J-*Kdm5b WT* and (B) C57BL/6J-*Kdm5b ΔARID* thoracic mammary glands at pd 18.5 (n=4 per group). Arrow denotes lumen containing fat globules. (C) Three randomly chosen 1mm^2 areas were selected and the perimeter of the alveoli determined using NanoZoomer Digital Pathology Software (n=3).

4.4 Discussion

In chapter 4 we have used *in situ* hybridisation, quantitative PCR, Western blot and immunohistochemistry analysis to describe the expression profile of KDM5B throughout mammary gland morphogenesis. Collectively these data suggest a role for KDM5B throughout the development of the mammary gland. Significantly, the nulliparous C57BL/6J-*Kdm5b ΔARID* female presents with fewer terminal end bud structures and a delay in ductal elongation together with reduced ductal side branching. Furthermore, after a delay in pregnancy associated mammary gland development, by late pregnancy the gross morphology of the mammary gland is comparable with that of the wild-type counterpart and the female can support her pups at parturition.

4.4.1 KDM5B is expressed during postnatal mammary gland morphogenesis and may suggest a role in epithelial cell proliferation, differentiation and survival.

Defining the spatial-temporal expression pattern of KDM5B is important in understanding the function of KDM5B during mammary gland morphogenesis. Examination of the KDM5B transcript level and protein expression profile demonstrated that KDM5B is expressed throughout murine mammary gland morphogenesis in the C57BL/6J mouse. Where an increase in *Kdm5b* transcription was seen - notably at pd18.5 and day 7 and 10 post weaning – an additional antibody reactive band at approximately 150KDa was also observed. Whether this antibody reactive band represents an alternative KDM5B splice variant or a degradation product has not been investigated. However the possibility of KDM5B splice variant protein products expressed during mammary gland development highlights the possibility of stage and epithelial cell-type specific functions. Furthermore, the KDM5B transcript detected in ductal and alveolar cells by *in situ* hybridisation used a probe designed to the same region used to study protein expression by Western blot analysis and immunohistochemistry. Interesting the *Kdm5b* transcript is expressed in only a proportion of epithelial cells in the TEB and ductal region at 4 weeks of age, yet is expressed in the majority of ductal epithelial cells in the adult as well as the ductal and alveolar epithelia during pregnancy. Furthermore, whilst *in situ* hybridisation and immunohistochemistry has demonstrated that KDM5B is expressed mainly in the epithelia, KDM5B expression is also detected in the stroma and specifically in adipocytes. These studies highlight the potential importance of KDM5B during proliferation, differentiation and survival of mammary gland epithelia and a potential role for KDM5B in a number of signalling pathways.

4.4.2 An increase in Kdm5b transcript level translates to a less abundant KDM5B protein in the C57BL/6J-*Kdm5b ΔARID female at pd 18.5.*

Examination of KDM5B expression in the C57BL/6J-*Kdm5b ΔARID* mammary gland female at pd18.5 confirmed the expression of a smaller less abundant protein but interestingly elevated *Kdm5b* transcript levels was observed, which may reflect a more stable *Kdm5b ΔARID* transcript. It is therefore plausible that expression of a ΔARID KDM5B protein may affect expression of the *Kdm5b* transcript indirectly. However, the increase in *Kdm5b* transcript levels detected in the C57BL/6J-*Kdm5b ΔARID* mammary gland female at pd18.5 could also be direct, suggesting the possibility of self-regulation. This hypothesis relies on the ability of KDM5B to function as a transcription repressor, with demethylase activity and therefore repressor function being dependent upon the presence of the ARID and JmJN domains. Alternatively the possible demethylase-independent ability of KDM5B to function as an activator of transcription raises the possibility of a switch in function whereby the ΔARID form of KDM5B can act as an activator of transcription at its own promoter. This interesting question could be addressed by examining *Kdm5b* promoter-luciferase activity after transfection with KDM5B and KDM5B ΔARID expression constructs. The PCR primers used to quantify the *Kdm5b* transcript in the C57BL/6J-*Kdm5b WT* and C57BL/6J-*Kdm5b* ΔARID mammary gland, do not necessarily detect a full-length transcript whereas the KDM5B specific antibody was raised again the 3' end of KDM5B (Barrett *et al*., 2002). This discrepancy between *Kdm5b ΔARID* transcript and protein level of expression could be due to incomplete translation of the *Kdm5b* transcript or due to the targeting of the KDM5B ΔARID protein product for degradation.

4.4.3 A function for KDM5B during nulliparous mammary gland development

Significantly the wild type *Kdm5b* transcript is expressed in the mammary bud at e14.5 (Madsen *et al*., 2002), a mammary gland developmental stage enriched for multi-potent progenitor cells (Van Keymeulen *et al*., 2011). This expression data indicates a potential role for KDM5B during lineage specification at the onset of pubertal mammary gland development, and could be addressed using genetic lineage tracing experiments.

Prior to parturition a rudimentary ductal system is established that responds at puberty with the formation of TEB structures. Although not examined here, it is possible, that the defect present in the C57BL/6J-*Kdm5b ΔARID* female mammary gland at 4 weeks of age is as a consequence of a defect in branching that presents at the embryonic

ductal tree developmental stage, resulting in reduced TEB structure formation in response to oestrogen signalling. Examination of the gross morphology of the newly born rudimentary ductal system would address this issue. However, examination of the extent of ductal ramification in the inguinal mammary gland at 4 weeks of age demonstrates that the C57BL/6J-*Kdm5b WT* female duct had ramified the fat pad as far as the lymph node, indicating that at 4 weeks of age puberty had already commenced. These data suggest that the C57BL/6J-*Kdm5b ΔARID* female may have not received the extrinsic stimulus to proliferate. This is of particular importance given that transplantation of ovarian hormone deprived CD24+CD29^{hi} stem cell enriched population into the clear fat pad of recipient adult females resulted in a delay in ductal morphogenesis and furthermore that oestrogen may be required for the survival of the luminal-enriched population (Asselin-Labat *et al*., 2006, Asselin-Labat *et al*., 2010, Shehata *et al*., 2012). Quantification of ovarian hormone serum levels would address these issues. We have not determined the weight of the C57BL/6J-*Kdm5b WT* and *ΔARID* murine lines. The size of the C57BL/6J-*Kdm5b ΔARID* mammary gland fat pad shown in Chapter 3, Figure 3.10B and C (page 95) as well as in Chapter 4, Figure 4.12C (page 126) are smaller than the wild type counterpart. The weight of the C57BL/6J-*Kdm5b ΔARID* fat pad should be normalised against body weight and compared to the wild type counterpart to accurately determine the extent of fat pad ramification (See final discussion, Chapter 7). Furthermore, images containing lymph nodes should be included to provide a reference point for ductal ramification.

Expression of *Kdm5b* in the TEB structure of the C57BL/6J-*Kdm5b WT* female suggests that KDM5B may play a role during ductal morphogenesis. The ability of the C57BL/6J-*Kdm5b ΔARID* female to generate a functional mammary gland suggests that the mammary gland stem cell population can differentiate toward the ductal lineage, albeit the delay in ductal elongation may represent a reduction in the proliferation of the ductal luminal progenitor population. Although we have not determined whether proliferation is affected in the C57BL/6J-*Kdm5b* ΔARID mammary gland at 4 weeks of age, studies have indicated a role for KDM5B in the control of the cell cycle (Yamane *et al*., 2007, Dey *et al*., 2008, Xie *et al*., 2011, Wong *et al*., 2012). It is therefore possible that a defect in proliferation at 4 weeks of age recovers by 12 weeks of age, as seen by the positive Ki67 epithelia, and these studies would therefore benefit from an increase in the number of pubertal stages examined for markers of proliferation. The expression of KDM5B is required for proper G1 to S phase transition of both ES cells (Dey *et al*., 2008, Xie *et al*., 2011) and the breast cancer cell line, MCF7 (Yamane *et al*., 2007, Wong *et al*., 2012). This requirement for *Kdm5b* at the G1 to S phase transition may be common to normal murine mammary epithelial cells and

account for the delayed ductal morphogenesis presented in the C57BL/6J-*Kdm5b* ΔARID nulliparous mammary gland. Mammary gland development in the adult heterozygous B6;129-*Kdm5b-Exon1* knock out murine line resembles that of the wild type counterpart. We have not compared the KDM5B expression levels in the heterozygous B6;129-*Kdm5b-Exon1* knock out female with the KDM5B ΔARID expression levels in the C57BL/6J-*Kdm5b* ΔARID female to determine if expressions levels are potentially a factor in effecting mammary gland ductal morphogenesis.

The delay in ductal elongation during puberty and side branching in the adult C57BL/6J-*Kdm5b ΔARID* mammary gland suggests an involvement of KDM5B in mediating some aspects of the oestrogen and progesterone signaling pathways. KDM5B can interact with the androgen receptor (AR) and potentiate transcription in a ligand dependent manner (Xiang *et al*., 2007). It is therefore possible that KDM5B may interact with ER alpha and potentiate transcription. In the adult mammary gland, at diestrous an increase in mammary gland cell number and mammary ductal side-branching (Cole *et al*., 1933, Fata *et al*., 2001) is attributable to PR expression (Joshi *et* al., 2010). If KDM5B potentiates transcription in a ligand dependent manner as described for when acting as an AR cofactor, then an interaction of KDM5B with ER alpha may also potentiate *Pgr* transcription.

The STAT family of proteins are involved in every stage of mammary gland development. STAT5 expression is not required for the generation of mammary gland ductal cells (Yamaji *et al*., 2009) and therefore ductal elongation during puberty proceeds as seen for the wild type counterpart but side branching is reduced (Santos *et al.,* 2010). The C57BL/6J-*Kdm5b ΔARID* female presents with a defect in ductal elongation and side branching suggesting that KDM5B may function to mediate both STAT5-dependent and STAT5-independent signalling pathways.

4.4.4 A function for KDM5B during pregnancy associated mammary gland morphogenesis

Three aspects dictate the successful development of the mammary gland during pregnancy and they are proliferation, differentiation and survival. KDM5B is expressed throughout this developmental period and interestingly a KDM5B splice variant is detected late in pregnancy (pd18.5). Of further interest, expression of a KDM5B ΔARID protein results in reduced side branching and alveoli development that recovers sufficiently for the female to support her pups at parturition. These data suggest that although expression of the KDM5B ΔARID protein is sufficient for ductal and alveolar

progenitor expansion and differentiation, a delay in alveolar progenitor cell proliferation is suggested by the presence of fewer alveoli at pd18.5. Although, we have not detected a difference in Ki67 levels compared to the wild type counterpart a delay in cell cycle could account for the ability of the C57BL/6J-*Kdm5b ΔARID* mammary gland to 'catch up' as suggested earlier.

Our analysis on KDM5B expression during mammary gland morphogenesis has extended the current knowledge on the expression profile of KDM5B during mammary gland development. Using Northern blot transfer, a previous study (Madsen *et al*., 2002) reported that the *Kdm5b* transcript was not expressed post forced weaning during the first and second phases of involution. However, we cannot confirm the absence of KDM5B expression during the first phase of involution (Madsen *et al*., 2002), as this stage of mammary gland involution was not included in this study, and this should be addressed. We have however detected KDM5B expression at day 3 post forced weaning suggesting a function for KDM5B during the second phase of involution. These studies would therefore benefit from a detailed analysis of the KDM5B expression profile during both the first and second phases of involution (12hrs, 24hrs, 48hrs, 96hrs and 6 days post forced weaning) and the gross morphology of the C57BL/6J-*Kdm5b ΔARID* involuting mammary gland examined (see final discussion Chapter 7). KDM5B is also detected at day 7 and day 10 post forced weaning. Interestingly the splice variant seen at day 18.5 of pregnancy when the mammary gland is differentiated is also detected at day 7 and day 10 post forced weaning and could indicate a stage specific function for KDM5B in the parous mammary gland.

We have generated a hypomorphic KDM5B murine line in which both the demethylase activity (Yamane *et al*., 2007, Xiang *et al*., 2007) and the DNA binding activity (Scibetta *et al*., 2007, Yao *et al*., 2010) have been compromised. The phenotype presented in the nulliparous C57BL/6J-*Kdm5b ΔARID* female, is suggestive of a function for KDM5B in ER alpha signalling. We will therefore use the C57BL/6J-*Kdm5b ΔARID* murine line to investigate the effect in the nulliparous mammary gland of KDM5B ΔARID protein expression on ER alpha target genes and those genes reported to be repressed by KDM5B (Scibetta *et al*., 2007). Mammary gland morphogenesis during pregnancy requires the integration of a number of signalling pathways. The oestrogen and progesterone receptors are required for alveologenesis (Lydon *et al*., 1998, Brisken *et al*., 1998, Mulac-Jericevic *et al*., 2003, Feng *et al.,* 2007) and signalling through these receptors could be affected in the C57BL/6J-*Kdm5b ΔARID* pregnant mammary gland. Developmental time windows are important during mammary gland morphogenesis. STAT5A is required for the generation of alveolar progenitors as well as their

proliferation, differentiation and survival (Yamaji *et al*., 2009, Cui *et al*., 2004), whilst STAT6 mediates proliferation and luminal cell commitment to an alveolar lineage during early pregnancy (Khaled *et al*., 2007). The phenotype in the pregnant C57BL/6J-*Kdm5b ΔARID* mammary gland is suggestive of a role for KDM5B in mediating the STAT signalling pathway. We will therefore use the C57BL/6J-*Kdm5b ΔARID* murine line to explore the effect of KDM5B ΔARID expression on the STAT signalling pathway.

4.5 Supplemental material

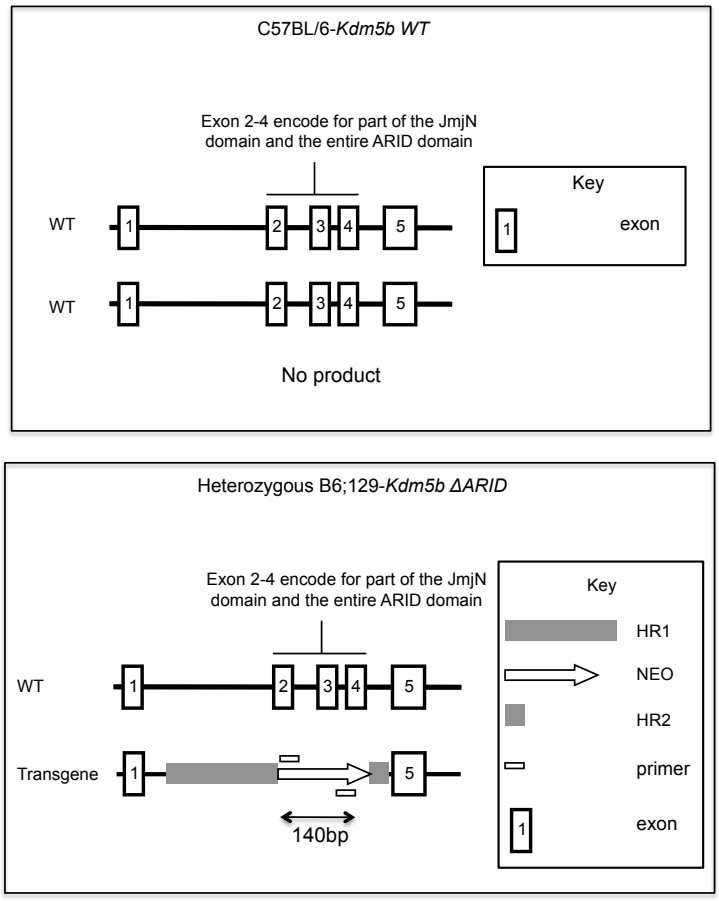


Figure 4S1 Screening strategy used to detect the engineered allele during the backcross of the chimeric heterozygous B6;129-*Kdm5b ΔARID* murine line onto the inbred C57BL/6J genetic strain. Schematic alignment of KDM5B WT allele and Neo targeting transgene with PCR primer location within the neomycin gene used to distinguish the engineered allele from the wild type allele

Chapter 5: Results

Investigation into the effect of KDM5B ΔARID expression on gene expression

Chapter 5. Investigation into the effect of KDM5B ΔARID expression on gene regulation

5.1 Aims: Using the C57BL/6J-*Kdm5b ΔARID* murine line we aim to investigate the effect of KDMB ΔARID expression on gene expression by:

(1) Examining the effect of KDM5B ΔARID expression on ER alpha target gene regulation during mammary gland development.
(2) Investigating the ability of KDM5B and KDM5B ΔARID to interact with ER alpha.
(3) Examining in the mammary gland, the effect of KDM5B ΔARID expression on the repression of demethylase-dependent KDM5B target genes in the adult mammary gland
(4) Examining in the mammary gland, the effect of KDM5B ΔARID expression on the AKT and STAT5 signaling pathways.

5.2 Introduction:

5.2.1 KDM5B and gene regulation

Several reports have demonstrated that the function of KDMB is context dependent, with protein interactions and genome binding location influencing function (Xiang *et al*., 2007, Secombe *et al*., 2007, Schmitz *et al*., 2011 and Xie *et al*., 2011). Using a differential expression system, approximately 100 genes have been identified as putative KDM5B target genes involved in cell cycle and signal transduction, of which 81% of these were silenced by KDM5B over expression. Of those genes identified, the promoter of the spindle checkpoint gene budding uninhibited by benzimidazole 1 (BUB1) was bound and the gene repressed by KDM5B concomitantly with a decrease in H3K4me3 methylation levels. Metallothionein 1F (MT1F) was also identified as a gene that was bound and repressed in a demethylase dependent manner by KDM5B (Scibetta *et al*., 2007, Breast Cancer Biology Group unpublished observation). Of interest, MT1F expression positively correlates with the histological grade of breast cancer, being expressed at significantly higher levels in grade 3 tumours (Jin *et al*., 2001). Furthermore, KDM5B can also bind and repress transcription of the tumour suppressor gene, breast cancer 1 (BRCA1) in a demethylase dependent manner (Yamane *et al*., 2007).

KDM5B can also function as an activator of transcription (Xiang *et al*., 2007, Xie *et al*., 2011), as KDM5B can bind to the androgen receptor and activate transcription from a *PSA-luciferase* reporter construct (Xiang *et al*., 2007). The ability of the KDM5 family to interact with nuclear receptors maybe conserved given that KDM5A can also interact with the retinoic acid receptor (RAR), the vitamin D receptor (VDR), the glucocorticoid receptor (GR) and ER alpha (Chan and Hong. 2001).

Signaling through nuclear receptors is of central importance in order to establish a competent mammary gland. Mammary gland ductal morphogenesis at puberty is dependent upon the formation of TEB structures, which in turn requires the expression of ER alpha (Mallepell *et al*., 2006, Feng *et al*., 2007). In addition to being required for ductal elongation during puberty, the epithelial expression of ER alpha is essential during pregnancy for alveologenesis and lactation (Feng *et al*., 2007). Ductal side branching in the adult mammary gland occurs during the diestrous stage of the estrous cycle a process requiring the expression of the progesterone receptor (PR), which results in the up-regulation of *Wnt4* expression and expansion of the mammary gland stem cell population (Joshi *et al*., 2010). Further ductal side branching during pregnancy as well as the development of alveoli structures, is also dependent upon PR expression (Brisken *et al*., 1998, Mulac-Jericevic *et al*., 2003) and mediated in a paracrine manner (Brisken *et al*., 1998, Beleut *et al*., 2010). One factor, namely WNT4 is implicated in mediating some of the mitogenic effects of progesterone (Brisken *et al*., 2000, Joshi *et al*., 2010). Genetic ablation of *Wnt4* results in reduced ductal side branching at mid-pregnancy (pd12.5) yet the mammary gland recovers morphologically by late pregnancy to produce a lactation-competent mammary gland (Brisken *et al*., 2000).

The STAT family of proteins play a central role during gestation (Hughes and Watson 2012). STAT6 expression is required for inducing proliferation and luminal cell commitment to the alveolar lineage (Khaled *et* al., 2007) and a number of studies have demonstrated the importance of the PRLR/JAK2/STAT5 signalling pathway during the development of the pregnant mammary gland. Mice that harbor genetic alterations in components of the PRLR/JAK2/STAT5 signaling pathway present with an absence of alveolar structures and failed lactation (Lui *et al*., 1997, Wagner *et al*., 2004, Horseman *et al*., 1997, Ormandy *et al*., 1997). An additional link to the established role of the PRLR/JAK2/STAT5 signalling pathway during pregnancy associated mammary gland development is the compelling evidence that even in the absence of developmental cues associated with pregnancy, AKT signaling is necessary and sufficient to induce

autocrine prolactin production by the mammary gland epithelia, STAT5 activation, and terminal epithelial differentiation (Chen *et al*., 2012).

We have developed the KDM5B ΔARID murine line that is expected to lack KDM5B demethylase activity – and therefore repressor function (Yamane *et al*., 2007) - as well as a potential mechanism for the recruitment of KDM5B to DNA (Scibetta *et al*., 2007, Yao *et al*., 2010). Given that the mammary gland of the C57BL/6J-*Kdm5b ΔARID* female presents with a phenotype suggestive of a defect in ER alpha signaling we examined whether KDM5B can interact with ER alpha. In addition we investigated if the levels of ER alpha target genes as well as some of those genes implicated in mammary gland ductal morphogenesis are altered in the C57BL/6J-*Kdm5b ΔARID* mammary gland. Given that genes involved in cell cycle control (*BUB1*) and breast cancer progression (*BRCA1*, *MT1F*) are repressed in a demethylase dependent manner by KDM5B in a breast cancer cell line*,* we examined the expression levels of these genes in the C57BL/6J-*Kdm5b ΔARID* female. The C57BL/6J-*Kdm5b ΔARID* female mammary gland also presents with a delay in pregnancy associated mammary gland development. We therefore examined whether expression of a KDM5B ΔARID protein affected the expression of a number of key factors whose ablation affects pregnancy associated mammary gland development including ER alpha, PR and WNT4 as well as STAT6 and the AKT and STAT5 signalling pathway.

5.3 Results

5.3.1 Studies on a possible role for KDM5B in ER alpha signalling

5.3.1.1 Analysis of transcription levels of Esr1 and its target genes in the C57BL/6J-Kdm5b ΔARID nulliparous mammary gland

In order to investigate a function for KDM5B in ER alpha signaling we sought to examine the effect of KDM5B ΔARID expression on the ER alpha transcript (*Esr1*) level of expression and on known ER alpha target genes, namely the progesterone receptor (*Pgr*) and the downstream transcriptional target of the progesterone receptor (PR), *Wnt4*. To achieve this, RNA was isolated from the mammary glands of estrous synchronized nulliparous C57BL/6J-*Kdm5b WT* and C57BL/6J-*Kdm5b ΔARID* females at the onset of adult mammary gland development (4 weeks) and in the adult (12 weeks). Quantitative PCR on the cDNA generated from the respective C57BL/6J-*Kdm5b WT* and C57BL/6J-*Kdm5b ΔARID* mammary glands demonstrated that there is no significant difference in the expression of *Esr1* transcript levels at 4 weeks of age (Fig 5). However by 12 weeks of age, although no significant difference in *Esr1* transcript levels were detected in the C57BL/6J-*Kdm5b ΔARID* nulliparous mammary gland compared to the C57BL/6J-*Kdm5b WT*, a trend indicating a reduction in the level of the *Pgr* transcript was observed (Fig.5.1) suggesting that KDM5B may function to positively regulate *Pgr* transcription. To verify an effect on ER alpha signaling in the adult nulliparous C57BL/6J-*Kdm5b ΔARID* female mammary gland we quantified the transcript levels of a progesterone receptor target gene *Wnt4*. As shown in Fig. 5.1 *Wnt4* transcript expression levels are significantly reduced compared to the C57BL/6J-*Kdm5b WT*. The reduced *Pgr* and *Wnt4* transcript levels in the C57BL/6J-*Kdm5b ΔARID* adult nulliparous mammary gland suggests that expression of the KDM5B *ΔARID* protein may perturb ER alpha signalling, culminating in defective mammary gland morphogenesis.

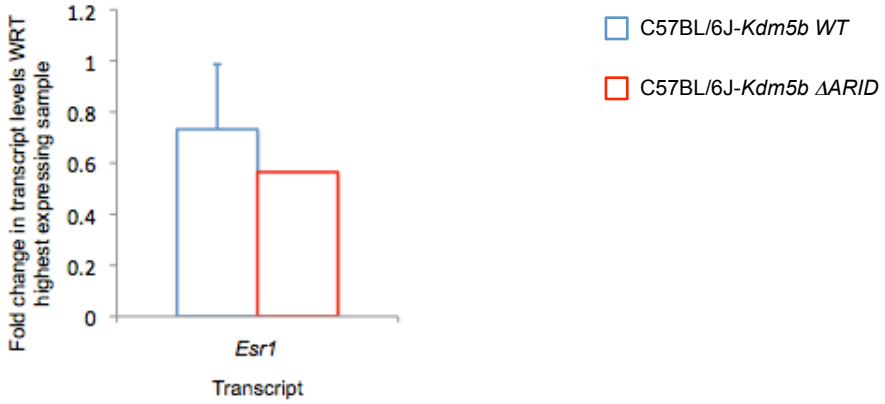


Figure 5 Relative transcript levels of *Esr1* in the C57BL/6J-*Kdm5b WT* and C57BL/6J-*Kdm5b ΔARID* nulliparous mammary gland at 4 weeks of age (WT n=3; ΔARID n=2). The acronym WRT is defined as 'with respect to'. The *Esr1* amplicon PCR cycle number was normalized against the 18S ribosomal RNA amplicon PCR cycle number.

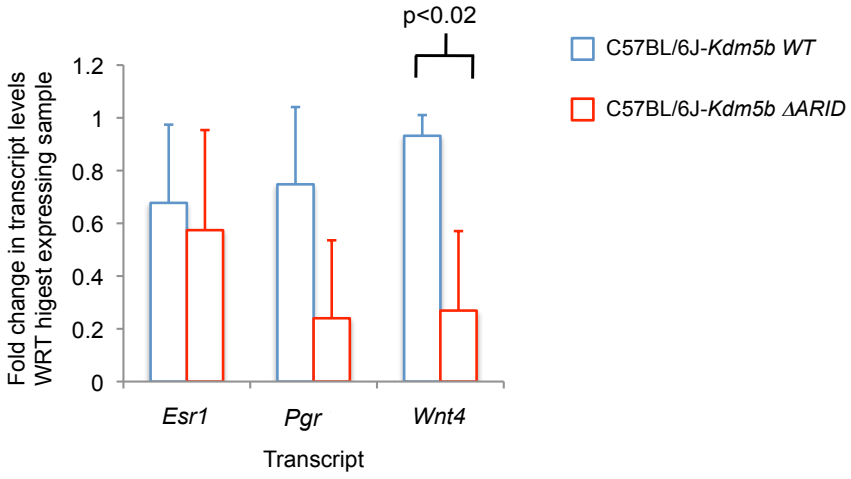


Figure 5.1 Relative transcript levels of *Esr1, Pgr*, and *Wnt4* in the C57BL/6J-*Kdm5b WT* and C57BL/6J-*Kdm5b ΔARID* nulliparous mammary gland at 12 weeks of age (WT n=3; ΔARID n=4).

5.3.1.2 KDM5B interacts with ER alpha in vivo in an ARID independent manner

To further explore a function for KDM5B in ER alpha signalling we examined whether KDM5B can interact with ER alpha, and whether any interaction is affected by the deletion of the ARID domain. In order to achieve this COS-7 cells were co-transfected with HA-tagged ER alpha and either MYC-HIS-tagged KDM5B or MYC-HIS-tagged KDM5B ΔARID expression constructs. Figure 5.2 demonstrates the ability of the α-HA or α-HIS antibodies to immunoprecipitate ER alpha or KDM5B respectively and the *in vivo* interaction confirmed by immunoblot detection of KDM5B and ER alpha by α-KDM5B and α-HA antibodies. Of interest, expression of the KDM5B ΔARID protein

does not abrogate an interaction with ER alpha *in vivo*, suggesting that any effects on ER alpha function are downstream of this interaction.

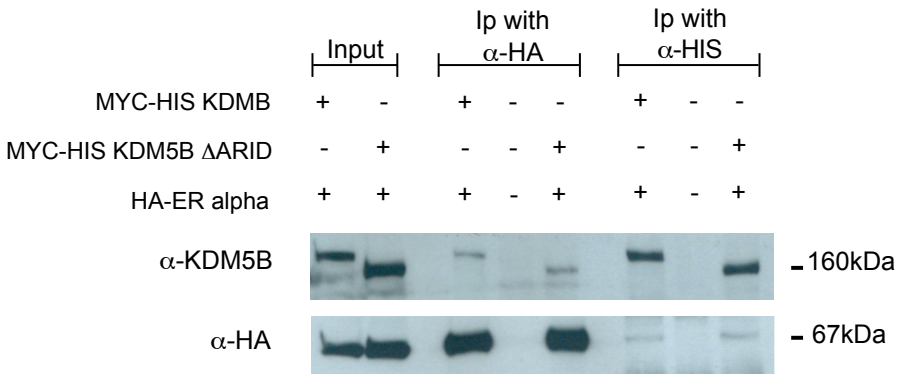


Figure 5.2 KDM5B interacts with ER alpha *in vivo* in an ARID independent manner. COS-7 cells were transfected with HA-ER alpha and MYC-HIS KDMB WT or MYC-HIS KDM5B ΔARID expression constructs and subject to immunoprecipitation with either HA-beads or HIS-beads and immunblotted with antibodies specific to either KDM5B or HA.

5.3.2 Studies on KDM5B repressor function in the adult C57BL/6J-Kdm5b ΔARID mammary gland

The ability of KDM5B to function as a transcriptional repressor is dependent upon its demethylase activity; a function ablated by the deletion of the ARID domain (Yamane *et al*., 2007, Xiang *et al*., 2007). As detailed in the introduction, a number of *in vitro* studies using cell lines have demonstrated that KDM5B can repress transcription from a number of promoters including *BUB1* (Breast Cancer Biology Group unpublished observation), *BRCA1* (Yamane *et al*., 2007) and *MT1F* (Scibetta *et al*., 2007). However, using quantitative PCR on cDNA generated from RNA isolated from the adult (12 weeks) C57BL/6J-*Kdm5b ΔARID* and C57BL/6J-*Kdm5b WT* mammary gland demonstrated that *Bub1*, *Brca1* and *Mt1F* transcript levels are unaffected in the adult C57BL/6J-*Kdm5b ΔARID* mammary gland compared with the C57BL/6J-*Kdm5b WT* counterpart (Fig5.3).

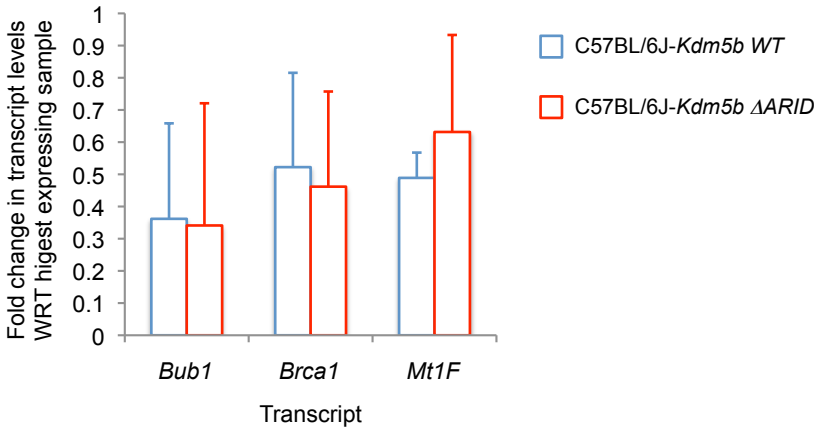


Figure 5.3 Relative transcript levels of *Bub1, Brca1* and *Mt1F* in the C57BL/6J-*Kdm5b WT* and C57BL/6J-*Kdm5b ΔARID* nulliparous mammary gland at 12 weeks of age (WT n=3; ΔARID n=4).

5.3.3 Molecular assessment of the role of KDM5B during development of the C57BL/6J-*Kdm5b ΔARID* pregnant mammary gland.

The delay in the development of the C57BL/6J-*Kdm5b ΔARID* pregnant mammary gland would suggest an affect on luminal/alveolar progenitor cell proliferation and differentiation. A number of factors mediate mammary gland epithelial cell hierarchy determination downstream of the ovarian and pituitary axis. To attempt to characterize the molecular pathways affected in the C57BL/6J-*Kdm5b ΔARID* mammary gland we analyzed the expression of ER alpha, PR, STAT6, STAT5, activated STAT5, AKT, activated AKT, WAP and beta casein at mid and late pregnancy.

5.3.3.1 Molecular analysis in the C57BL/6J-Kdm5b ΔARID mammary gland at mid-pregnancy (pd12.5)

(A) Steroid receptor expression at mid pregnancy

Where ER alpha and its cofactors are required for the orderly development of the pubertal mammary gland, during pregnancy ablation of ER alpha results in a loss in PR expression resulting in reduced side branching, alveolar structures and compromised milk production (Feng *et al*., 2007). Pregnancy-associated ductal side branching and lobuloalveolar development are markedly reduced in the *Prb* null murine line due to a decrease in ductal and alveolar epithelial cell proliferation and a decrease in the

survival of alveolar epithelia (Mulac-Jericevic *et al*., 2003). Furthermore, progesterone can induce WNT4 expression and is required for ductal side branching at pregnancy but is dispensible by late pregnancy (Brisken *et al.,* 2000), reminiscent of the phenotype presented in the C57BL/6J-*Kdm5b ΔARID* mammary gland. Using the adult C57BL/6J-*Kdm5b ΔARID* mammary gland, we have shown that whilst the transcript levels of *Esr1* are not significantly reduced, a trend indicating a reduction in the level of the *Pgr* transcript was observed, together with a significant reduction in *Wnt4* transcript levels (Fig5.1). These studies presented here suggest that KDM5B could be functioning to mediate some aspects of ER alpha signalling.

Therefore in the first instance we examined the expression of ER alpha, *Pgr* and *Wnt4* at mid pregnancy, a stage of development at which point the C57BL/6J-*Kdm5b ΔARID* mammary gland presents with a reduction in side branching and alveolar development. Figure 5.4 shows that the expression of ER alpha is not reduced compared to the wild type counterpart. Moreover, whilst a trend indicating a reduction in the expression level of *Pgr* was observed, *Wnt4* expression is not reduced (Fig. 5.5).

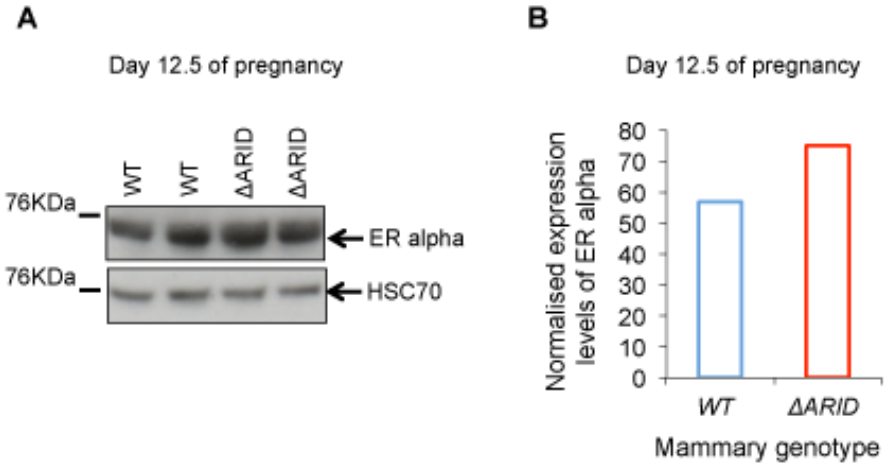


Figure 5.4 Expression of ER alpha in the C57BL/6J-*Kdm5b WT* and *ΔARID* mammary gland at mid-pregnancy.
(A) Western blot showing the expression of ER alpha and HSC70 in the C57BL/6J-*Kdm5b WT* and *ΔARID* mammary gland at mid-pregnancy. (B) ImageJ software was used to quantify the band intensity and a histogram plotted showing the expression level of ER alpha normalized against the expression level of HSC70 (n=2 per group).

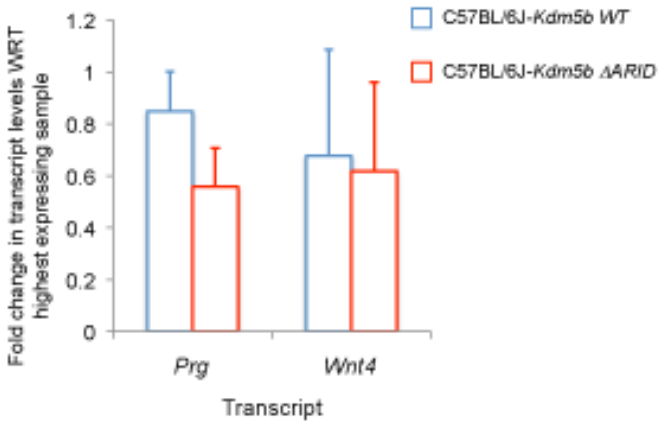


Figure 5.5 Transcript levels of *Pgr* and *Wnt4* in the C57BL/6J-*Kdm5b WT* and C57BL/6J-*Kdm5b ΔARID* mammary gland at pd12.5 (n=4 per group).

(B) Changes in the JAK/STAT and AKT signaling axis at mid pregnancy

STAT6 expression is required for inducing proliferation and luminal cell commitment to the alveolar lineage, but importantly, proliferation and full differentiation of the mammary gland is achieved by late pregnancy (Khaled *et al*., 2007). We therefore examined the impact of KDM5B ΔARID expression on STAT6 expression. Figure 5.6 shows that STAT6 expression is comparable between the C57BL/6J-*Kdm5b ΔARID* and the wild type mammary gland at mid pregnancy indicating that the expression of the KDM5B ΔARID protein has no effect of STAT6 expression.

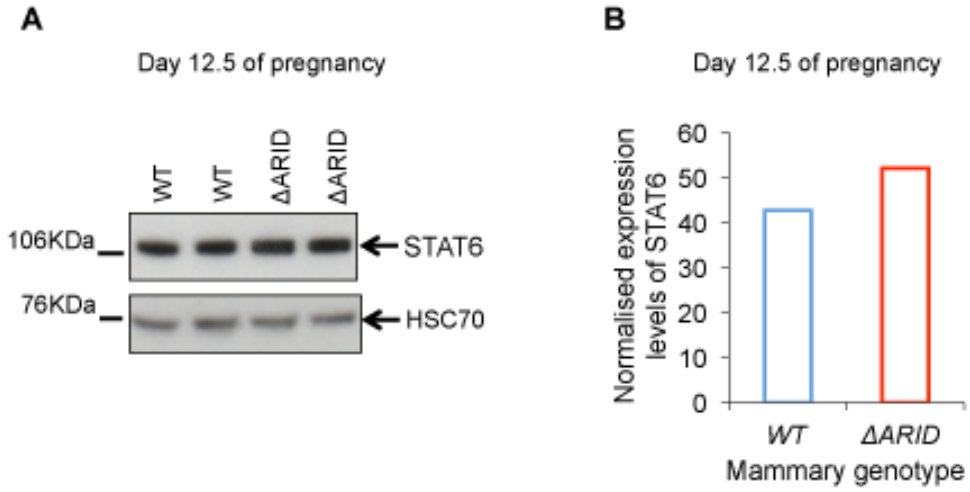


Figure 5.6 Expression of STAT6 in the C57BL/6J-*Kdm5b WT* and *ΔARID* mammary gland at mid-pregnancy.
(A) Western blot showing the expression of STAT6 and HSC70 in the C57BL/6J-*Kdm5b WT* and *ΔARID* mammary gland at mid-pregnancy. (B) ImageJ software was used to quantify the band intensity and a histogram plotted showing the expression level of STAT6 normalized against the expression level of HSC70 (n=2 per group).

The transcription factor STAT5 plays a pivotal role during mammary gland morphogenesis where it controls the development of alveolar progenitors from stem cells in the nulliparous mammary gland (Yamaji *et* al., 2009) and during pregnancy where STAT5A is required to promote alveolar proliferation, differentiation and activation of milk proteins as well as the survival of mammary gland epithelia (Cui *et al*., 2004, Yamaji *et al*., 2013). STAT5A is required for the development of alveoli structures as early as day 6 of pregnancy (Yamaji *et al*., 2013), however maximal STAT5 activation does not occur until mid to late pregnancy (Bednorz *et al*., 2011). Furthermore STAT5A expression is required to induce ductal side-branching in ovariectomised mice supplemented with pregnancy levels of ovarian hormone (Santos *et al*., 2010). Studies indicate that STAT5 positively regulates the transcription of the pro-survival protein AKT (Creamer et al., 2010), whose activation is required to initiate branch formation in a three-dimensional culture model of murine mammary epithelia (Zhu and Nelson, 2013).

Interestingly, Western blot analysis showed that although the expression level of the STAT5 protein is only marginally increased in the C57BL/6J-*Kdm5b ΔARID* mammary gland, there is a dramatic reduction in the relative ratio of pSTAT5 to STAT5 (76 percent) and in the level of pSTAT5 expressed in the C57BL/6J-*Kdm5b ΔARID* mammary gland compared to the wild type counterpart (Figure 5.7**)**. This could account for the reduction in ductal side branching and alveoli development seen in the C57BL/6J-*Kdm5b ΔARID* mammary gland at mid pregnancy.

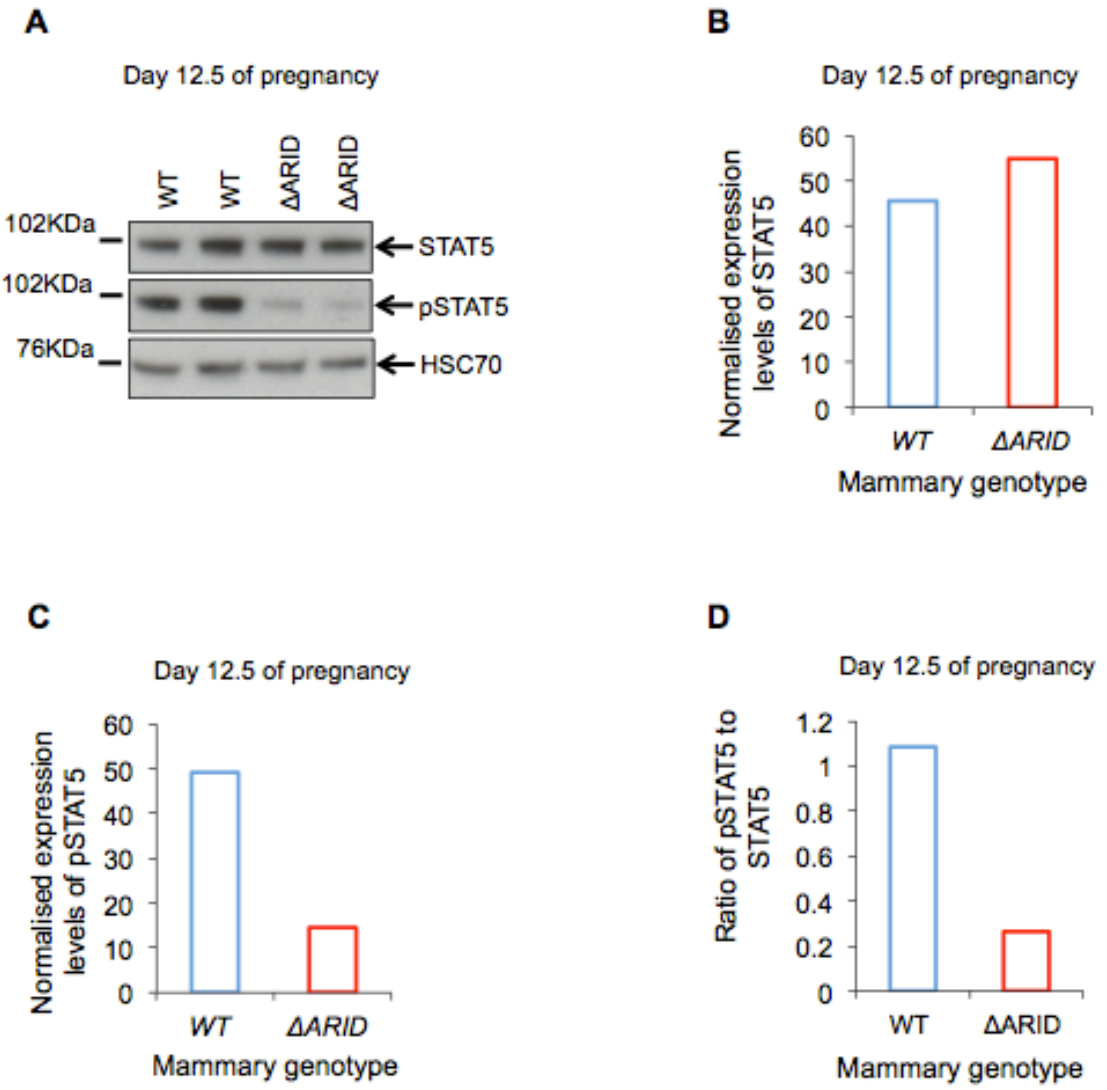


Figure 5.7 The relative ratio of pSTAT5 to STAT5 is reduced in the C57BL/6J-*Kdm5b ΔARID* mammary gland at mid pregnancy.
(A) Western blot showing the expression of STAT5, phosphorylated (p)STAT5 and HSC70 in the C57BL/6J-*Kdm5b WT* and *ΔARID* mammary gland at mid-pregnancy. ImageJ software was used to quantify the band intensity and a histogram plotted showing the expression level of (B) STAT5 and (C) pSTAT5 normalized against the expression of HSC70. (D) Histogram showing the relative ratio of pSTAT5 to STAT5 (n=2 per group).

Examination of genes positively regulated by STAT5 shows that in keeping with the reduced relative ratio of pSTAT5 to STAT5 protein levels, there is a marked reduction in AKT expression levels (63 percent) at mid-pregnancy compared to the wild-type mammary gland. Although the relative ratio of pAKT to AKT appears to be increased, the actual level of pAKT is still lower in the C57BL/6J-*Kdm5b ΔARID* mammary gland compared to the wild type counterpart (Fig. 5.8).

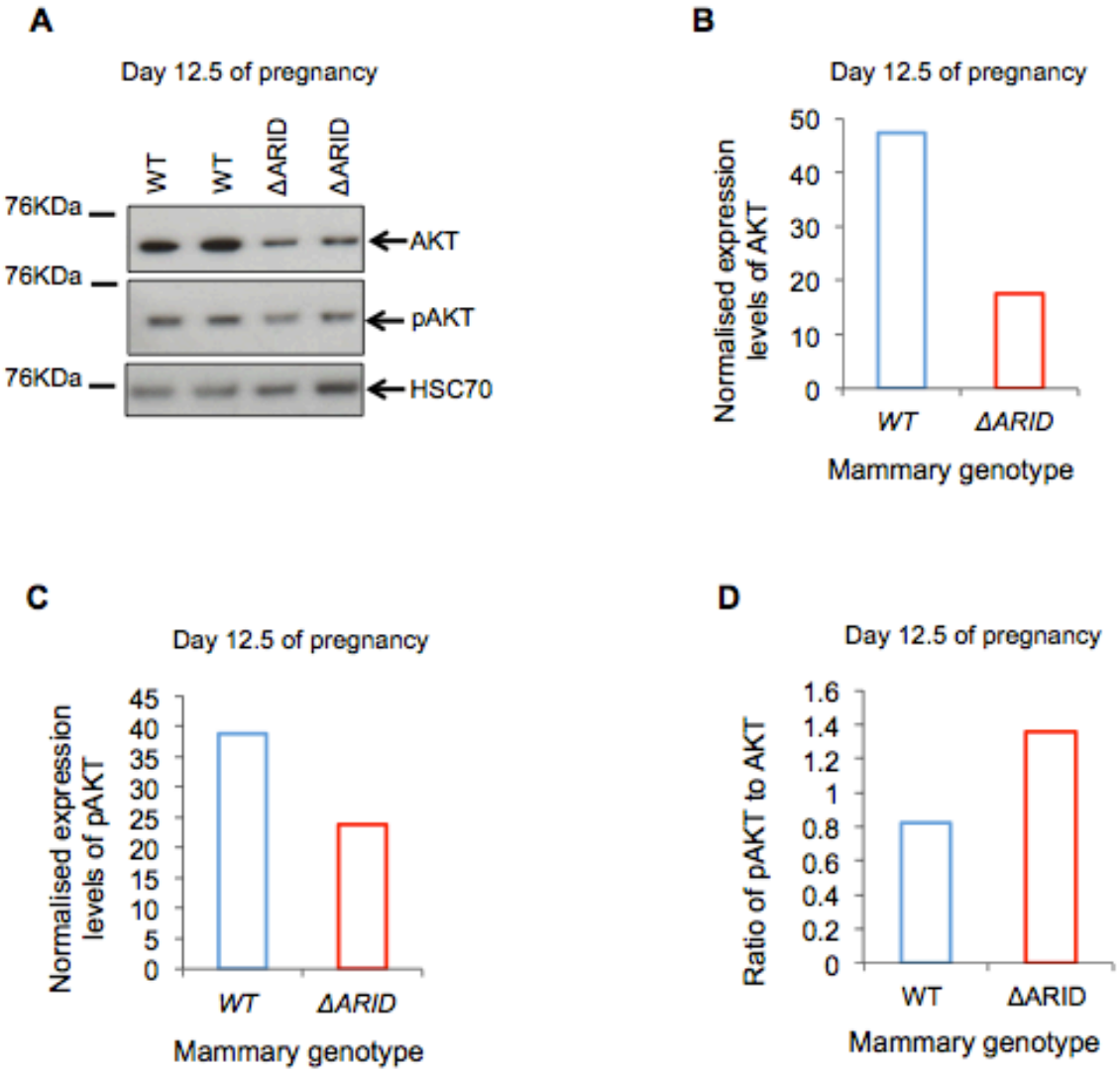


Figure 5.8 AKT expression is reduced in the C57BL/6J-*Kdm5b ΔARID* mammary gland at mid pregnancy.
(A) Western blot showing the expression of AKT, phosphorylated (p)AKT and HSC70 in the C57BL/6J-*Kdm5b WT* and *ΔARID* mammary gland at mid-pregnancy. ImageJ software was used to quantify the band intensity and a histogram plotted showing the expression levels of (B) AKT and (C) pAKT normalized against the expression of HSC70 and (D) Histogram showing the relative ratio of pAKT to AKT (n=2 per group).

The expression of milk proteins, are developmental biomarkers for mammary gland tissue. Therefore, as may have been predicted from the reduction in the levels of pSTAT5, beta casein expression at mid-pregnancy is dramatically reduced in the C57BL/6J-*Kdm5b ΔARID* mammary gland compared to the wild-type counterpart (89 percent) (Fig. 5.9). Furthermore, whey acidic protein is not expressed in the mammary gland of the C57BL/6J-*Kdm5b WT* or *ΔARID* female at mid pregnancy.

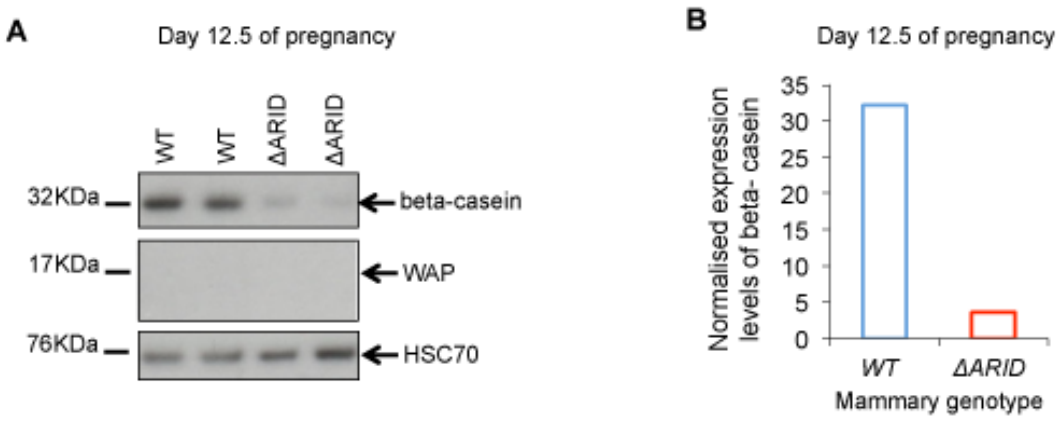


Figure 5.9 A delay in mammary gland differentiation is suggested by the reduced beta casein expression level in the C57BL/6J-*Kdm5b ΔARID* mammary gland at mid pregnancy.
(A) Western blot showing the expression of beta casein and whey acid protein in the C57BL/6J-*Kdm5b WT* and *ΔARID* mammary gland at mid-pregnancy. ImageJ software was used to quantify the band intensity and a histogram plotted showing the expression level of (B) beta casein normalized against the expression of HSC70. Note that whey acidic protein is not expressed in the C57BL/6J-*Kdm5b WT* or *ΔARID* mammary gland at mid pregnancy (n=2 per group).

5.3.3.2 Molecular analysis in the C57BL/6J-*Kdm5b ΔARID* mammary gland at late pregnancy (pd18.5)

(A) Steroid receptor expression at late pregnancy

The *C57BL/6J-Kdm5b ΔARID* female can support her pups at parturition and at a gross morphological level the mammary gland resembles that of the wild type counterpart. However, we have observed at late pregnancy a possible increase in fat globules secreted to the lumen in the C57BL/6J-*Kdm5b ΔARID* mammary gland. Ovariectomy at day 17 of pregnancy triggers premature milk secretion and accumulation of milk proteins in the ductal lumen (Neville et al., 2002), and the reduction in the expression of the progesterone receptor that occurs during late pregnancy contributes to the onset of lactation and terminal differentiation (Ismail et al., 2002). We therefore examined the expression of ER alpha by Western blot analysis and the expression of the progesterone receptor by immunohistochemistry. As seen at mid-pregnancy in the C57BL/6J-*Kdm5b ΔARID* mammary gland, only a marginal increase was observed in the level of ER alpha expressed in the C57BL/6J-*Kdm5b ΔARID* mammary gland at pd18.5 compared to the wild type counterpart (Fig. 5.10).

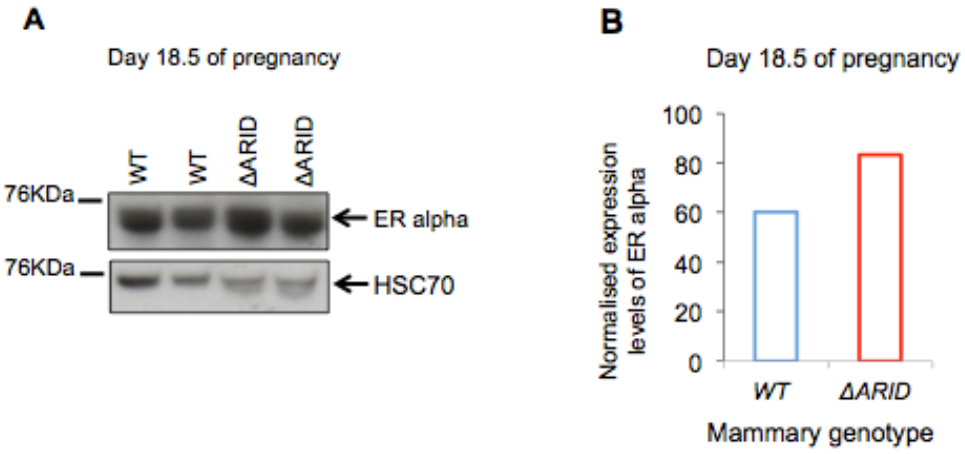


Figure 5.10 Expression of ER alpha in the C57BL/6J-*Kdm5b WT* and *ΔARID* mammary gland at late pregnancy.
(A) Western blot showing the expression of ER alpha and HSC70 in the C57BL/6J-*Kdm5b WT* and *ΔARID* mammary gland at late pregnancy. (B) ImageJ software was used to quantify the band intensity and a histogram plotted showing the expression level of ER alpha normalized against the expression of HSC70 (n=2 per group).

Of interest, progesterone receptor expression levels and the number of PR positive alveolar epithelia detected in the C57BL/6J-*Kdm5b ΔARID* female mammary gland is reduced compared to the wild type counterpart (Fig. 5.11**).** This could indicate that the reduction in PR expression may have accounted for the increase in fat globules secreted to the mammary gland lumen of the C57BL/6J-*Kdm5b ΔARID* female.

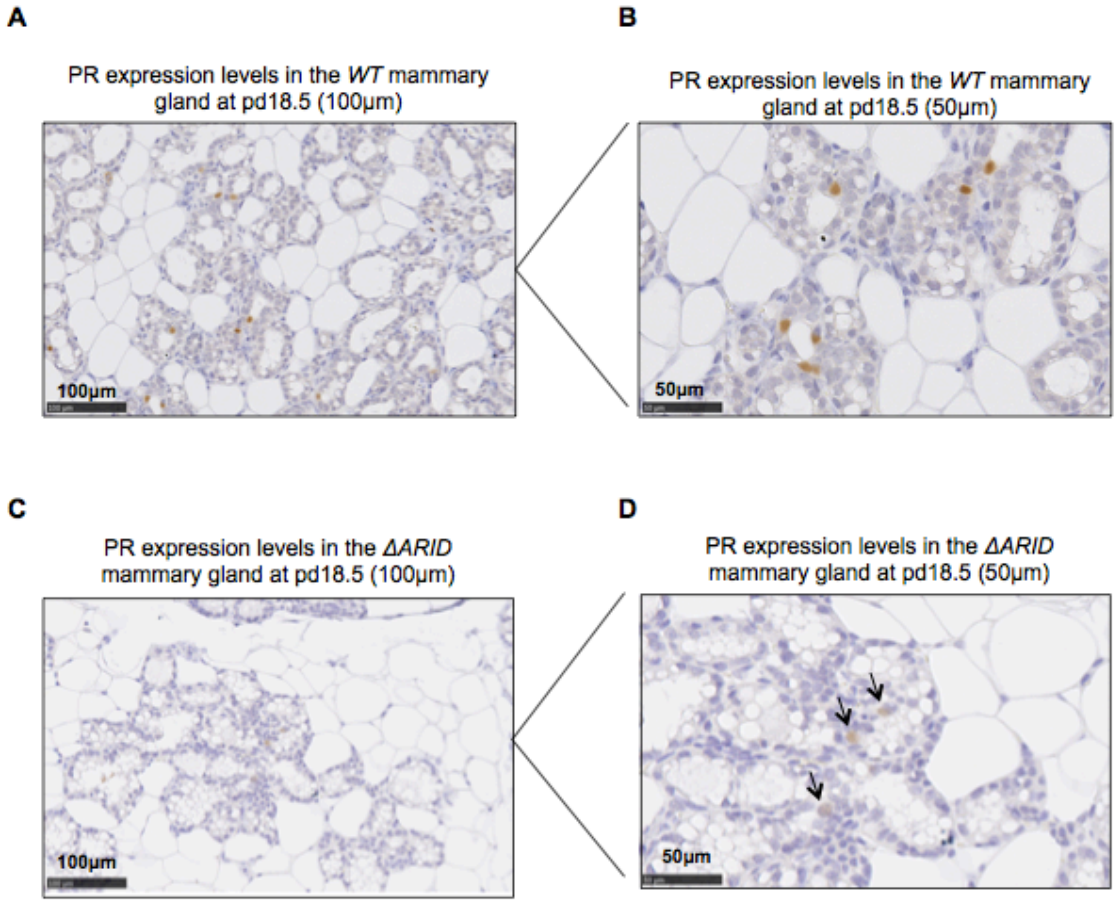


Figure 5.11 Progesterone receptor expression level is reduced in the C57BL/6J-*Kdm5b ΔARID* mammary gland at late-pregnancy.
Immunohistochemistry was performed for progesterone receptor expression on C57BL/6J-*Kdm5b WT* and *C57BL/6J-Kdm5b ΔARID* mammary gland sections at late pregnancy. Image of PR expression in the C57BL/6J-*Kdm5b WT* mammary gland at (A) x10 magnification and (B) x20 magnification. Image of PR expression in the *C57BL/6J-Kdm5b ΔARID* mammary gland at (C) x10 magnification and (D) x20 magnification. Arrow indicate weakly stained PR positive alveolar epithelia in the C57BL/6J-*Kdm5b ΔARID* mammary gland (n=2).

(B) Changes in the JAK/STAT and AKT signaling axis at late pregnancy

As seen at mid pregnancy the expression level of STAT6 in the C57BL/6J-*Kdm5b ΔARID* mammary gland is comparable with the wild type counterpart (Fig.5.6**),** indicating that expression of a KDM5B ΔARID protein is not overtly affecting STAT6 expression.

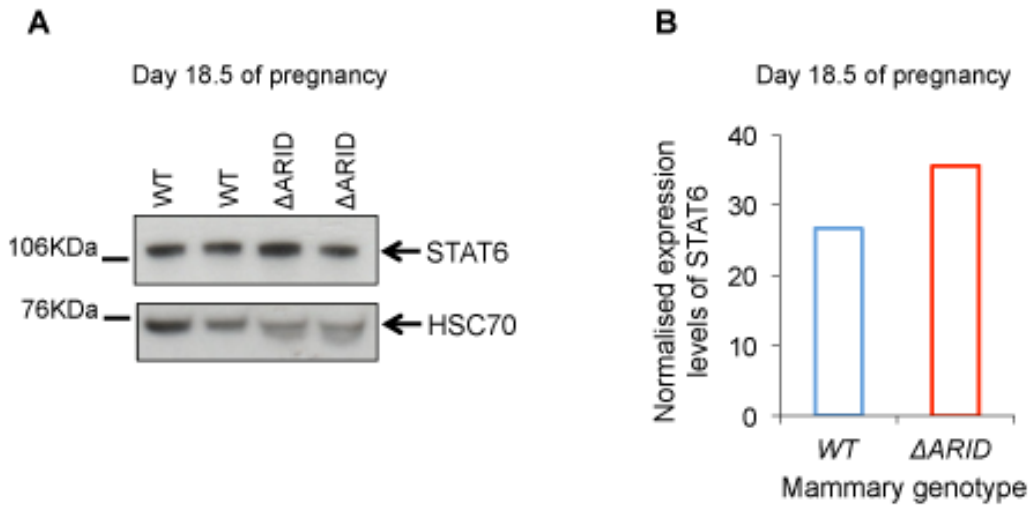


Figure 5.12 Expression of STAT6 in the C57BL/6J-*Kdm5b WT* and *ΔARID* mammary gland at late pregnancy.
(A) Western blot showing the expression of STAT6 and HSC70 in the C57BL/6J-*Kdm5b WT* and *ΔARID* mammary gland at late-pregnancy. (B) ImageJ software was used to quantify the band intensity and a histogram plotted showing the expression level of STAT6 normalized against the expression of HSC70 (n=2 per group).

As the gross morphology of the C57BL/6J-*Kdm5b ΔARID* mammary gland resembled that of the wild type by late pregnancy and the female can nurse her offspring at parturition we predicted that the relative ratio of pSTAT5 to STAT5 could be equivalent to the wild type counterpart. As shown in Figure 5.13, even though by late pregnancy expression of STAT5 is increased above the level expressed in the wild type counterpart (77 percent), the relative ratio of pSTAT5 to STAT5 is reduced compared to the relative ratio expressed in the wild type mammary gland (50 percent). Also, although western blot analysis on protein isolated from the whole mammary gland, suggests that the expression level of pSTAT5 is comparable with the wild type counterpart, immunohistochemistry analysis demonstrates that pSTAT5 expression is reduced in the alveolar epithelia (Fig.5.14). The discrepancy between the level of pSTAT5 expression seen by immunohistochemistry and Western blot could reflect sample loading. The quantification of pSTAT5 expression from the immunoblot is dependent on the normalization to HSC70. As seen in figure 5.13A, the resolution of the HSC70 bands from the C57BL/6J-*Kdm5b ΔARID* mammary gland samples is diffuse making accurate quantification less reliable.

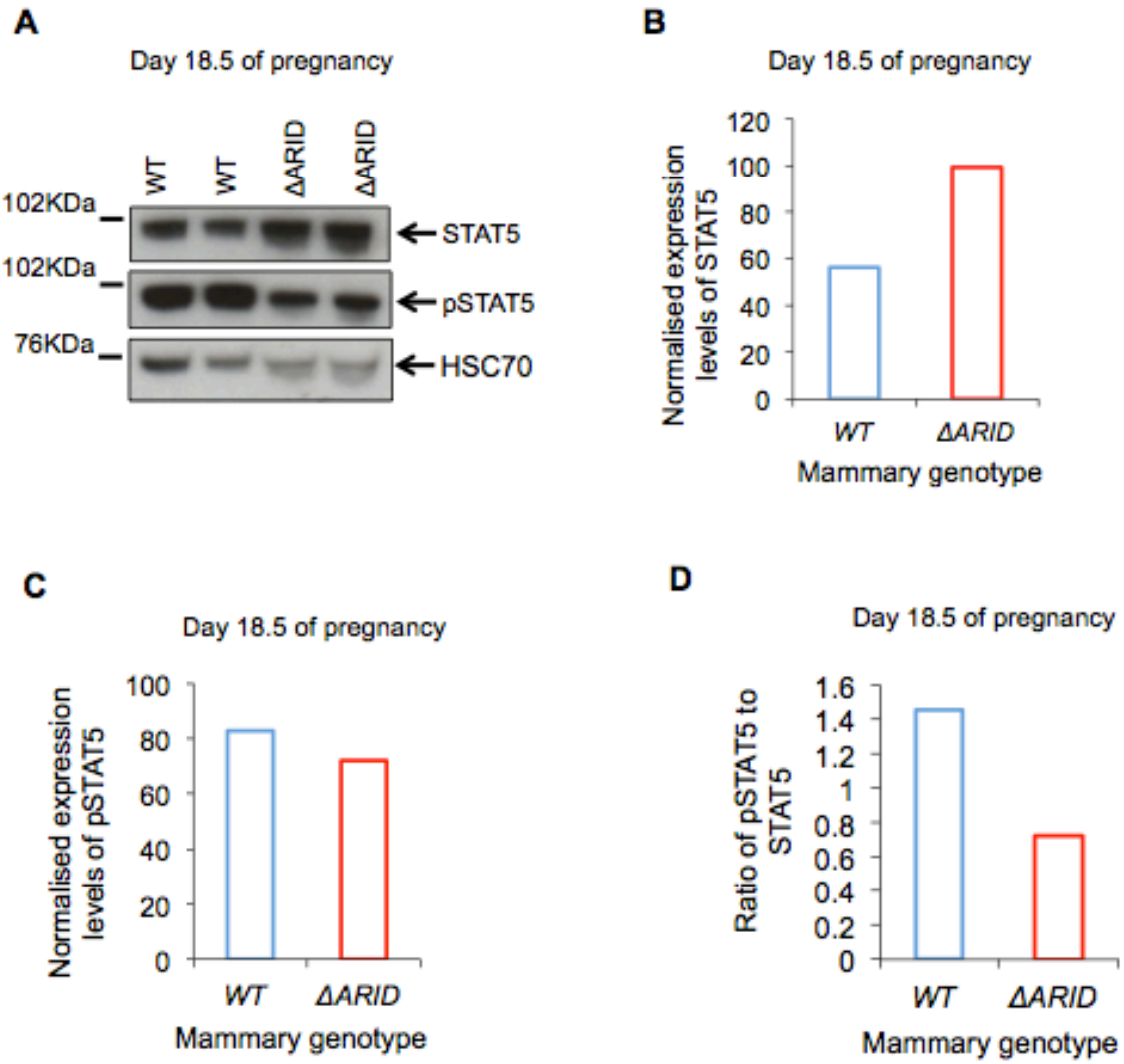


Figure 5.13 The relative ratio of pSTAT5 to STAT5 is reduced in the C57BL/6J-*Kdm5b ΔARID* mammary gland at late pregnancy.
(A) Western blot showing the expression of STAT5, phosphorylated (p)STAT5 and HSC70 in the C57BL/6J-*Kdm5b WT* and *ΔARID* mammary gland at late pregnancy. ImageJ software was used to quantify the band intensity and a histogram plotted showing the expression level of (B) STAT5 and (C) pSTAT5 normalized against the expression of HSC70 and (D) Histogram showing the relative ratio of pSTAT5 to STAT5 (n=2 per group).

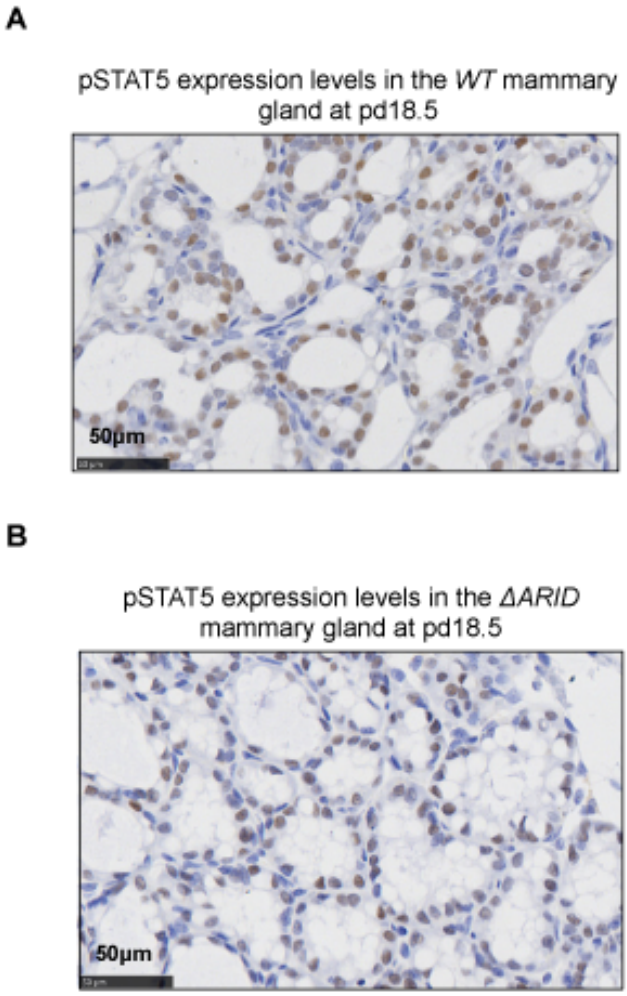


Figure 5.14 Phosphorylated STAT5 expression level is reduced in the C57BL/6J-*Kdm5b ΔARID* mammary gland at late pregnancy.
Immunohistochemistry was performed for phosphorylated STAT5 expression on (A) C57BL/6J-*Kdm5b WT* and (B) *C57BL/6J-Kdm5b ΔARID* mammary gland sections at late pregnancy (n=2)

In addition to the proposed role of activated AKT as part of a signalling pathway involved in mammary ductal branch initiation (Zhu *et al*., 2013), AKT can induce autocrine prolactin secretion from the mammary gland epithelia resulting in the activation of STAT5 and the development of a lactating mammary gland (Chen *et al*., 2012). Moreover, STAT5 positively regulates the transcription of *Akt* (Creamer *et al*., 2010). This indicates that a positive feedback loop exists between STAT5 and AKT. Even though the relative ratio of pSTAT5 to STAT5 in the C57BL/6J-*Kdm5b ΔARID* mammary gland is 50 percent less at late pregnancy compared to the wild type counterpart, this ratio has increased approximately two fold compared to the relative ratio of pSTAT5 to STAT5 expressed in the C57BL/6J-*Kdm5b ΔARID* mammary gland at mid-pregnancy. Interestingly, AKT expression increases to near wild type levels (29

percent increase above wild type) and the relative ratio of pAKT to AKT is only slightly reduced compared to the relative ratio expressed in the wild type counterpart (12% percent) (Fig.5.15**)**.

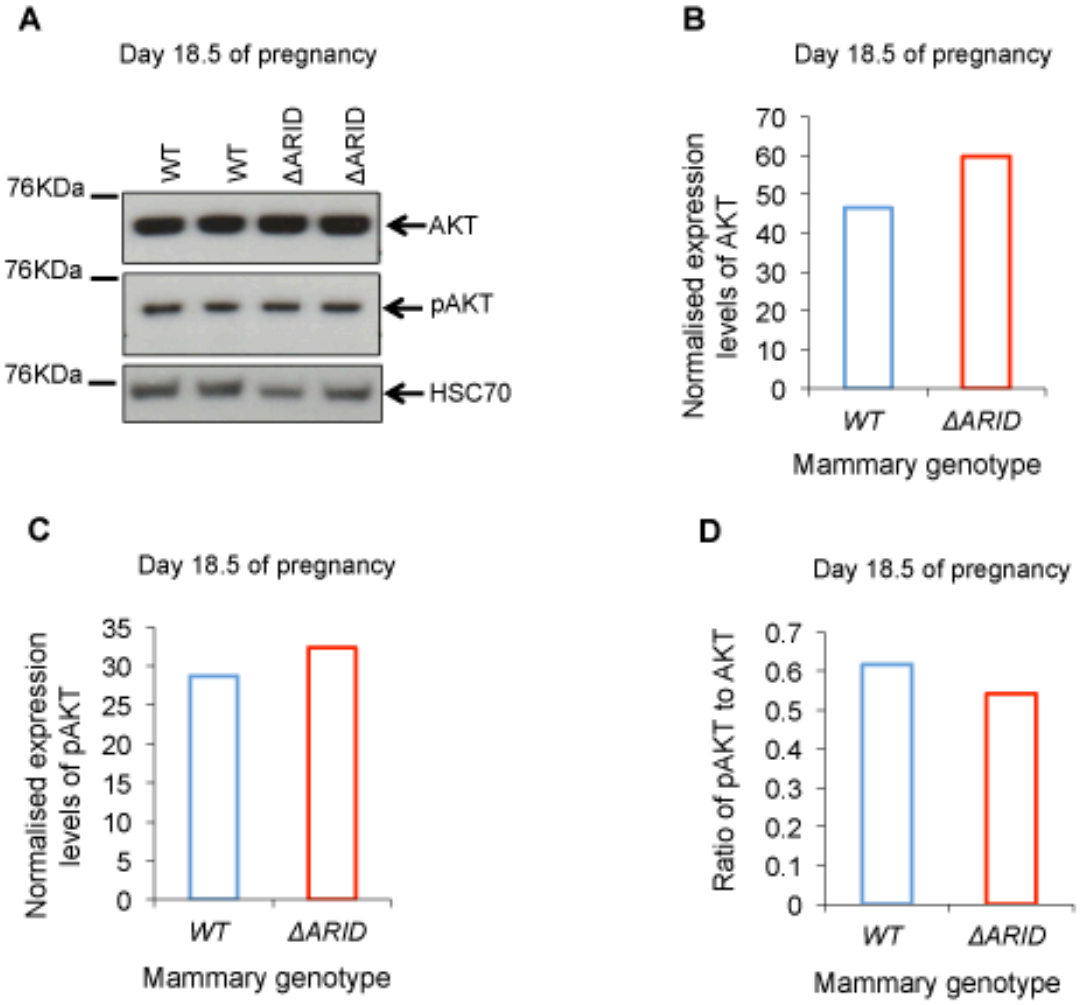


Figure 5.15 AKT expression in the C57BL/6J-*Kdm5b ΔARID* mammary gland at late pregnancy is comparable with the wild type counterpart.
(A) Western blot showing the expression of AKT, phosphorylated (p)AKT and HSC70 in the C57BL/6J-*Kdm5b WT* and *ΔARID* mammary gland at late pregnancy. ImageJ software was used to quantify the band intensity and a histogram plotted showing the expression level of (B) AKT and (C) pAKT normalized against the expression of HSC70 and (D) Histogram showing the relative ratio of pAKT to AKT (n=2 per group).

The expression levels of STAT5 are important for gene regulation. For example only 10-15% of total STAT5 expression is sufficient to induce a five-fold increase in beta-casein expression, whereas expression of 30% of the total STAT5 levels resulted in a reduction in the expression levels of WAP by 85% (Yamaji *et al*., 2013). Given that the

relative ratio of pSTAT5 to STAT5 is reduced by 50 percent in the C57BL/6J-*Kdm5b ΔARID* mammary gland at late pregnancy compared with the wild type relative ratio, we examined beta casein and whey acidic expression in the C57BL/6J-*Kdm5b ΔARID* mammary gland at late pregnancy.

Interestingly, compared to the wild type counterpart, beta casein expression increased by 71% and WAP expression increased by 60% in the C57BL/6J-*Kdm5b ΔARID* mammary gland (Fig.5.16). These data suggest that the relative ratio of pSTAT to STAT5 is sufficient, or other mechanisms exist that account for the increase in beta casein and WAP expression detected in the C57BL/6J-*Kdm5b ΔARID* mammary gland at late pregnancy.

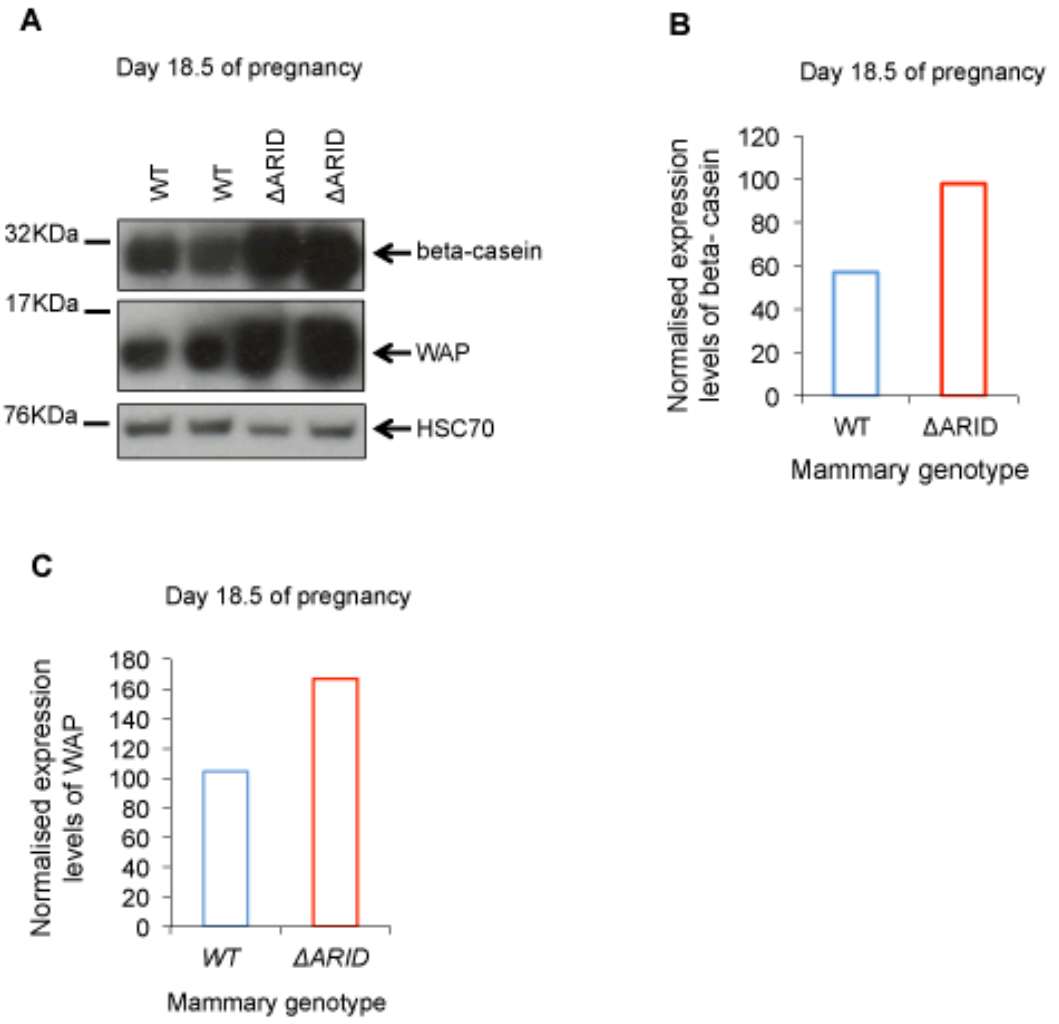


Figure 5.16 Beta casein and WAP expression in the C57BL/6J-*Kdm5b ΔARID* mammary gland at late pregnancy indicative of full differentiation.
(A) Western blot showing the expression of beta casein and whey acid protein in the C57BL/6J-*Kdm5b WT* and *ΔARID* mammary gland at late pregnancy. ImageJ software was used to quantify the band intensity and a histogram plotted showing the expression level of (B) beta casein and (C) whey acidic protein normalized against the expression of HSC70 (n=2 per group).

(C) Analysis of Kdm5a transcript expression in the C57BL/6J-*Kdm5b WT* and *ΔARID* mammary gland *at late pregnancy*

Studies suggest that KDM5A and KDM5B may compete for binding, and this competition is related to KDM5 expression levels (Islam *et al*., 2011b). The delay in differentiation observed in the C57BL/6J-*Kdm5b ΔARID* mammary gland could suggest that KDM5A compensates for the expression of a less abundant KDM5B ΔARID protein at late pregnancy. We therefore examined the *Kdm5a* transcript levels in the C57BL/6J-*Kdm5b WT* and C57BL/6J-*Kdm5b ΔARID* mammary gland at late pregnancy. Although the expression level of the *Kdm5a* transcript was not significantly altered in the C57BL/6J-*Kdm5b ΔARID* mammary gland compared to the wild type counterpart, the expression of KDM5A at pd18.5 could be sufficient for mammary gland recovery; a functional compensation which maybe unique to mammary gland development at late pregnancy (Fig 5.17).

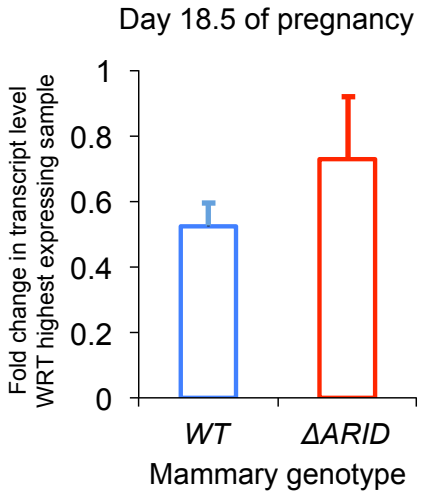


Figure 5.17 Expression of *Kdm5a* in the C57BL/6J-*Kdm5b WT and ΔARID* mammary gland at late pregnancy

Our studies have demonstrated that the expression of a KDM5B ΔARID protein results in a delay in mammary gland development and the female can nurse her pups at parturition. The sample number used for molecular analysis was unavoidably small and is therefore insufficient for statistical analysis. The graphical representation of the immunoblot data is provided solely as a visual tool since loading was not always equal. Therefore the information that it provides is limited. However a couple of notable points are highlighted. These studies would benefit from a larger sample size and further analysis by immunohistochemistry.

As collated in figure 5.18 below, our molecular analysis at mid-pregnancy (pd12.5) demonstrates that whilst the expression of ER alpha, STAT6 and STAT5 are comparable or only slightly increased compared to the wild type counterpart at mid-pregnancy (pd12.5), phosphorylated STAT5 and the relative ratio of phosphorylated to un-phosphorylated STAT5 are dramatically reduced in the *C57BL/6J-Kdm5b ΔARID* female mammary gland. In keeping with this beta casein, a STAT5 target gene (Yamaji *et al*., 2013) is also dramatically reduced indicating a less differentiated phenotype. Furthermore AKT, also a STAT5 target gene (Creamer *et al*., 2010), is markedly reduced and could account for the reduction in the number of side branches observed (Zhu and Nelson, 2013). By late pregnancy (pd18.5), prior to parturition, the level of STAT5 expression increases above the wild type counterpart expression level, and although the relative ratio of phosphorylated to un-phosphorylated STAT5 increases beyond that seen at mid pregnancy (pd12.5), the levels are below that detected in the wild type counterpart at late pregnancy. The expression level of STAT5 is important for gene regulation and may account for the activation of AKT to near wild type levels. In keeping with the ability of the C57BL/6J-*Kdm5b ΔARID* female to nurse her offspring, the expression level of beta casein and whey acidic protein increases, in fact, above that expressed in the wild type counterpart.

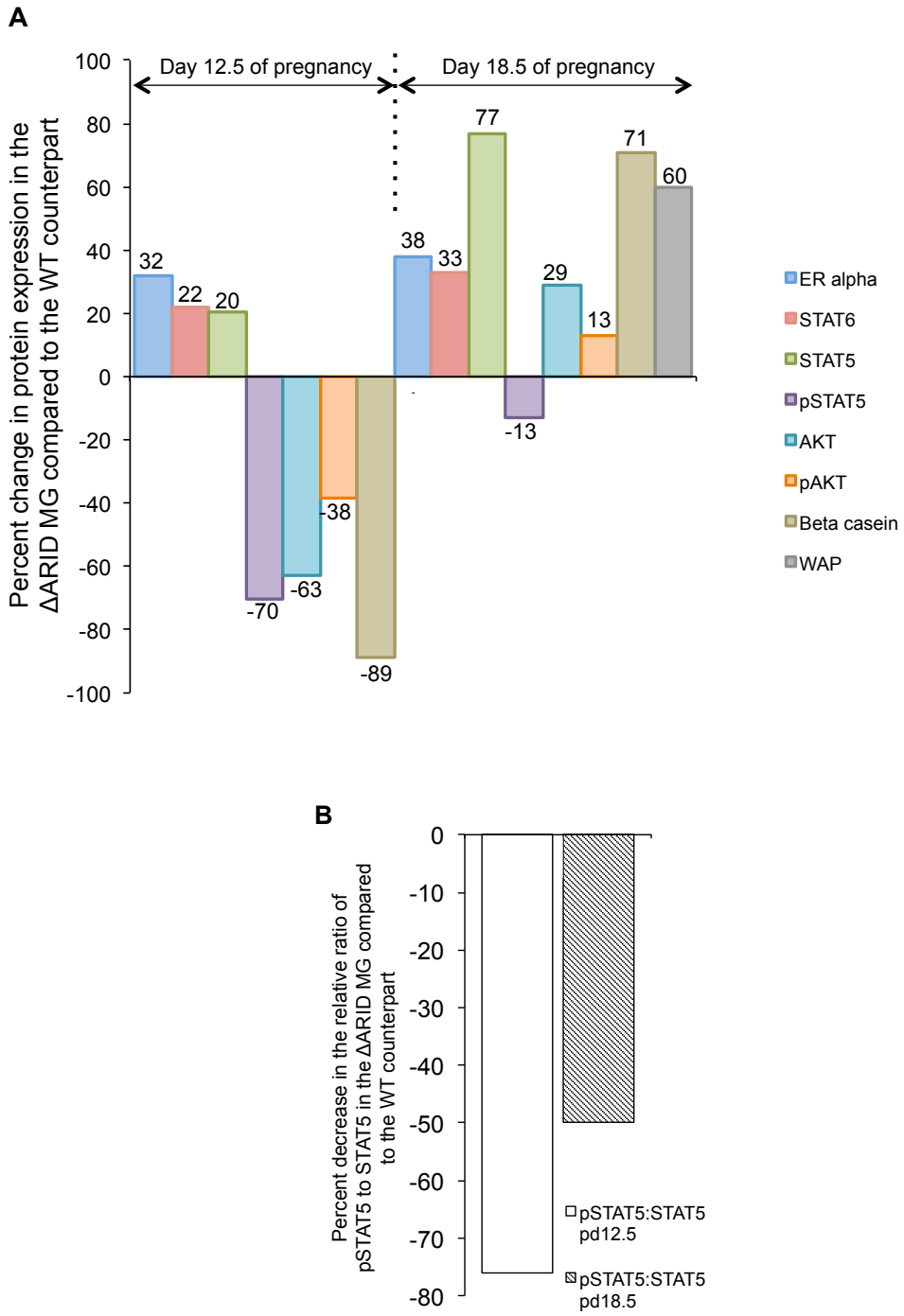


Figure 5.18 Summary of molecular analysis in the C57BL/6J-*Kdm5b ΔARID* mammary gland. (A) Histogram showing the percentage change in expression of ER alpha, STAT6, STAT5, pSTAT5, AKT, pAKT. beta casein and whey acidic protein in the C57BL/6J-*Kdm5b ΔARID* mammary gland compared to the wild type counterpart at mid and late pregnancy. (B) Histogram showing the decrease in the relative ratio of pSTAT5 to STAT5 expressed in the C57BL/6J-*Kdm5b ΔARID* mammary gland compared to the wild type counterpart.

5.4 Discussion

5.4.1 A potential role for KDM5B during oestrogen receptor signaling in the pubertal mammary gland

Development of the mammary gland requires interpretation of upstream hormonal signalling at the level of the genome resulting in the alteration of chromatin structure that permits gene regulation, progenitor cell expansion and lineage determination. Changes in histone methylation patterns are associated with gene expression changes during lineage restriction (Pal *et* al., 2013) and is therefore a likely mediator of the mammary epithelial cell hierarchy. Expression of a KDM5B protein lacking the ARID sequence would indicate a loss in demethylase activity and DNA binding via the ARID sequence resulting in an alteration in chromatin structure and therefore gene expression. The contribution of the KDM5B ΔARID domain to KDM5B function during mammary gland development will be discussed later in the final discussion.

ER alpha expression is a prerequisite for pubertal mammary gland development (Feng *et al*., 2007). As *Esr1* transcript levels are not affected in the C57BL/6J-*Kdm5b ΔARID* mammary gland at 4 weeks of age, but the C57BL/6J-*Kdm5b ΔARID* mammary gland presents with a delay in ductal elongation suggests that KDM5B could function as a ER alpha cofactor and regulate a subset of ER alpha responsive genes. The studies reported here using tagged proteins indicate that KDM5B can form a complex with ER alpha *in vivo*, independent of the ARID domain. Given that the C57BL/6J-*Kdm5b ΔARID* adult mammary gland also presents with reduced side branching and we have seen a trend in the reduction in progesterone transcript levels, suggests that KDM5B via the ARID domain recruits ER alpha to the genome and is partially responsible for the activation of progesterone receptor expression. To substantiate this, these studies require further investigation. In the first instance, the expression level of *Esr1*, *Pgr* and *Wnt4* transcripts would need to be examined on a larger sample size. Furthermore, immunohistochemistry would confirm whether ER alpha and KDM5B are co-expressed, and immunoprecipitation of endogenous ER alpha and KDM5B/KDM5B ΔARID would confirm an *in vivo* interaction. To determine whether the interaction between ER alpha and KDM5B is direct could be achieved by pull down experiments with glutathione s-transferase (GST) tagged ER alpha and *in vitro* translated KDM5B or *visa versa.* Furthermore ChIp for KDM5B/KDM5B ΔARID on the progesterone receptor gene would determine if the ARID domain is responsible for DNA binding and re-ChIp with an ER alpha antibody to establish whether KDM5B and ER alpha are localized to the

same region of the progesterone receptor gene. If proven, this could suggest that KDM5B may function in the context of a luminal epithelial hormone-sensing cell. In this case, KDM5B could potentially regulate mammary gland stem cell expansion and cell fate determination during the development of the nulliparous mammary gland and during gestation (Asselin-Labat *et al*., 2010, Joshi *et al*., 2010). One proposed paracrine mediator of progesterone signaling responsible for an increase in mammary gland stem cell number is WNT4, transcript levels of which are reduced in the adult C57BL/6J-*Kdm5b ΔARID* mammary gland.

5.4.2 Analysis of KDM5B target genes in the adult C57BL/6J-Kdm5b ΔARID mammary gland

Expression of a KDM5B protein without the ARID domain is expected to lack demethylase activity (Yamane *et al*., 2007, Xiang *et al*., 2007). Although *BUB1*, *MT1F*, and *BRCA1* genes are bound and repressed in a demethylase dependent manner by KDM5B in the human breast cancer cell line MCF7, the observation that the levels of these transcripts do not change in the adult nulliparous C57BL/6J-*Kdm5b ΔARID* mammary gland could be due to a number of considerations. Firstly, a redundant function for KDM5A and KDM5B has been described (Islam *et al*., 2011b, Chicas *et al*., 2012). For example, during pRb associated repression of senescence-associated genes, siRNA mediated suppression of either *KDM5A* or *KDM5B* expression in senescent cells did not affect the expression of most cell cycle genes tested. However, targeted knocked down of both *KDM5A* and *KDM5B* expression cooperated to prevent the repression of these E2F target genes (Chicas *et al*., 2012). Functional cooperation between KDM5A and KDM5B is not restricted to genes involved in senescence. Similarly, KDM5B was recruited to multiple KDM5A target genes in both *KDM5A* siRNA targeted cells and *Kdm5a null* MEFs (Islam *et al*., 2011b). As KDM5B is the most abundant KDM5 family member expressed in MCF7 cells (Krishnakumar *et al*., 2010, SC and JTP unpublished observation) the expression level of KDM5A maybe insufficient to compensation for KDM5B mediated gene repression of *BUB1*, *MT1F* and *BRCA1*. Although not examined here, If KDM5A is expressed in the nulliparous adult mammary gland, KDM5A may compensate for the demethylase activity of KDM5B, accounting for the lack of change in *Bub1*, *Mt1F* and *Brca1* transcript levels expressed in the C57BL/6J-*Kdm5b ΔARID* mammary gland at 12 weeks of age.

5.4.3 Importance of epigenetic factors in mammary gland development

Given that KDM5B is expressed in embryonic stem cells (Dey *et* al., 2007, Schmitz *et al*., 2011, Xie *et al*., 2011, Kidder *et al*., 2013) we cannot exclude a possible role for KDM5B in mammary gland stem self-renewal and cell-fate determination. Whilst it is not clear whether KDM5B regulates ES cell self-renewal (Schmitz *et al*., 2010, Xie *et* al., 2011, Kidder *et al*., 2013), the absence of KDM5B impairs differentiation (Schmitz *et al*., 20011, Kidder *et al*., 2013) due to the inappropriate expression of pluripotency genes (Schmitz *et al*., 2011, Kidder *et al*., 2013) as well as germ cell genes (Schmitz *et* al., 2011) and the under-expression of developmental genes (Schmitz *et al*., 2011, Kidder *et al*., 2013). KDM5B binding is associated with polycomb protein complex target genes enriched in bivalent domains (Schmitz *et al*., 2010), Interestingly in the absence of EZH2, mammary gland stem cell and luminal activity is reduced and manifests in a delay in pubertal mammary gland development. However although during pregnancy alveoli progenitor cells differentiate, pups die at birth due to a reduction in alveoli structures and therefore insufficient milk production (Pal *et al*., 2013). Even though alveologenesis proceeds in the C57BL/6J-*Kdm5b ΔARID* mammary gland, the similar nulliparous mammary gland phenotype to that presented in the mammary gland specific *Ezh2* knockout may further implicate KDM5B in mediating gene regulation as part of an EZH2 containing polycomb complex. KDM5A is also implicated in mediating polycomb protein complex target genes (Pasini *et al*., 2008) and could be responsible for the 'recovery' seen in the C57BL/6J-*Kdm5b ΔARID* mammary gland by late pregnancy.

5.4.4 KDM5B function during pregnancy associated mammary gland development

(A) Early to mid-pregnancy

In the adult nulliparous mammary gland STAT5 expression is required to generate alveolar progenitor cells (Yamaji *et* al., 2009) that expand and differentiate during pregnancy. Expression from either one allele of *Stat5a* or *Stat5b* during pregnancy is sufficient to promote alveoli bud formation, whilst expression from two alleles initiates differentiation similar to expression from all four alleles of *Stat5* (Yamaji *et* al., 2013). Thus, lower levels of activated STAT5 appear to be sufficient to promote alveolar bud formation at mid-pregnancy in the C57BL/6J-*Kdm5b ΔARID* mammary gland but not differentiation to the level seen in the wild type counterpart. Given that KDM5B expression is required to fully activate STAT5 could suggest that fewer alveolar

progenitor cells reside in the adult nulliparous C57BL/6J-*Kdm5b ΔARID* mammary gland and/or an effect of alveolar progenitor cell expansion/differentiation during early pregnancy (Cui *et al*., 2004).

Whist STAT6 expression is not required for the development of the nulliparous mammary gland, during early pregnancy STAT6 expression is required for proliferation and commitment to the alveolar lineage (Khaled *et al*., 2007). Whilst the studies reported here cannot exclude a function for KDM5B in mediating STAT6 signaling, STAT6 expression levels are relatively unperturbed in the KDM5B ΔARID mammary gland during pregnancy. An attempt was made to examine pSTAT6 expression levels by Western blot but the antibody failed to detect expression. In future the expression of activated STAT6 should be investigated. However activated STAT5, AKT and beta casein levels are reduced at mid-pregnancy indicating a delay in differentiation. Activated STAT5 positively regulates AKT expression (Creamer *et al*., 2010) and activated AKT is required to initiate branch formation in a three-dimensional culture model of murine mammary epithelia (Zhu *et al*., 2013). This agrees with the lack of side branches manifest in the C57BL/6J-*Kdm5b ΔARID* mammary gland at this stage of pregnancy.

The level of ER alpha expression in the C57BL/6J-*Kdm5b ΔARID* mammary gland at mid pregnancy is comparable with the wild type counterpart. However whilst a trend in the reduction of *Pgr* transcript expression is observed, *Wnt4* transcript level in the C57BL/6J-*Kdm5b ΔARID* mammary gland is comparable with the wild type counterpart. Given that we have seen a trend in the reduction in *Pgr* transcript expression and moreover a significant reduction in *Wnt4* transcript expression levels in the nulliparous mammary gland, it is possible that KDM5B functions to mediate signaling pathways at distinct mammary gland developmental windows. This observation would be confirmed using immunohistochemical analysis by co-staining for PR and WNT4 expression in the C57BL/6J-*Kdm5b WT* and *ΔARID* mammary gland at these stages of development.

Although WNT4 expression is required for ductal side branching at mid-pregnancy (Brisken *et al*., 2000), other factors such as RANKL and ID4 also mediate side branching and alveologenesis (Fernandez-Valdivia *et al*., 2009, Dong *et al*., 2011). Of Interest, ovarian hormone replacement in a *Stat5a* null genetic background failed to induce *Rankl* expression (Santos *et al*., 2010). Furthermore, a PR/STAT5 complex can bind to the *Id4* gene in response to prolactin and progesterone to elicit an increase in *Id4* expression (Fernandez-Valdivia *et al*., 2009), highlighting that cross talk between the PRL/JAK2/STAT5 and progesterone signaling pathways is important in mediating

mammary gland morphogenesis. Given the reduction in activated STAT5 levels at mid-pregnancy, RANKL and ID4 are likely candidates in mediating the downstream effects of progesterone and prolactin signaling and could be reduced in the C57BL/6J-*Kdm5b ΔARID* mammary gland.

(B) Late pregnancy

By late pregnancy, pSTAT5 levels are still reduced compare to the wild type but increased in relation to the activated pSTAT5 levels seen at mid pregnancy in the KDM5B ΔARID mammary gland. The induction of beta casein and whey acidic protein expression would indicate that pSTAT5 levels at this stage of pregnancy are sufficient to induce full differentiation (Yamaji *et al*., 2013). Interestingly beta casein and WAP are expressed at levels higher in the C57BL/6J-*Kdm5b ΔARID* mammary gland than in the wild-type counterpart, even though the mammary gland consists of fewer alveoli structures at late pregnancy (See Chapter 4). This suggests that activated AKT may be inducing WAP and beta-casein expression in ductal luminal cells in the absence of alveoli structures (Chen *et al*., 2012).

The level of ER alpha expression in the C57BL/6J-*Kdm5b ΔARID* mammary gland is comparable with the wild type counterpart at late pregnancy, yet the expression level of the progesterone receptor is reduced. We attempted to confirm the reduction in progesterone receptor expression seen using immunohistochemistry by Western blot. However the antibodies used failed to detect expression. The progressive reduction in progesterone receptor expression that occurs during late pregnancy has also been suggested to contribute to the onset of lactation and terminal differentiation (Ismail et al., 2002), and may possibly be accelerated in the C57BL/6J-*Kdm5b ΔARID* female. This could also reflect the suggestion that an increase in fat globules has been observed in the lumen (Chapter 4) and could be examined by immunohistochemistry using a perillipin specific antibody. Furthermore accelerated differentiation is also in keeping with the increase in beta casein and WAP proteins detected in the C57BL/6J-*Kdm5b ΔARID* mammary gland compared to the wild type at late pregnancy.

5.4.5 The relative ratio of phosphorylated to un-phosphorylated STAT5

The activated STAT5 levels are reduced in the C57BL/6J-*Kdm5b ΔARID* mammary gland altering the ratio of un-phosphorylated to phosphorylated STAT5 protein levels. Interestingly, it has been reported that un-phosphorylated STAT1 and STAT3 regulate expression of target genes that are distinct from those controlled by activated STAT1

and STAT3 pathways (Yang and Stark, 2008). Studies in *D. melanogaster* using a leukemia model have demonstrated that the un-phosphorylated form of STAT is localized in heterochromatin in association with HP1 and upon STAT activation results in a loss of heterochromatin formation (Shi *et al*., 2008). Significantly, un-phosphorylated STAT5 binds to heterochromatin protein 1 alpha (HP1-alpha) and stabilizes heterochromatin formation (Hu *et al*., 2013). These studies highlight the importance of the non-canonical function of STAT5 and may indicate a function for the increased level of un-phosphorylated STAT5 in the C57BL/6J-*Kdm5b ΔARID* mammary gland.

5.4.6 The regulation of STAT5 activation

In mammary gland epithelial cells STAT5 can be activated by a number of different signalling pathways that could be affected in the C57BL/6J-*Kdm5b ΔARID* mammary gland, however JAK2 is a key signaling node for the activation of STAT5 (Wagner *et al.,* 2004), and is mediated by prolactin binding to the prolactin receptor (Horseman *et al*., 1997. Ormandy *et al*., 1997). The expression of AKT is essential for the activation of STAT5 via the PRLR/PRL/JAK2 signalling pathway (Chen *et al*., 2012), yet although AKT expression levels in the C57BL/6J-*Kdm5b ΔARID* mammary gland at late pregnancy are comparable with the wild type, activated STAT5 is reduced. It would therefore be important to examine prolactin and prolactin receptor expression levels in the C57BL/6J-*Kdm5b ΔARID* mammary gland. Furthermore STAT5 activation in the mammary gland is also controlled by negative regulators, whose expression could be affected in the C57BL/6J-*Kdm5b ΔARID* mammary gland including Caveolin-1 (Sotgia *et al*., 2006), suppressor of cytokine signaling-2 (SOCS2) (Harris *et al*., 2006), PI3-kinase enhancer A (PIKE-A) (Chan *et al*., 2010), protein tyrosine phosphatase 1B (PTP1B) (Milani *et al*., 2013) and p21-activated kinase 1 (PAK1) (Wang *et al*., 2003).

Chapter 6: Results

Investigation into the effect of KDM5B ΔARID expression on mammary gland tumour development

Chapter 6. Investigation into the effect of KDM5B ΔARID expression on mammary gland tumour development

6.1 Aims: Using the C57BL/6J-*Kdm5b ΔARID* murine line we aim to investigate the effect of KDMB ΔARID expression on mammary gland tumour development.

6.2 Introduction:

KDM5B was first reported as being expressed in breast cancer (Lu *et al*., 1999). Since then, KDM5B dys-regulation has been reported in several types of solid tumors, including prostate cancer (Xiang *et al*., 2007), bladder cancer (Hayami *et al*., 2010) and melanoma (Roesch *et al*., 2005, 2006, 2008, 2010), in which KDM5B expression defines a subset of slow cycling melonoma cells that are required for continuous tumour growth (Roesch *et al*., 2010). Using transplantable tumour models of human (Catchpole *et al*., 2011) and murine (Yamane *et al*., 2007) cell lines and by knocking down *KDM5B* expression using RNA interference, it has been shown by us (Catchpole *et al*., 2011) and others (Yamane *et al*., 2007) that KDM5B expression is required for mammary tumour growth. We therefore sought to expand our studies by examining the effect of the KDM5B ΔARID protein on murine mammary gland tumour development.

To examine how expression of a KDM5B ΔARID protein can affect tumour development an endogenous tumour model expressing the KDM5B ΔARID protein is required. This can be achieved by introducing an oncogene, driven by a mammary gland specific promoter, into the C57BL/6J-*Kdm5b ΔARID* murine line. We therefore made use of the polyoma middle T murine model that expresses the polyoma middle T antigen driven from the mouse mammary tumour virus (MMTV) promoter. This results in the development of spontaneous mammary gland tumours with a 100 percent penetrance.

6.3 Results

6.3.1 The expression of a KDM5B ΔARID protein results in a delay in mammary gland tumour development

To investigate the role of KDM5B in mammary gland tumour development two parallel breeding programs were initiated; the test group was bred over 3 generations to generate females homozygous for the *ΔARID* allele and heterozygous for the polyoma middle T antigen, whilst the control group was bred over the same number of generations in order to control for genetic variability (Fig. 6).

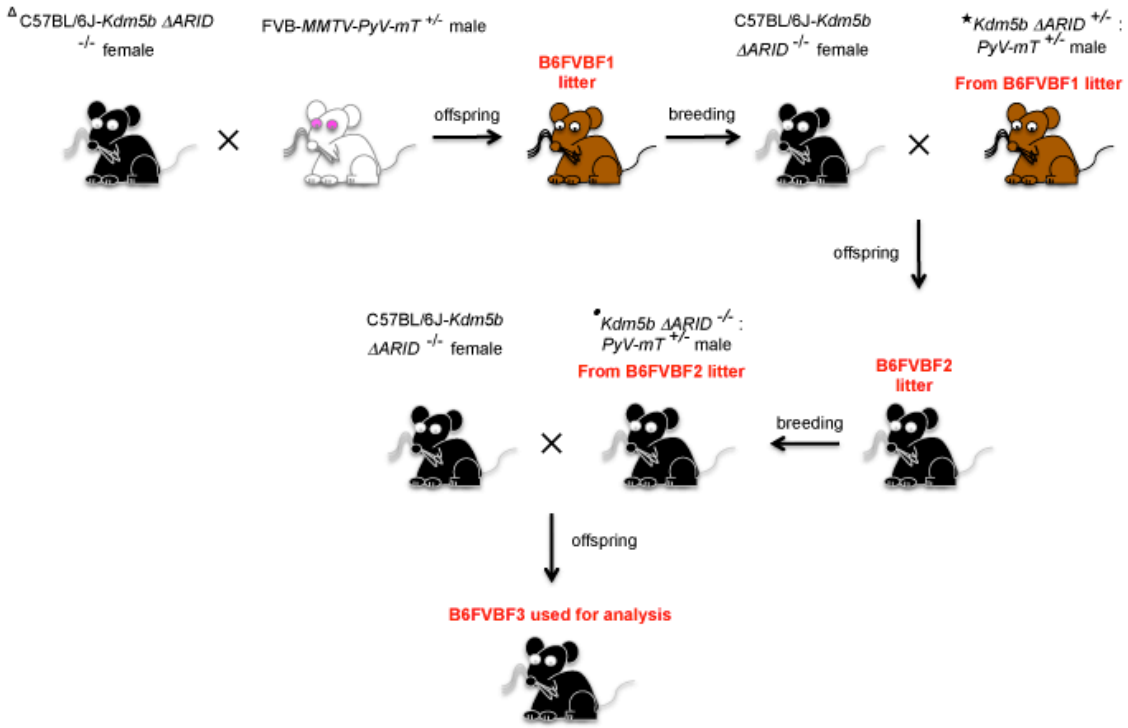


Figure 6 Schematic representation of the B6;FVB-*Kdm5b ΔARID* -/- : *PyV-mT* +/- breeding program. Δ**,** for the control murine line, the C57BL/6J-*Kdm5b WT* female was bred with the FVB-*MMTV-PyV-mT +/-* male over three generations as detailed for the test study. ★, •, genotype selected for subsequent breeding programs. B6FVBF1, B6FVBF2, B6FVBF3: F1, F2, F3 generations derived from the breeding program between C57BL/6J and FVB murine strains (See Fig. 6.1, 6.2, 6.3).

A breeding program was established between a C57BL/6J-*Kdm5b ΔARID -/-* female and a FVB-*MMTV-PyV-mT +/-* male. In order to identify and select a breeding male heterozygous for both the *Kdm5b ΔARID* and polyoma middle T antigen alleles (B6FVBF1), genomic DNA was isolated and screened by PCR for the presence of the polyoma middle T antigen allele (Fig 6.1).

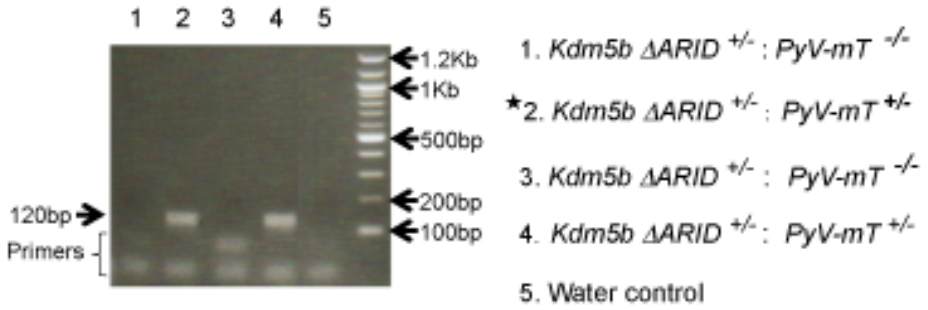


Figure 6.1 PCR generated genotype results of a litter from the C57BL/6J-*Kdm5b ΔARID -/-* female : FVB-*MMTV-PyV-mT +/-* male breeding program (B6FVBF1). The male identified as positive for the polyoma middle T antigen allele (lane 2, ★) was paired with a C57BL/6J-*Kdm5b ΔARID -/-* female to generate the B6FVBF2 generation.

Once identified, the B6;FVB-*Kdm5b ΔARID* +/- : *PyV-mT +/-* male was paired with a C57BL/6J-*Kdm5b ΔARID -/-* female and the offspring (B6FVBF2) screened for the presence of the *ΔARID* allele by Southern blot and the polyoma middle T antigen by PCR (Fig. 6.2 A and B respectively). The final breeding program was then initiated between the C57BL/6J-*Kdm5b ΔARID* -/- female and the B6;FVB-*Kdm5b ΔARID -/-* : *PyV-mT +/-* male and the *ΔARID* homozygous status confirmed by Southern blot (Fig 6.3A); the presence of the polyoma middle T antigen confirmed by PCR (Fig 6.3B). Third generation homozygous B6;FVB-*Kdm5b ΔARID* or B6;FVB-*Kdm5b* WT females heterozygous for the polyoma middle T antigen were monitored from birth and time in days to tumour development noted (See Table 5S1 in the supplemental material).

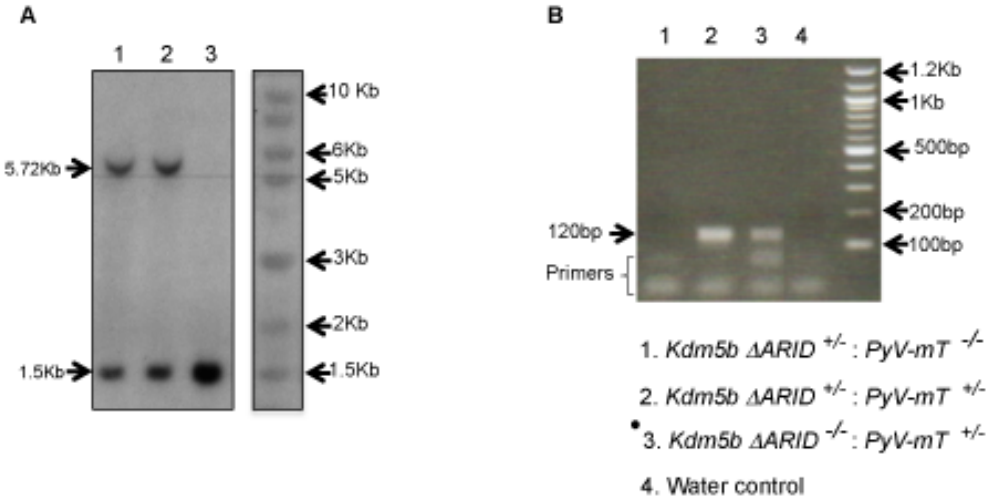


Figure 6.2 Genotype results of a litter from the B6;FVB-*Kdm5b ΔARID* +/- : *PyV-mT +/-* male and a C57BL/6J-*Kdm5b ΔARID -/-* female breeding program (B6FVBF2). The offspring were screened for the presence of the (A) *KDM5B ΔARID* allele by Southern blot and (B) the polyoma middle T antigen by PCR. Lane 3 (•) represents the genotype result for a B6;FVB-*Kdm5b ΔARID* -/- : *PyV-mT +/-* male used to pair with a C57BL/6J-*Kdm5b ΔARID -/-* female to generate the B6FVBF3 generation.

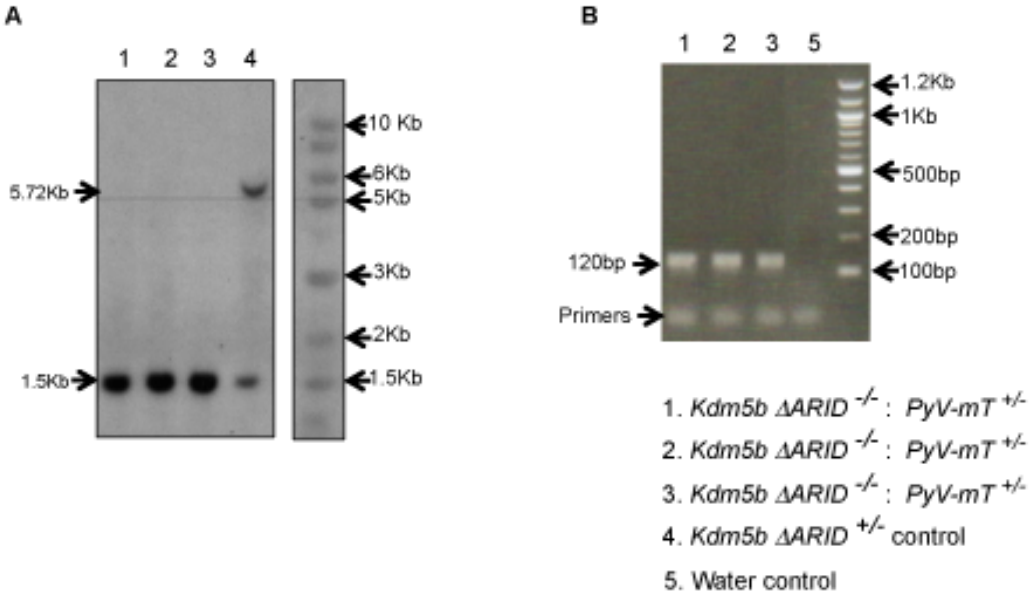


Figure 6.3 Genotype results of a litter from the B6;FVB-*Kdm5b ΔARID* -/- : *PyV-mT* +/- male and a C57BL/6J-*Kdm5b ΔARID* -/- female breeding program (B6FVBF3). The offspring were screened for the presence of the (A) *KDM5B ΔARID* allele by Southern blot and (B) the polyoma middle T antigen by PCR. B6FVBF3 offspring were used to monitor tumour development.

The results showed that expression of a KDM5B ΔARID protein, which is expected to lack demethylase activity, results in a delay in spontaneous mammary gland tumour growth ($p<0.05$). The box-plot in Figure 6.4 demonstrates that the time taken for the B6;FVB- *Kdm5b WT*:*PyV-mT* +/- female to present with tumours is varied, ranging from 46 days to 156 days with a median value of 96 days and an interquartile range of 27. In comparison, the time taken for the B6;FVB-*Kdm5b ΔARID* -/- : *PyV-mT* +/- female to present with tumours is less varied ranging from 76 days to 130 days with one mammary gland tumour presenting at 162 days being represented as an outlier (See Table 6S1 in the supplemental material). The median value for the time to tumour development in the B6;FVB-*Kdm5b ΔARID* -/- : *PyV-mT* +/- female is 108 days with an interquartile range of 21 days. Representing the data as a Kaplan-Meier plot additionally highlights that mammary gland tumours develop earlier in the B6;FVB-*Kdm5b WT*: *PyV-mT* +/- female than in the B6;FVB-*Kdm5b ΔARID* -/- : *PyV-mT* +/- female. The later appearance of mammary tumours in the B6;FVB-*Kdm5b ΔARID* -/- : *PyV-mT* +/- females may reflect the delay in mammary gland development.

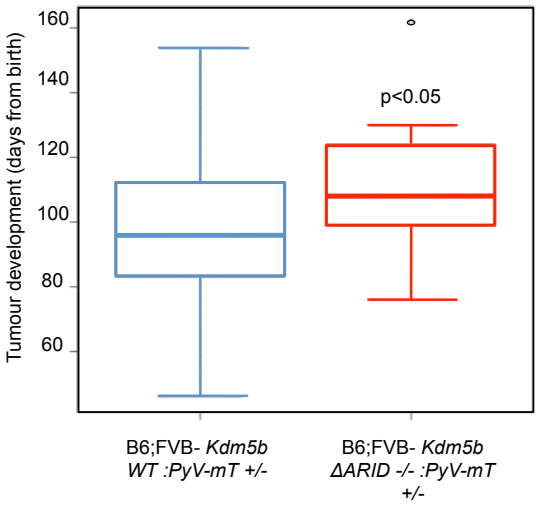


Figure 6.4 Box plot showing the distribution of time (in days) taken to develop mammary gland tumours; the median value, 25th and 75th percentile range; sample maximum, minimum and outlier values in the B6;FVB- *Kdm5b WT*:*PyV-mT +/-* and B6;FVB-*Kdm5b ΔARID -/-* : *PyV-mT +/-* females (n=23 per group)

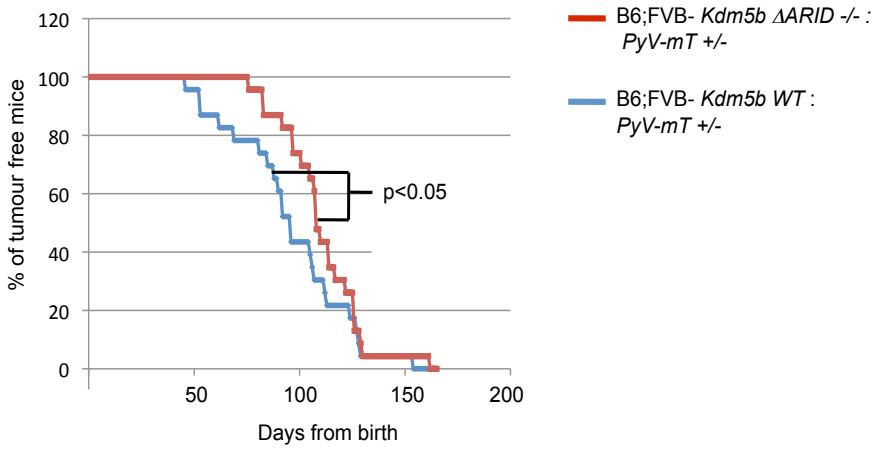


Figure 6.5 Kaplan-Meier plot showing time to tumour development in the B6;FVB- *Kdm5b ΔARID -/-*:*PyV-mT +/-* and B6;FVB- *Kdm5b WT*:*PyV-mT +/-* female mammary gland. The B6;FVB- *Kdm5b ΔARID -/-*:*PyV-mT +/-* female presents with an initial delay in spontaneous mammary gland tumour development (n=23 per group).

6.4 Discussion

6.4.1 KDM5B ΔARID expression and breast cancer

Studies in this laboratory have shown that on a cohort of over 300 breast cancers that KDM5B is widely expressed in all breast cancer sub-types (unpublished observation). Activated STAT5 is also detected in all sub-types of breast cancer but primarily ER+ tumours and when so, is associated with a more differentiated phenotype, responsiveness to endocrine therapy and an increase in the patient survival rate (Cotarla *et al*., 2004, Nevalainen et al., 2004, Yamashita et al., 2006, Peck *et al*., 2011). It would therefore be of interest to correlate expression levels of KDM5B with that of activated STAT5.

Our studies indicate that KDM5B may regulate some aspects of ER alpha signaling and studies suggest that knockdown of *KDM5B* expression impairs breast cancer cell proliferation *in vivo* and *in vitro* (Yamane *et al*., 2007, Catchpole *et al*., 2011). Whereas knock down of *KDM5B* dramatically affects tumour growth *in vivo* using the ER positive breast cancer cell line MCF7 (Catchpole *et al*., 2011), reduced expression levels of a KDM5B ΔARID protein in a ER-negative spontaneous mammary gland tumour model (PyV-mT), delays the time to first tumour appearance and the initial growth. This delayed tumour development in the C57BL/6J-*Kdm5b ΔARID* female possibly reflects the presence of fewer mammary gland epithelial cells. However, breast cancer growth may be dependent upon KDM5B expression levels. This data could suggest that the oncogenic potential of KDM5B may reside in either the demethylase activity of KDM5B, it's DNA binding ability or both. Interestingly, hemizygous loss of the *Stat5* allele also delayed the first appearance of SV40-T antigen mediated tumours (208 days compared with 188 days) (Ren *et al*., 2002).

Given that polyoma middle T antigen induces tumours that are ER negative whereas the epithelial breast cancer cell line, MCF7 is ER alpha positive and was isolated from a metastatic site, makes comparisons between these two tumour models difficult. The C57BL/6J-*Kdm5b ΔARID* murine line should therefore be crossed to an ER positive tumour model (Kumar *et al*., 2007, Chan *et al*., 2012). However as noted above KDM5B is expressed in all human breast cancer sub-types.

Interestingly, the luminal progenitor gene signature correlates with the gene signature transcribed in the ER-negative polyoma middle T tumour model (Lim *et al*., 2010). Furthermore, the ER-negative luminal progenitor population most likely represents the alveolar progenitor population (Shehata *et al*., 2012). By analogy then, given that

STAT5 expression is required for the generation and proliferation of alveolar progenitors suggests that this is the population affected during normal mammary gland development in the C57BL/6J-*Kdm5b ΔARID* murine line.

Whilst activation of STAT5 has been shown to be tumourigenic, with mice expressing a constitutively activated STAT5 protein developing occasional adenocarcinomas after a long latency of between 8 and 12 months (Iavnilovitch *et* al., 2004, Vafaizadeh *et al*., 2012), activation of STAT5 via constitutive activation of JAK2 required additional oncogenic insults for tumour development (Caffarel *et al*., 2012). Activation of JAK2 circumvents apoptosis (Creamer *et* al., 2010, Caffarel *et al*., 2012) that is a hallmark of cancer (reviewed Hanahan and Weinberg, 2011). Studies show that activated JAK2 expression and therefore activated STAT5 not only induces proliferation and resistance to cell death but can enhance the expression of differentiation markers *in vitro* (Caffarel *et al*., 2012). These authors suggest that activation of the JAK2/STAT5 pathway may have a dual role whereby STAT5 promotes the earlier steps of tumour progression, but maintains the differentiation status of established breast cancers (Caffarel *et al*., 2012). This may account for the improved prognosis of breast cancer patients expressing activated STAT5 and markers of differentiation.

Studies are currently underway to identify KDM5B specific inhibitors (Sayegh *et al*., 2013) and significantly, knock down of KDM5B sensitizes cells to genotoxic insults (Li *et al*., 2014). Collectively this suggests that inhibition of KDM5B in combination with genotoxic drugs, in pSTAT5 positive tumours during the early stages of tumour progression could impinge on two important cellular processes subverted during cancer. (1) inhibition of KDM5B through chemical inhibition would inhibit alveolar hyperplasia by down-regulating the JAK2/STAT5 signaling pathway and (2) upon a second oncogenic insult fail to repair double strand breaks resulting in genomic instability and sensitizing the tumour to genotoxic drugs.

6.5 Supplemental material

B6;FVB- *Kdm5b WT:PyV-mT +/-*	Tumour development (Days from birth)	B6;FVB- *Kdm5b ΔARID -/-:PyV-mT +/-*	Tumour development (Days from birth)
1	154	A	162
2	129	B	130
3	128	C	129
4	127	D	126
5	124	E	126
6	113	F	126
7	112	G	122
8	107	H	117
9	106	I	114
10	105	J	114
11	96	K	110
12	96	L	108
13	92	M	108
14	92	N	108
15	90	O	107
16	88	P	105
17	85	Q	101
18	81	R	97
19	69	S	97
20	62	T	92
21	53	U	83
21	53	V	83
23	46	W	76

Table 6S1: Table showing time to tumour development (in days from birth) in the B6;FVB- *Kdm5b ΔARID -/-*:*PyV-mT +/-* and B6;FVB- *Kdm5b WT*:*PyV-mT +/-* female mammary gland (n=23 per group).

Chapter 7: Discussion

Chapter 7 Discussion

7.1 Summary

In this thesis the attempts to generate a constitutive *Kdm5b* null murine line is described. Generation of one model, called the B6;129-*Kdm5b-Exon1* knock out murine line resulted in constitutive *Kdm5b* deletion and demonstrated that KDM5B maybe required for embryonic development. A second model, called the C57BL/6J-*Kdm5b ΔARID* murine line resulted in the expression of a truncated hypomorphic KDM5B protein that lacked 5 of the 42 amino acids that constitute the JMJN domain and the entire ARID domain that would result in a loss of demethylase activity and interfere with direct chromatin interaction. Although otherwise developmentally normal, the C57BL/6J-*Kdm5b Δ*ARID female presented with a delay in ductal morphogenesis at puberty suggestive of a role for KDM5B in mediating oestrogen receptor signalling. In line with this the expression levels of an oestrogen receptor target gene, the progesterone receptor, and a downstream target of the progesterone receptor, *Wnt4* are reduced in the adult nulliparous C57BL/6J-*Kdm5b Δ*ARID mammary gland. Furthermore it has been demonstrated that an *in vivo* interaction between epitope tagged ER alpha and KDM5B is independent of the ARID domain. As the ARID domain is one potential mechanism by which KDM5B can be recruited to the genome we propose that KDM5B may be involved in the recruitment of ER alpha to some regions of the genome. Our analysis of the C57BL/6J-*Kdm5b Δ*ARID pregnant mammary gland showed a delay in mammary gland morphogenesis and the female could nurse her pups at parturition. Investigation into the molecular mechanisms that may relate to this showed that KDM5B expression is required to positively regulate the PRLR/JAK2/STAT5 signalling pathway associated with mammary gland development during gestation. Interestingly, beta casein levels are reduced at mid-pregnancy in the C57BL/6J-*Kdm5b Δ*ARID mammary gland indicating a delay in alveolar differentiation. However, by late pregnancy expression of beta casein exceeds wild type expression level and progesterone receptor expression is reduced indicating premature differentiation.

7.2 The KDM5B null phenotype

The studies presented in this thesis, were the first to report on a *Kdm5b* null genetic line and these studies demonstrated that KDM5B is essential for embryonic

development (Catchpole *et al*., 2011). During the writing of this thesis Zou and colleagues (2014) also reported on a *Kdm5b* null genetic line. Whereas the *Kdm5b* null murine line reported in this thesis is on the mixed (B6;129) genetic background, using the C57BL/6J genetic background studies have yielded contrasting phenotypes (Albert et al., 2013, Zou *et al*., 2014). Albert and colleagues (2013) reported that deletion of the *Kdm5b* gene resulted in major neonatal lethality (Albert et al., 2013), whereas in the *Kdm5b* null murine line reported by Zou and colleagues (2014) the offspring are viable but presented with increased mortality, decreased body weight and the females were infertile beyond three months of age. Furthermore the deletion of *Kdm5b* resulted in the formation of fewer TEB structures and a delay in pubertal mammary gland development. Given that KDM5B expression (Madsen et al., 2002) and molecular mechanisms (Yamane et al., 2007, Pasini et al., 2008, Hao et al., 2012, Kidder *et al*., 2013) could account for the phenotypes presented in the *Kdm5b* null murine lines reported (Catchpole *et al*., 2011, Albert *et al*., 2013, Zou *et al*., 2014) makes resolving these discrepancies difficult, particularly for those studies on the same genetic background.

However, as discussed in Chapter 3, the neomycin-targeting vector used to generate the *Kdm5b-Exon 1* knock out murine line was designed to replace *Kdm5b* exon 1. The presence of the endogenous *Kdm5b* promoter, and the described cryptic splice sites contained within the neomycin gene (Jin et al., 2005) could potentially lead to the expression of hybrid transcripts consisting of both the neomycin and *Kdm5b* gene sequences (Shearman et al., 2000, Kos et al., 2002). Furthermore, the presence of the neomycin promoter contained within the neomycin targeting vector could drive transcription that could potentially result in the expression of a truncated *Kdm5b* transcript lacking exon 1 of *Kdm5b.* We are currently crossing the B6;129-*Kdm5b-Exon1* knock out murine line with a FVB/N-Tg(ACTB-cre)2Mrt/J murine line to remove the neomycin gene in order to address this discrepancy on the role for KDM5B during embryonic development.

7.3 Deciphering the role of the KDM5 family of proteins during development

Understanding the function of KDM5B during development is further complicated by the co-expression of the KDM5 family of proteins in a number of tissues and a propensity for compensation. In particular all four of the KDM5 family members are expressed in the embryonic brain (Sheardown et al., 2006, Madsen et al., 2002, Xu et al., 2002, Outchkourov et al., 2013) and KDM5B and KDM5D are expressed

during spermatogenesis (Madsen et al., 2003, Akimoto et al., 2008). Furthermore, KDM5A, KDM5B and KDM5C are also expressed in the haematopoietic system (Sheardown et al., 1996, Islam et al., 2011a). Our studies in the murine mammary gland have shown that KDM5B is involved in STAT5 activation and so could potentially affect the development of the lymphocyte system in the C57BL/6J-*Kdm5b ΔARID* murine line. In conclusion, a better understanding of the KDM5 family of proteins during embryonic development and most likely postnatal development of the mammary gland and spermatogenesis awaits combined knock out studies.

However it is worth noting at this stage that the KDM5B ΔARID murine line are fertile beyond three months of age and although the mortality rate was not examined, no obvious survival phenotype was apparent. This suggests that the expression level of a KDM5B ΔARID are sufficient, or other domains of KDM5B are required to rescue some of the phenotypes presented on the *Kdm5b* null genetic background reported by Zou and colleague (2014). However as discussed below the ARID domain of KDM5B could be required for KDM5B binding to chromatin and the recruitment of cofactors thereby promoting gene expression changes toward the luminal cell lineage.

Despite the reduced body weight in the *Kdm5b* null murine line reported by Zou and colleagues (2014), when normalised the fat pad was comparable with the wild type counterpart, indicating an intrinsic effect on ductal elongation (Zou *et al*., 2014). Furthermore oestrogen levels were reduced in the absence of KDM5B (Zou *et al*., 2014) further highlighting the need to examine hormone levels in the C57BL/6J-*Kdm5b ΔARID* murine line. However, whilst extrinsic effects on pubertal mammary development occur, KDM5B also controls gene regulation as discussed below.

7.4 KDM5B function during pubertal mammary gland

Signalling through the oestrogen receptor regulates pubertal mammary gland ductal elongation and is delayed when a KDM5B protein lacking the ARID domain is expressed (Catchpole *et al*., 2011 and this thesis), and also in the *Kdm5b* null murine line (Zou *et al*., 2014), indicating that the phenotype is attributable to the absence of the ARID domain. In the C57BL/6J-*Kdm5b Δ*ARID murine line, DNA binding is compromised and demethylase activity is lost providing an important tool to study the role of the KDM5B ARID domain in gene regulation. Importantly, KDM5B promotes

FoxA1 and *Stat5a* expression by binding directly to their promoters and facilitating recruitment of the master luminal regulator GATA3. Significantly, an absence of KDM5B results in a decrease in H3K4me3 levels at the activated promoters (Zou *et al*., 2014) indicating a demethylase independent mechanism for KDM5B-mediated gene activation and is discussed later. It is therefore possible that not only is the ARID domain of KDM5B responsible for the recruitment of cofactors to DNA but it is also the DNA interacting domain that distinguishes between gene activation and repression. Interestingly *FoxA1* and *Stat5a* expression is not entirely dependent upon KDM5B expression and so is only reduced in its absence (Zou *et al*., 2014). This is in keeping with *FoxA1* null mammary epithelia failing to develop beyond the rudimentary ductal structure, whereas *FoxA1* haploinsufficiency result in a delay in ductal elongation (Bernado *et al*., 2010). Furthermore, STAT5A expression is dispensable for ductal elongation but required for ductal side branching during oestrus (Santo *et al*., 2010), phenotypes affected in the C57BL/6J-*Kdm5b* ΔARID mammary gland. To substantiate this, FOXA1 and STAT5A expression levels should therefore be examined in the nulliparous C57BL/6J-*Kdm5b* ΔARID mammary gland and furthermore ChIp-Seq analysis together with RNA-Seq performed to correlation KDM5B binding with H3K4 methylation levels and gene expression. Whilst further investigation is required, in chapter 4 we propose that KDM5B via the ARID domain recruits ER to the progesterone receptor and is partially responsible for gene activation. In keeping with this, the expression level of the *Pgr* transcript is also reduced in the *Kdm5b* null genetic background (Zou *et al*., 2014) further suggesting a function for the KDM5B ARID domain in gene activation.

If the expression of KDM5B is required for the recruitment of ER alpha to the genome resulting in gene expression as proposed in this thesis, and KDM5B can recruit GATA3 to the promoter of *FoxA1* and facilitate expression (Zou *et al*., 2014), the question is whether there is a causal relationship between ER alpha, GATA3, FOXA1 and KDM5B. Genome wide mapping of ER alpha, GATA3 and FOXA1 in the breast cancer cell line MCF7 has demonstrated that 45 percent of ER alpha binding sites map to GATA3 binding sites, 37 percent of ER alpha binding sites map to FOXA1 binding sites and 30 percent of ER alpha binding sites were co-occupied by GATA3 and FOXA1 (Kong *et al*., 2011). An important first step would be to correlate KDM5B genome wide binding with that of ER alpha, GATA3 and FOXA1. Genome wide mapping of ER alpha, GATA3 and FOXA1 after RNAi-mediated silencing of *KDM5B*

expression would go someway in establishing if KDM5B expression is required to recruit these factors to the genome.

The role of KDM5B during nuclear receptor signalling is not clear, with KDM5B being implicated in both the activation and repression of hormone inducible genes. While KDM5B binds to AR and activates transcription from a *PSA-Luc* reporter construct (Xiang *et al*., 2007) in a hormone dependent manner, KDM5B forms a repressor complex with progesterone receptor in the absence of hormone (Vincent *et al*, 2011, 2013). These findings if extrapolated may suggest a function for KDM5B as a gate-keeper to hormone induction. For instance, where the role of KDM5B is to keep genes repressed in the absence of hormones, this would require the demethylase activity of KDM5B. Conversely, in the presence of hormones KDM5B may switch to an activator of transcription and would require DNA interaction via the ARID domain.

7.5 KDM5B, stem cells and progenitor cells

In vitro binding studies (EMSA) and expression of KDM5B mutant constructs in cell lines have shown that the KDM5B ARID domain is required for DNA binding (Scibetta *et al*., 2007, Yao *et al*., 2010) and demethylase activity (Xiang *et al*., 2007, Yamane *et al*., 2007) and therefore repression. We have developed a murine model in which KDM5B mediated activation as well as repression can be studied. In the *Kdm5b* null murine line, gene expression analysis suggests that KDM5B expression not only promotes gene expression changes toward the luminal cell lineage but also represses stem cell associated genes during nulliparous mammary gland development (Zou *et al*., 2014). This is analogous to the role of KDM5B in embryonic stem cells in which *Kdm5b* depletion results in a delay in the expression of neuronal differentiation markers in part due to the expression of pluripotent genes (Schmitz *et* al., 2011, Kidder *et al*., 2013). The phenotype presented in the postnatal C57BL/6J-*Kdm5b ΔARID* mammary gland could be due therefore to continue self-renewal even in the presence of differentiation signals (Kidder *et al*., 2013) resulting in perturbed postnatal mammary gland development. KDM5B positively regulates *Stat5a* expression in the adult nulliparous mammary gland (Zou *et al*., 2014) suggesting that the population of alveolar progenitor cells present in the nulliparous C57BL/6J-*Kdm5b Δ*ARID mammary gland, and expanded upon pregnancy, is reduced. Whilst the mammary gland cell hierarchy is not alter in the nulliparous mammary gland in

the absence of KDM5B (Zou *et* al., 2014) an effect on the cell cycle is possible given that KDM5B expression is required for the transition from the G1 phase of the cell cycle (Dey *et al*., 2007, Yamane *et al*., 2007).

7.6 KDM5B, pregnancy and involution

7.6.1 KDM5B and the STAT signalling pathway

Our morphological and molecular characterisation of the C57BL/6J-*Kdm5b* ΔARID mammary gland at mid pregnancy suggests an effect at the very least on luminal ductal progenitor expansion and the expansion/differentiation of the alveolar progenitor pool at mid-pregnancy. The adult mammary gland provides the ductal and alveolar progenitor population that expand during pregnancy providing the mature luminal ductal system and differentiated alveolar structures. The delay in C57BL/6J-*Kdm5b* ΔARID mammary gland ductal side branching and alveologenesis observed during pregnancy may originally reside in the adult nulliparous mammary gland. Although the morphology of the C57BL/6J-*Kdm5b* ΔARID mammary gland by late pregnancy resembles the wild type counterpart, significantly fewer alveoli are present, suggesting reduced proliferation. However no difference in Ki67 levels were detected at two stages, mid pregnancy (pd12.5) and late pregnancy (pd18.5). KDM5B expression is required for proper G1 to S phase transition of both ES cells (Dey *et al*., 2008, Xie *et al*., 2010) and the breast cancer cell line, MCF7 (Yamane *et al*., 2007, Wong *et al*., 2012). This requirement for *Kdm5b* at the G1 to S phase transition may be common to normal murine mammary epithelial cells during pregnancy. However we have shown a reduction in the pro-survival protein AKT at mid pregnancy, which could indicate an increase in apoptosis at this stage, resulting in fewer alveoli at late pregnancy even in the presence of near normal AKT expression levels. This question could be resolved by examining the expression of cleaved caspase 3 and 6 by immunohistochemistry.

As discussed above KDM5B recruits GATA3 to the *FoxA1* and *Stat5a* promoter resulting in gene expression during nulliparous mammary gland development (Zou *et al*., 2014). KDM5B most likely mediates transcription of only a subset of GATA3 responsive genes given that GATA3 expression is required for placode formation and postnatal mammary gland ductal and alveolar progenitor differentiation (Asselin-Labat *et al*., 2007). Therefore an effect on a subset of GATA3 responsive genes in

the C57BL/6J-*Kdm5b* *Δ*ARID mammary gland during pregnancy-associated development is also possible.

GATA3 expression is required for the expression of Th2 cytokines *IL4*, *IL5*, and *IL13* during T cell differentiation (Sasaki *et al*., 2013). The expression of IL4 and IL13 activates STAT6 leading to proliferation and luminal cell commitment to an alveolar lineage (Khaled *et al*., 2007). It is certainly intriguing to imagine that during early mammary gland differentiation KDM5B is involved in the recruitment of GATA3 to the *IL4* and *IL13* genes leading to expression, STAT6 activation and mammary gland differentiation, which is delayed in the C57BL/6J-*Kdm5b* *Δ*ARID mammary gland. To further substantiate this, while total STAT5 protein levels remain comparable, activated STAT5 levels are also reduced in the *Stat6* null (Khaled *et* al., 2007) and C57BL/6J-*Kdm5b* *Δ*ARID genetic backgrounds throughout gestation. These studies would therefore be greatly enhanced by a morphological and molecular characterisation of early gestation stages in the C57BL/6J-*Kdm5b* *Δ*ARID mammary gland. GATA3 has also been shown to activate STAT5 in the hematopoietic system (Bhattacharya *et al*., 2001), via the expression of *IL5* and by the same analogy maybe reduced in the C57BL/6J-*Kdm5b* *Δ*ARID mammary gland.

Given that overexpression and forced activation of STAT5 delays post-lactational involution (Iavnilovitch *et* al., 2004) could suggest that involution in the C57BL/6J-*Kdm5b* *Δ*ARID mammary gland is accelerated and therefore the gross morphology of the mammary gland should be examined post forced weaning. Furthermore, as detailed above, the recent evidence that KDM5B is involved in the recruitment of GATA3 to specific genes (Zou *et* al., 2014) could implicate KDM5B in mediating STAT6 activation. This could suggest that KDM5B is involved in the general activation of STAT family members and raises the question whether KDM5B is involved in the activation of STAT3?

As discussed below KDM5B is likely to be involved in a number of signalling pathways that control mammary gland morphogenesis. In keeping with this, although activated STAT5 is required for alveolar progenitor expansion and differentiation it is dispensable for ductal development (Liu *et al*., 1997, Cui *et al*., 2004, Yamaji *et al*., 2009), suggesting that STAT5 dependent and independent pathways are affected in the C57BL/6J-*Kdm5b* *Δ*ARID mammary gland. The same analogy applies to STAT6 signalling given that the *Stat6* null nulliparous mammary gland presents with no

apparent defect and AKT expression levels are unaffected during pregnancy. To further these studies and define the function of KDM5B and particularly the role the of the ARID sequence, requires defining those genes that KDM5B directly interacts with and regulates, together with changes in H3K4 methylation patterns in the different subpopulations of mammary gland epithelia. In the first instance therefore, it could prove informative to examine in the C57BL/6J-*Kdm5b ΔARID* mammary gland throughout mammary gland morphogenesis, the effect of KDM5B ΔARID expression on H3K4 methylation patterns by immunohistochemistry.

Multiple signalling pathways are integrated permitting cell proliferation, migration and differentiation, in order to establish the pattern of the mammary gland. KDM5B can elicit its function as part of a multi-protein complex that contain other chromatin-modifying factors (Barrett *et al*., 2007, Banck *et al*., 2009) to control transcription through the modulation of chromatin structure. The function of KDM5B has been implicated in the control of a number of different signalling pathways including those involved in cell cycle (Yamane *et al*., 2007, Dey *et al*., 2008, Xie *et al*., 2011, Wong *et al*., 2012), differentiation (Schmitz *et* al., 2011, Kidder *et al*., 2013) and migration (Li *et al*., 2011, Yoshida *et al*., 2011), which are important during mammary gland morphogenesis.

7.7 KDM5B, signalling pathways and the development of the mammary gland.

Most significantly, *KDM5B* was initially identified as a transcript down regulated in response to inhibition of the c-ErbB2 signalling pathway in a human mammary gland epithelial cell line (Lu *et al*., 1999). As seen for the C57BL/6J-*Kdm5b ΔARID* murine line, ablation of *Erbb2* expression also result in a delay in pubertal ductal morphogenesis and the female can support her offspring at parturition (Jackson-Fisher *et al*., 2004, Andrechek *et al*., 2005) Although changes in mammary gland morphology during pregnancy were not examined in the *Erbb2* null female these studies may further support a role for KDM5B downstream of the c-ErbB2 signalling pathway.

The NOTCH signalling pathway plays a central role during mammary gland morphogenesis by not only directing mammary gland stem cells toward a luminal cell fate during puberty (Bouras *et al*., 2008), but by also maintaining the luminal cell fate

during pregnancy and thereby regulating alveolar development (Buono *et al*., 2006). Although studies have not been conducted in order to examine a function for KDM5B as part of the NOTCH signalling pathway, KDM5A and the *D. Melanogaster* Lid can interact with the NOTCH pathway effector protein, RBP-J in mammals and repress NOTCH target genes (Moshkin *et al*., 2009, Liefke *et al*., 2010). This may suggest that the KDM5 family of proteins may function as NOTCH signalling pathway effector proteins. Loss of RBP-J expression in mammary gland stem cells lead to the expansion of basal cells (Bouras *et al*., 2008) as did the loss of RBP-J expression from luminal cells during pregnancy (Buono *et al*., 2006).

Reduced TEB number has been reported for a number of cytokine and chemokine deficient murine models. Studies have also implicated KDM5B in the regulation of immune mediators (Li *et al*., 2011) further highlighting a function for KDM5B during the invasion and ductal patterning of the murine mammary gland. Although the functional consequence of KDM5B promoter binding was not assessed, never-the-less gene ontology analysis has categorized KDM5B as a protein whose binding is enriched at promoter sites of genes encoding members of the chemokine pathway (Li *et al*., 2011). In addition, in order for myeloid progenitor cells to differentiate to macrophages, expression of the micro-RNA-17-92 cluster is repressed in a demethylase dependent manner by KDM5B (Pospisil *et al*., 2011). In deed macrophages are recruited to the TEB by CSF1 (colony stimulating factor 1) and mice homozygous null for *Csf1* present with a depleted macrophage population, and impaired TEB formation, ductal elongation and side branching (Gouon-Evans *et al*., 2000, Van Nguyen *et al*., 2002).

During mammary gland morphogenesis epithelial cells become incompletely polarized, multi-layered and remodel cell junctions to allow cell rearrangement (Ewald *et al.,* 2008). A genome wide transcriptional analysis of TEB structures revealed an increase in the epithelial to mesenchmal-related transcripts including *Snai1* and *Snai2* (Kouros-Mehr *et al*., 2006). Support for an EMT-like event during mammary gland ductal patterning was further suggested by the observation that green fluorescent protein driven from the vimentin promoter was detected at branch points using an *in vitro* system to control ductal patterning (Nelson *et al*., 2006). Interestingly, KDM5B has also been implicated in promoting the epithelial to mesenchyme transition in both cancer cell lines as well as the mouse mammary epithelial cell line NMuMG. The expression of KDM5B can repress the expression of the microRNA-200 (miRNA-200) family resulting in an increase in ZEB1 and ZEB2

levels followed by downregulation of E-cadherin and upregulation of mesenchymal marker genes, *Snai1* and *Snai2* (Enkhbaatar *et al*., 2013).

7.8 Demethylase independent function of the KDM5 family of proteins

The expression of a KDM5B lacking part of the JMJN domain and the entire ARID domain indicates that other demethylase independent aspects of KDM5B function are preserved. This highlights the importance of defining the demethylase independent functions of KDM5B, which to date have not been addressed. However, a demethylase independent function for other members of the KDM5 family have been described, a function that is potentially conserved.

The lower organisms *D. Melanogaster* and *C. Elegans* express only a single orthologue of the KDM5 family namely Lid and rbr-2 respectively. The viability of *D. Melanogaster* is not dependent on the demethylase activity of Lid (Li *et al*., 2010), and a mutant strain of *C.Elegans* expressing *rbr-2* lacking demethylase activity presents with only a defect in vulvamorphogenesis highlighting the functional importance of the other domains of the KDM5 family of proteins (Christensen *et al*., 2007). Studies have shown that the enzyme activity of histone modifying enzymes can be modulated through the association with other proteins (Lee *et al*., 2009, DiTacchio *et al*., 2011). Interestingly, KDM5A and Lid inhibit the deacetylase activity of HDAC1 and Rpd3 (a HDAC homologue) respectively to activate transcription at specific loci (Lee *et al*., 2009, DiTacchio *et al*., 2011). The co-expression of Lid and MYC potentiates transcription and a Lid/MYC interaction inhibits Lid demethylase activity (Secombe *et al*., 2007). Furthermore KDM5B and MYC interact *in vivo* (SC and JTP, unpublished observation) suggesting functional conservation. Although the mechanism for gene activation was not addressed by these authors (Secombe *et al*., 2007), deacetylase inhibition by Lid, in a demethylase independent manner is plausible. Taken together this data suggest that the KDM5 family may perform two independent functions. One function is to demethylate H3K4 resulting in gene repression, whereas the other is to antagonize HDAC activity to promote transcription.

A potential model for KDM5B function is summarised below. The studies reported in this thesis together with published data suggest that expression of a KDM5B ΔARID protein potentially negates DNA binding activity and GATA3 recruitment to the genome resulting in reduced *FoxA1* and *Stat5a* expression in the nulliparous

mammary gland. In the C57BL/6J-*Kdm5b* *Δ*ARID mammary gland, KDM5B demethylase activity and repression is also negated resulting in an increase in the stem cell gene signature. The overall effect of KDM5B ΔARID expression is a delay in pubertal mammary gland development. During pregnancy, expression of a KDM5B ΔARID protein could potentially negate KDM5B DNA binding activity and GATA3 recruitment to the *IL4, IL5*, *IL13* genes resulting in reduced expression. The consequence is reduced activation of STAT6 and a delay in pregnancy associated mammary gland development. Reduced *IL5* expression results in a lower level of STAT5 activation resulting in a reduction in AKT and beta casein expression at mid-pregnancy. Elevated expression levels of activated STAT5 at late pregnancy are potentially sufficient to induce AKT, beta casein and whey acidic protein expression and thus a lactating mammary gland.

The work reported in this thesis has contributed to our knowledge of the function of KDM5B in the development of the mammary gland. This work has opened the way forward to further investigations.

Chapter 8: References

Chapter 8 References

ABAD, M., MORENO, A., PALACIOS, A., NARITA, M., BLANCO, F., MORENO-BUENO, G. & PALMERO, I. (2011) The tumor suppressor ING1 contributes to epigenetic control of cellular senescence. *Aging Cell,* 10**,** 158-71.

ABELL, K., BILANCIO, A., CLARKSON, R. W., TIFFEN, P. G., ALTAPARMAKOV, A. I., BURDON, T. G., ASANO T., VANHAESEBROECK, B. & WATSON C. J. (2005) Stat3-induced apoptosis requires a molecular switch in PI(3)K subunit composition. *Nat Cell Biol,* 7, 392-8.

AGULNIK, A. I., MITCHELL, M. J., LERNER, J. L., WOODS, D. R. & BISHOP, C. E. (1994b) A mouse Y chromosome gene encoded by a region essential for spermatogenesis and expression of male-specific minor histocompatibility antigens. *Hum Mol Genet,* 3**,** 873-8.

AGULNIK, A. I., MITCHELL, M. J., MATTEI, M. G., BORSANI, G., AVNER, P. A., LERNER, J. L. & BISHOP, C. E. (1994a) A novel X gene with a widely transcribed Y-linked homologue escapes X-inactivation in mouse and human. *Hum Mol Genet,* 3**,** 879-84.

AKASAKA, T., KANNO, M., BALLING, R., MIEZA, M. A., TANIGUCHI, M. & KOSEKI, H. (1996) A role for mel-18, a Polycomb group-related vertebrate gene, during the anteroposterior specification of the axial skeleton. *Development,* 122**,** 1513-22.

AKIMOTO, C., KITAGAWA, H., MATSUMOTO, T. & KATO, S. (2008) Spermatogenesis-specific association of SMCY and MSH5. *Genes Cells,* 13**,** 623-33.

ALBERT, M., SCHMITZ, S. U., KOOISTRA, S. M., MALATESTA, M., MORALES TORRES, C., REKLING, J. C., JOHANSEN, J. V., ABARRATEGUI, I. & HELIN, K. (2013) The histone demethylase Jarid1b ensures faithful mouse development by protecting developmental genes from aberrant H3K4me3. *PLoS Genet,* 9**,** e1003461.

ANDERSON, S. M., RUDOLPH, M. C., MCMANAMAN, J. L. & NEVILLE, M. C. (2007) Key stages in mammary gland development. Secretory activation in the mammary gland: it's not just about milk protein synthesis! *Breast Cancer Res*, 9, 204.

ANDRECHEK, E. R., WHITE, D. & MULLER, W. J. (2005) Targeted disruption of ErbB2/Neu in the mammary epithelium results in impaired ductal outgrowth. *Oncogene,* 24**,** 932-7.

APTER, D., REINILA, M. & VIHKO, R. (1989) Some endocrine characteristics of early menarche, a risk factor for breast cancer, are preserved into adulthood. *Int J Cancer,* 44**,** 783-7.

ASSELIN-LABAT, M. L., SHACKLETON, M., STINGL, J., VAILLANT, F., FORREST, N. C., EAVES, C. J., VISVADER, J. E. & LINDEMAN, G. J. (2006) Steroid hormone receptor status of mouse mammary stem cells. *J Natl Cancer Inst,* 98**,** 1011-4.

ASSELIN-LABAT, M. L., SUTHERLAND, K. D., BARKER, H., THOMAS, R.,

SHACKLETON, M., FORREST, N. C., HARTLEY, L., ROBB, L., GROSVELD, F. G., VAN DER WEES, J., LINDEMAN, G. J. & VISVADER, J. E. (2007) Gata-3 is an essential regulator of mammary-gland morphogenesis and luminal-cell differentiation. *Nat Cell Biol,* 9**,** 201-9.

ASSELIN-LABAT, M. L., VAILLANT, F., SHERIDAN, J. M., PAL, B., WU, D., SIMPSON, E. R., YASUDA, H., SMYTH, G. K., MARTIN, T. J., LINDEMAN, G. J. & VISVADER, J. E. (2010) Control of mammary stem cell function by steroid hormone signalling. *Nature,* 465**,** 798-802.

BAI, L. & ROHRSCHNEIDER, L. R. (2010) s-SHIP promoter expression marks activated stem cells in developing mouse mammary tissue. *Genes Dev,* 24**,** 1882-92.

BALKO, J. M., MILLER, T. W., MORRISON, M. M., HUTCHINSON, K., YOUNG, C., RINEHART, C., SANCHEZ, V., JEE, D., POLYAK, K., PRAT, A., PEROU, C. M., ARTEAGA, C. L. & COOK, R. S. (2012) The receptor tyrosine kinase ErbB3 maintains the balance between luminal and basal breast epithelium. *Proc Natl Acad Sci U S A,* 109**,** 221-6.

BANCK, M. S., LI, S., NISHIO, H., WANG, C., BEUTLER, A. S. & WALSH, M. J. (2009) The ZNF217 oncogene is a candidate organizer of repressive histone modifiers. *Epigenetics,* 4**,** 100-6.

BARAK, O., LAZZARO, M. A., LANE, W. S., SPEICHER, D. W., PICKETTS, D. J. & SHIEKHATTAR, R. (2003) Isolation of human NURF: a regulator of Engrailed gene expression. *EMBO J,* 22**,** 6089-100.

BARRETT, A., MADSEN, B., COPIER, J., LU, P. J., COOPER, L., SCIBETTA, A. G., BURCHELL, J. & TAYLOR-PAPADIMITRIOU, J. (2002) PLU-1 nuclear protein, which is upregulated in breast cancer, shows restricted expression in normal human adult tissues: a new cancer/testis antigen? *Int J Cancer,* 101**,** 581-8.

BARRETT, A., SANTANGELO, S., TAN, K., CATCHPOLE, S., ROBERTS, K., SPENCER-DENE, B., HALL, D., SCIBETTA, A., BURCHELL, J., VERDIN, E., FREEMONT, P. & TAYLOR-PAPADIMITRIOU, J. (2007) Breast cancer associated transcriptional repressor PLU-1/JARID1B interacts directly with histone deacetylases. *Int J Cancer,* 121**,** 265-75.

BARSKI, A., CUDDAPAH, S., CUI, K., ROH, T. Y., SCHONES, D. E., WANG, Z., WEI, G., CHEPELEV, I. & ZHAO, K. (2007) High-resolution profiling of histone methylations in the human genome. *Cell,* 129**,** 823-37.

BAXTER, F. O., CAME, P. J., ABELL, K., KEDJOUAR, B., HUTH, M., RAJEWSKY, K., PASPARAKIS, M. & WATSON, C. J. (2006) IKKbeta/2 induces TWEAK and apoptosis in mammary epithelial cells. *Development,* 133, 3485-94.

BEDNORZ, N. L., BRILL, B., KLEIN, A., GÄBEL, K. & GRONER, B. (2011) Tracking the activation of Stat5 through the expression of an inducible reporter gene in a transgenic mouse line. *Endocrinology*, 152, 1935-47.

BELENKAYA, T. Y., HAN, C., STANDLEY, H. J., LIN, X., HOUSTON, D. W., HEASMAN, J. & LIN, X. (2002) Pygopus encodes a nuclear protein essential for wingless/Wnt signaling. *Development*, 129, 4089-101.

BELEUT, M., RAJARAM, R. D., CAIKOVSKI, M., AYYANAN, A., GERMANO, D., CHOI, Y., SCHNEIDER, P. & BRISKEN, C. (2010) Two distinct mechanisms underlie progesterone-induced proliferation in the mammary gland. *Proc Natl Acad Sci U S A,* 107**,** 2989-94.

BERNARDO, G. M., LOZADA, K. L., MIEDLER, J. D., HARBURG, G., HEWITT, S. C., MOSLEY, J. D., GODWIN, A. K., KORACH, K. S., VISVADER, J. E., KAESTNER, K. H., ABDUL-KARIM, F. W., MONTANO, M. M. & KERI, R. A. (2010) FOXA1 is an essential determinant of ERalpha expression and mammary ductal morphogenesis. *Development,* 137**,** 2045-54.

BERNSTEIN, B. E., MIKKELSEN, T. S., XIE, X., KAMAL, M., HUEBERT, D. J., CUFF, J., FRY, B., MEISSNER, A., WERNIG, M., PLATH, K., JAENISCH, R., WAGSCHAL, A., FEIL, R., SCHREIBER, S. L. & LANDER, E. S. (2006) A bivalent chromatin structure marks key developmental genes in embryonic stem cells. *Cell,* 125**,** 315-26.

BERNSTEIN, L. (2002) Epidemiology of endocrine-related risk factors for breast cancer. *J Mammary Gland Biol Neoplasia,* 7**,** 3-15.

BESHIRI, M. L., HOLMES, K. B., RICHTER, W. F., HESS, S., ISLAM, A. B., YAN, Q., PLANTE, L., LITOVCHICK, L., GEVRY, N., LOPEZ-BIGAS, N., KAELIN, W. G., JR. & BENEVOLENSKAYA, E. V. (2012) Coordinated repression of cell cycle genes by KDM5A and E2F4 during differentiation. *Proc Natl Acad Sci U S A,* 109**,** 18499-504.

BHATTACHARYA, S., STOUT, B. A., BATES, M. E., BERTICS, P. J. & MALTER, J. S. (2001) Granulocyte macrophage colony-stimulating factor and interleukin-5 activate STAT5 and induce CIS1 mRNA in human peripheral blood eosinophils. *Am J Respir Cell Mol Biol*, 24, 312-6.

BHAUMIK, S. R., SMITH, E. & SHILATIFARD, A. (2007) Covalent modifications of histones during development and disease pathogenesis. *Nat Struct Mol Biol,* 14**,** 1008-16.

BJORKMAN, M., OSTLING, P., HARMA, V., VIRTANEN, J., MPINDI, J. P., RANTALA, J., MIRTTI, T., VESTERINEN, T., LUNDIN, M., SANKILA, A., RANNIKKO, A., KAIVANTO, E., KOHONEN, P., KALLIONIEMI, O. & NEES, M. (2011) Systematic knockdown of epigenetic enzymes identifies a novel histone demethylase PHF8 overexpressed in prostate cancer with an impact on cell proliferation, migration and invasion. *Oncogene,* 31**,** 3444-56.

BOURAS, T., PAL, B., VAILLANT, F., HARBURG, G., ASSELIN-LABAT, M. L., OAKES, S. R., LINDEMAN, G. J. & VISVADER, J. E. (2008) Notch signaling regulates mammary stem cell function and luminal cell-fate commitment. *Cell Stem Cell,* 3, 429-41.

BOYER, L. A., PLATH, K., ZEITLINGER, J., BRAMBRINK, T., MEDEIROS, L. A., LEE, T. I., LEVINE, S. S., WERNIG, M., TAJONAR, A., RAY, M. K., BELL, G. W., OTTE, A. P., VIDAL, M., GIFFORD, D. K., YOUNG, R. A. & JAENISCH, R. (2006) Polycomb

complexes repress developmental regulators in murine embryonic stem cells. *Nature,* 441**,** 349-53.

BRADFORD, M. M. (1976) A rapid and sensitive method for the quantitation of microgram quantities of protein utilizing the principle of protein-dye binding. *Anal Biochem,* 72**,** 248-54.

BRISKEN, C., HEINEMAN, A., CHAVARRIA, T., ELENBAAS, B., TAN, J., DEY, S. K., MCMAHON, J. A., MCMAHON, A. P. & WEINBERG, R. A. (2000) Essential function of Wnt-4 in mammary gland development downstream of progesterone signaling. *Genes Dev,* 14**,** 650-4.

BRISKEN, C., PARK, S., VASS, T., LYDON, J. P., O'MALLEY, B. W. & WEINBERG, R. A. (1998) A paracrine role for the epithelial progesterone receptor in mammary gland development. *Proc Natl Acad Sci U S A,* 95**,** 5076-81.

BUONO, K. D., ROBINSON, G. W., MARTIN, C., SHI, S., STANLEY, P., TANIGAKI, K., HONJO, T. & HENNIGHAUSEN, L. (2006) The canonical Notch/RBP-J signaling pathway controls the balance of cell lineages in mammary epithelium during pregnancy. *Dev Biol*, 15, 565-80.

BURDON, T. G., MAITLAND, K. A., CLARK, A. J., WALLACE, R. & WATSON, C. J. (1994) Regulation of the sheep beta-lactoglobulin gene by lactogenic hormones is mediated by a transcription factor that binds an interferon-gamma activation site-related element. *Mol Endocrinol,* 8, 1528-36.

CAFFAREL, M. M., ZARAGOZA, R., PENSA, S., LI, J., GREEN, A. R. & WATSON, C. J. (2012) Constitutive activation of JAK2 in mammary epithelium elevates Stat5 signalling, promotes alveologenesis and resistance to cell death, and contributes to tumourigenesis. *Cell Death Differ*, 19, 511-22.

CAMPOS, E. I. & REINBERG, D. (2009) Histones: annotating chromatin. *Annu Rev Genet,* 43**,** 559-99.

CAO, R., WANG, L., WANG, H., XIA, L., ERDJUMENT-BROMAGE, H., TEMPST, P., JONES, R. S. & ZHANG, Y. (2002) Role of histone H3 lysine 27 methylation in Polycomb-group silencing. *Science*, 298, 1039-43.

CATCHPOLE, S., SPENCER-DENE, B., HALL, D., SANTANGELO, S., ROSEWELL, I., GUENATRI, M., BEATSON, R., SCIBETTA, A. G., BURCHELL, J. M. & TAYLOR-PAPADIMITRIOU, J. (2011) PLU-1/JARID1B/KDM5B is required for embryonic survival and contributes to cell proliferation in the mammary gland and in ER+ breast cancer cells. *Int J Oncol,* 38**,** 1267-77.

CATCHPOLE, S., TAVNER, F., LE CAM, L., SARDET, C. & WATSON, R. J. (2002) A B-myb promoter corepressor site facilitates in vivo occupation of the adjacent E2F site by p107 x E2F and p130 x E2F complexes. *J Biol Chem,* 277**,** 39015-24.

CELLOT, S., HOPE, K. J., CHAGRAOUI, J., SAUVAGEAU, M., DENEAULT, É., MACRAE, T., MAYOTTE, N., WILHELM, B. T., LANDRY, J. R., TING, S. B., KROSL, J.,

HUMPHRIES, K., THOMPSON, A. & SAUVAGEAU, G. (2013) RNAi screen identifies Jarid1b as a major regulator of mouse HSC activity. *Blood*, 122, 1545-55.

CHAKRABARTI, R., WEI, Y., ROMANO, RA., DECOSTE, C., KANG, Y. & SINHA, S. (2012) Elf5 regulates mammary gland stem/progenitor cell fate by influencing notch signaling. *Stem Cells,* 30, 1496-508.

CHAN, C. B, LIU, X., ENSSLIN, M. A., DILLEHAY, D. L., ORMANDY, C. J., SOHN, P., SERRA, R. & YE, K. (2010) PIKE-A is required for prolactin-mediated STAT5a activation in mammary gland development. *EMBO J*, 29, 956-68.

CHAN, S. R., VERMI, W., LUO, J., LUCINI, L., RICKERT, C., FOWLER, A. M., LONARDI, S., ARTHUR, C., YOUNG, L. J., LEVY, D. E., WELCH, M. J., CARDIFF, R. D. & SCHREIBER, R.D. (2012) STAT1-deficient mice spontaneously develop estrogen receptor α-positive luminal mammary carcinomas. *Breast Cancer Res*, 14, R16.

CHAN, S. W. & HONG, W. (2001) Retinoblastoma-binding protein 2 (Rbp2) potentiates nuclear hormone receptor-mediated transcription. *J Biol Chem,* 276**,** 28402-12.

CHAPMAN, R, S., LOURENCO, P. C., TONNER, E., FLINT, D. J., SELBERT, S., TAKEDA, K., AKIRA, S., CLARKE, A. R. & WATSON, C. J. (1999) Suppression of epithelial apoptosis and delayed mammary gland involution in mice with a conditional knockout of Stat3. *Genes Dev*, 13, 2604-16.

CHEN, C. C., STAIRS, D. B., BOXER, R. B., BELKA, G. K., HORSEMAN, N. D., ALVAREZ, J. V. & CHODOSH, L. A. (2012) Autocrine prolactin induced by the Pten-Akt pathway is required for lactation initiation and provides a direct link between the Akt and Stat5 pathways. *Genes Dev*, 26, 2154-68.

CHEN, C. D., WELSBIE, D. S., TRAN, C., BAEK, S. H., CHEN, R., VESSELLA, R., ROSENFELD, M. G. & SAWYERS, C. L. (2004) Molecular determinants of resistance to antiandrogen therapy. *Nat Med,* 10**,** 33-9.

CHEN, Z., ZANG, J., WHETSTINE, J., HONG, X., DAVRAZOU, F., KUTATELADZE, T. G., SIMPSON, M., MAO, Q., PAN, C. H., DAI, S., HAGMAN, J., HANSEN, K., SHI, Y. & ZHANG, G. (2006) Structural insights into histone demethylation by JMJD2 family members. *Cell,* 125**,** 691-702.

CHICAS, A., KAPOOR, A., WANG, X., AKSOY, O., EVERTTS, A. G., ZHANG, M. Q., GARCIA, B. A., BERNSTEIN, E. & LOWE, S. W. (2012) H3K4 demethylation by Jarid1a and Jarid1b contributes to retinoblastoma-mediated gene silencing during cellular senescence. *Proc Natl Acad Sci U S A,* 109**,** 8971-6.

CHODOSH, L. A., GARDNER, H. P., RAJAN, J. V., STAIRS, D. B., MARQUIS, S. T. & LEDER, P. A. (2000) Protein kinase expression during murine mammary development. *Dev Biol,* 219**,** 259-76.

CHOI, Y. S., CHAKRABARTI, R., ESCAMILLA-HERNANDEZ, R. & SINHA, S. (2009) Elf5 conditional knockout mice reveal its role as a master regulator in mammary alveolar development: failure of Stat5 activation and functional differentiation in the absence of Elf5. *Dev Biol*, 329, 227-41.

CHOMCZYNSKI, P. & SACCHI, N. (1987) Single-step method of RNA isolation by acid guanidinium thiocyanate-phenol-chloroform extraction. *Anal Biochem,* 162**,** 156-9.

CHRISTENSEN, J., AGGER, K., CLOOS, P. A., PASINI, D., ROSE, S., SENNELS, L., RAPPSILBER, J., HANSEN, K. H., SALCINI, A. E. & HELIN, K. (2007) RBP2 belongs to a family of demethylases, specific for tri-and dimethylated lysine 4 on histone 3. *Cell,* 128**,** 1063-76.

CIARLONI, L., MALLEPELL, S. & BRISKEN, C. (2007) Amphiregulin is an essential mediator of estrogen receptor alpha function in mammary gland development. *Proc Natl Acad Sci U S A,* 104**,** 5455-60.

CLARKSON, R. W., WAYLAND, M. T., LEE, J., FREEMAN, T. & WATSON, C. J. (2004) Gene expression profiling of mammary gland development reveals putative roles for death receptors and immune mediators in post-lactational regression. *Breast Cancer Res,* 6**,** R92-109.

COBLEIGH, M. A., VOGEL, C. L., TRIPATHY, D., ROBERT, N. J., SCHOLL, S., FEHRENBACHER, L., WOLTER, J. M., PATON, V., SHAK, S., LIEBERMAN, G. & SLAMON, D. J. (1999) Multinational study of the efficacy and safety of humanized anti-HER2 monoclonal antibody in women who have HER2-overexpressing metastatic breast cancer that has progressed after chemotherapy for metastatic disease. *J Clin Oncol,* 17**,** 2639-48.

COFFEY, K., ROGERSON, L., RYAN-MUNDEN, C., ALKHARAIF, D., STOCKLEY, J., HEER, R., SAHADEVAN, K., O'NEILL, D., JONES, D., DARBY, S., STALLER, P., MANTILLA, A., GAUGHAN, L. & ROBSON, C. N. (2013) The lysine demethylase, KDM4B, is a key molecule in androgen receptor signalling and turnover. *Nucleic Acids Res*, 41, 4433-46.

COLE H.A (1933) The mammary gland of the mouse, during the oestrous cycle, pregnancy and lactation. *Proc. R. Soc. B*. 114, 136-61

COLEMAN, J. A., CORREA, I., COOPER, L., BOHNENKAMP, H. R., POULSOM, R., BURCHELL, J. M. & TAYLOR-PAPADIMITRIOU, J. (2100) T cells reactive with HLA-A*0201 peptides from the histone demethylase JARID1B are found in the circulation of breast cancer patients. *Int J Cancer,* 128**,** 2114-24.

COTARLA, I., REN, S., ZHANG, Y., GEHAN, E., SINGH, B. & FURTH, P. A. (2004) Stat5a is tyrosine phosphorylated and nuclear localized in a high proportion of human breast cancers. *Int J Cancer,* 108, 665-71.

CREAMER, B. A., SAKAMOTO, K., SCHMIDT, J. W., TRIPLETT, A, A., MORIGGL, R. & WAGNER, K. U. (2010) Stat5 promotes survival of mammary epithelial cells through transcriptional activation of a distinct promoter in Akt1. *Mol Cell Biol*, 30, 2957-70.

CUI, Y., RIEDLINGER, G., MIYOSHI, K., TANG, W., LI, C., DENG, C. X., ROBINSON, G. W. & HENNIGHAUSEN, L. (2004) Inactivation of Stat5 in mouse mammary epithelium during pregnancy reveals distinct functions in cell proliferation, survival, and differentiation. *Mol Cell Biol*, 24, 8037-47.

CUZICK, J., SESTAK, I., BAUM, M., BUZDAR, A., HOWELL, A., DOWSETT, M. & FORBES, J. F. (2010) Effect of anastrozole and tamoxifen as adjuvant treatment for early-stage breast cancer: 10-year analysis of the ATAC trial. *Lancet Oncol,* 11**,** 1135-41.

DANIEL, C. W., SILBERSTEIN, G. B. & STRICKLAND, P. (1987) Direct action of 17 beta-estradiol on mouse mammary ducts analyzed by sustained release implants and steroid autoradiography. *Cancer Res,* 47**,** 6052-7.

DARNELL, J. E, JR., KERR, I. M. & STARK, G. R. (1994) Jak-STAT pathways and transcriptional activation in response to IFNs and other extracellular signaling proteins. *Science,* 264, 1415-21.

DEFEO-JONES, D., HUANG, P. S., JONES, R. E., HASKELL, K. M., VUOCOLO, G. A., HANOBIK, M. G., HUBER, H. E. & OLIFF, A. (1991) Cloning of cDNAs for cellular proteins that bind to the retinoblastoma gene product. *Nature,* 352**,** 251-4.

DEL MAR LORENTE, M., MARCOS-GUTIERREZ, C., PEREZ, C., SCHOORLEMMER, J., RAMIREZ, A., MAGIN, T. & VIDAL, M. (2000) Loss- and gain-of-function mutations show a polycomb group function for Ring1A in mice. *Development,* 127**,** 5093-100.

DENT, R., TRUDEAU, M., PRITCHARD, K. I., HANNA, W. M., KAHN, H. K., SAWKA, C. A., LICKLEY, L. A., RAWLINSON, E., SUN, P. & NAROD, S. A. (2007) Triple-negative breast cancer: clinical features and patterns of recurrence. *Clin Cancer Res,* 13**,** 4429-34.

DEY, B. K., STALKER, L., SCHNERCH, A., BHATIA, M., TAYLOR-PAPIDIMITRIOU, J. & WYNDER, C. (2008) The histone demethylase KDM5b/JARID1b plays a role in cell fate decisions by blocking terminal differentiation. *Mol Cell Biol,* 28**,** 5312-27.

DITACCHIO, L., LE, H. D., VOLLMERS, C., HATORI, M., WITCHER, M., SECOMBE, J. & PANDA, S. (2011) Histone lysine demethylase JARID1a activates CLOCK-BMAL1 and influences the circadian clock. *Science,* 333**,** 1881-5.

DONG, J., HUANG, S., CAIKOVSKI, M., JI, S., MCGRATH, A., CUSTORIO, M.G., CREIGHTON. C. J., MALIAKKAL, P., BOGOSLOVSKAIA, E., DU, Z., ZHANG, X., LEWIS, M. T., SABLITZKY, F., BRISKEN, C. & LI, Y. (2011) ID4 regulates mammary gland development by suppressing p38MAPK activity. *Development*, 138, 5247-56.

EBCTCG (Early Breast Cancer Trialists' Collaborative Group). (2005) Effects of chemotherapy and hormonal therapy for early breast cancer on recurrence and 15-year survival: an overview of the randomized trials. Lancet 365, 1687-1717

EISSENBERG, J. C., LEE, M. G., SCHNEIDER, J., ILVARSONN, A., SHIEKHATTAR, R. & SHILATIFARD, A. (2007) The trithorax-group gene in Drosophila little imaginal discs encodes a trimethylated histone H3 Lys4 demethylase. *Nat Struct Mol Biol,* 14**,** 344-6.

ENKHBAATAR, Z., TERASHIMA, M., OKTYABRI, D., TANGE, S., ISHIMURA, A., YANO, S. & SUZUKI, T. (2013) KDM5B histone demethylase controls epithelial-mesenchymal transition of cancer cells by regulating the expression of the microRNA-200 family. *Cell Cycle*, 12, 2100-12.

EWALD, A. J., BRENOT, A., DUONG, M., CHAN, B. S. & WERB, Z. (2008) Collective

epithelial migration and cell rearrangements drive mammary branching morphogenesis. *Dev Cell,* 14**,** 570-81.

FATA, J. E., CHAUDHARY, V. & KHOKHA, R. (2001) Cellular turnover in the mammary gland is correlated with systemic levels of progesterone and not 17beta-estradiol during the estrous cycle. *Biol Reprod,* 65**,** 680-8.

FENG, Y., MANKA, D., WAGNER, K. U. & KHAN, S. A. (2007) Estrogen receptor-alpha expression in the mammary epithelium is required for ductal and alveolar morphogenesis in mice. *Proc Natl Acad Sci U S A,* 104**,** 14718-23.

FENG, Z., MARTI, A., JEHN, B., ALTERMATT, H. J., CHICAIZA, G. & JAGGI, R. (1995) Glucocorticoid and progesterone inhibit involution and programmed cell death in the mouse mammary gland. *J Cell Biol,* 131**,** 1095-103.

FERNANDEZ-VALDIVIA, R., MUKHERJEE, A., YING, Y., LI, J., PAQUET, M., DEMAYO, F. J. & LYDON, J. P. (2009) The RANKL signaling axis is sufficient to elicit ductal side-branching and alveologenesis in the mammary gland of the virgin mouse. *Dev Biol*, 328, 127-39.

FIEDLER, M., SÁNCHEZ-BARRENA, M. J, NEKRASOV, M., MIESZCZANEK, J., RYBIN, V., MÜLLER, J., EVANS, P. & BIENZ, M. (2008) Decoding of methylated histone H3 tail by the Pygo-BCL9 Wnt signaling complex. *Mol Cell*, 30, 507-18.

FLOWERS, S., BECK, G. R., JR. & MORAN, E. (2010) Transcriptional activation by pRB and its coordination with SWI/SNF recruitment. *Cancer Res,* 70**,** 8282-7.

FLOWERS, S., XU, F. & MORAN, E. (2013) Cooperative activation of tissue-specific genes by pRB and E2F1. *Cancer Res,* 73**,** 2150-8.

FORSSMANN, U., HARTUNG, I., BALDER, R., FUCHS, B., ESCHER, S. E., SPODSBERG, N., DULKYS, Y., WALDEN, M., HEITLAND, A., BRAUN, A., FORSSMANN, W. G. & ELSNER, J. (2004) n-Nonanoyl-CC chemokine ligand 14, a potent CC chemokine ligand 14 analogue that prevents the recruitment of eosinophils in allergic airway inflammation. *J Immunol,* 173**,** 3456-66.

FORSTER, C., MAKELA, S., WARRI, A., KIETZ, S., BECKER, D., HULTENBY, K., WARNER, M. & GUSTAFSSON, J. A. (2002) Involvement of estrogen receptor beta in terminal differentiation of mammary gland epithelium. *Proc Natl Acad Sci U S A,* 99**,** 15578-83.

FRANKENBERG, S., SMITH, L., GREENFIELD, A. & ZERNICKA-GOETZ, M. (2007) Novel gene expression patterns along the proximo-distal axis of the mouse embryo before gastrulation. *BMC Dev Biol,* 7**,** 8.

GAUGHAN, L., STOCKLEY, J., COFFEY, K., O'NEILL, D., JONES, D. L., WADE, M., WRIGHT, J., MOORE, M., TSE, S., ROGERSON, L. & ROBSON, C. N. (2013) KDM4B is a Master Regulator of the Estrogen Receptor Signalling Cascade. *Nucleic Acids Res*.

GAWENIS, L. R., GREEB, J. M., PRASAD, V., GRISHAM, C., SANFORD, L. P., DOETSCHMAN, T., ANDRINGA, A., MILLER, M. L. & SHULL, G. E. (2005) Impaired

gastric acid secretion in mice with a targeted disruption of the NHE4 Na+/H+ exchanger. *J Biol Chem,* 280**,** 12781-9.

GILDEA, J. J., LOPEZ, R. & SHEARN, A. (2000) A screen for new trithorax group genes identified little imaginal discs, the Drosophila melanogaster homologue of human retinoblastoma binding protein 2. *Genetics,* 156**,** 645-63.

GORDON, K. E., BINAS, B., CHAPMAN, R. S., KURIAN, K. M., CLARKSON, R. W., CLARK, A. J., LANE, E. B. & WATSON, C. J. (2000) A novel cell culture model for studying differentiation and apoptosis in the mouse mammary gland. *Breast Cancer Res*, 2, 222-35.

GOUON-EVANS, V., ROTHENBERG, M. E. & POLLARD, J. W. (2000) Postnatal mammary gland development requires macrophages and eosinophils. *Development*. 127, 2269-82.

GROTE, D., SOUABNI, A., BUSSLINGER, M. & BOUCHARD, M. (2006) Pax 2/8-regulated Gata 3 expression is necessary for morphogenesis and guidance of the nephric duct in the developing kidney. *Development,* 133**,** 53-61.

GU, B., SUN, P., YUAN, Y., MORAES, R. C, LI, A., TENG, A., AGRAWAL, A., RHÉAUME, C., BILANCHONE, V., VELTMAAT, J. M., TAKEMARU, K., MILLAR, S., LEE, E. Y., LEWIS, M. T., LI, B. & DAI, X. (2009) Pygo2 expands mammary progenitor cells by facilitating histone H3 K4 methylation. *J Cell Biol*, 185, 811-26.

GU, B., WATANABE, K., SUN, P., FALLAHI, M. & DAI, X. (2013) Chromatin effector Pygo2 mediates Wnt-notch crosstalk to suppress luminal/alveolar potential of mammary stem and basal cells. *Cell Stem Cell*, 13, 48-61.

GUNTHER, E. J., BELKA, G. K., WERTHEIM, G. B., WANG, J., HARTMAN, J. L., BOXER, R. B. & CHODOSH, L. A. (2002) A novel doxycycline-inducible system for the transgenic analysis of mammary gland biology. *FASEB J,* 16**,** 283-92.

HANAHAN, D. & WEINBERG, R. A. (2011) Hallmarks of cancer: the next generation. *Cell*, 144, 646-74.

HAO, H., KIM, D. S., KLOCKE, B., JOHNSON, K. R., CUI, K., GOTOH, N., ZANG, C., GREGORSKI, J., GIESER, L., PENG, W., FANN, Y., SEIFERT, M., ZHAO, K. & SWAROOP, A. (2012) Transcriptional regulation of rod photoreceptor homeostasis revealed by in vivo NRL targetome analysis. *PLoS Genet,* 8**,** e1002649.

HAPP, B. & GRONER, B. (1993) The activated mammary gland specific nuclear factor (MGF) enhances in vitro transcription of the beta-casein gene promoter. J Steroid *Biochem Mol Biol*, 47, 21-30.

HARRIS, J., STANFORD, P. M., SUTHERLAND, K., OAKES, S. R., NAYLOR, M. J., ROBERTSON, F. G., BLAZEK, K. D., KAZLAUSKAS, M., HILTON, H. N., WITTLIN, S., ALEXANDER, W. S., LINDEMAN, G. J., VISVADER, J. E. & ORMANDY, C. J. (2006) Socs2 and elf5 mediate prolactin-induced mammary gland development. *Mol Endocrinol*, 20, 1177-87.

HASLAM, S. Z. & SHYAMALA, G. (1979) Progesterone receptors in normal mammary glands of mice: characterization and relationship to development. *Endocrinology,* 105**,** 786-95.

HAYAKAWA, T., OHTANI, Y., HAYAKAWA, N., SHINMYOZU, K., SAITO, M., ISHIKAWA, F. & NAKAYAMA, J. (2007) RBP2 is an MRG15 complex component and down-regulates intragenic histone H3 lysine 4 methylation. *Genes Cells,* 12**,** 811-26.

HAYAMI, S., YOSHIMATSU, M., VEERAKUMARASIVAM, A., UNOKI, M., IWAI, Y., TSUNODA, T., FIELD, H. I., KELLY, J. D., NEAL, D. E., YAMAUE, H., PONDER, B. A., NAKAMURA, Y. & HAMAMOTO, R (2010). Overexpression of the JmjC histone demethylase KDM5B in human carcinogenesis: involvement in the proliferation of cancer cells through the E2F/RB pathway. *Mol Cancer,* 9**,** 59.

HEBBAR, P. B. & ARCHER, T. K. (2008) Altered histone H1 stoichiometry and an absence of nucleosome positioning on transfected DNA. *J Biol Chem,* 283**,** 4595-601.

HEINTZMAN, N. D., HON, G. C., HAWKINS, R. D., KHERADPOUR, P., STARK, A., HARP, L. F., YE, Z., LEE, L. K., STUART, R. K., CHING, C. W., CHING, K. A., ANTOSIEWICZ-BOURGET, J. E., LIU, H., ZHANG, X., GREEN, R. D., LOBANENKOV, V. V., STEWART, R., THOMSON, J. A., CRAWFORD, G. E., KELLIS, M. & REN, B. (2009) Histone modifications at human enhancers reflect global cell-type-specific gene expression. *Nature,* 459**,** 108-12.

HORSEMAN, N. D., ZHAO, W., MONTECINO-RODRIGUEZ, E., TANAKA, M., NAKASHIMA, K., ENGLE, S. J., SMITH, F., MARKOFF, E. & DORSHKIND, K. (1997) Defective mammopoiesis, but normal hematopoiesis, in mice with a targeted disruption of the prolactin gene. *EMBO J*, 16, 6926-35.

HOWLIN, J., MCBRYAN, J., NAPOLETANO, S., LAMBE, T., MCARDLE, E., SHIODA, T. & MARTIN, F. (2006) CITED1 homozygous null mice display aberrant pubertal mammary ductal morphogenesis. *Oncogene,* 25**,** 1532-42.

HU, X., DUTTA, P., TSURUMI, A., LI, J., WANG, J., LAND, H. & LI, W. X. (2013) Unphosphorylated STAT5A stabilizes heterochromatin and suppresses tumor growth. *Proc Natl Acad Sci U S A*, 110, 10213-8.

HUGHES, K. & WATSON, C. J. (2012) The spectrum of STAT functions in mammary gland development. JAKSTAT, 1, 151-158.

HUGHES, K., WICKENDEN, J. A., ALLEN, J. E. & WATSON, C. J. (2012) Conditional deletion of Stat3 in mammary epithelium impairs the acute phase response and modulates immune cell numbers during post-lactational regression. *J Pathol*, 227, 106-17.

HUMPHREYS, R. C., BIERIE, B., ZHAO, L., RAZ, R., LEVY, D. & HENNIGHAUSEN, L. (2002) Deletion of Stat3 blocks mammary gland involution and extends functional competence of the secretory epithelium in the absence of lactogenic stimuli. *Endocrinology,* 143, 3641-50.

IAVNILOVITCH, E., CARDIFF, R. D., GRONER, B. & BARASH, I. (2004) Deregulation of Stat5 expression and activation causes mammary tumors in transgenic mice. *Int J Cancer*, 112, 607-19.

IHLE, J. N. & KERR, I. M. (1995) Jaks and Stats in signaling by the cytokine receptor superfamily. *Trends Genet*, 11, 69-74.

ISLAM, A. B., RICHTER, W. F., JACOBS, L. A., LOPEZ-BIGAS, N. & BENEVOLENSKAYA, E. V. (2011a) Co-regulation of histone-modifying enzymes in cancer. *PLoS One,* 6**,** e24023.

ISLAM, A. B., RICHTER, W. F., LOPEZ-BIGAS, N. & BENEVOLENSKAYA, E. V. (2011b) Selective targeting of histone methylation. *Cell Cycle,* 10**,** 413-24.

ISMAIL, P, M., LI, J., DEMAYO, F.J., O'MALLEY, B. W. & LYDON, J. P. (2002) A novel LacZ reporter mouse reveals complex regulation of the progesterone receptor promoter during mammary gland development. *Mol Endocrinol*, 16, 2475-89.

IWASE, S., LAN, F., BAYLISS, P., DE LA TORRE-UBIETA, L., HUARTE, M., QI, H. H., WHETSTINE, J. R., BONNI, A., ROBERTS, T. M. & SHI, Y. (2007) The X-linked mental retardation gene SMCX/JARID1C defines a family of histone H3 lysine 4 demethylases. *Cell,* 128**,** 1077-88.

JACKSON-FISHER, A. J., BELLINGER, G., BREINDEL, J. L., TAVASSOLI, F. A., BOOTH, C. J., DUONG, J. K. & STERN, D. F. (2008) ErbB3 is required for ductal morphogenesis in the mouse mammary gland. *Breast Cancer Res,* 10**,** R96.

JACKSON-FISHER, A. J., BELLINGER, G., RAMABHADRAN, R., MORRIS, J. K., LEE, K. F. & STERN, D. F. (2004) ErbB2 is required for ductal morphogenesis of the mammary gland. *Proc Natl Acad Sci U S A,* 101**,** 17138-43.

JACOBSON, N. G., SZABO, S. J., WEBER-NORDT, R. M., ZHONG, Z., SCHREIBER, R. D., DARNELL, J. E. JR. & MURPHY, K. M. (1995) Interleukin 12 signaling in T helper type 1 (Th1) cells involves tyrosine phosphorylation of signal transducer and activator of transcription (Stat)3 and Stat4. *J Exp Med*, 181, 1755-62.

JENSEN, L. R., AMENDE, M., GUROK, U., MOSER, B., GIMMEL, V., TZSCHACH, A., JANECKE, A. R., TARIVERDIAN, G., CHELLY, J., FRYNS, J. P., VAN ESCH, H., KLEEFSTRA, T., HAMEL, B., MORAINE, C., GECZ, J., TURNER, G., REINHARDT, R., KALSCHEUER, V. M., ROPERS, H. H. & LENZNER, S. (2005) Mutations in the JARID1C gene, which is involved in transcriptional regulation and chromatin remodeling, cause X-linked mental retardation. *Am J Hum Genet,* 76**,** 227-36.

JIN, R., BAY, B. H., CHOW, V. T. & TAN, P. H. (2001) Metallothionein 1F mRNA expression correlates with histological grade in breast carcinoma. *Breast Cancer Res Treat,* 66**,** 265-72.

JIN, S. G. & MANN, J. R. (2005) Synthetic neomycin-kanamycin phosphotransferase, type II coding sequence for gene targeting in mammalian cells. *Genesis,* 42**,** 207-9.

JONES, P. H., HARPER, S. & WATT, F. M. (1995) Stem cell patterning and fate in

human epidermis. *Cell,* 80**,** 83-93.

JOSHI, P. A., JACKSON, H. W., BERISTAIN, A. G., DI GRAPPA, M. A., MOTE, P. A., CLARKE, C. L., STINGL, J., WATERHOUSE, P. D. & KHOKHA, R. (2010) Progesterone induces adult mammary stem cell expansion. *Nature,* 465**,** 803-7.

JUAN, A. H., DERFOUL, A., FENG, X., RYALL, J. G., DELL'ORSO, S., PASUT, A., ZARE, H., SIMONE, J. M., RUDNICKI, M. A. & SARTORELLI, V. (2011) Polycomb EZH2 controls self-renewal and safeguards the transcriptional identity of skeletal muscle stem cells. *Genes Dev*, 25, 789-94.

KANG, K., YAMAJI, D., YOO, K. H., ROBINSON, G. W. & HENNIGHAUSEN, L. (2014) Mammary-specific gene activation is defined by progressive recruitment of STAT5 during pregnancy and the establishment of H3K4me3 marks. *Mol Cell Biol,* 34, 464-73.

KAPLAN, M. H., SCHINDLER, U., SMILEY, S. T. & GRUSBY, M. J. (1996) Stat6 is required for mediating responses to IL-4 and for development of Th2 cells. *Immunity*, 4, 313-9.

KAWAZU, M., SASO, K., TONG, K. I., MCQUIRE, T., GOTO, K., SON, D. O., WAKEHAM, A., MIYAGISHI, M., MAK, T. W. & OKADA, H. (2011) Histone demethylase JMJD2B functions as a co-factor of estrogen receptor in breast cancer proliferation and mammary gland development. *PLoS One,* 6**,** e17830.

KENNEY, N. J., SMITH, G. H., ROSENBERG, K., CUTLER, M. L. & DICKSON, R. B. (1996) Induction of ductal morphogenesis and lobular hyperplasia by amphiregulin in the mouse mammary gland. *Cell Growth Differ,* 7**,** 1769-81.

KESSLER, R., HAUSMANN, G. & BASLER, K. (2009) The PHD domain is required to link Drosophila Pygopus to Legless/beta-catenin and not to histone H3. *Mech Dev*, 126, 752-9.

KHALED, W. T, READ, E. K., NICHOLSON, S. E., BAXTER, F. O., BRENNAN, A. J., CAME, P. J., SPRIGG, N., MCKENZIE, A. N & WATSON, C. J. (2007) The IL-4/IL-13/Stat6 signalling pathway promotes luminal mammary epithelial cell development. *Development*. 134, 2739-50.

KIDDER, B. L., HU, G., YU, Z. X., LIU, C. & ZHAO, K. (2013) Extended self-renewal and accelerated reprogramming in the absence of Kdm5b. *Mol Cell Biol*, 33, 4793-810.

KIM, Y. W., OTTERSON, G. A., KRATZKE, R. A., COXON, A. B. & KAYE, F. J. (1994) Differential specificity for binding of retinoblastoma binding protein 2 to RB, p107, and TATA-binding protein. *Mol Cell Biol,* 14**,** 7256-64.

KLEIN, B. J., PIAO, L., XI, Y., RINCON-ARANO, H., ROTHBART, S. B., PENG, D., WEN, H., LARSON, C., ZHANG, X., ZHENG, X., CORTAZAR, M. A., PEÑA, P. V., MANGAN, A., BENTLEY, D. L., STRAHL, B. D., GROUDINE, M., LI, W., SHI, X. & KUTATELADZE, T, G. (2014) The histone-H3K4-specific demethylase KDM5B binds to its substrate and product through distinct PHD fingers. *Cell Rep*, 6, 325-35.

KLOSE, R. J., YAMANE, K., BAE, Y., ZHANG, D., ERDJUMENT-BROMAGE, H., TEMPST, P., WONG, J. & ZHANG, Y. (2006) The transcriptional repressor JHDM3A demethylates trimethyl histone H3 lysine 9 and lysine 36. *Nature,* 442**,** 312-6.

KLOSE, R. J., YAN, Q., TOTHOVA, Z., YAMANE, K., ERDJUMENT-BROMAGE, H., TEMPST, P., GILLILAND, D. G., ZHANG, Y. & KAELIN, W. G., JR. (2007) The retinoblastoma binding protein RBP2 is an H3K4 demethylase. *Cell,* 128**,** 889-900.

KLOVER, P. J., MULLER, W. J., ROBINSON, G. W., PFEIFFER, R. M., YAMAJI, D. & HENNIGHAUSEN, L. (2010) Loss of STAT1 from mouse mammary epithelium results in an increased Neu-induced tumor burden. *Neoplasia*, 12, 899-905.

Kong, S. L., Li, G., Loh, S. L., Sung, W. K. & Liu, E. T. (2011) Cellular reprogramming by the conjoint action of ERα, FOXA1, and GATA3 to a ligand-inducible growth state. *Mol Syst Biol,* 7:526.

KORNBERG, R. D. (1974) Chromatin structure: a repeating unit of histones and DNA. *Science,* 184**,** 868-71.

KOS, M., DENGER, S., REID, G., KORACH, K. S. & GANNON, F. (2002) Down but not out? A novel protein isoform of the estrogen receptor alpha is expressed in the estrogen receptor alpha knockout mouse. *J Mol Endocrinol,* 29**,** 281-6.

KOUROS-MEHR, H. & WERB, Z. (2006) Candidate regulators of mammary branching morphogenesis identified by genome-wide transcript analysis. *Dev Dyn*, 235, 3404-12.

KRAMPS, T., PETER, O., BRUNNER, E., NELLEN, D., FROESCH, B., CHATTERJEE, S., MURONE, M., ZÜLLIG, S. & BASLER, K. (2002) Wnt/wingless signaling requires BCL9/legless-mediated recruitment of pygopus to the nuclear beta-catenin-TCF complex. *Cell*, 109, 47-60.

KREGE, J. H., HODGIN, J. B., COUSE, J. F., ENMARK, E., WARNER, M., MAHLER, J. F., SAR, M., KORACH, K. S., GUSTAFSSON, J. A. & SMITHIES, O. (1998) Generation and reproductive phenotypes of mice lacking estrogen receptor beta. *Proc Natl Acad Sci U S A,* 95**,** 15677-82.

KREUZALER, P. A., STANISZEWSKA, A. D., LI, W., OMIDVAR, N., KEDJOUAR, B., TURKSON, J., POLI, V., FLAVELL, R. A., CLARKSON, R. W. & WATSON, C. J. (2011) Stat3 controls lysosomal-mediated cell death in vivo. *Nat Cell Biol,* 13**,** 303-9.

KRISHNAKUMAR, R. & KRAUS, W. L. (2010) PARP-1 regulates chromatin structure and transcription through a KDM5B-dependent pathway. *Mol Cell,* 39**,** 736-49.

KRITIKOU, E. A., SHARKEY, A., ABELL, K., CAME, P. J., ANDERSON, E., CLARKSON, R. W. & WATSON, C. J. (2003) A dual, non-redundant, role for LIF as a regulator of development and STAT3-mediated cell death in mammary gland. *Development*, 130, 3459-68.

KUMAR, M. J., PONVIJAY, K. S., NANDHINI, R., NAGARAJAN, R. S., JOSE, J., SRINIVAS, G., NAGARAJAN, P., VENKATESAN, R., KUMAR, K. & SINGH, S. (2007) A

mouse model for luminal epithelial like ER positive subtype of human breast cancer. *BMC Cancer*, 7, 180.

KUZBICKI, L., LANGE, D., STRACZYNSKA-NIEMIEC, A. & CHWIROT, B. W. (2013) JARID1B expression in human melanoma and benign melanocytic skin lesions. *Melanoma Res,* 23**,** 8-12.

LEE, C. G., DA SILVA, C.A., DELA CRUZ, C. S., AHANGARI, F., MA, B., KANG, M.J., HE, C.H., TAKYAR, S. & ELIAS, J.A. (2011) Role of chitin and chitinase/chitinase-like proteins in inflammation, tissue remodeling, and injury. *Annu Rev Physiol,* 73, 479-501.

LEE, H.J., GALLEGO-ORTEGA, D., LEDGER, A., SCHRAMEK, D., JOSHI, P., SZWARC, M. M., CHO, C., LYDON, J. P., KHOKHA, R., PENNINGER, J. M. & ORMANDY, C. J. (2013) Progesterone drives mammary secretory differentiation via RankL-mediated induction of Elf5 in luminal progenitor cells. *Development*, 140, 1397-401.

LEE, N., ZHANG, J., KLOSE, R. J., ERDJUMENT-BROMAGE, H., TEMPST, P., JONES, R. S. & ZHANG, Y. (2007) The trithorax-group protein Lid is a histone H3 trimethyl-Lys4 demethylase. *Nat Struct Mol Biol,* 14**,** 341-3.

LEMAY, D.G., NEVILLE, M. C., RUDOLPH, M. C., POLLARD, K. S. & GERMAN, J. B. (2007) Gene regulatory networks in lactation: identification of global principles using bioinformatics. *BMC Syst Biol,* 1**,** 56.

LI, A., SIMMONS, P. J. & KAUR, P. (1998) Identification and isolation of candidate human keratinocyte stem cells based on cell surface phenotype. *Proc Natl Acad Sci U S A,* 95**,** 3902-7.

LI, L., GREER, C., EISENMAN, R. N. & SECOMBE, J. (2010). Essential functions of the histone demethylase lid. *PLoS Genet,* 6**,** e1001221.

LI, M., LIU, X., ROBINSON, G., BAR-PELED, U., WAGNER, K. U., YOUNG, W. S., HENNIGHAUSEN, L. & FURTH, P. A. (1997) Mammary-derived signals activate programmed cell death during the first stage of mammary gland involution. *Proc Natl Acad Sci U S A,* 94**,** 3425-30.

LI, S. & ROSEN, J. M. (1995) Nuclear factor I and mammary gland factor (STAT5) play a critical role in regulating rat whey acidic protein gene expression in transgenic mice. *Mol Cell Biol*, 15, 2063-70.

LI, Q., SHI, L., GUI, B., YU, W., WANG, J., ZHANG, D., HAN, X., YAO, Z. & SHANG, Y. (2011) Binding of the JmjC demethylase JARID1B to LSD1/NuRD suppresses angiogenesis and metastasis in breast cancer cells by repressing chemokine CCL14. *Cancer Res,* 71**,** 6899-908.

LI, W., FERGUSON, B. J., KHALED, W. T., TEVENDALE, M., STINGL, J., POLI, V., RICH, T., SALOMONI, P. & WATSON, C. J. (2009) PML depletion disrupts normal mammary gland development and skews the composition of the mammary luminal cell progenitor pool. *Proc Natl Acad Sci U S A,* 106**,** 4725-30.

LI, X., LIU L., YANG, S., SONG, N., ZHOU, X., GAO, J., YU, N., SHAN, L., WANG, Q., LIANG, J., XUAN, C., WANG, Y., SHANG, Y. & SHI, L. (2014) Histone demethylase KDM5B is a key regulator of genome stability. *Proc Natl Acad Sci U S A*, Apr 28. [Epub ahead of print]

LIEFKE, R., OSWALD, F., ALVARADO, C., FERRES-MARCO, D., MITTLER, G., RODRIGUEZ, P., DOMINGUEZ, M. & BORGGREFE, T. (2010) Histone demethylase KDM5A is an integral part of the core Notch-RBP-J repressor complex. *Genes Dev,* 24**,** 590-601.

LIM, E., WU, D., PAL, B., BOURAS, T., ASSELIN-LABAT, M. L., VAILLANT, F., YAGITA, H., LINDEMAN, G. J., SMYTH, G. K. & VISVADER, J. E. (2010) Transcriptome analyses of mouse and human mammary cell subpopulations reveal multiple conserved genes and pathways. *Breast Cancer Res,* 12**,** R21.

LIN, W., CAO, J., LIU, J., BESHIRI, M. L., FUJIWARA, Y., FRANCIS, J., CHERNIACK, A. D., GEISEN, C., BLAIR, L. P., ZOU, M. R., SHEN, X., KAWAMORI, D., LIU, Z., GRISANZIO, C., WATANABE, H., MINAMISHIMA, Y. A., ZHANG, Q., KULKARNI, R. N., SIGNORETTI, S., RODIG, S. J., BRONSON, R. T., ORKIN, S. H., TUCK, D. P., BENEVOLENSKAYA, E. V., MEYERSON, M., KAELIN, W. G., JR. & YAN, Q. (2011) Loss of the retinoblastoma binding protein 2 (RBP2) histone demethylase suppresses tumorigenesis in mice lacking Rb1 or Men1. *Proc Natl Acad Sci U S A,* 108**,** 13379-86.

LIU, X., ROBINSON, G.W., GOUILLEUX, F., GRONER, B. & HENNIGHAUSEN, L. (1995) Cloning and expression of Stat5 and an additional homologue (Stat5b) involved in prolactin signal transduction in mouse mammary tissue. *Proc Natl Acad Sci U S A.* 92, 8831-5.

LIU, X., ROBINSON, G. W. & HENNIGHAUSEN, L. (1996) Activation of Stat5a and Stat5b by tyrosine phosphorylation is tightly linked to mammary gland differentiation. *Mol Endocrinol,* 10, 1496-506.

LIU, X., ROBINSON, G. W., WAGNER, K. U., GARRETT, L., WYNSHAW-BORIS, A. & HENNIGHAUSEN, L. (1997) Stat5a is mandatory for adult mammary gland development and lactogenesis. *Genes Dev*, 11, 179-86.

LOPEZ-BIGAS, N., KISIEL, T. A., DEWAAL, D. C., HOLMES, K. B., VOLKERT, T. L., GUPTA, S., LOVE, J., MURRAY, H. L., YOUNG, R. A. & BENEVOLENSKAYA, E. V. (2008) Genome-wide analysis of the H3K4 histone demethylase RBP2 reveals a transcriptional program controlling differentiation. *Mol Cell,* 31**,** 520-30.

LU, P., EWALD, A. J., MARTIN, G. R. & WERB, Z. (2008) Genetic mosaic analysis reveals FGF receptor 2 function in terminal end buds during mammary gland branching morphogenesis. *Dev Biol,* 321**,** 77-87.

LU, P. J., SUNDQUIST, K., BAECKSTROM, D., POULSOM, R., HANBY, A., MEIER-EWERT, S., JONES, T., MITCHELL, M., PITHA-ROWE, P., FREEMONT, P. & TAYLOR-PAPADIMITRIOU, J. (1999) A novel gene (PLU-1) containing highly conserved putative DNA/chromatin binding motifs is specifically up-regulated in breast cancer. *J Biol Chem,* 274**,** 15633-45.

LUETTEKE, N. C., QIU, T. H., FENTON, S. E., TROYER, K. L., RIEDEL, R. F., CHANG, A. & LEE, D. C. (1999) Targeted inactivation of the EGF and amphiregulin genes reveals distinct roles for EGF receptor ligands in mouse mammary gland development. *Development,* 126**,** 2739-50.

LUGER, K., MADER, A. W., RICHMOND, R. K., SARGENT, D. F. & RICHMOND, T. J. (1997) Crystal structure of the nucleosome core particle at 2.8 A resolution. *Nature,* 389**,** 251-60.

LUND, L. R., ROMER, J., THOMASSET, N., SOLBERG, H., PYKE, C., BISSELL, M. J., DANO, K. & WERB, Z. (1996) Two distinct phases of apoptosis in mammary gland involution: proteinase-independent and -dependent pathways. *Development,* 122**,** 181-93.

LYDON, J. P., DEMAYO, F. J., FUNK, C. R., MANI, S. K., HUGHES, A. R., MONTGOMERY, C. A JR., SHYAMALA, G., CONNEELY, O. M. & O'MALLEY, B. W. (1995) Mice lacking progesterone receptor exhibit pleiotropic reproductive abnormalities. *Genes Dev*, 9, 2266-78.

MA, K., SHARKEY, A., KIRSCH, S., VOGT, P., KEIL, R., HARGREAVE, T. B., MCBEATH, S. & CHANDLEY, A. C. (1992) Towards the molecular localisation of the AZF locus: mapping of microdeletions in azoospermic men within 14 subintervals of interval 6 of the human Y chromosome. *Hum Mol Genet,* 1**,** 29-33.

MACIAS, H. & HINCK, L. (2012) Mammary gland development. *Wiley Interdiscip Rev Dev Biol*, 1, 533-57.

MADSEN, B., SPENCER-DENE, B., POULSOM, R., HALL, D., LU, P. J., SCOTT, K., SHAW, A. T., BURCHELL, J. M., FREEMONT, P. & TAYLOR-PAPADIMITRIOU, J. (2002) Characterisation and developmental expression of mouse Plu-1, a homologue of a human nuclear protein (PLU-1) which is specifically up-regulated in breast cancer. *Gene Expr Patterns,* 2**,** 275-82.

MADSEN, B., TARSOUNAS, M., BURCHELL, J. M., HALL, D., POULSOM, R. & TAYLOR-PAPADIMITRIOU, J. (2003) PLU-1, a transcriptional repressor and putative testis-cancer antigen, has a specific expression and localisation pattern during meiosis. *Chromosoma,* 112**,** 124-32.

MALLEPELL, S., KRUST, A., CHAMBON, P. & BRISKEN, C. (2006) Paracrine signaling through the epithelial estrogen receptor alpha is required for proliferation and morphogenesis in the mammary gland. *Proc Natl Acad Sci U S A,* 103**,** 2196-201.

MARTI, A., FENG, Z., ALTERMATT, H. J. & JAGGI, R. (1997) Milk accumulation triggers apoptosis of mammary epithelial cells. *Eur J Cell Biol,* 73**,** 158-65.

MARTI, A., RITTER, P.M., JÄGER, R., LAZAR, H., BALTZER, A., SCHENKEL, J., DECLERCQ, W., VANDENABEELE, P. & JAGGI, R. (2001) Mouse mammary gland involution is associated with cytochrome c release and caspase activation. *Mech Dev,* 104, 89-98.

MCBRYAN, J., HOWLIN, J., KENNY, P. A., SHIODA, T. & MARTIN, F. (2007) ERalpha-CITED1 co-regulated genes expressed during pubertal mammary gland development: implications for breast cancer prognosis. *Oncogene,* 26**,** 6406-19.

MCGRAW, S., VIGNEAULT, C. & SIRARD, M. A. (2007) Temporal expression of factors involved in chromatin remodeling and in gene regulation during early bovine in vitro embryo development. *Reproduction,* 133**,** 597-608.

MENCHON, C., EDEL, M. J. & IZPISUA BELMONTE, J. C. (2011) The cell cycle inhibitor p27Kip(1) controls self-renewal and pluripotency of human embryonic stem cells by regulating the cell cycle, Brachyury and Twist. *Cell Cycle,* 10**,** 1435-47.

METIVIER, R., PENOT, G., HUBNER, M. R., REID, G., BRAND, H., KOS, M. & GANNON, F. (2003) Estrogen receptor-alpha directs ordered, cyclical, and combinatorial recruitment of cofactors on a natural target promoter. *Cell,* 115**,** 751-63.

MEYERS, E. N., LEWANDOSKI, M. & MARTIN, G. R. (1998) An Fgf8 mutant allelic series generated by Cre- and Flp-mediated recombination. *Nat Genet,* 18**,** 136-41.

MICHALAK, E.M., NACERDDINE, K., PIETERSEN, A., BEUGER, V., PAWLITZKY, I., CORNELISSEN-STEIJGER, P., WIENTJENS, E., TANGER, E., SEIBLER, J., VAN LOHUIZEN, M. & JONKERS, J. (2013) Polycomb group gene Ezh2 regulates mammary gland morphogenesis and maintains the luminal progenitor pool. *Stem Cells*, 31, 1910-20.

MIKKELSEN, T. S., KU, M., JAFFE, D. B., ISSAC, B., LIEBERMAN, E., GIANNOUKOS, G., ALVAREZ, P., BROCKMAN, W., KIM, T. K., KOCHE, R. P., LEE, W., MENDENHALL, E., O'DONOVAN, A., PRESSER, A., RUSS, C., XIE, X., MEISSNER, A., WERNIG, M., JAENISCH, R., NUSBAUM, C., LANDER, E. S. & BERNSTEIN, B. E. (2007) Genome-wide maps of chromatin state in pluripotent and lineage-committed cells. *Nature,* 448**,** 553-60.

MILANI, E.S., BRINKHAUS, H., DUEGGELI, R., KLEBBA, I., MUELLER, U., STADLER, M., KOHLER, H., SMALLEY M. J. & BENTIRES-ALJ, M. (2013) Protein tyrosine phosphatase 1B restrains mammary alveologenesis and secretory differentiation. *Development,* 140, 117-25.

MILLS, C. D. (2012) M1 and M2 Macrophages: Oracles of Health and Disease. *Crit Rev Immunol*, 32, 463-88.

MITRA, D., DAS, P. M., HUYNH, F. C. & JONES, F. E. (2011) Jumonji/ARID1 B (JARID1B) protein promotes breast tumor cell cycle progression through epigenetic repression of microRNA let-7e. *J Biol Chem,* 286**,** 40531-5.

MOSHKIN, Y. M., KAN, T. W., GOODFELLOW, H., BEZSTAROSTI, K., MAEDA, R. K., PILYUGIN, M., KARCH, F., BRAY, S. J., DEMMERS, J. A. & VERRIJZER, C. P. (2009) Histone chaperones ASF1 and NAP1 differentially modulate removal of active histone marks by LID-RPD3 complexes during NOTCH silencing. *Mol Cell,* 35**,** 782-93.

MULAC-JERICEVIC, B., LYDON, J. P., DEMAYO, F. J. & CONNEELY, O. M. (2003) Defective mammary gland morphogenesis in mice lacking the progesterone receptor B isoform. *Proc Natl Acad Sci U S A*. 100, 9744-9.

NAGY, A., MOENS, C., IVANYI, E., PAWLING, J., GERTSENSTEIN, M., HADJANTONAKIS, A. K., PIRITY, M. & ROSSANT, J. (1998) Dissecting the role of N-myc in development using a single targeting vector to generate a series of alleles. *Curr Biol,* 8**,** 661-4.

NANDI, S. (1958) Endocrine control of mammary gland development and function in the C3H/ He Crgl mouse. *J Natl Cancer Inst,* 21**,** 1039-63.

NAYLOR, M. J. & ORMANDY, C. J. (2002) Mouse strain-specific patterns of mammary epithelial ductal side branching are elicited by stromal factors. *Dev Dyn,* 225**,** 100-5.

NELSON, C. M., VANDUIJN, M. M., INMAN, J. L., FLETCHER, D. A. & BISSELL, M. J. (2006) Tissue geometry determines sites of mammary branching morphogenesis in organotypic cultures. *Science*, 314, 298-300.

NEVALAINEN, M. T., XIE, J., TORHORST, J., BUBENDORF, L., HAAS, P., KONONEN, J., SAUTER, G. & RUI, H. (2004) Signal transducer and activator of transcription-5 activation and breast cancer prognosis. *J Clin Oncol*, 22, 2053-60.

NEVILLE, M. C., MCFADDEN, T. B. & FORSYTH, I. (2002) Hormonal regulation of mammary differentiation and milk secretion. *J Mammary Gland Biol Neoplasia*, 7, 49-66.

NIJWENING, J. H., GEUTJES, E. J., BERNARDS, R. & BEIJERSBERGEN, R. L. (2011) The histone demethylase Jarid1b (Kdm5b) is a novel component of the Rb pathway and associates with E2f-target genes in MEFs during senescence. *PLoS One,* 6**,** e25235.

OAKES, S. R., NAYLOR, M. J., ASSELIN-LABAT, M. L., BLAZEK, K.D., GARDINER-GARDEN, M., HILTON, H.N., KAZLAUSKAS, M., PRITCHARD, M. A., CHODOSH, L. A., PFEFFER, P. L., LINDEMAN, G. J., VISVADER, J. E. & ORMANDY, C. J. (2008) The Ets transcription factor Elf5 specifies mammary alveolar cell fate. *Genes Dev*, 22, 581-6.

O'BRIEN, J., LYONS, T., MONKS, J., LUCIA, M.S., WILSON, R.S., HINES, L., MAN, Y.G., BORGES, V. & SCHEDIN, P. (2010) Alternatively activated macrophages and collagen remodeling characterize the postpartum involuting mammary gland across species. *Am J Pathol,* 176, 1241-55.

O'CARROLL, D., ERHARDT, S., PAGANI, M., BARTON, S. C., SURANI, M. A. & JENUWEIN, T. (2001) The polycomb-group gene Ezh2 is required for early mouse development. *Mol Cell Biol*, 21, 4330-6.

OLIVER, C. H. & WATSON, C. J. (2013) Making milk: A new link between STAT5 and Akt1. *JAKSTAT*, 2, e23228

OLSON, E. N., ARNOLD, H. H., RIGBY, P. W. & WOLD, B. J. (1996) Know your neighbors: three phenotypes in null mutants of the myogenic bHLH gene MRF4. *Cell,* 85**,** 1-4.

ORMANDY, C. J., CAMUS, A., BARRA, J., DAMOTTE, D., LUCAS, B., BUTEAU, H., EDERY, M., BROUSSE, N., BABINET, C., BINART, N. & KELLY, P. A. (1997) Null mutation of the prolactin receptor gene produces multiple reproductive defects in the mouse. *Genes Dev*, 11, 167-78.

OUTCHKOUROV, N. S., MUINO, J. M., KAUFMANN, K., VAN IJCKEN, W. F., GROOT KOERKAMP, M. J., VAN LEENEN, D., DE GRAAF, P., HOLSTEGE, F. C., GROSVELD, F. G. & TIMMERS, H. T. (2013) Balancing of histone H3K4 methylation states by the Kdm5c/SMCX histone demethylase modulates promoter and enhancer function. *Cell Rep,* 3**,** 1071-9.

PAL, B., BOURAS, T., SHI, W., VAILLANT, F., SHERIDAN, J. M., FU, N., BRESLIN, K., JIANG, K., RITCHIE, M. E., YOUNG, M., LINDEMAN, G. J., SMYTH, G. K. & VISVADER, J. E. (2013). Global changes in the mammary epigenome are induced by hormonal cues and coordinated by Ezh2. *Cell Rep*. 3, 411-26.

PASINI, D., HANSEN, K. H., CHRISTENSEN, J., AGGER, K., CLOOS, P. A. & HELIN, K. (2008) Coordinated regulation of transcriptional repression by the RBP2 H3K4 demethylase and Polycomb-Repressive Complex 2. *Genes Dev,* 22**,** 1345-55.

PECK, A. R., WITKIEWICZ, A. K., LIU, C., STRINGER, G. A., KLIMOWICZ, A. C., PEQUIGNOT, E., FREYDIN, B., TRAN, T. H., YANG, N., ROSENBERG, A. L., HOOKE, J. A., KOVATICH, A. J., NEVALAINEN, M. T., SHRIVER, C. D., HYSLOP, T., SAUTER, G., RIMM, D. L., MAGLIOCCO, A. M. & RUI, H. (2011) Loss of nuclear localized and tyrosine phosphorylated Stat5 in breast cancer predicts poor clinical outcome and increased risk of antiestrogen therapy failure. *J Clin Oncol*, 29, 2448-58.

PEROU, C. M., SORLIE, T., EISEN, M. B., VAN DE RIJN, M., JEFFREY, S. S., REES, C. A., POLLACK, J. R., ROSS, D. T., JOHNSEN, H., AKSLEN, L. A., FLUGE, O., PERGAMENSCHIKOV, A., WILLIAMS, C., ZHU, S. X., LONNING, P. E., BORRESEN-DALE, A. L., BROWN, P. O. & BOTSTEIN, D. (2000) Molecular portraits of human breast tumours. *Nature,* 406**,** 747-52.

PHILP, J. A., BURDON, T. G. & WATSON, C. J. (1996) Differential activation of STATs 3 and 5 during mammary gland development. *FEBS Lett*. 396, 77-80.

POKHOLOK, D. K., HARBISON, C. T., LEVINE, S., COLE, M., HANNETT, N. M., LEE, T. I., BELL, G. W., WALKER, K., ROLFE, P. A., HERBOLSHEIMER, E., ZEITLINGER, J., LEWITTER, F., GIFFORD, D. K. & YOUNG, R. A. (2005) Genome-wide map of nucleosome acetylation and methylation in yeast. *Cell,* 122**,** 517-27.

POND, A. C., BIN, X., BATTS, T., ROARTY, K., HILSENBECK, S. & ROSEN, J. M. (2009) Fibroblast growth factor receptor signaling is essential for normal mammary gland development and stem cell function. *Stem Cells,* 31**,** 178-89.

POSPISIL, V., VARGOVA, K., KOKAVEC, J., RYBAROVA, J., SAVVULIDI, F., JONASOVA, A., NECAS, E., ZAVADIL, J., LASLO, P. & STOPKA T. (2011) Epigenetic silencing of the oncogenic miR-17-92 cluster during PU.1-directed macrophage differentiation. *EMBO J*, 30, 4450-64.

RADBERGER, P., RADBERGER, A., BYKOV, V. J., SEREGARD, S. & ECONOMOU, M.

A. (2012) JARID1B protein expression and prognostic implications in uveal melanoma. *Invest Ophthalmol Vis Sci,* 53**,** 4442-9.

RAYMAN, J. B., TAKAHASHI, Y., INDJEIAN, V. B., DANNENBERG, J. H., CATCHPOLE, S., WATSON, R. J., TE RIELE, H. & DYNLACHT, B. D. (2002) E2F mediates cell cycle-dependent transcriptional repression in vivo by recruitment of an HDAC1/mSin3B corepressor complex. *Genes Dev,* 16**,** 933-47.

REIJO, R., LEE, T. Y., SALO, P., ALAGAPPAN, R., BROWN, L. G., ROSENBERG, M., ROZEN, S., JAFFE, T., STRAUS, D., HOVATTA, O. & ET AL. (1995) Diverse spermatogenic defects in humans caused by Y chromosome deletions encompassing a novel RNA-binding protein gene. *Nat Genet,* 10**,** 383-93.

REIS-FILHO, J. S. & TUTT, A. N. (2008) Triple negative tumours: a critical review. *Histopathology,* 52**,** 108-18.

REN, S., CAI, H. R., LI, M. & FURTH, P. A. (2002) Loss of Stat5a delays mammary cancer progression in a mouse model. *Oncogene*, 21, 4335-9.

RESNITZKY, D., HENGST, L. & REED, S. I. (1995) Cyclin A-associated kinase activity is rate limiting for entrance into S phase and is negatively regulated in G1 by p27Kip1. *Mol Cell Biol,* 15**,** 4347-52.

RIETZE, R. L., VALCANIS, H., BROOKER, G. F., THOMAS, T., VOSS, A. K. & BARTLETT, P. F. (2001) Purification of a pluripotent neural stem cell from the adult mouse brain. *Nature,* 412**,** 736-9.

RIJNKELS, M., FREEMAN-ZADROWSKI, C., HERNANDEZ, J., POTLURI, V., WANG, L., LI, W., & LEMAY, D. G. (2013) Epigenetic modifications unlock the milk protein gene loci during mouse mammary gland development and differentiation. *PLoS One*, 8

ROESCH, A., BECKER, B., MEYER, S., WILD, P., HAFNER, C., LANDTHALER, M. & VOGT, T. (2005) Retinoblastoma-binding protein 2-homolog 1: a retinoblastoma-binding protein downregulated in malignant melanomas. *Mod Pathol,* 18**,** 1249-57.

ROESCH, A., BECKER, B., SCHNEIDER-BRACHERT, W., HAGEN, I., LANDTHALER, M. & VOGT, T. (2006) Re-expression of the retinoblastoma-binding protein 2-homolog 1 reveals tumor-suppressive functions in highly metastatic melanoma cells. *J Invest Dermatol,* 126**,** 1850-9.

ROESCH, A., FUKUNAGA-KALABIS, M., SCHMIDT, E. C., ZABIEROWSKI, S. E., BRAFFORD, P. A., VULTUR, A., BASU, D., GIMOTTY, P., VOGT, T. & HERLYN, M. A (2010) Temporarily distinct subpopulation of slow-cycling melanoma cells is required for continuous tumor growth. *Cell,* 141**,** 583-94.

ROESCH, A., MUELLER, A. M., STEMPFL, T., MOEHLE, C., LANDTHALER, M. & VOGT, T. (2008) RBP2-H1/JARID1B is a transcriptional regulator with a tumor suppressive potential in melanoma cells. *Int J Cancer,* 122**,** 1047-57.

RUTHENBURG, A. J., ALLIS, C. D. & WYSOCKA, J. (2007) Methylation of lysine 4 on histone H3: intricacy of writing and reading a single epigenetic mark. *Mol Cell,* 25**,** 15-30.

SANTOS-REBOUCAS, C. B., FINTELMAN-RODRIGUES, N., JENSEN, L. R., KUSS, A. W., RIBEIRO, M. G., CAMPOS, M., JR., SANTOS, J. M. & PIMENTEL, M. M. (2011) A novel nonsense mutation in KDM5C/JARID1C gene causing intellectual disability, short stature and speech delay. *Neurosci Lett,* 498**,** 67-71.

SANTOS, S. J., HASLAM, S. Z. & CONRAD, S. E. (2008) Estrogen and progesterone are critical regulators of Stat5a expression in the mouse mammary gland. *Endocrinology*. 149, 329-38.

SANTOS, S. J., HASLAM, S. Z. & CONRAD, S. E. (2010) Signal transducer and activator of transcription 5a mediates mammary ductal branching and proliferation in the nulliparous mouse. *Endocrinology*, 151, 2876-85.

SASAKI, T., ONODERA, A., HOSOKAWA, H., WATANABE, Y., HORIUCHI, S., YAMASHITA, J., TANAKA, H., OGAWA, Y., SUZUKI, Y. & NAKAYAMA, T. (2013) Genome-Wide Gene Expression Profiling Revealed a Critical Role for GATA3 in the Maintenance of the Th2 Cell Identity. *PLoS One*, 8, e66468.

SAYEGH, J., CAO, J., ZOU, M. R., MORALES, A., BLAIR, L. P., NORCIA, M., HOYER, D., TACKETT, A. J., MERKEL, J. S. & YAN, Q. (2013) Identification of small molecule inhibitors of Jumonji AT-rich interactive domain 1B (JARID1B) histone demethylase by a sensitive high throughput screen. *J Biol Chem*, 288, 9408-17.

SCACHERI, P. C., CRABTREE, J. S., NOVOTNY, E. A., GARRETT-BEAL, L., CHEN, A., EDGEMON, K. A., MARX, S. J., SPIEGEL, A. M., CHANDRASEKHARAPPA, S. C. & COLLINS, F. S. (2001) Bidirectional transcriptional activity of PGK-neomycin and unexpected embryonic lethality in heterozygote chimeric knockout mice. *Genesis,* 30**,** 259-63.

SCHERE-LEVY, C., BUGGIANO, V., QUAGLINO, A., GATTELLI, A., CIRIO, M. C., PIAZZON, I., VANZULLI, S. & KORDON, E. C. (2003) Leukemia inhibitory factor induces apoptosis of the mammary epithelial cells and participates in mouse mammary gland involution. *Exp Cell Res,* 282, 35-47.

SCHINDLER, C. & DARNELL, J. E, JR. (1995) Transcriptional responses to polypeptide ligands: the JAK-STAT pathway. *Annu Rev Biochem,* 64, 621-51.

SCHMITZ, S. U., ALBERT, M., MALATESTA, M., MOREY, L., JOHANSEN, J. V., BAK, M., TOMMERUP, N., ABARRATEGUI, I. & HELIN, K. (2011) Jarid1b targets genes regulating development and is involved in neural differentiation. *EMBO J,* 30**,** 4586-600.

SCHWERTFEGER, K. L., RICHERT, M. M. & ANDERSON, S. M. (2001) Mammary gland involution is delayed by activated Akt in transgenic mice. *Mol Endocrinol,* 15, 867-81.

SCIBETTA, A. G., SANTANGELO, S., COLEMAN, J., HALL, D., CHAPLIN, T., COPIER, J., CATCHPOLE, S., BURCHELL, J. & TAYLOR-PAPADIMITRIOU, J. (2007) Functional analysis of the transcription repressor PLU-1/JARID1B. *Mol Cell Biol,* 27**,** 7220-35.

SEBASTIAN, J., RICHARDS, R. G., WALKER, M. P., WIESEN, J. F., WERB, Z., DERYNCK, R., HOM, Y. K., CUNHA, G. R. & DIAUGUSTINE, R. P. (1998) Activation

and function of the epidermal growth factor receptor and erbB-2 during mammary gland morphogenesis. *Cell Growth Differ,* 9**,** 777-85.

SECOMBE, J., LI, L., CARLOS, L. & EISENMAN, R. N. (2007) The Trithorax group protein Lid is a trimethyl histone H3K4 demethylase required for dMyc-induced cell growth. *Genes Dev,* 21**,** 537-51.

SEKI, Y., HAYASHI, K., MATSUMOTO, A., SEKI, N., TSUKADA, J., RANSOM, J., NAKA, T., KISHIMOTO, T., YOSHIMURA, A. & KUBO, M. (2002) Expression of the suppressor of cytokine signaling-5 (SOCS5) negatively regulates IL-4-dependent STAT6 activation and Th2 differentiation. *Proc Natl Acad Sci U S A*, 99, 13003-8.

SEWARD, D. J., CUBBERLEY, G., KIM, S., SCHONEWALD, M., ZHANG, L., TRIPET, B. & BENTLEY, D. L. (2007) Demethylation of trimethylated histone H3 Lys4 in vivo by JARID1 JmjC proteins. *Nat Struct Mol Biol,* 14**,** 240-2.

SHACKLETON, M., VAILLANT, F., SIMPSON, K. J., STINGL, J., SMYTH, G. K., ASSELIN-LABAT, M. L., WU, L., LINDEMAN, G. J. & VISVADER, J. E. (2006) Generation of a functional mammary gland from a single stem cell. *Nature,* 439**,** 84-8.

SHEARDOWN, S., NORRIS, D., FISHER, A. & BROCKDORFF, N. (1996) The mouse Smcx gene exhibits developmental and tissue specific variation in degree of escape from X inactivation. *Hum Mol Genet,* 5**,** 1355-60.

SHEARMAN, L. P., JIN, X., LEE, C., REPPERT, S. M. & WEAVER, D. R. (2000) Targeted disruption of the mPer3 gene: subtle effects on circadian clock function. *Mol Cell Biol,* 20**,** 6269-75.

SHEHATA, M., TESCHENDORFF, A., SHARP, G., NOVCIC, N., RUSSELL, A., AVRIL, S., PRATER, M., EIREW, P., CALDAS, C., WATSON, C. J. & STINGL, J. (2012) Phenotypic and functional characterization of the luminal cell hierarchy of the mammary gland. *Breast Cancer Res,* 14**,** R134.

SHI, L., SUN, L., LI, Q., LIANG, J., YU, W., YI, X., YANG, X., LI, Y., HAN, X., ZHANG, Y., XUAN, C., YAO, Z. & SHANG, Y. (2011) Histone demethylase JMJD2B coordinates H3K4/H3K9 methylation and promotes hormonally responsive breast carcinogenesis. *Proc Natl Acad Sci U S A,* 108**,** 7541-6.

SHI, S., LARSON, K., GUO, D., LIM, S. J., DUTTA, P., YAN, S. J. & LI, W. X. (2008) Drosophila STAT is required for directly maintaining HP1 localization and heterochromatin stability. *Nat Cell Biol*, 10, 489-96.

SHI, X., HONG, T., WALTER, K. L., EWALT, M., MICHISHITA, E., HUNG, T., CARNEY, D., PENA, P., LAN, F., KAADIGE, M. R., LACOSTE, N., CAYROU, C., DAVRAZOU, F., SAHA, A., CAIRNS, B. R., AYER, D. E., KUTATELADZE, T. G., SHI, Y., COTE, J., CHUA, K. F. & GOZANI, O. (2006) ING2 PHD domain links histone H3 lysine 4 methylation to active gene repression. *Nature,* 442**,** 96-9.

SHI, Y., LAN, F., MATSON, C., MULLIGAN, P., WHETSTINE, J. R., COLE, P. A. & CASERO, R. A. (2004) Histone demethylation mediated by the nuclear amine oxidase homolog LSD1. *Cell,* 119**,** 941-53.

SLAMON, D. J., CLARK, G. M., WONG, S. G., LEVIN, W. J., ULLRICH, A. & MCGUIRE, W. L. (1987) Human breast cancer: correlation of relapse and survival with amplification of the HER-2/neu oncogene. *Science,* 235**,** 177-82.

SLEEMAN, K. E., KENDRICK, H., ROBERTSON, D., ISACKE, C. M., ASHWORTH, A. & SMALLEY, M. J. (2007) Dissociation of estrogen receptor expression and in vivo stem cell activity in the mammary gland. *J Cell Biol,* 176**,** 19-26.

SMITH, C. L. & HAGER, G. L. (1997) Transcriptional regulation of mammalian genes in vivo. A tale of two templates. *J Biol Chem,* 272**,** 27493-6.

SORLIE, T., PEROU, C. M., TIBSHIRANI, R., AAS, T., GEISLER, S., JOHNSEN, H., HASTIE, T., EISEN, M. B., VAN DE RIJN, M., JEFFREY, S. S., THORSEN, T., QUIST, H., MATESE, J. C., BROWN, P. O., BOTSTEIN, D., LONNING, P. E. & BORRESEN-DALE, A. L. (2001) Gene expression patterns of breast carcinomas distinguish tumor subclasses with clinical implications. *Proc Natl Acad Sci U S A,* 98**,** 10869-74.

SOTGIA, F., SCHUBERT, W., PESTELL, R. G. & LISANTI, M. P. (2006) Genetic ablation of caveolin-1 in mammary epithelial cells increases milk production and hyper-activates STAT5a signaling. *Cancer Biol Ther*, 5, 292-7.

STEIN, T., MORRIS, J. S., DAVIES, C. R., WEBER-HALL, S. J., DUFFY, M. A., HEATH, V. J., BELL, A. K., FERRIER, R. K., SANDILANDS, G. P. & GUSTERSON, B. A. (2004) Involution of the mouse mammary gland is associated with an immune cascade and an acute-phase response, involving LBP, CD14 and STAT3. *Breast Cancer Res,* 6**,** R75-91.

STERNLICHT, M. D., SUNNARBORG, S. W., KOUROS-MEHR, H., YU, Y., LEE, D. C. & WERB, Z. (2005) Mammary ductal morphogenesis requires paracrine activation of stromal EGFR via ADAM17-dependent shedding of epithelial amphiregulin. *Development,* 132**,** 3923-33.

STINGL, J., EIREW, P., RICKETSON, I., SHACKLETON, M., VAILLANT, F., CHOI, D., LI, H. I. & EAVES, C. J. (2006) Purification and unique properties of mammary epithelial stem cells. *Nature,* 439**,** 993-7.

STRATMANN, A. & HAENDLER, B. (2011) The histone demethylase JARID1A regulates progesterone receptor expression. *FEBS J,* 278**,** 1458-69.

SVOTELIS, A., BIANCO, S., MADORE, J., HUPPÉ, G., NORDELL-MARKOVITS, A., MES-MASSON, A. M. & GÉVRY, N. (2011) H3K27 demethylation by JMJD3 at a poised enhancer of anti-apoptotic gene BCL2 determines ERα ligand dependency. *EMBO J*, 30, 3947-61.

TAHILIANI, M., MEI, P., FANG, R., LEONOR, T., RUTENBERG, M., SHIMIZU, F., LI, J., RAO, A. & SHI, Y. (2007) The histone H3K4 demethylase SMCX links REST target genes to X-linked mental retardation. *Nature,* 447**,** 601-5.

TEGLUND, S., MCKAY, C., SCHUETZ, E., VAN DEURSEN, J. M., STRAVOPODIS, D., WANG, D., BROWN, M., BODNER, S., GROSVELD, G. & IHLE, J. N. (1998) Stat5a and Stat5b proteins have essential and nonessential, or redundant, roles in cytokine responses. *Cell*, 93, 841-50.

TERRANOVA, R., AGHERBI, H., BONED, A., MERESSE, S. & DJABALI, M. (2006) Histone and DNA methylation defects at Hox genes in mice expressing a SET domain-truncated form of Mll. *Proc Natl Acad Sci U S A,* 103**,** 6629-34.

THIERFELDER, W. E., VAN DEURSEN, J. M., YAMAMOTO, K., TRIPP, R. A., SARAWAR, S. R., CARSON, R. T., SANGSTER, M. Y., VIGNALI, D. A., DOHERTY, P. C., GROSVELD, G. C. & IHLE, J. N. (1996) Requirement for Stat4 in interleukin-12-mediated responses of natural killer and T cells. *Nature*, 382, 171-4.

THOMPSON, B., TOWNSLEY, F., ROSIN-ARBESFELD, R., MUSISI, H. & BIENZ, M. (2002) A new nuclear component of the Wnt signalling pathway. *Nat Cell Biol*, 4, 367-73.

TING, C. N., OLSON, M. C., BARTON, K. P. & LEIDEN, J. M. (1996) Transcription factor GATA-3 is required for development of the T-cell lineage. *Nature,* 384**,** 474-8.

TREWICK, S. C., MCLAUGHLIN, P. J. & ALLSHIRE, R. C. (2005) Methylation: lost in hydroxylation? *EMBO Rep,* 6**,** 315-20.

TRICHOPOULOS, D., MACMAHON, B. & COLE, P. (1972) Menopause and breast cancer risk. *J Natl Cancer Inst,* 48**,** 605-13.

TU, S., TENG, Y. C., YUAN, C., WU, Y. T., CHAN, M. Y., CHENG, A. N., LIN, P. H., JUAN, L. J. & TSAI, M. D. (2008) The ARID domain of the H3K4 demethylase RBP2 binds to a DNA CCGCCC motif. *Nat Struct Mol Biol,* 15**,** 419-21.

TZSCHACH, A., LENZNER, S., MOSER, B., REINHARDT, R., CHELLY, J., FRYNS, J. P., KLEEFSTRA, T., RAYNAUD, M., TURNER, G., ROPERS, H. H., KUSS, A. & JENSEN, L. R. (2006) Novel JARID1C/SMCX mutations in patients with X-linked mental retardation. *Hum Mutat,* 27**,** 389.

VAFAIZADEH, V., KLEMMT, P. A. & GRONER, B. (2012) Stat5 assumes distinct functions in mammary gland development and mammary tumor formation. *Front Biosci*, 17, 1232-50.

VAN AMERONGEN, R., BOWMAN, A. N. & NUSSE, R. (2012) Developmental stage and time dictate the fate of Wnt/beta-catenin-responsive stem cells in the mammary gland. *Cell Stem Cell,* 11**,** 387-400.

VAN KEYMEULEN, A., ROCHA, A. S., OUSSET, M., BECK, B., BOUVENCOURT, G., ROCK, J., SHARMA, N., DEKONINCK, S. & BLANPAIN, C. (2011) Distinct stem cells contribute to mammary gland development and maintenance. *Nature,* 479**,** 189-93.

VAN NGUYEN, A. & POLLARD, J. W. (2002) Colony stimulating factor-1 is required to recruit macrophages into the mammary gland to facilitate mammary ductal outgrowth. *Dev Biol*, 247, 11-25.

VAN OEVELEN, C., WANG, J., ASP, P., YAN, Q., KAELIN, W. G., JR., KLUGER, Y. & DYNLACHT, B. D. (2008) A role for mammalian Sin3 in permanent gene silencing. *Mol Cell,* 32**,** 359-70.

VERMEULEN, M., MULDER, K. W., DENISSOV, S., PIJNAPPEL, W. W., VAN SCHAIK,

F. M., VARIER, R. A., BALTISSEN, M. P., STUNNENBERG, H. G., MANN, M. & TIMMERS, H. T. (2007) Selective anchoring of TFIID to nucleosomes by trimethylation of histone H3 lysine 4. *Cell,* 131**,** 58-69.

VICENT, G. P., NACHT, A. S., FONT-MATEU, J., CASTELLANO, G., GAVEGLIA, L., BALLARE, C. & BEATO, M. (2011) Four enzymes cooperate to displace histone H1 during the first minute of hormonal gene activation. *Genes Dev,* 25**,** 845-62.

VICENT, G. P., NACHT, A. S., ZAURIN, R., FONT-MATEU, J., SORONELLAS, D., LE DILY, F., REYES, D. & BEATO, M. (2013) Unliganded progesterone receptor-mediated targeting of an RNA-containing repressive complex silences a subset of hormone-inducible genes. *Genes Dev,* 27**,** 1179-97.

VOGT, T., KROISS, M., MCCLELLAND, M., GRUSS, C., BECKER, B., BOSSERHOFF, A. K., RUMPLER, G., BOGENRIEDER, T., LANDTHALER, M. & STOLZ, W. (1999) Deficiency of a novel retinoblastoma binding protein 2-homolog is a consistent feature of sporadic human melanoma skin cancer. *Lab Invest,* 79**,** 1615-27.

VOMACHKA, A. J., PRATT, S. L., LOCKEFEER, J. A. & HORSEMAN N, D. (2000) Prolactin gene-disruption arrests mammary gland development and retards T-antigen-induced tumor growth. *Oncogene*, 19, 1077-84.

WAGNER, K. U., KREMPLER, A., TRIPLETT, A. A., QI, Y., GEORGE, N. M., ZHU, J. & RUI, H. (2004) Impaired alveologenesis and maintenance of secretory mammary epithelial cells in Jak2 conditional knockout mice. *Mol Cell Biol*, 24, 5510-20.

WANG, G. G., SONG, J., WANG, Z., DORMANN, H. L., CASADIO, F., LI, H., LUO, J. L., PATEL, D. J. & ALLIS, C. D. (2009a) Haematopoietic malignancies caused by dysregulation of a chromatin-binding PHD finger. *Nature,* 459**,** 847-51.

WANG, R. A., VADLAMUDI, R. K., BAGHERI-YARMAND, R., BEUVINK, I., HYNES, N. E & KUMAR, R. (2003) Essential functions of p21-activated kinase 1 in morphogenesis and differentiation of mammary glands. *J Cell Biol*, 161, 583-92.

WANG, Z., LI, G., TSE, W. & BUNTING, K. D. (2009b) Conditional deletion of STAT5 in adult mouse hematopoietic stem cells causes loss of quiescence and permits efficient nonablative stem cell replacement. *Blood*, 113, 4856-65.

WATSON, C. J., GORDON, K. E., ROBERTSON, M. & CLARK, A. J. (1991) Interaction of DNA-binding proteins with a milk protein gene promoter in vitro: identification of a mammary gland-specific factor. *Nucleic Acids Res*, 19, 6603-10.

WATSON, C. J. & KHALED, W. T. (2008) Mammary development in the embryo and adult: a journey of morphogenesis and commitment. *Development*,135, 995-1003.

WONG, P. P., MIRANDA, F., CHAN, K. V., BERLATO, C., HURST, H. C. & SCIBETTA, A. G. (2012) Histone demethylase KDM5B collaborates with TFAP2C and Myc to repress the cell cycle inhibitor p21(cip) (CDKN1A). *Mol Cell Biol,* 32**,** 1633-44.

WU, J., SALIDO, E. C., YEN, P. H., MOHANDAS, T. K., HENG, H. H., TSUI, L. C., PARK, J., CHAPMAN, V. M. & SHAPIRO, L. J. (1994) The murine Xe169 gene escapes

X-inactivation like its human homologue. *Nat Genet,* 7**,** 491-6.

WYSOCKA, J., SWIGUT, T., XIAO, H., MILNE, T. A., KWON, S. Y., LANDRY, J., KAUER, M., TACKETT, A. J., CHAIT, B. T., BADENHORST, P., WU, C. & ALLIS, C. D. (2006) A PHD finger of NURF couples histone H3 lysine 4 trimethylation with chromatin remodelling. *Nature,* 442**,** 86-90.

XIANG, Y., ZHU, Z., HAN, G., YE, X., XU, B., PENG, Z., MA, Y., YU, Y., LIN, H., CHEN, A. P. & CHEN, C. D. (2007) JARID1B is a histone H3 lysine 4 demethylase up-regulated in prostate cancer. *Proc Natl Acad Sci U S A,* 104**,** 19226-31.

XIE, L., PELZ, C., WANG, W., BASHAR, A., VARLAMOVA, O., SHADLE, S. & IMPEY, S. (2011) KDM5B regulates embryonic stem cell self-renewal and represses cryptic intragenic transcription. *EMBO J,* 30**,** 1473-84.

XU, J., BURGOYNE, P. S. & ARNOLD, A. P. (2002) Sex differences in sex chromosome gene expression in mouse brain. *Hum Mol Genet,* 11**,** 1409-19.

YAGI, H., DEGUCHI, K., AONO, A., TANI, Y., KISHIMOTO, T. & KOMORI, T. (1998) Growth disturbance in fetal liver hematopoiesis of Mll-mutant mice. *Blood,* 92**,** 108-17.

YAHATA, T., SHAO, W., ENDOH, H., HUR, J., COSER, K. R., SUN, H., UEDA, Y., KATO, S., ISSELBACHER, K. J., BROWN, M. & SHIODA, T. (2001) Selective coactivation of estrogen-dependent transcription by CITED1 CBP/p300-binding protein. *Genes Dev,* 15**,** 2598-612.

YAMAJI, D., KANG, K., ROBINSON, G. W. & HENNIGHAUSEN, L. (2013) Sequential activation of genetic programs in mouse mammary epithelium during pregnancy depends on STAT5A/B concentration. *Nucleic Acids Res,* 41, 1622-36.

YAMAJI, D., NA, R., FEUERMANN, Y., PECHHOLD, S., CHEN, W., ROBINSON, G. W. & HENNIGHAUSEN, L. (2009) Development of mammary luminal progenitor cells is controlled by the transcription factor STAT5A. *Genes Dev*, 23, 2382-7.

YAMANE, K., TATEISHI, K., KLOSE, R. J., FANG, J., FABRIZIO, L. A., ERDJUMENT-BROMAGE, H., TAYLOR-PAPADIMITRIOU, J., TEMPST, P. & ZHANG, Y. (2007) PLU-1 is an H3K4 demethylase involved in transcriptional repression and breast cancer cell proliferation. *Mol Cell,* 25**,** 801-12.

YAMASHITA, H., NISHIO, M., ANDO, Y., ZHANG, Z., HAMAGUCHI, M., MITA, K., KOBAYASHI, S., FUJII, Y. & IWASE, H. (2006) Stat5 expression predicts response to endocrine therapy and improves survival in estrogen receptor-positive breast cancer. *Endocr Relat Cancer*, 13, 885-93.

YANG, J. & STARK, G. R. (2008) Roles of unphosphorylated STATs in signaling. *Cell Res,* 18, 443-51

YAO, W., PENG, Y. & LIN, D. (2010) The flexible loop L1 of the H3K4 demethylase JARID1B ARID domain has a crucial role in DNA-binding activity. *Biochem Biophys Res Commun,* 396**,** 323-8.

YAO, Z., CUI, Y., WATFORD, W. T., BREAM, J. H., YAMAOKA, K., HISSONG, B. D., LI, D., DURUM, S. K., JIANG, Q., BHANDOOLA, A., HENNIGHAUSEN, L. & O'SHEA, J. J. (2006) Stat5a/b are essential for normal lymphoid development and differentiation. *Proc Natl Acad Sci U S A,* 103, 1000-5.

YOSHIDA, M., ISHIMURA, A., TERASHIMA, M., ENKHBAATAR, Z., NOZAKI, N., SATOU, K. & SUZUKI, T. (2011) PLU1 histone demethylase decreases the expression of KAT5 and enhances the invasive activity of the cells. *Biochem J,* 437**,** 555-64.

YU, B. D., HESS, J. L., HORNING, S. E., BROWN, G. A. & KORSMEYER, S. J. (1995) Altered Hox expression and segmental identity in Mll-mutant mice. *Nature,* 378**,** 505-8.

ZENG, Y. A. & NUSSE, R. (2010) Wnt proteins are self-renewal factors for mammary stem cells and promote their long-term expansion in culture. *Cell Stem Cell*, 6, 568-77.

ZHAO, L., HART, S., CHENG, J., MELENHORST, J. J., BIERIE, B., ERNST, M., STEWART, C., SCHAPER, F., HEINRICH, P. C., ULLRICH, A., ROBINSON, G. W. & HENNIGHAUSEN, L. (2004) Mammary gland remodeling depends on gp130 signaling through Stat3 and MAPK. *J Biol Chem*, 279, 44093-100.

ZHU, W. & NELSON, C. M. (2013) PI3K regulates branch initiation and extension of cultured mammary epithelia via Akt and Rac1 respectively. *Dev Biol*, 379, 235-45.

ZOU, M. R., CAO, J., LIU, Z., HUH, S. J., POLYAK, K. & YAN, Q. (2014) Histone Demethylase Jumonji AT-Rich Interactive Domain 1B (JARID1B) Controls Mammary Gland Development by Regulating Key Developmental and Lineage Specification Genes. *J Biol Chem*, May 6. [Epub ahead of print]